Fabrication and characterisation of organic monolithic columns for the separation of small molecules using HPLC-MS
The Frame Problem Revisited

Aljohani, Wael Hamad H

Awarding institution:
King's College London

KING'S College LONDON

Fabrication and characterisation of organic monolithic columns for the separation of small molecules using HPLC-MS

By

Wael H Aljohani

A thesis submitted in partial fulfilment of the requirements for the degree Doctor of Philosophy

December 2016

Abstract

Monolithic columns are continuous interconnected networks with large through-pore channels. This structure results in a decrease in the diffusion path and affords high permeability, which result in obtaining good separation efficiency. Ideally, the structure of monoliths should be bi-model consisting of meso-pores and macro-pores responsible for retention time and flow of mobile phase respectively. The structure also enhances the mechanical strength, and the large through-pore channels afford very low flow resistance. This combination therefore results in the ability of smaller diameter monolithic columns to be employed under high flow rates, increasing both sensitivity and throughput simultaneously. Additionally, the unique structure of monoliths improves permeability and mass transfer leading to a decrease in band broadening.

The first stage of the project was focused on the fabrication and characterisation of an organic monolithic column namely poly (SMA-co-EDMA) followed by quantification of caffeine in Arabic coffee. Since the efficiency of the above monolith was low due to the low number of mesopores (low surface area), the second stage was centered on improving the efficiency of organic monoliths via the use of a longer crosslinker namely 1,6-HEDA. This novel monolith column poly (HMA-co-1,6-HEDA) afforded high efficiency, good porosity, high permeability and excellent reproducibility. Next, this monolith was applied to several applications namely separation of neutral non-polar analytes, weak acids, and strong bases, followed by a quantification of amitriptyline in commercial pharmaceutical tablets. Since the results obtained for this novel monolith using capillary liquid chromatography were encouraging, the third stage was investigating the possibilities of coupling narrow fused silica capillaries with mass spectrometry (MS). In this stage, the novel monolith (HMA-co-1,6-HEDA) lacked stability under high pressure due to either the low concentration of the

crosslinker (1,6-HEDA) in the polymerisation mixture or the ratio between the monomer mixture (HMA and 1,6-HEDA) and porogen system (1-propanol and 1,4-butanediol). Hence, a move towards using nano-flow to couple narrow fused silica capillaries to the MS was utilised and was successful in separating two basic drugs (amitriptyline and nortriptyline). Finally, in order to widen the application of reversed- phase monoliths, a new monolithic material namely poly (GMA-co-EDMA) was synthesised followed by incorporation of high purity Congo red (CR) which contains several functional groups including SO_3H, and then evaluating by separation of some reversed phase and HILIC mixtures.

Acknowledgements

First, I would like to express my appreciation to my wonderful supervisor Dr. Norman Smith, who I will never forget, for his continuous support throughout my PhD journey. He has taught me chromatography and has helped me to build contact within chromatography community. He also influxed me with English idioms during the coffee breaks some of which are donkeys years, white elephant, costs fortune, jerry built, and as useful as a chocolate teapot. I would like to thank my first supervisor Dr. Cristina Legido-Quigley for her guide and advise during my studies. I wish to thank sincerely our post-docs including Dr. Chris Knappy and Dr. Arundhuti Sen who assisted and gave me invaluable advice during the tough period in getting my thesis together. I also wish to express my thankfulness to all PhD students in our group with whom I share the happiness and sadness times together and for holding fruitful discussions regarding the matters in our research. I would like to show gratitude toward my parents for their financial and spiritual support and wish for my dad a good health. I have been missing you both. I would like to show my recognition to my lovely wife Shaima for her continuous support during the difficult times in the UK, am gifted with her and I love her sincerely. I also wish her good luck with her PhD. Finally, I would like to say to my children Daimah and Fasial that I love you so much and am sorry for not being with you at all times during my PhD. I also encourage my kids to seek knowledge as it does build your personality and character.

Tables (created using word software):

Table of Figures (created using word software):

List of symbols and abbreviations

HPLC	High Performance Liquid Chromatography
logP	The partition coefficient of a molecule between an aqueous and lipophilic phases
Nano-HPLC	Nano-High Performance Liquid Chromatography
NPLC	Normal phase chromatography
RP-HPLC	Reversed-phase liquid chromatography
IE	Ion exchange
SEC	Size exclusion chromatography
HILIC	Hydrophilic interaction liquid chromatography
EPG	Embedded polar group stationary phases
C_{18}	Octadecyl
SPE	Zwitterion phase (N,N-Dimethyl-N-(2-methacryloyloxyethyl) -N-(3-sulfopropyl)ammonium betaine
t_0/V_0	Dead/Void volume
t_R	Retention time
k	Retention factor
α	Selectivity factor
Rs	Resolution
A_s	Asymmetry Factor
N	Column Efficiency
HETP	Height equivalent to a theatrical plate
MS	Mass spectrometry
m/z	Mass-to-charge ratios
EI	Electron ionisation
CI	Chemical ionisation
ESI	Electrospray ionisation
CRM	Charged residue model
IEM	Ion evaporation model
APCI	Atmospheric pressure chemical ionisation
APPI	Atmospheric pressure photoionisation
T.O.F	Time of flight
HCl	Hydrochloric acid
H_2SO_4	Sulphuric acid
TFA	Trifluoroacetic acid
LLE	Liquid-liquid extraction
SPE	Solid phase extraction
API	Atmospheric pressure ionisation
μ	linear velocity
A	Eddy diffusion
B	Axial diffusion
C	Resistance to mass transfer
d_p	Particle size
γ	Packing coefficient

D_M	Diffusion coefficient
UHPLC	Ultra-High performance Liquid Chromatography
i.d.	Internal diameter
CEC	Capillary Electro Chromatography
GC	Gas Chromatography
METAM	Methacryloyloxy ethyl-trimethyl ammonium methylsulphate
GMA	Glycol methacrylate
HMA	Hexyl methacrylate
EDMA	Ethylene dimethacrylate
1,6-HEDA	1,6-hexanediol ethoxylate diacrylate
η	Dynamic viscosity
K	Permeability
Ɛ	Porosity
SEM	Electron microscopy
RSD	Relative standard deviation
SMA	Stearyl methacrylate
ICH	International Conference on Harmonisation
L.O.D	Limit of detection
L.O.Q	Limit of quantification
SPE	(N, N-dimethyl-N-methacryloxyethyl-N-(3-sulfopropyl) ammonium betaine
SPDA	*N*,*N*-dimethyl-*N*-acryloyloxyethyl-*N*-(3-sulfopropyl) ammonium
MBA	*N*,*N*′-methylenebisacrylamide
PEGMEMA	poly(ethylene glycol) methyl ether methacrylate
γ-MAPS	3-(trimethoxysilyl) propyl methacrylate
NaOH	Sodium hydroxide
MeOH	Methanol
ACN	Acetonitrile
M	Molar (Concentration unit)
PEEK	Polyether ether ketone
FTIR	Fourier transform infrared spectroscopy
UV	Ultra violate
CR	Congo red
µ-HPLC	Micro-high performance liquid chromatography
NMR	Nuclear magnetic resonance spectroscopy
pH	Potential of hydrogen
CE	Capillary electrophoresis
AIBN	Azobisisobutyronitrile
MPa	Megapascal (pressure unit)
mM	milliMolar (concentration unit)
S	Slope
σ	Standard deviation
ROMP	Ring-opening metathesis polymerisation
o.d.	Outer dimension
LMA	Lauryl Methacrylate
R^2	Correlation coefficient
AOD	3-methylacryloyl-3-oxapropyl-3-(N,N-dioctadecylcarbamoyl)-propionate
PEDAS	Pentaerythritol diacrylate monostearate

SEMA	2-(sulphooxy) ethyl methacrylate
TEA	Triethylamine
HPLC-MS	High liquid chromatography coupled with mass spectrometry
GC-MS	Gas chromatography-Mass Spectrometry
PB	Particle beams
cf-FAB	Continuous flow fast atom bombardment
DLI	Direct liquid introduction
TSP	Thermospray
CI	Chemical ionisation
EI	Electron ionisation
1,4-BDDMA	1,4-butanediol dimethacrylate
1,10-DMDMA	1,10-decamethylene dimethacrylate
PEEKsil	Fused silica tubing sheathed in PEEK polymer
TMPTA	Trimethylolpropane triacrylate
MDPC	12-Methacryloyl dodecylphosphocholine
MDPS	12-methacryloyl dodecylphosphoserine
MO	Methyl orange
PAHs	Poly-aromatic hydrocarbons
DMF	N,N-dimethylformamide
EtOH	Ethanol
DMSO	Dimethyl sulfoxide
SPP	N, N-dimethyl-N-(3-methacryl-amidopropyl)-N-(3-(sulfopropyl) ammonium betaine
SFC	supercritical fluid chromatography
CO_2	Carbon dioxide

Chapter 1

Introduction

1. Introduction

1.1. Basic principles of High Performance Liquid Chromatography (HPLC)

Liquid chromatography can be described as a physical separation technique in which the components of a mixture are separated based on their differential interaction between two phases, namely, a stationary phase and a mobile phase. The former is usually a porous solid placed inside a cylindrical column; the latter is liquid [1]. Based on the nature of analyte (chemical structure and logP), the mode of separation is selected [2], will be discussed briefly in section 1.3.

If the concentration of the mobile phase is fixed throughout the analysis, this type of chromatography is called isocratic elution. When the concentration of the mixture of the mobile phase and thus its polarity is changed throughout the analysis, this is called gradient elution. The isocratic elution is mainly employed for assay, dissolution and routine analysis when required to resolve 2 to 3 compound in a single run [3]. Gradient elution, on the other hand, is used when required to separate more complex mixtures of analytes with a range of polarities need to be separate in a single run. Furthermore, gradient elution is appropriate for degradation studies, impurities profiling, and separation of complex herbal extracts, amongst other applications [3].

In isocratic elution, peak width broadens linearly as the retention times increases in accordance with the equation of efficiency, and this will be illustrated in section 1.3 (equation 1.6) below. This broadening can often result in late eluting peaks being very flat to the extent that they are sometimes not recognized as peaks.

This retention time dependent broadening is reduced with gradient elution, which decreases the retention time of the late-eluting peaks leading to narrower and taller peaks. Moreover, peak shapes improve due to the increased concentration of the organic eluent resulting in pushing the tailing part of a peak forward [3].

The mobile phase consists of at least two solvents; one behaving like a strong solvent while the other behaves as a weak solvent. This classification is based on the position of the solvent in the relevant eluotropic series. The eluotropic series classifies solvents in order of their influence to elute a given compound via a stationary phase (silica or C_{18}). This order of the solvents runs in the order of their polarity. The eluotropic series is thus dependent on the stationary phase used and the compound that needs to be separated [4]. Table 1.1 below shows some of the solvents used in chromatography with their eluotropic series. It is also believed that the strong solvent interacts with the stationary phase more readily than the weak one. Examples of strong solvents in reversed-phase chromatography and normal phase chromatography are acetonitrile and chloroform respectively [5].

Table1-1: Eluent Strength based on eluotropic of solvent for adsorption chromatography on silica, adopted from [5].

Solvent	Eluent Strength based on elutropic series*[a]
Hexane	0.01
Heptane	0.01
Toluene	0.22
Chloroform	0.26
Diethyl ether	0.43
Acetonitrile	0.52
Acetone	0.53
Tetrahydrofuran	0.53
2-Propanol	0.60
Methanol	0.70
Water	1.00

[a] The values are calculated with respect to water.

1.2. Nano- High Performance Liquid Chromatography (Nano-HPLC)

Reproducible Nano-HPLC requires a pumping system capable of consistently delivering a very low flow rate on the order of nl/min. Nano flow, therefore, can be generated using an incorporating flow splitter with a conventional HPLC pump leading to the removal of excessive flow from the HPLC system. Nano flow can alternatively be generated via the use of splitless nano flow pumping system which has become available in the market [6]. Schematics of both types of pump are shown in Fig. 1.1. It is worth noting that when the term Nano-HPLC is used, it means the column's ID used is between 20-100 µm, while when the term capillary-HPLC is used, the column's ID is between 100-500 µm, micro-HPLC uses column ID's of between 0.5-1.0 mm [7, 8].

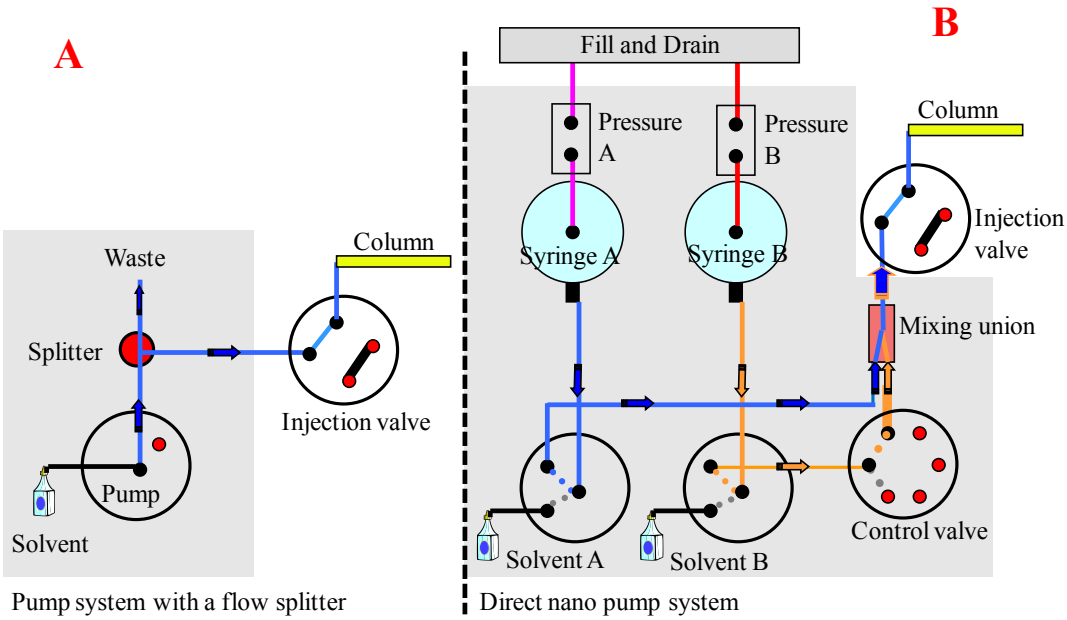

Figure 1-1: Nano flow pump system employing a flow splitter (A) and splitless technology (B), reproduced with permission[6].

The Dina nano-flow pumping system used in this project employs built-in syringe pumps to draw and store liquids from solvent reservoirs A and B. After the syringes are filled in the flushing mode, solvents A and B are drained out via the draining valve sets located near the pressure regulators of each syringe. In the operational mode, solvent A is delivered from a syringe direct to a mixing union, while solvent B travels through the control valve before being introduced to the union. The solvents (A and B) mix in the union, then travel to the injection valve and column and finally to the detector [6]. A photograph of the Nano-HPLC is illustrated in Fig.1.2 below.

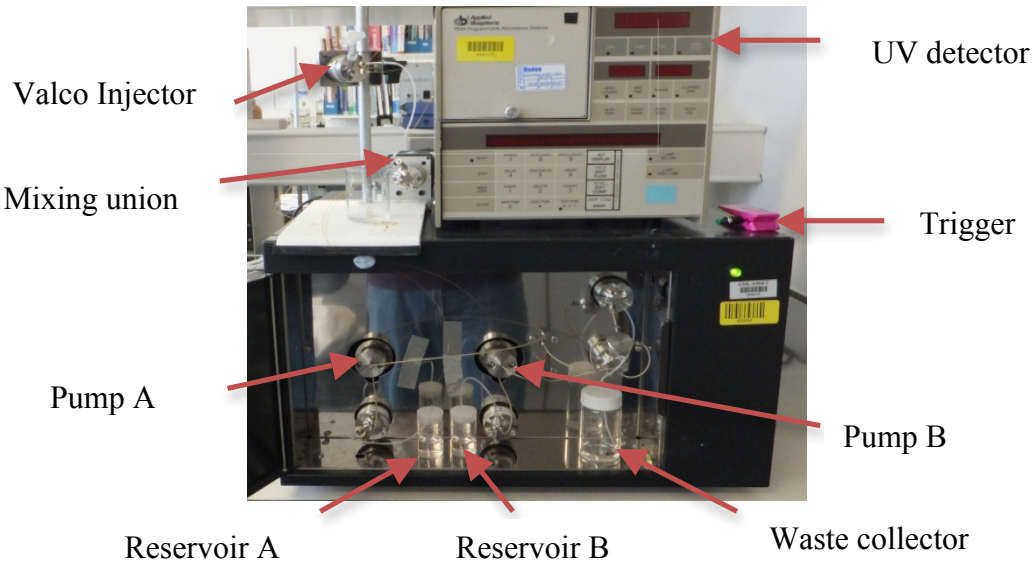

Figure 1-2: photograph of Dina system.

As shown in Fig 1.2, a fixed volume of the sample (100 nl) is injected into a small loop at atmospheric pressure (with the injection valve in load position). Then, the sample is introduced into the column via a loop injector in the following manner: when the injection valve is switched from the load to the inject mode, the mobile phase flows through the loop and carries the sample to the column where the separation takes place. Then, the sample components illustrate different affinities towards the mobile and stationary phases: the higher the affinity of a component towards the stationary phase, the longer its retention in the

column. Once eluted, the flow path leads to a detector producing signals which correspond to the component's physical characteristics. Then, the signals are transformed to interpretable data, known as chromatograms. In our project for the detection, a window for use with UV detection is created on the capillary column (online-detection); the detector cell is positioned so that the light beam passes through the window [1].

1.3. Modes of HPLC

As previously mentioned, there are several modes of liquid chromatography which can be used depending on the nature of analyte of interest. The main modes are normal phase chromatography (NPLC), reversed-phase liquid chromatography (RP-HPLC), ion exchange (IE), size exclusion chromatography (SEC), and hydrophilic interaction liquid chromatography (HILIC). The scope of this thesis will only be tackling the RP-HPLC, and HILIC modes as these are the modes most frequently employed.

1.3.1. **Reversed-phase Liquid chromatography (RP-HPLC)**

In RP-HPLC, the stationary phase is non-polar, and as a result, the analyte of interest is non-polar, and the mobile phase overall polarity is polar, typically mixtures of aqueous/organic solvents. The elution order of the analytes is based on their polarity/hydrophobicity. The more non-polar the analytes, the longer they are retained on the column. An example of a common stationary phase used in RP-HPLC is silica bonded with either a C_8 or C_{18} ligand which imparts the hydrophobicity to the stationary phase. Additionally, the stationary phase can be altered chemically in order to impart polar functional groups. This functionalization can widen its application in terms of selectivity and reduce the amount of method development for particular compounds.

For instance, incorporating phenyl groups to silica-C_{18} helps to separate the aromatic compounds via π-π interaction, in comparison with pure silica-C_8 or C_{18}.

Moreover, incorporating either amino or cyano groups to the silica-C_{18} assists in resolving polar compounds through dipole-dipole interaction, which are not prevalent on classical silica-C_{18}. Fig 1.3 shows the chemical structure of the C_{18} moiety, with and without additional functional groups; the latter are incorporated to obtain different selectivities [9]. These types of columns with polar sites are known as embedded polar group stationary phases (EPG).

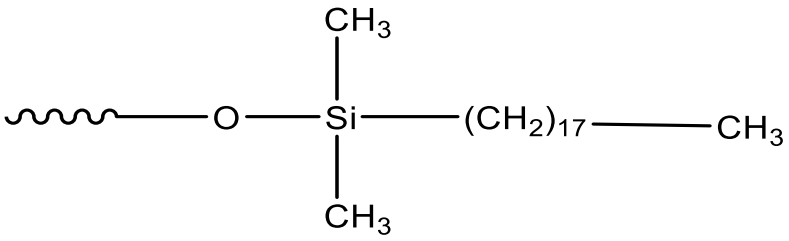

Octadecyl (C_{18})

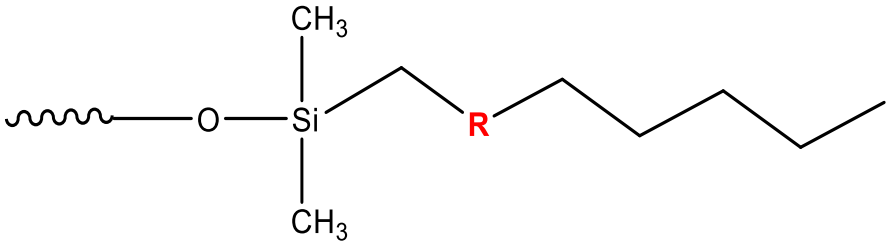

(EPG)

Where R: Functional group	Chemical Structure
Urea	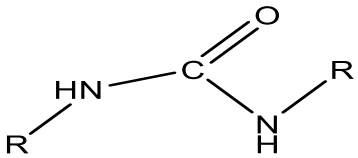
Amide	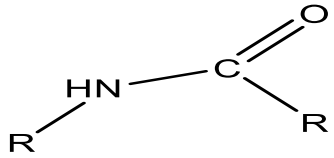
Carbamate	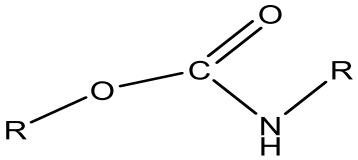

Figure 1-3: Examples of C18 columns and embedded polar group on C_{18}, where R in the table could be any functional group and is different to the R presented in the EPG structure [10].

1.3.2. **Hydrophilic interaction chromatography (HILIC)**

RP-HPLC is a handy technique which gives adequate separation for most of the analytes that we deal with. According to columns sales, around 70-80% of analytes can be resolved by RP-HPLC [11].

The high purity type of silica-based columns is robust in the range of $2 < pH < 8$. In addition, there are many columns available in the market that can work well to pH 10. When developing a method for charged analytes in HPLC, the first choice is to work at low pH. Under low pH, acids will be ion suppressed, neutral, and as a result will be more retained under RP-HPLC. While for bases, they will be ionised, positively charged, and as a result will be poorly/un-retained under RP-HPLC. If the pH parameter is not effective, there is another type of stationary phase named as 'polar embedded group'[11]. With these types of columns, 100% aqueous mobile phases in RP-HPLC can be used without any issues, phase de-wetting phenomenon (column damage), more details about this phenomenon can be reviewed elsewhere [12]. When these types of columns also are not effective, ion pairing reagents or ion- exchange phases can be the way forward with charged analytes.

How is ion pairing used with highly polar and ionic compounds?

The ion pairing reagent possesses an ionic end (charged part) and non-polar tail, as illustrated in Fig. 1.4. Firstly, the ion pairing reagent is added to the mobile phase and is left for equilibrium with the column. Then, the non-polar end is, as a result, adsorbed strongly into non-polar stationary phase causing the charged functional group of the reagent to stick out into the mobile phase and bind with the analyte of interest possessing the charged polar functional group. This binding, therefore, causes/increases the retention of the analyte of interest [11].

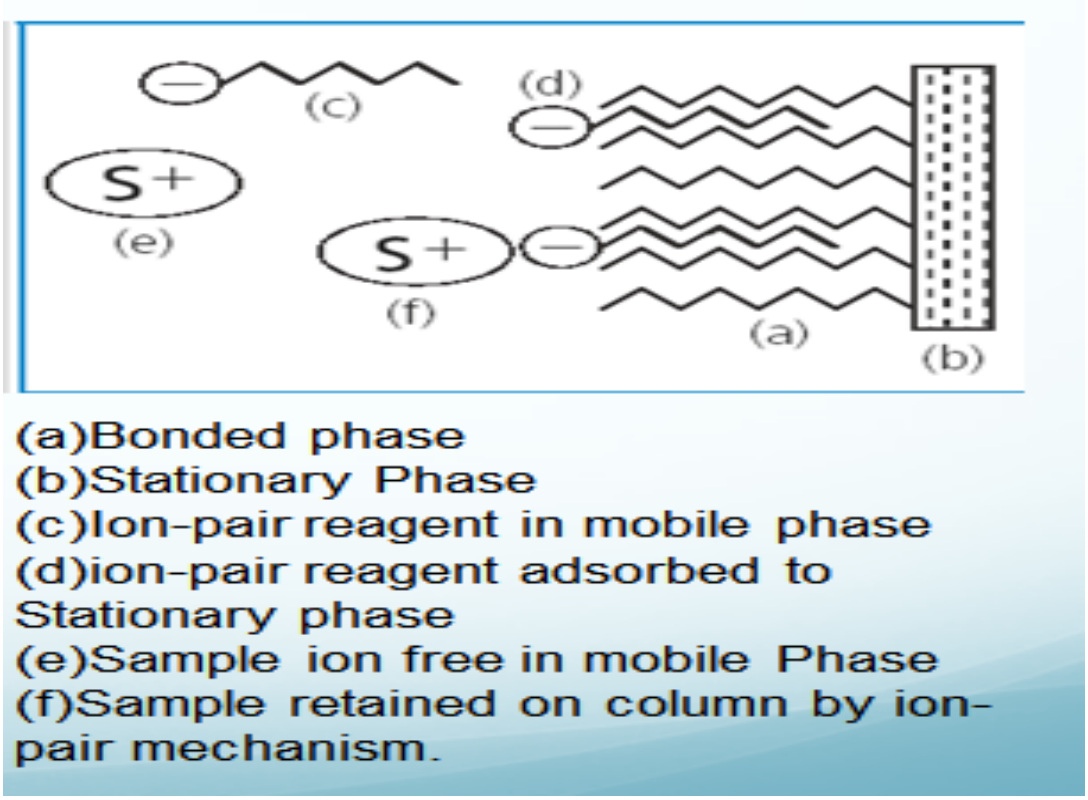

Figure 1-4: schematic of an ion pairing structure adopted from [11].

How is ion- exchange used with highly polar and ionic compounds?

Ion exchange chromatography (IEC) uses stationary phases with charged functional groups. IEC is based on the affinities of the charged analytes for charged functional groups embedded in the stationary phase or adsorbed counter ions. The embedded functional group on the surface of the stationary phase can either be an anion-exchanger (positive functional groups) and is used to attract negatively charged analytes. Alternatively, the embedded functional group is a cation exchanger (negative functional groups) and is used to attract positively charged analytes, as shown in Fig 1.5.

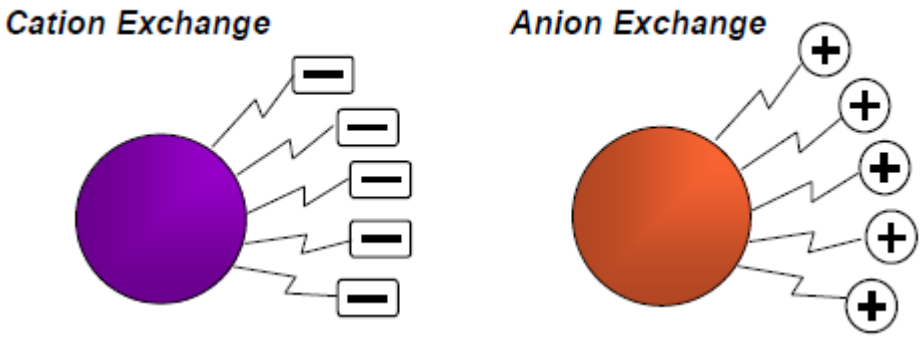

Figure 1-5: Schematic of an anion and cation exchange stationary phase adopting from [13].

Retention in IEC is based on the degree of the affinity of different analytes counter ions for the charged surface of the stationary phase along with a number of other solution parameters. These parameter include ionic strength, counter ion type, pH, and so on and so forth. Table 1.2 below gives some examples of embedded functional groups that can be used for IEC.

Table 1-2: Ion exchange: embedded functionality, Adopted with modification [13].

IEC	Cation	Anion
weak	COO^- Na^+ (Carboxylic Acid)	$NH(CH_3)_2^+$ Cl^- (Tertiary amine)
strong	SO_3^- Na^+ (Sulfonic Acid)	$N(CH_3)_3^+$ Cl^- (Quaternary amine)

However, a large group of strongly polar analytes which are not ionisable in solution could not be retained using the approaches mentioned above. This challenge has been overcome by two approaches including GC derivatisation or the recent mode in chromatography known as HILIC [14].

While Alpert first suggested the use of the term 'HILIC' to describe the associated separation mechanism in 1990, this separation mode has become widely used in the past two decades. HILIC is considered as a variant of NPLC, with a far more complicated mechanism. HILIC uses a polar stationary phase and mobile phase consisting of high organic such as ACN (> 80%) with a small portion of water or buffer [15]. It is believed that the water is adsorbed onto the polar stationary phase, thus forming a water-rich layer at the stationary phase and water-deficient mobile phase. The polar analytes are separated based on interactions with the adsorbed layer and mobile phase, as shown in Fig. 1.6.

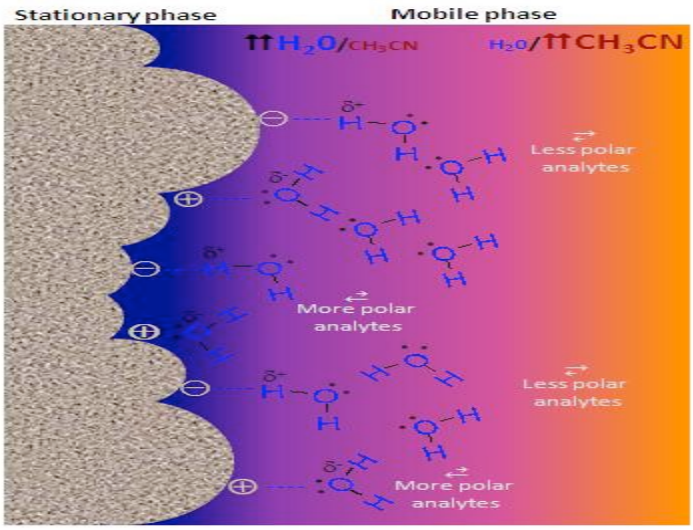

Figure 1-6: Illustration of HILIC separation, adopted from [16].

Two mechanisms are primarily involved in contributing to the overall separation of compounds: hydrogen bonding interaction between polar analytes and the water layer formed with the stationary phase, the weak electrostatic interaction between charged analytes and the stationary phase [17]. The order of elution is opposite to the RP-HPLC mode described above. Fig.1.7 below illustrates some of the stationary phases employed in HILIC. Additionally, the figure shows a zwitterion phase which contains both a positive and negative functional group; this widens the application area of these HILIC materials [17].

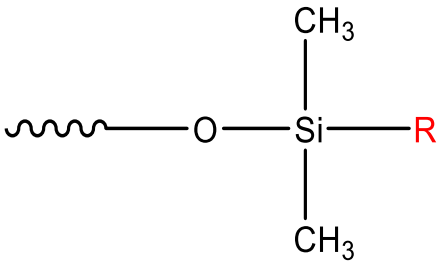

Where R: Functional group	Structure
Cyano bonded phase [18]	
Amino bonded phase [19]	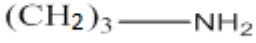
Zwitterion phase (N,N-Dimethyl-N-(2-methacryloyloxyethyl) -N-(3-sulfopropyl)ammonium betaine (SPE) [20]	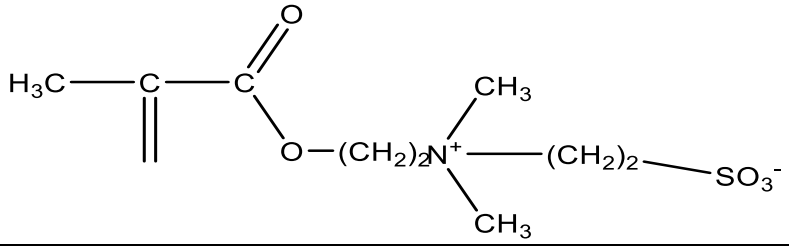

Figure:1-7: Stationary phases used in HILIC separation.

HILIC provides a solution to resolve a wide range of separation challenges including separation of basic drugs, small organic acids, metabolic profiling [21], clinical and diagnostic applications [17], and many other neutral and charged compounds.

Additionally, the high concentration of organic solvent used in the mobile phase for HILIC separation is very useful for coupling to MS detectors.

1.4. Characteristics of chromatographic separation

All chromatographic separation can be characterised by a set of parameters that aid in the identification and quantification of the separated compounds. Several of these parameters are illustrated in Fig. 1.8.

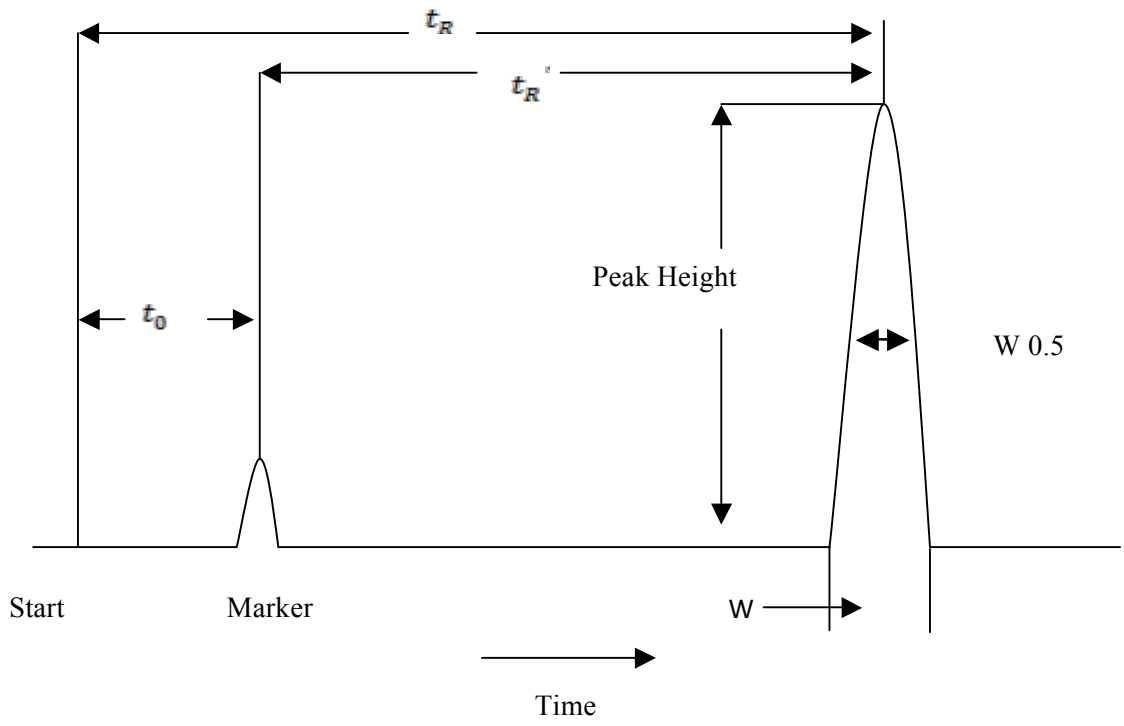

Figure: 1-8: The Chromatographic parameters.

1.4.1. Dead/Void volume (t_0/V_0)

This is the volume of the mobile phase to reach the detector from the injection point. As can be observed from the Fig 1.8, the first eluted peak represents the retention time of the un-retained peak, known as a marker. This is also used to indicate the void volume. The main characteristic of the marker used to indicate the dead volume is the absence of interaction with the stationary phase. Generally, thiourea and toluene are used as un-retained analytes in RP-HPLC and HILIC respectively [22].

1.4.2. **Retention time (t_R)**

This refers to the time spent by an analyte from the injection point until reaching a detector, as shown in Fig. 1.8. The void time (t_0) is an indication of the time spent by any analytes in only the mobile phase, while t_R is the total time spent by the analyte in both mobile and stationary phases. Therefore, the corrected retention time is calculated via equation 1.1 below.

$$t_R' = t_R - t_0 \qquad 1.1$$

t_R and t_0 are the retention times for the analyte of interest and an unretained analyte respectively [22].

1.4.3. **Retention factor (k)**

The retention factor or k provides an estimate of how well an analyte is retained on the column relative to the retention of an un-retained (t_0) marker. The retention factor is calculated through the equation below 1.2.

$$k = \frac{t_R - t_0}{t_0} \qquad 1.2$$

When $1 < k < 10$ for a given analyte, this suggests that an isocratic elution may be used to elute the analyte in a reasonable time. If the range of k is wider, then it is necessary to consider gradient elution. If k for a specific compound is ≤ 1, this is an indication of chromatographic interference at the beginning of the chromatogram and is considered to be an un-retained compound [23].

1.4.4. **Selectivity factor (α)**

This is a measure of the difference in retention behavior of two consecutive analytes and can be calculated using the equation below, 1.3.

$$\alpha = \frac{t_2 - t_0}{t_1 - t_0} = \frac{k_2}{k_1} \qquad 1.3$$

Where t_1 and t_2 are the retention times for any two successive peaks and k_1 and k_2 are their associated retention factors.

From the above equation, 1.3, if the selectivity factor is higher than 1, then it is acceptable, and there is a separation between the two analytes. Otherwise, the selectivity needs to be improved [22].

1.4.5. **Resolution (R_s)**

Peak resolution expresses the degree of separation of two analytes and also provides an indication of column performance and the contribution of peak broadening to changes in resolution, as shown in equation 1.4.

$$R_s = \frac{(t_{R_2} - t_{R_1})}{0.5(w_{b_1} + w_{b_2})} \qquad 1.4$$

Where w_{b_1} and w_{b_2} are the width of the first and the second peaks respectively.

If the resolution value is 1.5 or higher, this indicates the complete separation which assumes a Gaussian peak shape. However, the Gaussian peak shape does not take into account the phenomenon of co-elution [22], as observed in Fig 1.9.

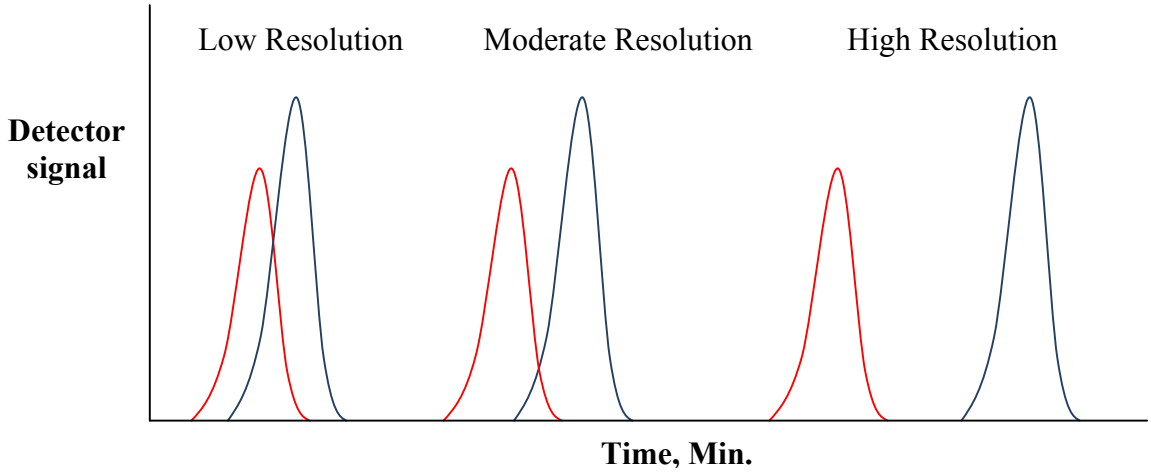

Figure 1-9: An example of the degree of resolution.

1.4.6. **Peak symmetry: Asymmetry Factor (A_s)**

Ideally, chromatographic peaks should display Gaussian shapes. However, in practices, such ideal shapes are not frequently observed. Peaks often demonstrate either fronting or tailing as shown in Fig. 1.10. leading to several issues including lower peak height resulting in higher detection limits, an undesirable problem when dealing with toxic analytes or those with low concentration [24]. Another issue that arises due to peak asymmetry is difficulty in peak integration, resulting in imprecise and irreproducible peak areas and ultimately imprecise quantification. The peak integration becomes more challenging when the difference in peak area between two adjacent peaks is high leading to the possibility that smaller peaks are overlooked, this is one of the fundamental challenges involved in impurity profiling [24].

Peak tailing originates from several sources including the type and purity of the stationary phase used, the choice of the mobile phase, and analyte-related factors including sample overload, sample solvent, and metal complexation [23].

Peak symmetry can be gauged by the peak asymmetry factor 'As' using equation 1.5, typically measured employing the peak width at 10% of peak height [23].

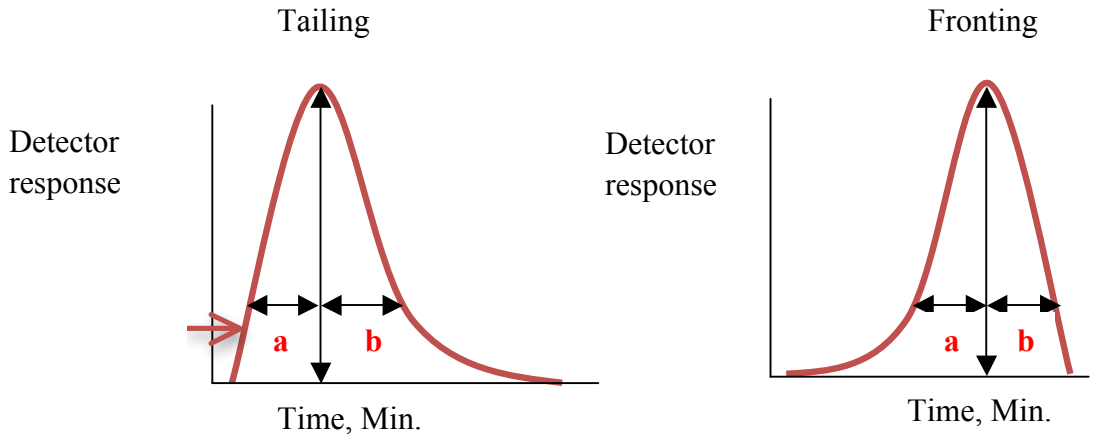

Figure 1-10: Peak tailing and fronting.

$$As = \frac{B}{A} \qquad 1.5$$

As is typically calculated from the peak width measured at 10% of peak height. An As of 1 suggests that excellent peak symmetry. A value less than 1 (b < a) indicates peak fronting while a value more than 1 (b > a) is an indication of peak tailing.

Fig. 1.11 demonstrates some of the common peak tailing issues observed in HPLC, and the acceptable limits of peak asymmetry values [24].

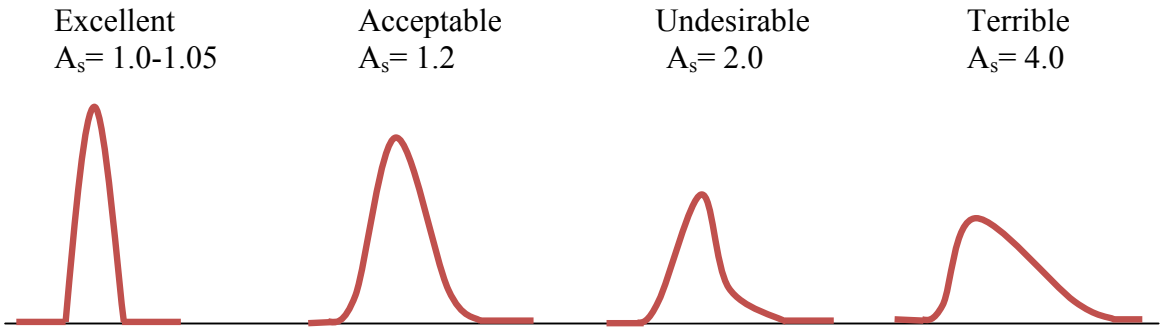

Figure 1-11: Examples of peak tailing, adopted with modification from [23].

1.4.7. **Column Efficiency (N)**

This indicates the performance of a chromatographic column through sharpness and symmetry of eluted peak. Efficiency is calculated via one of the two equations stated below, 1.6 and 1.7. Both equations can be used interchangeably, however, if there was a shoulder or a good baseline is not obtained, the equation used the peak width at half height would then be recommended [24].

$$\mathbf{N = 16\left(\frac{t_R}{w_b}\right)^2} \qquad 1.6$$

$$\mathbf{N = 5.54\left(\frac{t_R}{w_{1/2}}\right)^2} \qquad 1.7$$

Where $w_{1/2}$ is the peak width at half height and N is the number of plates.

The number of plates originates from the distillation column theory whereby equilibrium takes place between the stationary and the mobile phase between every plate. In a HPLC column, it is believed that a column consists of a series of plates where the equilibrium occurs between the two phases: the more plates the column possesses, the more efficient the column will be [24].

The number of plates is employed to compare the performance of different columns, so long as the test mixture and particle size used and other chromatographic conditions (mobile phase, temperature, flow rate) used are identical [24].

Another tool that indicates the performance of a column is the height equivalent to a theatrical plate (HETP), which is inversely proportional to a number of plates. This is calculated via equation 1.8 below.

$$\mathbf{HETP} = \frac{\mathbf{L}}{\mathbf{N}} \qquad 1.8$$

Where L is the length of the column in cm [24].

1.5. Mass Spectrometry (MS)

When working with MS, certain terms are significant and need to be clarified at the outset, including:

Mass resolution: The capacity of a mass analyser to distinguish one mass from an adjacent mass.

Mass accuracy: The closeness of a mass measurement to the true mass of the analyte of interest.

Mass spectrometry is an advanced analytical technique widely employed for the identification and quantification of ionisable molecules. MS can be used to detect any compound with at least one ionisable functional group, conferring an advantage over spectroscopic techniques (UV/VIS), which require a chromophore [25]. A key benefit of MS is its very low analytical detection limit (typically in the pg range); particularly advantageous for investigation of forensic or toxic samples. A further advantage is its potential for hyphenation with chromatography, affording spectral information for components in mixtures, discussed in details in the following section. In MS, analytes are ionised and are separated based on mass-to-charge ratios *(m/z)* using one of a variety of mass analysers and detected. Since electric or magnetic fields are used to resolve ions, the ions must be present in or converted to the gas phase. Amongst a range of applications, MS can be used to

determine molecular mass, to elucidate the chemical structure, quantification and to determine elemental composition [25].

Fig. 1.12 demonstrates a general schematic of a mass spectrometer, consisting of a sample inlet system, an ionisation source , a mass analyser , a detector and a data system [24]. The function of each component is illustrated below.

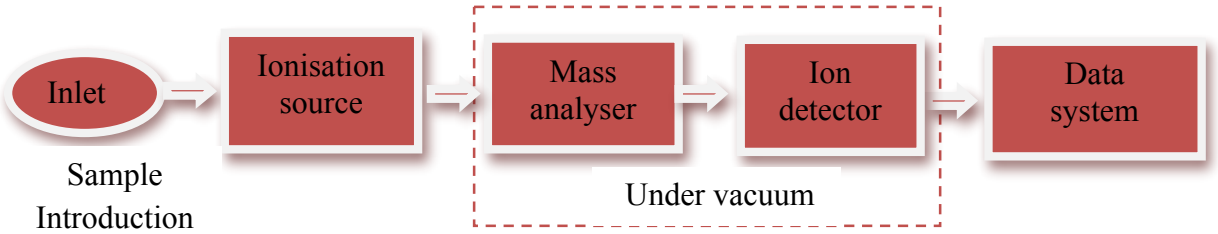

Figure 1-12: A schematic of MS.

1.5.1. HPLC-MS interface

A major focus has been directed towards the interface between HPLC and MS. The reason for this focus was due to the challenges of the coupling including HPLC which employs high pressures for separation, with a high associated gas load. MS, on the other hand, requires a vacuum and a limited gas load. For instance, a typical HPLC flow rate is 1 ml/min, which, when converted to vapour at atmospheric pressure, produces around 11000 ml/min; far higher than the 1 ml/min vapour load which MS can accommodate and handle [26]. Additionally, HPLC usually runs at ambient temperature, whereas MS requires an elevated temperature. Moreover, HPLC can utilise volatile and non-volatile buffers as mobile phase additives, whereas MS is only amenable to volatile buffers [26] , as will be reasoned in Table 1.2 below. Therefore, various approaches to couple HPLC to MS have been developed in order to overcome these issues. This includes particle beams (PB), moving belt/wire setups,

coupling with continuous flow fast atom bombardment (cf-FAB), direct liquid introduction or atmospheric pressure ionisation modes including electrospray ionisation (ESI), atmospheric pressure chemical ionisation (APCI) and atmospheric pressure photoionisation (APPI). [27]. These can be used in conjunction with flow splitting devices to reduce the rate of introduction of the eluent. For some interface techniques, there is a serious disadvantage to employing a splitting device, namely a reduction in sensitivity. The typical flow rate used with a classic 4.6 mm i.d. column is 1 ml/min, tolerable by techniques such as atmospheric pressure chemical ionization (APCI) and thermospray (TSP), negating the need for flow splitting in these cases. Electrospray (ESI), on the other hand, has a working range from 200 nl/min to 0.2 ml/min [27]. Additionally, the ESI signal is dependent on the concentration of sample as opposed to the amount injected, differing from other interface techniques (e.g. APCI, TSP). Consequently, ESI signals are virtually independent of flow rate, facilitating the use of splitters in order to decrease the amount of HPLC eluent introduced to MS without compromising sensitivity. This advantage has led to the utilisation of ESI in the area of HPLC miniaturisation; i.e. exploiting the use of capillary (300 μm i.d., 4 μL/min flow rates) and nano (75 μm i.d., 200–300 nL/min flow rate) dimensions [27]. The following section will provide a brief introduction on how some of these interfaces are coupled to the MS.

1.5.1.1. **Direct liquid introduction**

The first efforts to introduce HPLC eluent into MS using EI/CI sources centred on the reduction of the HPLC eluent via the use of a splitter or use of small i.d. columns. A vacuum system is used to remove the residual HPLC eluent leaving the analyte in the gas phase ready for ionisation. The maintenance of the vacuum is ensured via the use of a large pump system and differential pumping. In order to facilitate the evaporation of the HPLC eluent, a heated

desolvation chamber can also be used. Fig. 1.13 shows a schematic of a direct liquid introduction interface.

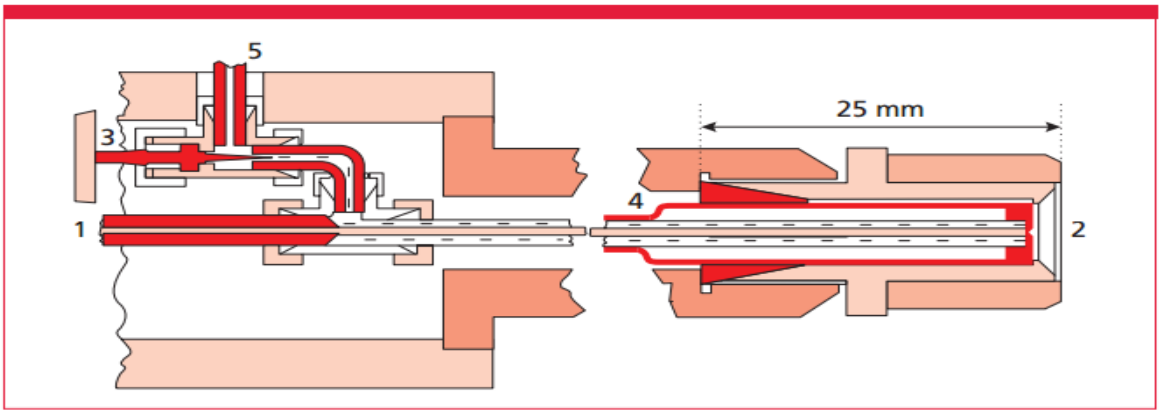

Figure 1-13: : Schematic of DLI. 1: Connection to HPLC column, 2: Diaphragm 5 µm opening to MS, 3: Needle valve, 4: Cooling region, 5: to UV detector or waste, adopted from [27].

1.5.1.2. Atmospheric pressure ionisation (API)

The aforementioned interfaces (DLI, moving belt/wire), although used for specific applications, have several operational issues, including limited sensitivity and lack of robustness [27].

The overwhelming rise in HPLC-MS applications is thought to be virtually due to the advent of sensitive and rugged API techniques. API terminology is used to describe all ionisation techniques by which ions are formed at atmospheric pressure. The main atmospheric pressure techniques are ESI and APCI [27].

In API interfaces, the ions are formed at atmospheric pressure and then transferred from the source to the vacuum of the analyser via one or more differentially pumped stages separated by skimmers. The application of appropriate electric fields directs and focuses the ions through the skimmer openings into the MS analyser [27]. For API interfaces, there are

various source designs, ion optic configurations, pumping systems, and other experimental nuances.

However, as shown in Fig.1.14 , some basic features are common to all API interfaces [28]. There are several advantages of API interfaces. As examples, APCI can accommodate the typical flow rate used in HPLC, whereas ESI is suitable for the analysis of polar, non-volatile, and thermally unstable compounds [27].

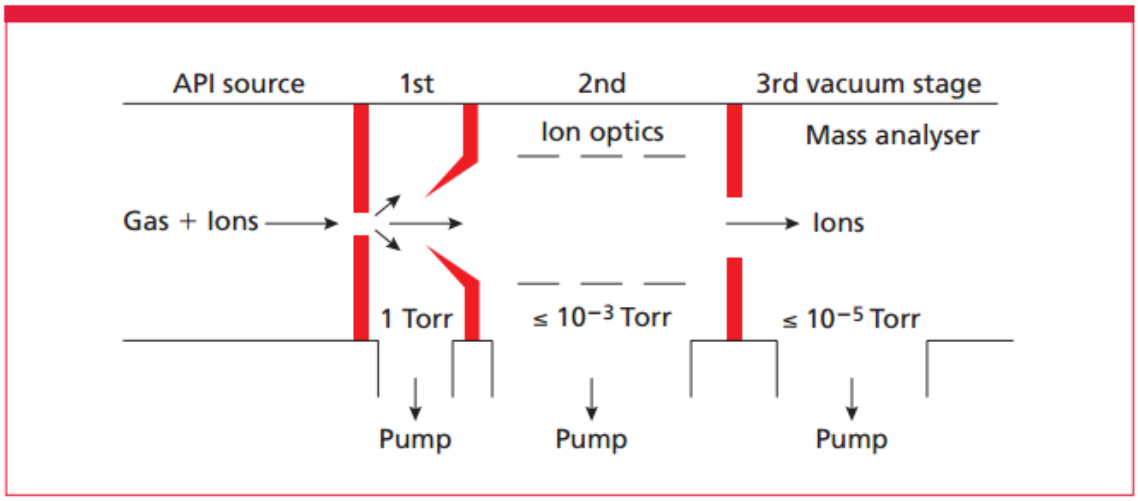

Figure 1-14: Overview of a differentially pumped API source coupled to a mass spectrometer, adopted from [27].

1.6. The Ionisation source

For many decades, readily available ionisation sources were limited to electron ionisation (EI) and chemical ionisation (CI). The EI technique is a hard ionisation, involving the use of high energy (70 eV), and leading to extensive fragmentations. This, in turn, yields detailed mass spectra which, when interpreted skillfully, can afford significant information regarding

the molecular structure and help elucidate the nature of the unknown sample. Compound identification is achieved via the direct comparison of the spectrum with mass spectral libraries recorded under the same MS conditions. In contrast, CI operates at lower energies (< 10 eV), leading to greater molecular preservation for improved determination of molecular mass.

Both EI and CI require high vacuum conditions for operation. [24]. [24]; work described in this thesis exclusively utilised ESI and this technique is discussed in detail below.

1.6.1.1. **Electrospray ionisation (ESI)**

ESI is a soft ionisation technique and was introduced by John Fenn in 1989 [29, 30]. The soft ionisation utilises a low energy, leading to little fragmentations. Molecular features, therefore, predominantly remain intact during the process [29]. ESI proved a major advance in coupling HPLC with MS and remains the most commonly used modern ionisation source, with a wide range of applications in small molecule analysis (e.g. metabolomics). Additionally, a key advantage of ESI is the ability to ionise very large macromolecules (e.g. proteins and lipids) and transfer them to the gaseous phase. Neutral compounds are converted to a charged form either in solution or in the gaseous phase by protonation or cationisation (in positive mode), or by deprotonation or anion adduction (in negative mode) [25]. Ionic analytes with pre-existing charges in solution are merely transferred to the gas phase, often leading to increased sensitivity to such components. As shown in Fig.1.15, ESI utilises nebulization and an electrical potential to help generate gaseous phase ions.

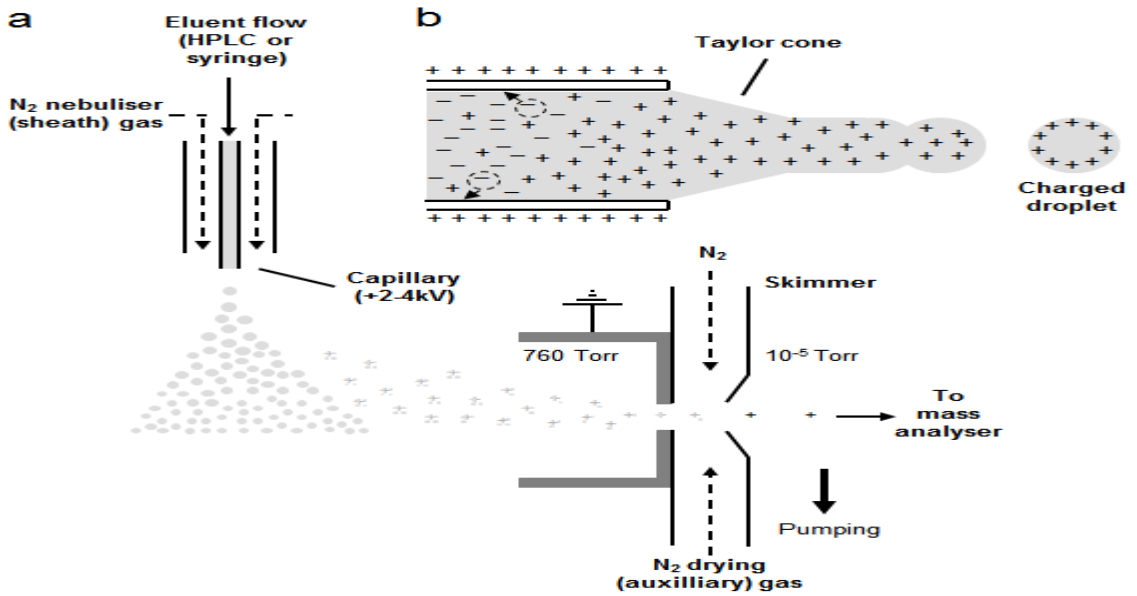

Figure 1-15: Illustration of an orthogonal ESI source, operated in positive ion mode, b) Magnification of the capillary tip, showing the formation of the spray, adopted from [31].

ESI is well-suited to analytes that are moderate to highly polarity, possess molecular weights up to 100,000 Dalton, and ionise in solution conceivably with multiple charges. Additionally, ESI favours the analytes of interest to be in the ionised form before being introduced to the API [32]. Examples of analytes that can carry charge in solution include molecules containing hetero-atoms, such as, 1,2 di-chloro benzene. These types of molecules can carry a proton in solution via the association with an unpaired electron. Another suitable type of analyte is the molecule that produces a charge via an inductive effect, for instance, azobenzene [32]. Other types of molecules are those capable of holding multiple charges, for example, proteins and peptides, with the multiple basic amino acid sites on these molecules when the correct pH is chosen [32].

There are two modes in ESI, as shown in Fig. 1,16, including positive and negative mode and based on the nature of the analyte of interest, the mode is selected. In positive mode, the capillary is the positive electrode (anode), and the sampling aperture is the negative electrode (cathode). The positive ions present in the HPLC eluent are repelled from the inner walls of the sprayer needle and as a result, the positive ions electrophoretically move into the body of the droplet formed at the capillary tip [32]. The mode induces the positive ions to cluster the sprayed droplet predominantly. Furthermore, the mode is employed with analytes forming cations in solution, for instance, bases. In negative mode, the reversed situation takes place in which the capillary is the negative electrode, and the sampling aperture is the positive electrode. Similarly, the mode induces the negative ions to cluster the sprayed droplet predominantly. Moreover, the mode is employed with analytes forming anions in solution, for instance, acids [32].

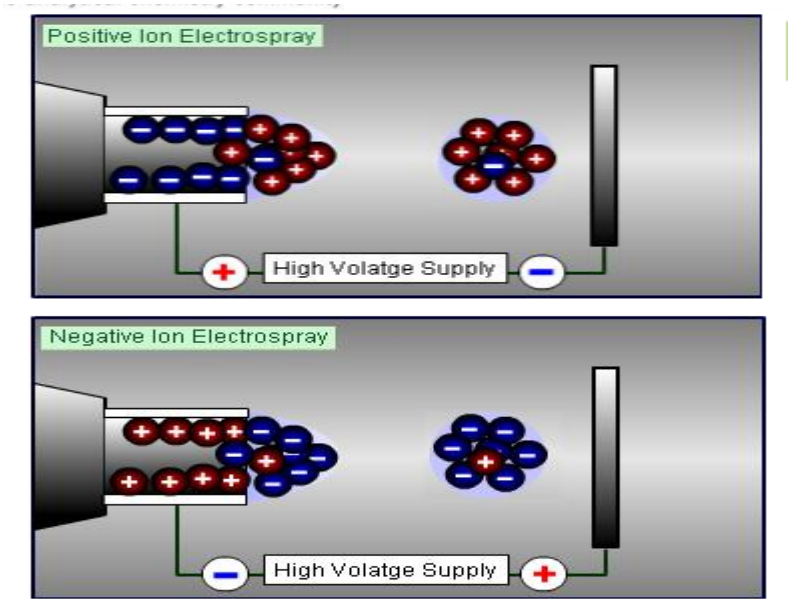

Figure 1-16: Schematic of Charged droplet formation at the capillary tip, adopted from [32].

In ESI, the transfer of charged species from solution into the gaseous phase proceeds via a series of discrete steps [25]. Firstly, a spray of highly charged droplets having the same polarity as the capillary voltage is formed at the sample capillary. The use of a nebulising gas, usually nitrogen, causes shearing around the eluent spray from the HPLC, leading to an enhanced sample flow rate. The droplets that are formed at the exit of the electrospray tip travel through a pressure and electrical potential gradient in the direction of the mass analyser. Using a second auxilliary stream of nitrogen and/or an elevated ESI-source temperature, the size of the charged droplets is reduced in a continuous manner through solvent evaporation. This results in an increase in surface density and a decrease in droplet radius. The electric field strength within the charged droplet ultimately reaches a point at which ions at the surface of the droplets have sufficient kinetic energy to be ejected into the gaseous phase; this phenomenon is called Columbic repulsion [29]. Subsequently, the ejected ions are focused via a sampling skimmer and accelerated into the mass analyser for separation [25].

1.6.1.2. Formation of gas- phase analyte ions from the charged droplets

There are two main mechanisms being proposed tackling the formation of gas-phase analyte ions from small highly charged ESI droplets. These mechanisms include charge residue model (CRM) [33] and ion evaporation model (IEM) [34].

1.6.1.2.1. Charge residue model

This mechanism was proposed by Dole and is based upon the droplets undergoing a series of solvent evaporation and Coulomb fissions [35]. Consequently, very small droplets are formed containing only analyte molecules. Desolvation of this droplet induces its charges (on the surface) to land on the analyte molecules.

The name of this mechanism comes from the fact that the residual droplet charge at the final stage of the desolvation in the ESI process is retained by the analyte molecule in the gas phase [35]. Another study supporting this mechanism was conducted by Schmelzeisen-Redeker et al. [36]. Fig 1.17 below is an illustration of this proposed mechanism

Figure 1-17: Illustration of Charge residue model, adopted from [32].

1.6.1.2.2. Ion evaporation model

This mechanism was proposed by Iribarne and Thomson. They proposed that below a droplet radius of 10 nm, an ion is capable of evaporating from within the droplets [34, 37]. Iribarne and Thomson based their hypothesis on the ion mobility studies that illustrate the production of the huge amount of gas phase ions at times when the majority of the charged droplets are expected to possess multiple charges and to some extent large radii [32]. The ion mobility studies demonstrate highly mobile gas phase that was identified spectroscopically as ion-solvent cluster molecules of the type $M^+ (H_2O)_{n,}$ where n=3-7 and M is the analyte species.

It is thought that this mechanism is the most widely accepted for the formation of gas- phase analyte ions from the charged droplets [32]. Fig.1.18 illustrates the ion evaporation model.

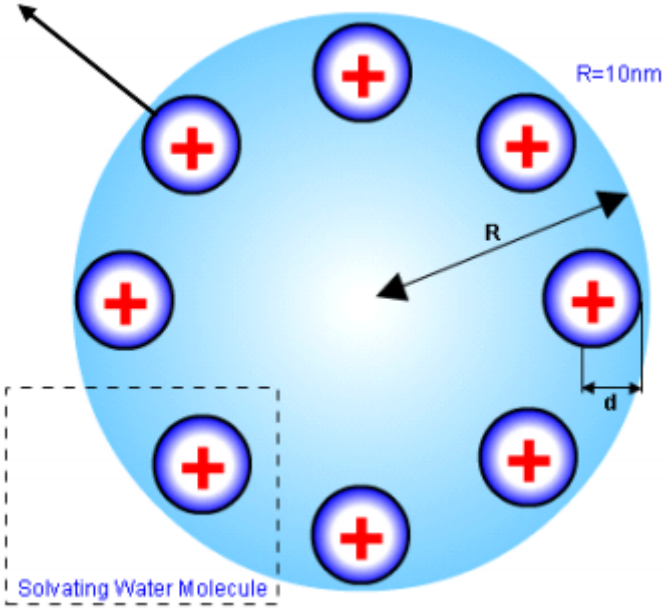

Figure 1-18: Schematic of IEM, adopted from [32].

1.6.2. **Mass analyser**

The role of a mass analyser is to separate ions based on their *m/z*. Several mass analysers have been employed with HPLC including quadrupole, time of flight (T.O.F), orbitrap, and ion trap analysers. For the research described in this thesis, only the ion trap analyser was employed and is discussed in further detail.

In the 1960s, the first mode of ion trap operation allowed the stabilisation of ions of a single *m/z* within a 3D evacuated environment. Two decades later, an alternative mode, mass instability mode, was introduced by Stafford [31]. In this mode, ions possessing different *m/z* are trapped simultaneously before being ejected sequentially [31].

As shown in Fig. 1.19, the ion trap is comprised of three hyperbolic electrodes, two of which are curved end caps placed in opposition to each other at a distance of $2z_0$. The other electrode is a ring electrode, oriented at a 90° angle to the end caps. One of the end caps possesses an inlet aperture which permits ions to enter the trap, whereas the other end cap possesses many small perforations permitting ions to leave the trap and ultimately travel to the detector [31].

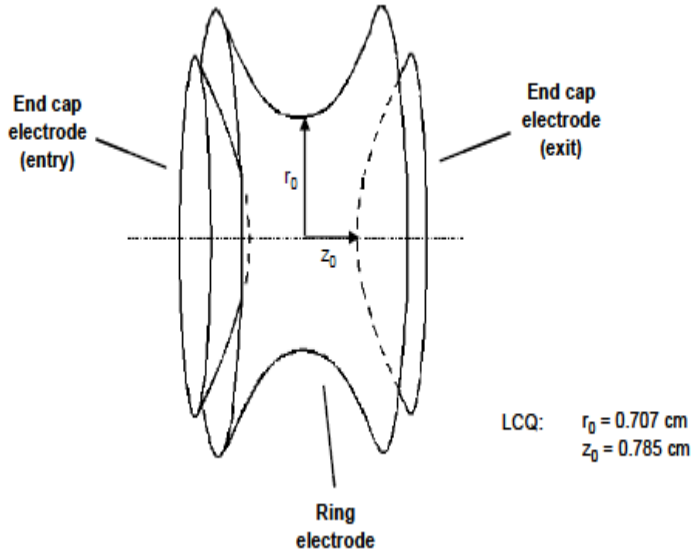

Figure 1-19: Ion trap analyser, reproduced with permission [31].

During operation, an oscillating potential at radio frequency is applied to the ring electrode, while the end cap electrodes are grounded. This results in the creation of a quadrupolar field within the trap [31]. Ions entering this field undergo oscillatory motion at a frequency distinctive to each *m/z*. Ions oscillating with stable trajectories are stored in the trap, while unstable ions are ejected via the end-cap electrodes. Through ramping of the potential of the ring electrode, plus the addition of a small supplementary oscillating potential to the end cap electrodes, ions are purposefully ejected and subsequently transmitted to a detector, generating a mass spectrum [31].

1.6.3. **Considerations for HPLC-MS hyphenation**

Analyte ionisation and the formation of a stable MS spray can be influenced by several factors including instrument hardware or design, analyte characteristics, and the chromatographic conditions (e.g. solvent, temperature) via which the analyte is introduced into the MS [24]. Consideration of such factors is key to effective experimental design.

1.6.3.1. **Mobile phase compositions**

The solvent used to introduce analytes into the MS source can have major influences on the ionisation behavior of the analytes. Ionisation tends to increase as the concentration of organic solvent in the mobile phase increases due to characteristics such as reduced viscosity, conductivity and surface tension [24]. However, in order to obtain an acceptable chromatographic separation, particular for charged molecules or basic analytes, HPLC methods frequently use buffers or ion pairing agents. Some of these mobile phase additives are not compatible with MS, due to low volatilities, signal suppression and/or long term negative impacts on the spectrometer. Table 1.3 lists the compatibility of various mobile-phase agents with MS. Notably, even the use of a compatible buffer can produce surface-active electrolytes, which will compete with the target analyte and ultimately cause ion suppression and loss of sensitivity [24].

Table 1-3: Buffers compatibility with MS.

Buffer and additive	Compatibility with MS	Comments
Phosphates	NO	Non-volatile, can deposit on lens elements causing reduced sensitivity
Inorganic acids (e.g. HCl, H_2SO_4)	NO	Damage the source components
Ammonium acetate	YES	Volatile
Citrates	NO	Non-volatile
Trifluoroacetic acid (TFA) (0.1%)	YES	Higher concentrations lead to deposit on the cones or the ion source, causing damage. Also, Ion suppression problem
Phosphoric acid (0.1%)	NO	Deposit on the cones or the ion source causing damage
Surfactants (e.g. Triton-x 100)	NO	Cause ion suppression and coating of ion optics.
Ammonium formate	YES	Volatile
Ammonium bicarbonate	YES	Volatile

1.6.3.2. **Ion suppression**

When choosing a method, it is important to assess and quantify the sample matrix effects. The matrix has the potential to suppress or enhance ionisation. This consideration is particularly important when dealing with bio-fluid samples such as urine, serum or plasma. Likewise, determination of how the matrix affects the MS signal is vital when optimising a chromatographic method for HPLC-MS in which quantification is required [24]. When matrix effects are identified, they can often be reduced and in some cases eliminated using common sample pre-treatments such as liquid-liquid extraction (LLE) or solid phase extraction (SPE). When sensitivity is not of importance, either a direct sample dilution and injection approach or centrifugation and injection approach can be employed without concern [24].

1.7. The rate theory of chromatography

This theory, also known as the van Deemter concept, investigates the parameters leading to the band broadening phenomenon during the chromatographic procedure. The degree of band broadening can either be due to the column itself or extra-column sources including the injector, connection tubing and detector [38].

The van Deemter equation takes into account the factors resulting in band broadening and represents them in relation to HETP on the linear velocity of the mobile phase. The linear velocity is calculated using equation 1.9 below.

$$\mu = \frac{\mathbf{L\,(mm)}}{\mathbf{to(sec)}} \qquad 1.9$$

Where μ is the linear velocity, L is the length of the column, and to is the retention time of un-retained molecule.

1.7.1. van Deemter equation

This is described as the dependence of HETP upon the linear velocity of the mobile phase, as observed in equation 1.10 below.

$$\mathbf{HETP = A + \frac{B}{u} + cu} \qquad 1.10$$

Where the A term represents the eddy diffusion, the B term represents the axial diffusion of the solute in the mobile phase, while the C term is referred to as the resistance to mass transfer in the mobile and stationary phases, and u is the linear velocity of the mobile phase [38].

1.7.1.1. **Eddy diffusion (A)**

The band broadening effect stems from the fact that the analyte molecules take different pathways when travelling through a packed column. These different pathways lead to band broadening [38], as observed in Fig 1.120.

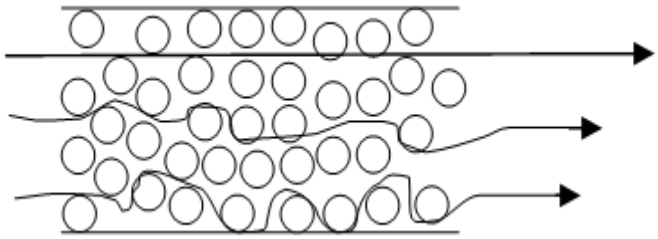

Figure 1-20: Demonstration of Eddy diffusion.

The eddy diffusion is dependent on particle size, the distribution of inter-particle channels and bad uniformities in the packing, as illustrated in equation 1.11 below.

$$\mathbf{A = 2\gamma d_p} \qquad 1.11$$

Where d_p is the particle size and γ is the packing coefficient.

As can be seen from the equation above, eddy diffusion is directly proportional to the particle diameter: the smaller the particle diameter is, the lower the value of A is and, as a result, the band broadening effect is reduced [38].

1.7.1.2. **Axial diffusion (B)**

This originates from the longitudinal diffusion of an analyte in the mobile phase through the column axis resulting in the band broadening effect [38]. The degree of axial diffusion is subject to two factors including the time spent by the analyte in the column and the diffusion coefficient of the molecule in the mobile phase, as illustrated in equation 1.12. The negative impact of this factor can be observed greatly when the analyte remains inside the column for a long time [38], as seen in Fig 1.21.

$$\frac{\mathbf{B}}{\mathbf{u}} = \frac{\mathbf{2\gamma D_m}}{\mathbf{u}} \qquad 1.12$$

Where D_M is the diffusion coefficient, γ is the factor concerned with diffusion restriction by column packing.

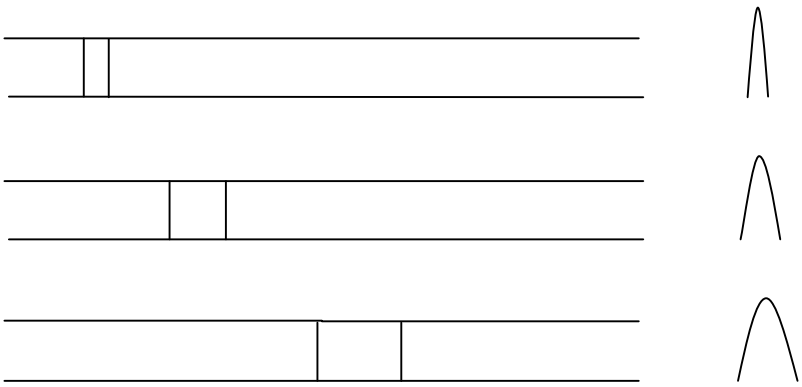

Figure 1-21: Illustration of axial diffusion.

1.7.1.3. **Resistance to mass transfer (C)**

This is thought to be the most important parameter affecting the efficiency of a column. It can be divided into the resistance to mass transfer of an analyte in the mobile and stationary phases [24].

While the sample components travel through a packed column, the sample is in continuous equilibrium between the two phases. Any delay or negative impact on the equilibrium will result in the effect of band broadening, as observed in equation 1.13.

$$\mathbf{Cu} = \frac{\boldsymbol{\gamma u d_p^2}}{\mathbf{D_m}} \qquad 1.13$$

Stationary phase mass transfer effects originates from the difference in the diffusion of an analyte into the phase which results in delaying the time of the analyte returning back to the mobile phase. That is, molecules that diffuse deeper into the stationary phase will need a longer time than those just on the surface to return back to the mobile phase and as a result, this difference leads to the effect of band broadening [24, 38].

1.7.1.4. **Factors affecting van Deemter curve**

The Fig.1.22 illustrates a typical van Deemter curve at the point by which the total dispersion from the factors (A, B, and C) leading to band broadening issue giving rise to the lowest HETP value and as a result, the best linear velocity which ultimately results in obtaining the best efficiency.

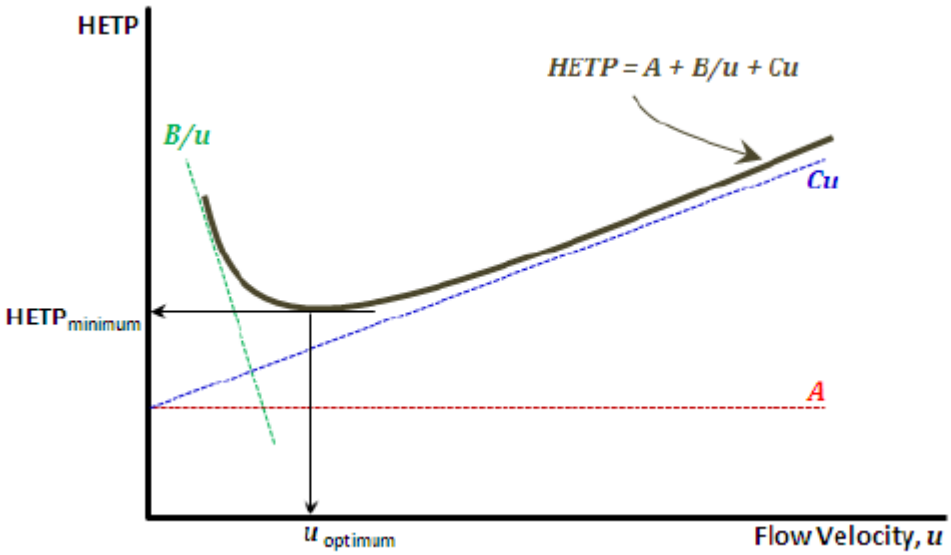

Figure 1-22: van Deemter curve illustrating the contribution of the factors leading to band broadening phenomena, adopted from [16].

The need to reduce the effects of the factors relating to the van Deemter equation, namely eddy diffusion, axial diffusion, and resistance to mass transfer, has resulted in a variety of solutions to overcome band broadening. One solution is decreasing the diameter of the packed particles, the effect of which is shown in Fig. 1.23. However, this approach leads to a decrease in the permeability of the packed columns observed by an increase in back pressure. This consequently results in the application of a lower flow rate resulting in longer analysis times. It could also be seen from Fig.1.23 that smaller particles result in higher efficiency and thus this relation between the particle size and efficiency is the driving force for the relatively recent reductions in column particle diameter and the introduction of Ultra-High performance Liquid Chromatography (UHPLC) [24].

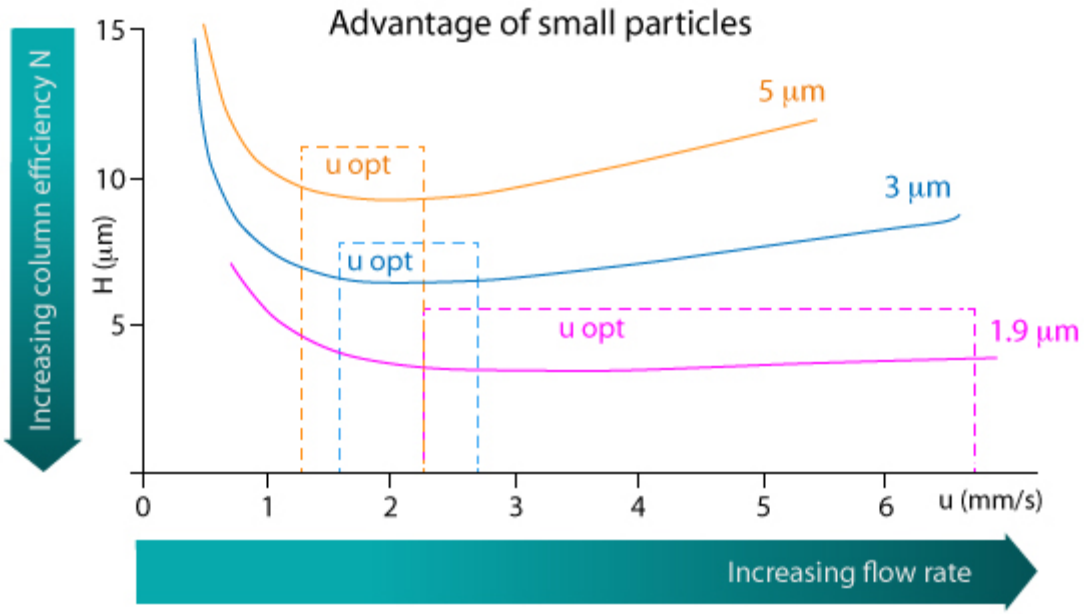

Figure 1-23: Particle size effects, adopted from [39].

1.7.2. **The Knox equation**

Giddings was the pioneer in proposing the dimensionless factors so as to tackle band broadening owing to the relationship between diffusive and convective velocities [40, 41]. These relate to the velocities along the column and the relative to the packing particle diameter. Equations 1.14 and 1.15 are the reduced plate height (h) and linear velocity (v) parameters illustrated as a function of general plate height (H), linear velocity (µ), diffusing coefficient (D_m), and particle diameter (d_p) [41].

$$\textbf{Reduced linear velocity} = \mu\, d_p / D_m \qquad 1.14$$

$$\textbf{Reduced plate height} = H / d_p \qquad 1.15$$

Knox then developed the idea further to make a comparison between different stationary phases in terms of their performances for HPLC. Knox's development is useful if the particle sizes of the columns compared are different but these columns possess the same substrate silica [41]. Equation 1.16 illustrates the Knox equation [42].

$$\mathbf{H \bullet B/v + A v^{1/3} + C v} \qquad 1.16$$

Similar to the van Deemter equation, there are three components to the Knox equation, but they show the dispersion in the packed bed in relation to the bed's structure or packing quality. The A-term is usually used as an indication, or a measure of the packing quality and its contribution to h is around 1. However, the A term has no influence on the gradient of the Knox curve. The B-term demonstrates the axial molecular diffusion, and its usual contribution to h is 2-4. The C-term illustrates slow equilibration in the column bed, and its contribution to h is always 0.1. It is thought that around 2 for the reduced plate height is an indication for a well packed column [41].

There are drawbacks in using Knox's equation, as there is a dependence on the value employed for the determination of diffusion coefficient and the mean particle diameter. As proposed by Jorgenson et al. [43]., diffusion coefficients are usually predicated via the Wilke-Chang equation employing either capillary time-of-flight (CTOF) or Aris-Taylor open tubular method. The particle size distribution is primarily determined using either scanning electron microscopy (SEM) or transmission electron microscopy (TEM) [44].

1.7.3. **Kinetic performance plots**

With the development of stationary phases, particle size and particle shape, there has been an increased interest in comparing different formats with one another. Although the van Deemter curve is fruitful for such comparison for the same particle diameter, the plot, unfortunately, does not consider the permeability, the pressure drop, or the time taken to appreciate a given number of theoretical plates (N) [24]. The kinetic plot, as a result, has become a very popular approach in which different columns can be compared. The very basic Kinetic plot of N *vs.* analysis time was proposed by Giddings in 1965 [45]. The plot was used to provide an explanation for column performance and attain information on the compromise between the plate number and the analysis time that can be obtained for a given particle size and pressure limit. Fig. 1.24 illustrates an example for kinetic plots for different particle sizes. As seen in the Fig 1.24, for a short analysis time, the particle size 2.5 µm performs better than the other particle sizes (3.5 and 5 µm). Whereas, with longer analysis times, the particle size 5 µm performs the best. This behaviour can be interpreted by the fact that for large particles (5 µm) the diffusion controlled section for the plot is reached at a longer analysis time than for small particles (2.5 µm) [24].

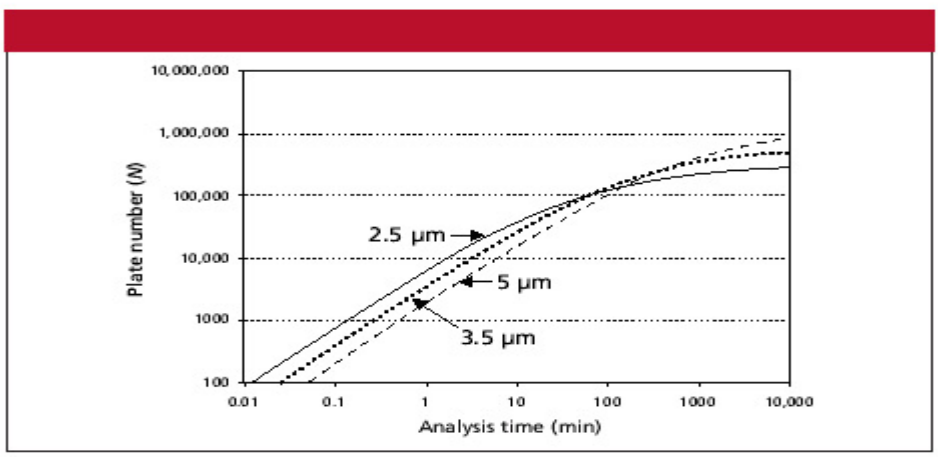

Figure 1-24: Kinetic plot of plate number vs. analysis time for 2.5, 3.5, and 5 µm particles, adopted from [46].

This basic plot by Giddings was then modified by Poppe who coined the concept of plate time. This concept is to calculate the time needed to generate one theoretical plate [47]. The t_R vs. N can be converted readily into a Poppe plot via firstly inverting the axis in order to give N in the x-axis and the analysis time in the y-axis. In addition, the analysis time is changed to the retention time of an un-retained molecule (t_0) (column dead time) [24], as shown in Fig. 1.25.

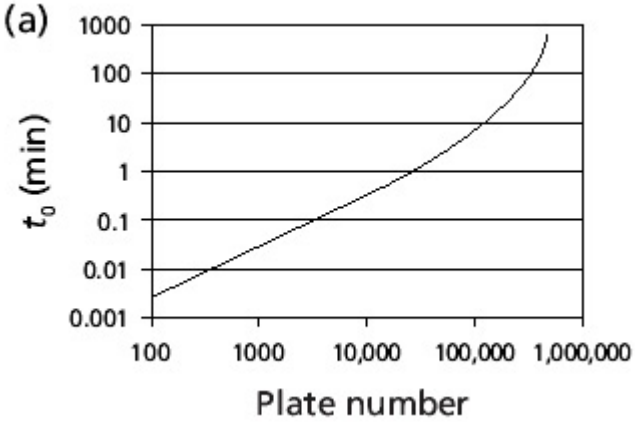

Figure 1-25: Kinetic plot of column dead time vs. plate number for 2.5 µm particles, adopted from [46]

Poppe's plot is usually employed to compare column performance under different chromatographic conditions. Furthermore, dividing t_0 by N and then plotting it versus N gives the classical Poppe plot illustrating the maximum N for a given particle size, as shown in Fig. 1.26.

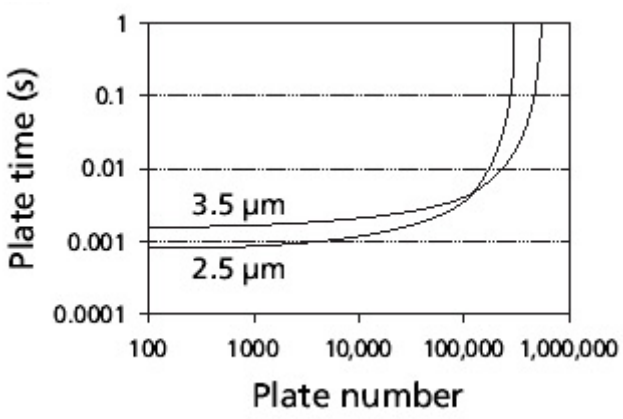

Figure 1-26: Poppe's kinetic plot plate time vs. plate number for 2.5 and 3.5 µm particles, adopted from [46].

Although Poppe's plot provides useful information, it does not take into account a relationship between the back pressure needed for operating a column and the column dead time. Due to this drawback, it would be difficult to compare particles of different porosities [24]. Consequently, Desmet et al. managed to further expand Poppe's plot via employing separation impedance (E), which was originally proposed by Bristow and Knox, as a tool for assessing column performance [42]. Desmet's expansion was to generate a host of kinetic plots. The t_0 plot suffers from a condensed y-axis which makes it challenging to read easily. Therefore, in order to maximise the view of the y-axis, t_0 could be divided by N^2 which then makes the plot $t_{0/} N^2$ *vs.* N, as illustrated in Fig. 1.27. Furthermore, Desmet and his co-workers inverted the N axis of the plot so that it looks like the van Deemter curve [24, 48].

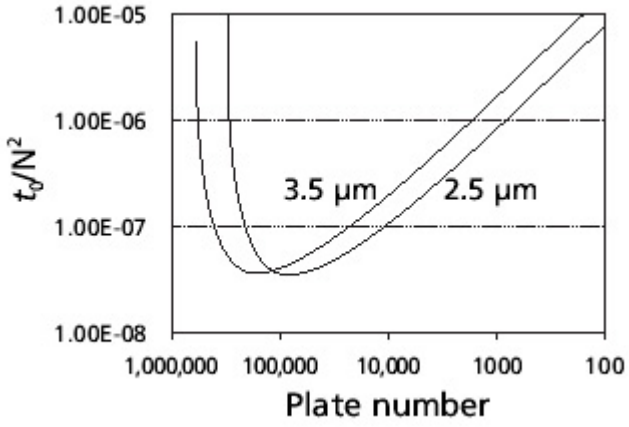

Figure 1-27: Desmet's kinetic plot demonstrating the comparison between 2.5 and 3.5 µm particles, adopted from[46].

1.7.4. **Extra-column Effects**

In addition to band broadening originating from on-column effects, there are other factors known as extra-column effects that can severely affect the performance of a chromatographic separation. The extra-column effects can arise from factors including injector design, tube connections for the whole system, and detector design. These effects are more noticeable when the internal diameter (i.d.) of the column is less than 2.1 mm, and the particle size is less than 3 µm [24].

1.8. Monolithic columns

Over the past decades, great interest has been directed towards HPLC owing to its rapid development in various applications, including the life sciences, the pharmaceutical industry, and the environmental sciences. However, due to the inherent limitations of conventional packed columns including slow mass transfer and the large void volumes, these ultimately lead to a negative impact on efficiency [49]. When Capillary Electro Chromatography (CEC) surfaced in the late 1980's, significant technical difficulties arose when packing capillaries with very small internal diameters using small diameter particles as packing such capillaries requires a high level of technical experience. In addition, when using CEC, significant difficulties arise in making retaining frits (used to hold the packing material within a column). However, there are now various approaches being used to overcome the problem of frit manufacturing some of which are packing the column with silica particles before the initiation of sol-gel or sintering particles to consolidate the packed bed [50-52].

There has been a trend over the past two decades towards the reduction of column dimension in HPLC so as to benefit from several advantages. These advantages include reduced solvent consumption and disposal, increased sensitivity, lower diffusion, and the straightforwardness of hyphenation to MS. This tendency of the miniaturisation process has accelerated since the dawn of the proteomics era, and the subsequent need for higher sensitivities with lower sample volumes and larger sample numbers. With increasing demand for high throughput and highly efficient methods, HPLC practitioners began to use shorter columns with lower particles size while increasing the flow rate of the mobile phase, as mentioned previously (section 1.7.1.3). However, operating under these conditions resulted in the generation of high back pressure [53], as shown previously in Fig. 1.123. This required the development of a new generation of UHPLC instruments that were designed to operate at significantly higher back pressures compared with the conventional HPLC systems.

Additionally, researchers began to embrace the alternative approaches to stationary phase design which could address the problem of low permeability and less efficient mass transfer (further details are provided in Fig.1.28). One of these alternative column designs is now known as a monolith and is described in detail below.

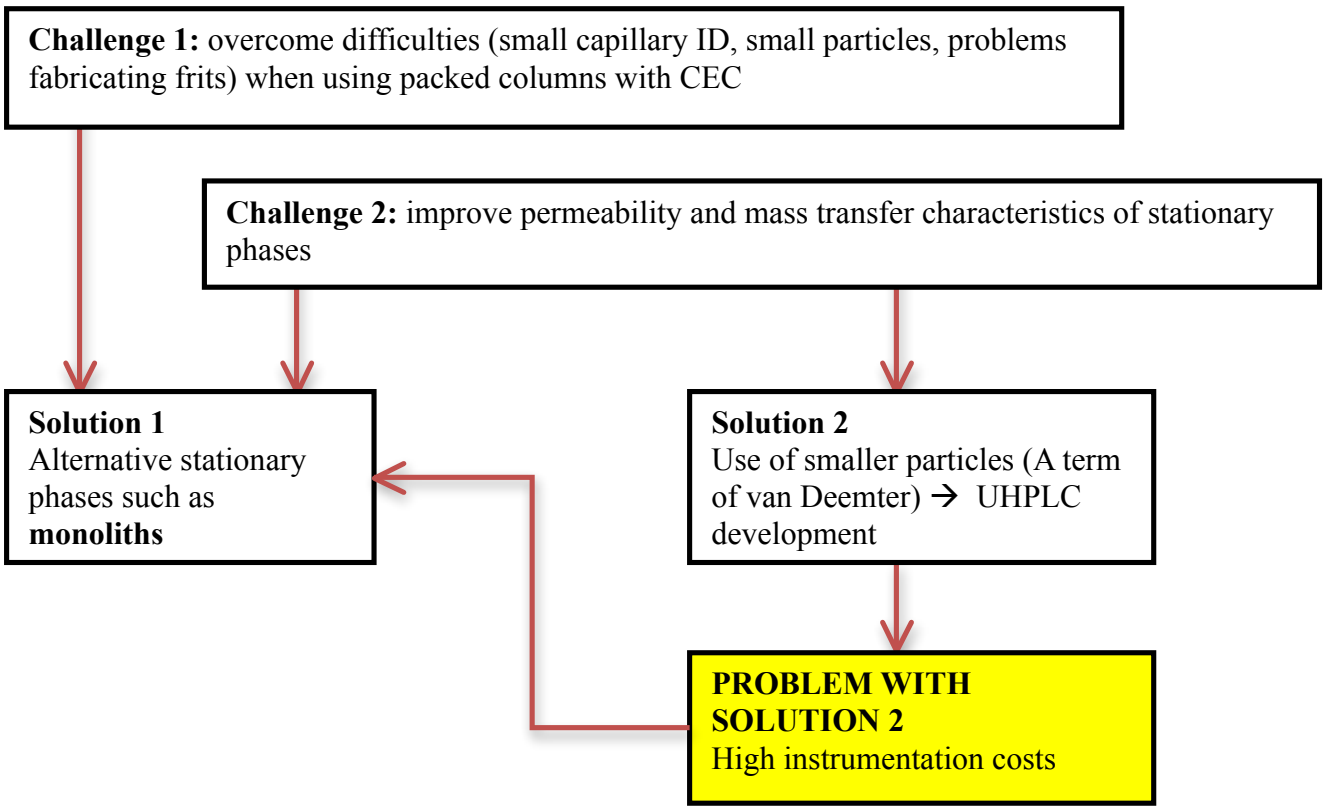

Figure 1-28: Motives led to the development of new material (known as monoliths).

Monoliths comprise of a single rigid piece of a porous material possessing a unique bimodal pore structure distribution (its structure bed is illustrated in Fig 1.29). The µm-sized (> 50 nm) through-pores are known as macropores and nm-sized (2-50 nm) pores [54, 55]. Macropores improve the column porosity and therefore reduce the analysis time through the application of high flow rates, whereas mesopores form the fine porous structure and afford a large active surface area to the interacting analytes, so leading to high efficiency and chromatographic interaction [56].

Furthermore, monolithic stationary phases have gained noticeable interest in all domains of chromatographic techniques, and it has become widely accepted that monoliths can be used as separation media for all types of chromatographic separation modes for the analysis of both small and large molecules [54].

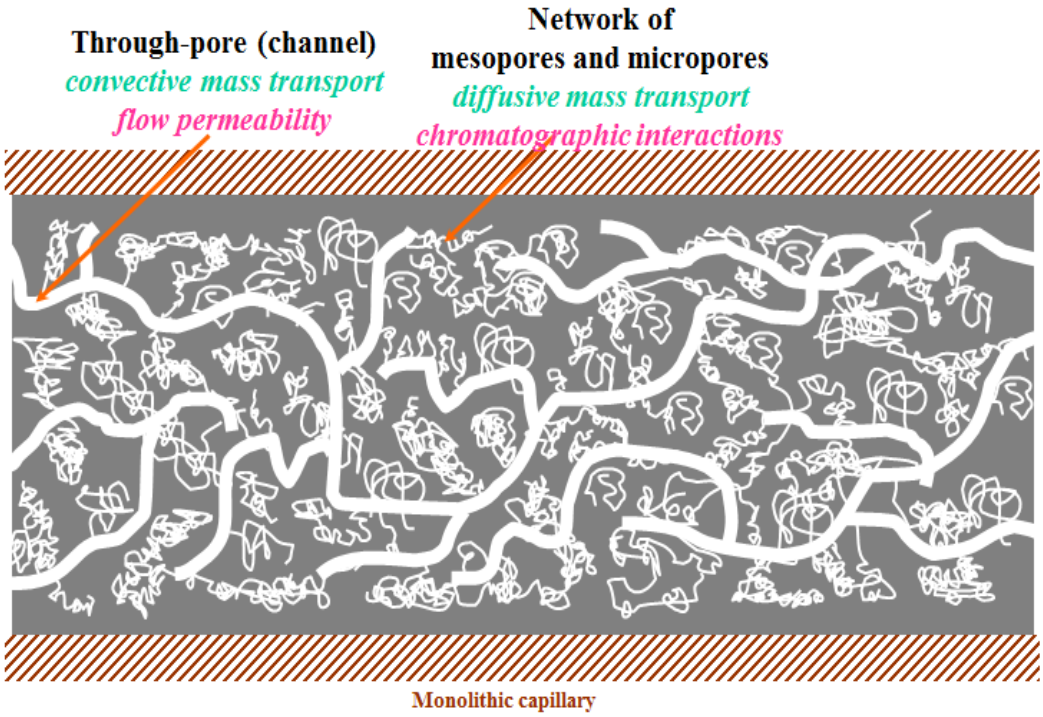

Figure 1-29: Structural features of monolith bed, reproduced with permission [6].

How is permeability enhanced?

Monolithic columns are continuous interconnected networks with large through-pore channels. This structure, therefore, leads to a decrease in the diffusion path and affords high permeability which results in obtaining good separation efficiency [50]. Additionally, the core structure improves the mechanical strength of the material, and the large through-pores channels are characterised by very low flow resistance. This combination of mechanical stability and low flow rate resistance permits the use of smaller diameter monolithic columns with relatively high flow-rates, so leading to simultaneous improvement in sensitivity and throughput [50].

How is mass transfer improved?

Since monoliths consist of a single piece bed, with interconnecting channels through which the mobile phase flow. Such structures, therefore, do not contain interparticle void volumes seen in particle columns channels, and thus the monolith occupies the whole column. This, as a result, leads to the elimination of any of the interparticle void volume, thereby improving the mass transfer kinetics of the analyte of interest between the mobile and stationary phases. This results in the whole mobile phase travelling through the monolith, consequently improving the efficiency of the separation, unlike in particle columns where the mobile phase travels in between the particles [50].

Various approaches led to the development of the current approach used for monoliths fabrication:

It is thought that Kubin *et al.* pioneered monolith synthesis in the late 1960s when they synthesised a swollen poly (2-hydroxyethyl methacrylate) material for SEC in order to resolve proteins under low pressure. However, due to the issue of low permeability, the prepared monolith could not be used for the analysis [57]. Another attempt was made by Ross to prepare monolithic open-pore polyurethane for HPLC and GC. Although the permeability was adequate, the monoliths were reported to suffer from swelling and softening when certain solvents were used, which limited their use for further applications [58]. In the 1980s, other approaches to monolith fabrication emerged which included rolled woven matrices [59], stacked membranes [60], rolled cellulose sheets [61], and macroporous disks [62]. In addition, it was reported that a compressed soft poly(acrylamide) gel was the first successful continuous bed to be employed in separation science [63].

In the 1990s, a completely new class of continuous bed consisting of rigid macroporous polymers were synthesised by a straightforward procedure introduced by Svec and Fréchet. Owing to their unique properties, these types of material have become the industry standard for monolithic columns, and have been used for various applications [64]. In 1996, a silica based monolith was introduced following scientific research by N. Tanaka [65]; these materials have been extensively reviewed elsewhere [66].

The unique structures of monoliths possess several advantages over conventional packed columns including fast mass transfer and high permeability. These features lead to high separation efficiencies and fast separations. Moreover, a wide variety of functional starting materials (monomers and cross-linkers) can be utilised enabling the preparation of monoliths for a specific mode of separation (RPHPLC, HILIC). Furthermore, the porogenic solvent can be chosen to match its polarity to the type of monolith to be synthesized [67]. Additionally, the fabrication of monolithic columns in capillary formats has facilitated the direct coupling of micro-HPLC with MS, as will be shown in Chapter **5** [50].

1.8.1. **Types of monolithic columns**

There are two main types of monolithic column, organic based monoliths and silica based monoliths. Since this project only deals with organic based monoliths, the latter will, therefore, be excluded in the discussion.

1.8.2. **Preparation of organic monoliths**

There are four main steps involved in synthesising a monolithic column including pre-treatment of the fused silica capillary followed by the introduction of the polymerisation mixture into the pre-treated fused silica capillary [56]. Then, commencing the polymerisation process either thermally or photochemically followed by washing out un-reacted monomers and porogens using organic solvents. More insight into the prepartion of monoliths with some care and hints will be described in the following Chapter, while a simplified process for the preparation of a monolith is illustrated in Fig 1.30.

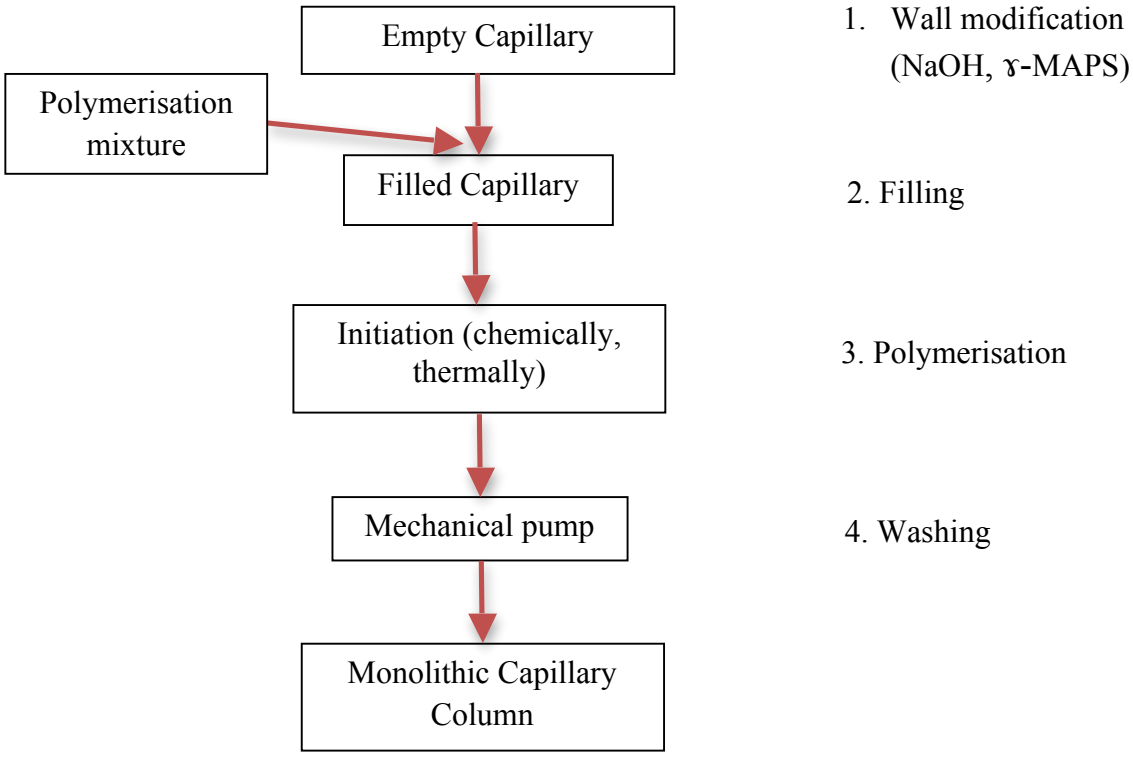

Figure1-30: A simplified illustration of the synthesis in a monolithic column.

The function of each component of the polymerisation mixture used to form the monolith is illustrated in Table 1.4. Polymethacrylate, polystyrenes, and polyacrylamides based materials are among the most reported monoliths used at present [68].

Table 1-4: Role of each component in polymerisation mixture.

Component	The role
Monomers	Characterisation of the stationary phase (mode of the chromatography)
Cross-linker	Its amount determines the porosity and rigidity
Macro-Porogen	Creating external (macro) pores in the monolith
Meso-porogen	Creating internal (micro) pores in the monolith

Fig.1.31 shows some of the more common monomers and cross-linkers used for monolith synthesis. These display important structural features, for example, the monomer 2-methacryloyloxy ethyl-trimethyl ammonium methylsulphate (METAM) possesses a quaternary amine group which can provide a positive charge acting as an anion exchanger. Additionally, chemical functionalisation of the monomer is occasionally required in order to utilise and obtain a better selectivity via a chemical modification of the surface of the monolith; in such cases, glycol methacrylate (GMA) is often used as it contains reactive epoxy group [69], as will be shown in Chapter **6**.

Monomers

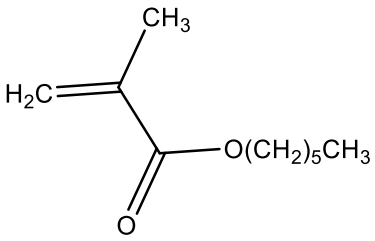

Hexyl methacrylate (HMA)

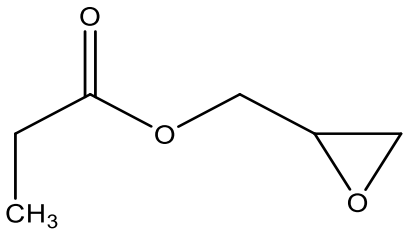

Glycol methacrylate (GMA)

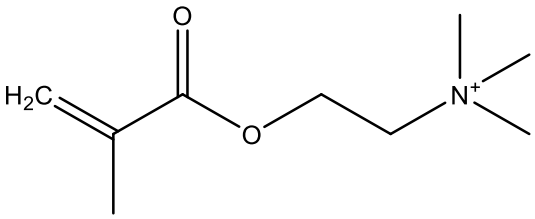

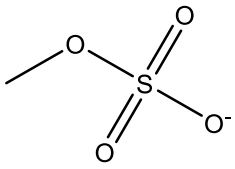

2-(methacryloyloxy) ethyl-trimethyl ammonium methylsulphate (METAM)

Crosslinkers

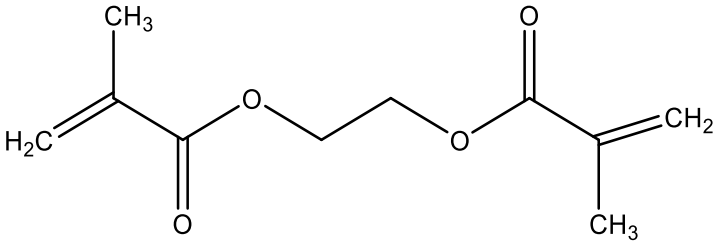

Ethylene dimethacrylate (EDMA)

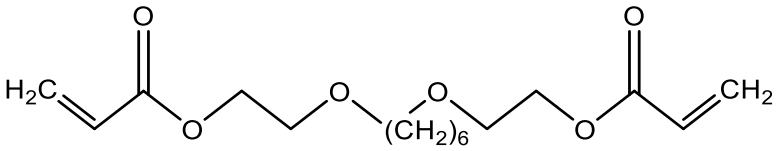

1,6-hexanediol ethoxylate diacrylate (1,6-HEDA)

Figure 1-31: Some examples of monomers and crosslinkers.

1.8.3. **The polymerisation process**

There are different types of polymerisation that can be employed to initiate the polymerisation process. The type of polymerisation used in this project is a free radical polymerisation. The free radical polymerisation involves three kinetic steps, initiation, propagation, and termination, as illustrated in Fig.1.32. The initiation step starts when the initiator molecule has sufficient energy to take apart the molecule forming free radical molecules, which become very reactive. Then, the free radical molecules react with one monomer, for example, $CH_2=CH_2$. This reaction will lead to the formation of a new a new free radical via the breaking of the double bond. This new fee radical will again react with a new monomer and the same process takes place (breaking the double bond) forming a new free radical. This process continues to take place and is responsible for forming the polymer chain. This process is called the propagation step. The propagation step comes to an end when either all monomers become polymerised or by quenching (stop the reaction). The final step starts, when one polymer chain containing the free radical meets another polymer chain also containing a free radical forming the complete polymer chain. [6].

Step 1: Initiation

I (initiator) → I• + I•

Step 2: Propagation

I• + M (monomer) → I–M•

I–M• + M → I–M–M• (or a propagating chain P_n•)

Step 3: Termination

(a) P_1• + P_2• → P

(b) P_1• + P_2• → P_1 + P_2

Figure 1-32: Schematic flow of a conventional free radical polymerisation, adopted from [16].

1.8.3.1. **Pore formation in monolith**

Understanding the process of pore formation is vital to understand the process which leads ultimately to an efficient monolith. As mentioned earlier, the monolith consists of a solid skeleton of the polymer possessing small pores named as internal-pores combined with large through-pores named as external pores that are empty spaces between porons (the continuous bed, i.e., the monolith itself). The internal pores offer retention and selectivity, whereas the external pores are responsible for allowing mobile phase to travel through the whole monolith, shown previously in Fig.1.29. For the sake of chromatography, the relative concentration of the internal and external pores is significant so as to obtain high efficiency and fast separation [6]. Pores formation within monoliths occurs into two steps which are nucleation and phase separation, as illustrated in Fig. 1.33 below.

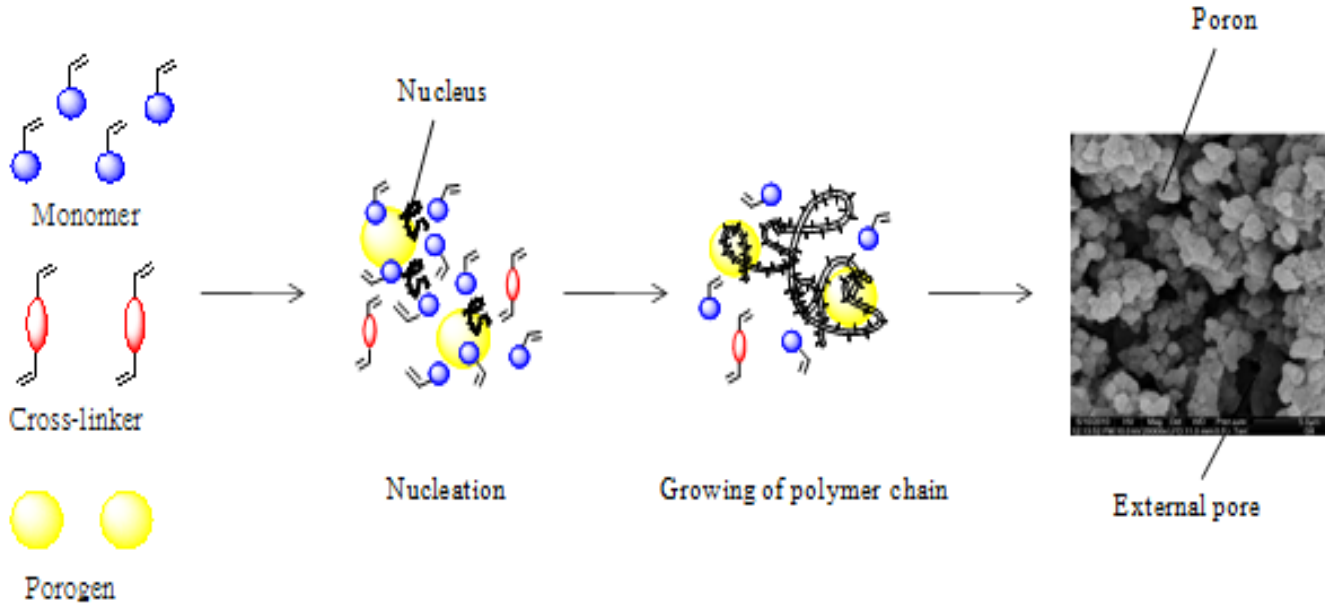

Figure 1-33: Formation of monolith's pores, reproduced with permission [6].

The nucleation is the commencement of the formation of nuclei of the polymer as the monomer mixture starts to bond with each other to form insoluble gel-like species. The polymer nuclei grow larger and larger as the polymerisation proceeds and the long chain polymer subsequently aggregate and form a poron (monolith) with external pores. When the polymer chain develops sufficiently, the separation phase takes place [6].

The separation phase is the process taking place when the growing solid polymer becomes insoluble in the porogenic solvents and separates during the polymerisation process, leading to the formation of a porous structure for the monoliths. Therefore, the porous properties depend to a large extent on the solvation power of porogenic solvents and their concentration in the polymerisation mixture. Therefore, solvents possessing good solvation capability for components of the monomer mixture (monomer and cross-linker) will lead to a prolonged separation process. This, therefore, affords small pores, while those having bad solvation properties result in a short separation phase. Consequently they form a macro-porous structure ultimately causing a negative impact on efficiency owing to the presence of high void volumes [70].

1.8.3.2. **Factors controlling monolith's pores formation**

There are several parameters affecting the preparation of the monoliths and adjusting the average pore size of monoliths including the concentration of porogenic solvents, the concentration of cross-linkers, the polymerisation temperature, and the polymerisation time. The effect of each parameter is discussed below [71].

Porogenic solvents can tune the properties of a monolith without changing its final chemical structure. Poorer solvents, not highly soluble in the polymerisation mixture, are believed to provide large pore sizes as the separation phase in the polymerisation process becomes faster as explained in the section above [71].

Cross-linkers can also change the properties of a monolith without changing its final chemical structure. The high concentration of cross-linker decreases the average pore size due to the early formation of highly cross-linked polymer globules leading to a dense bed [71].

The polymerisation temperature affects the kinetics of the polymerisation mixture, whereby higher temperature leads to a more rapid polymerisation rate and as a result smaller pores. At high temperature, the production of initiator free radicals is increased, and hence large number of nuclei and globules are formed, leading to a small pore size and a high surface area being formed [71].

The polymerisation time influences the conversion of monomers (all monomer become polymerised) and the use of a shorter time than is needed for full monomer conversion results in high permeability. Lastly, a high concentration of initiators leads to the formation of more number of radicals species and consequently a larger number of nuclei, which results in smaller pores being formed [72].

1.8.4. **Characterisation of monolithic columns**

There are several properties used to investigate a synthesised monolith including permeability, porosity, reproducibility, and mode of separation [73].

1.8.4.1. **Permeability**

This describes the degree of resistance of the prepared monolith to the flow of mobile phase and this can be calculated via the Darcy equation below, 1.17.

$$\boldsymbol{k} = \frac{\boldsymbol{\mu L}}{\boldsymbol{\Delta p}}\boldsymbol{\eta} \qquad 1.17$$

Where μ is the linear velocity of the eluent (mm/s), η is the dynamic viscosity of the eluent (c.Pa), L is the effective length of the column (cm), and ΔP is the back pressure (Pa).

Permeability analysis attempts to determine whether or not the prepared monolith has suffered from the phenomenon of shrinking or swelling. The calculation of permeability is undertaken after pumping different mobile phases under different flow rates using a dead-volume marker, for instance, thiourea or toluene, for RPHPLC and HILIC respectively [73].

1.8.4.2. **Porosity**

The point of undertaking such measurements is to investigate how porous a prepared monolith is. If the prepared monolith is porous, then it should be capable of withstanding high pressures, and consequently, a high flow rate can be used to obtain fast separations.

There are various ways to examine the porosity of the monolith, including scanning electron microscopy (SEM), mercury intrusion measurements, and micro-HPLC. Equation 1.18 is used with micro-HPLC to investigate the porosity of a monolith [20].

$$\varepsilon = \frac{4Ft_0}{d^2\pi L} \qquad 1.18$$

Where F is the flow rate ml/min, t_0 is the retention time for un-retained analyte (min), d is the internal diameter (cm), and L the length of a monolithic capillary (cm).

1.8.4.3. **Reproducibility**

This is conducted to prove that obtained results from the prepared monolith are reproducible, which is an important parameter in an analytical domain. The reproducibility of a monolith is evaluated via the preparation of three monolithic columns from different batches then calculating the relative standard deviation (RSD) of the retention time of the test mixture including thiourea, dimethyl phthalate, anisole, and naphthalene [74]. Fig. 1.34 demonstrates the structures of common standards for this purpose (using RPHPLC conditions) and their associated logP [75] .

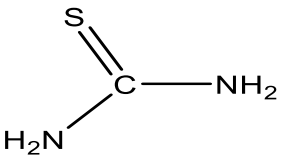

Thiourea (logP -0.46)

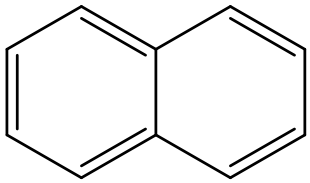

Naphthalene (logP 3.3)

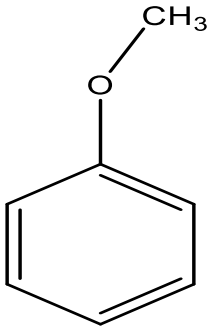

Anisole (logP 2.1)

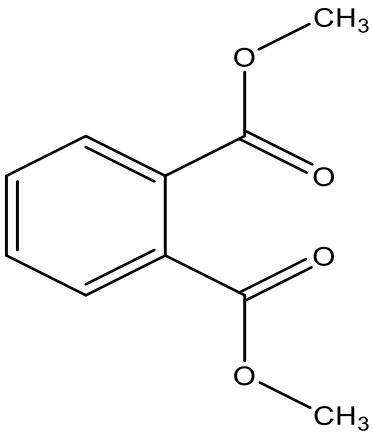

Dimethyl phthalate (logP 1.6)

Figure 1-34: Structures of common standards used in test mixtures for reproducibility analysis of prepared monoliths.

1.8.4.4. **Mode of separation**

Analysis of the mode of separation is performed using newly synthesised monoliths so that the predominant separation mechanism can be identified. Such analysis is based on the calculation of retention factors of injected standards (thiourea, dimethyl phthalate, anisole, and naphthalene) and their behavior in relation to the concentration of ACN in the mobile phase. If the log of retention factors (log k) decreases linearly with the increase of the concentration of ACN, then the mode of separation is RP-HPLC. If the reverse behavior is observed, then the mode of separation is HILIC [50].

1.8.5. **Limitations of organic monoliths**

In spite of the advantages mentioned earlier, there are still some drawbacks associated with organic monoliths. These include the fact that many monoliths suffer from swelling under high organic solvent compositions, which ultimately has a negative impact on the stability of the monolith and low efficiency. In addition, separation efficiencies and peak symmetry of polymeric monoliths are very often not high enough for the analysis of small molecules due to the production of large micro-pores in the total pore volume [68].

1.8.6. **Types of organic monoliths**

There are several types of organic monolith employed in HPLC, including hydrophobic monoliths, hydrophilic monoliths, ion exchange monoliths, affinity monoliths, and chiral organic polymeric monoliths. The work described herein only focused on hydrophobic and hydrophilic monoliths, and hence these will be discussed in subsequent sections. Several previous studies have investigated the synthesis of organic monoliths for RPHPLC and HILIC with varying results.

Smith et al. [74] synthesised a long alkyl chain methacrylate monolith by co-polymerisation of stearyl methacrylate (SMA) with ethylene dimethacrylate (EDMA) in a 100 μm i.d. fused silica capillary for the use as a stationary phase in capillary liquid chromatography. This monolith was found to behave in a similar fashion to a classical C_{18} (ODS) in terms of its retention characteristics. In relation to various ratios they attempted, it was observed that 35% wt of monomer, 65% wt of porogenic, 1% of the initiator with respect to the monomer

afforded the best porosity and permeability, 0.721% and 0.5×10−14 m^2 respectively. Consequently, this composition provided a monolith with good performance efficiency and selectivity. The prepared monolith was also evaluated through the separation of mixtures of weak acids, and neutral and basic molecules, and this monolith was also shown to work for peptide analysis.

Al-Othman et al. [56] fabricated a monolith for the determination of caffeine in various matrices including coffee, tea, and cocoa by co-polymerisation of hexyl methacrylate (HMA) with EDMA using a thermo-initiation. The analytical method developed was validated based on International Conference on Harmonisation (ICH) guidelines in terms of linearity, precision, ruggedness, limit of detection (L.O.D), and limit of quantification (L.O.Q) [56]. The linearity was measured over the range 0.016-250 µg/ml and gave (r^2 > 0.995). The L.O.D and L.O.Q were 0.05 and 0.16 µg/ml respectively. Furthermore, the concentration of caffeine was found to be highest in tea followed by coffee and cocoa. In addition, the recoveries for the extraction were found to be in the range of 89-116% illustrating that the extraction method was in the acceptable range based on ICH guidelines (80-120%). Subsequently, the results obtained with the monolithic column were compared to a conventional packed C_{18} column, in terms of porosity, permeability, pressure drop, retention time, L.O.D, and solvent consumption; the comparison was made under identical chromatographic conditions to obtain a reliable comparison. For these parameters, the prepared monolith showed noticeable advantages over the packed column.

Jiang et al. [20] used thermal initiation to prepare a novel porous poly (SPE-co-EDMA) monolith, for use in HILIC mode, consisting of poly (N, N-dimethyl-N-methacryloxyethyl-N-(3-sulfopropyl) ammonium betaine (SPE) and EDMA. The prepared monolith was intended to resolve polar charged and uncharged molecules. They showed that uncharged molecules were resolved based only on hydrophilic interaction, while charged ones were

separated by a combination of electrostatic and hydrophilic interactions, as indicated by results at different mobile phase pHs values. It was also noted that there was no sign of swelling or shrinking of the prepared monolith when different polarity solvents were used for permeability tests; this result indicated that the prepared monolith was stable under different solvent conditions. Additionally, the phenomenon of switching from RPHPLC to HILIC mechanism was observed through modifying the content of ACN and water in the mobile phase, specifically at above 65 % of ACN. This event of switching from RPHPLC to HILIC is known as a 'critical transition' and is used as an indication of the polarity of the stationary phase. The lower the critical transition is, the more polar the stationary phase will be [76], as shown in the study below.

Guangxin Yuan et al. [73] synthesised thermally, a novel HILIC monolith by co-polymerisation of *N*,*N*-dimethyl-*N*-acryloyloxyethyl-*N*-(3-sulfopropyl) ammonium (SPDA) with *N*,*N*′-methylenebisacrylamide (MBA), to produce the poly (SPDA-co-MBA) monolith. In this study, three different monolithic columns namely poly (SPE-co-EDMA), (SPDA-co-EDMA), and the novel monolith (SPDA-co-MBA) were synthesised and compared in terms of their hydrophilicity. It was observed that the novel poly (SPDA-co-MBA) monolith demonstrated the highest hydrophilicity among these three prepared monoliths, reflected by the value of the lowest 'critical transition' (at 5% ACN vs. 65% for both SPE-co-EDMA and SPDA-co-EDMA). The novel monolith poly (SPDA-co-MBA) showed good permeability with no sign of shrinking or swelling proving its high stability. Using a HILIC mixture consisting of three analytes including toluene, acrylamide and thiourea, the monolith illustrated high efficiency (70,000 plates/m) for the thiourea at a linear velocity of 1.95 mm/s. In addition, investigation of the influence of the mobile phase pH and salt concentration were performed using the novel monolith, and weak electrostatic repulsion for the negatively charged analytes at low concentrations of ACN was hypothesised.

This novel monolith showed excellent selectivity for a series of polar analytes including phenols, bases, and small peptides. Using the novel monolith, a method was successfully established for the analysis of two highly polar analytes, namely urea and allantoin in cosmetics products. The amount of urea and allantoin found in the cosmetic product were 43 mg/g and 1.4 mg/g, respectively. These results confirmed that the novel monolith was a promising stationary phase for resolving highly polar analytes.

1.9. Aim of this research project

This research project was focused on investigating alternative separation media (known as monoliths) as stationary phases for capillary liquid chromatography, owing to their merits as mentioned previously in sections 1.8. Therefore, the aims of this project were as follows:

- Synthesis of new organic monoliths to be utilised as stationary phases and employed for the analysis of small molecules.
- Exploring approaches in synthesising organic monoliths enabling them to be employed with small molecules.
- Investigation the possibilities of hyphenating small fused silica capillaries with classical mass spectrometry.
- Demonstrate how the fabricated monoliths can be utilised to analyse real samples (caffeine in Arabic coffee, amitriptyline in commercial tablets).
- To confirm that these monoliths can be made reproducibly.

Chapter 2

General protocol for monolith fabrications

2. Methodology

2.1. Fabrication of monolithic columns

As mentioned in the previous Chapter, there are four main steps involved in the fabrication of monoliths. These are as follows:

- Treatment of the inner fused-silica capillary with an alkaline media, in our case 1M NaOH was employed, to activate the surface via conversion the inner surface from Si-O-Si (Silicon) to Si-OH (Silanol group), shown in Fig 2.1.

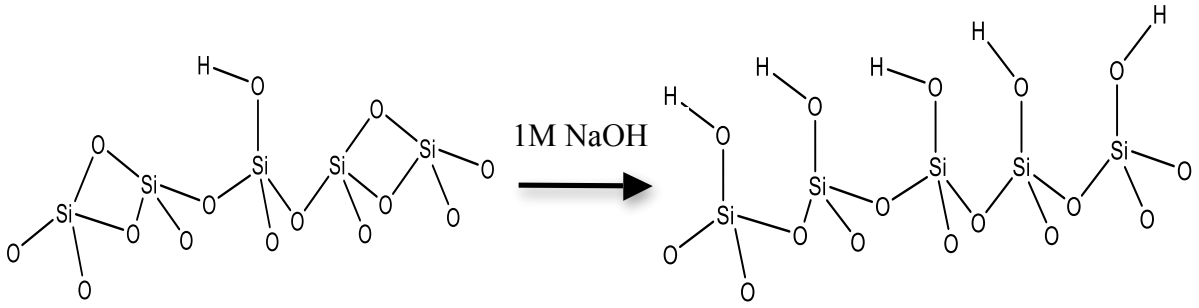

Figure 2-1: Activation of the inner surface of fused silica capillary.

- Use of 3-(trimethoxysilyl) propyl methacrylate (γ-MAPS) to derivatise the silanol group on the inner surface of the fused-silica capillary, illustrated in Fig 2.2 below. The treatment of the capillary with γ-MAPS solution produces vinyl groups on the wall surface of the capillary. This production of vinyl groups, as a result, binds covalently with the polymerisation mixture when introduced at a later stage [16, 77].

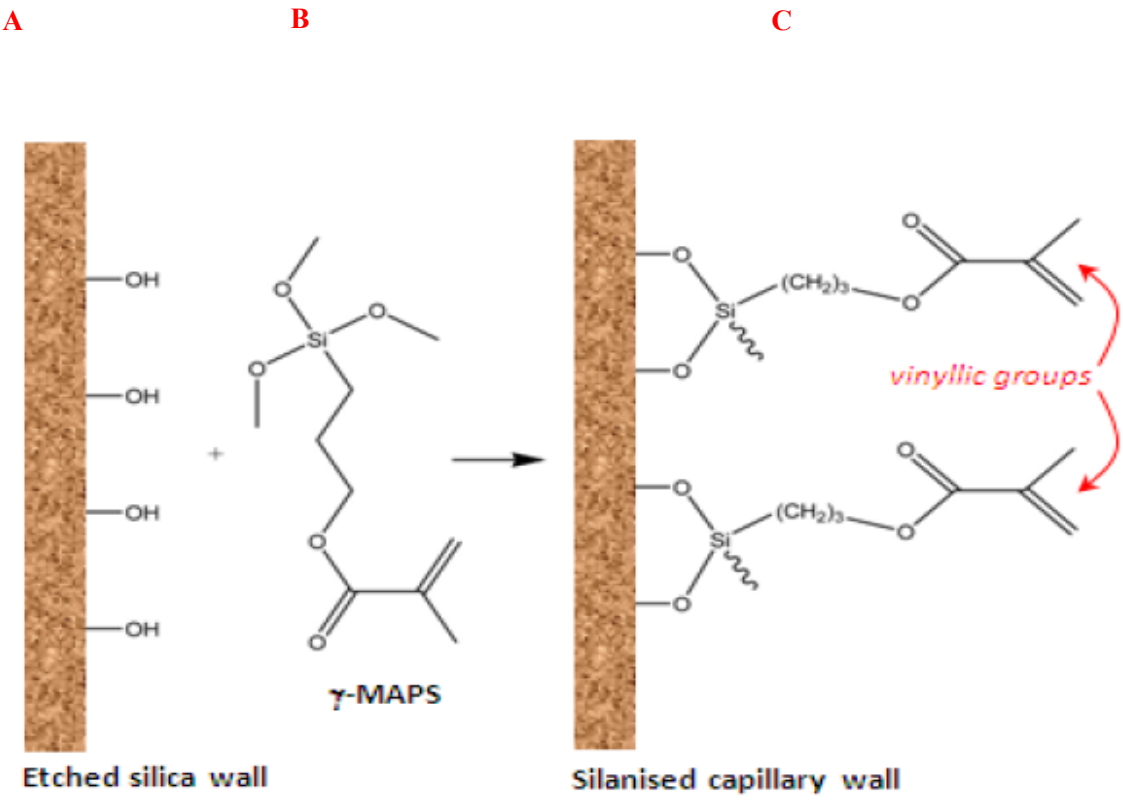

A: Silica superficial silanol groups

B: 3-(trimethoxysilyl) propyl-methacrylate

C: silanised capillary wall

Figure 2-2: Derivatisation the silanol group with γ-MAPS, adopted from [16].

- In situ thermal polymerisation of a monomer with a cross-linker in the presence of a porogen system and an initiator at a specific temperature for a certain period of time.
- Thorough washing with an organic solvent in order to wash out un-reacted materials and porogens. Fig 2.3. is a summary of the monolithic fabrication process.

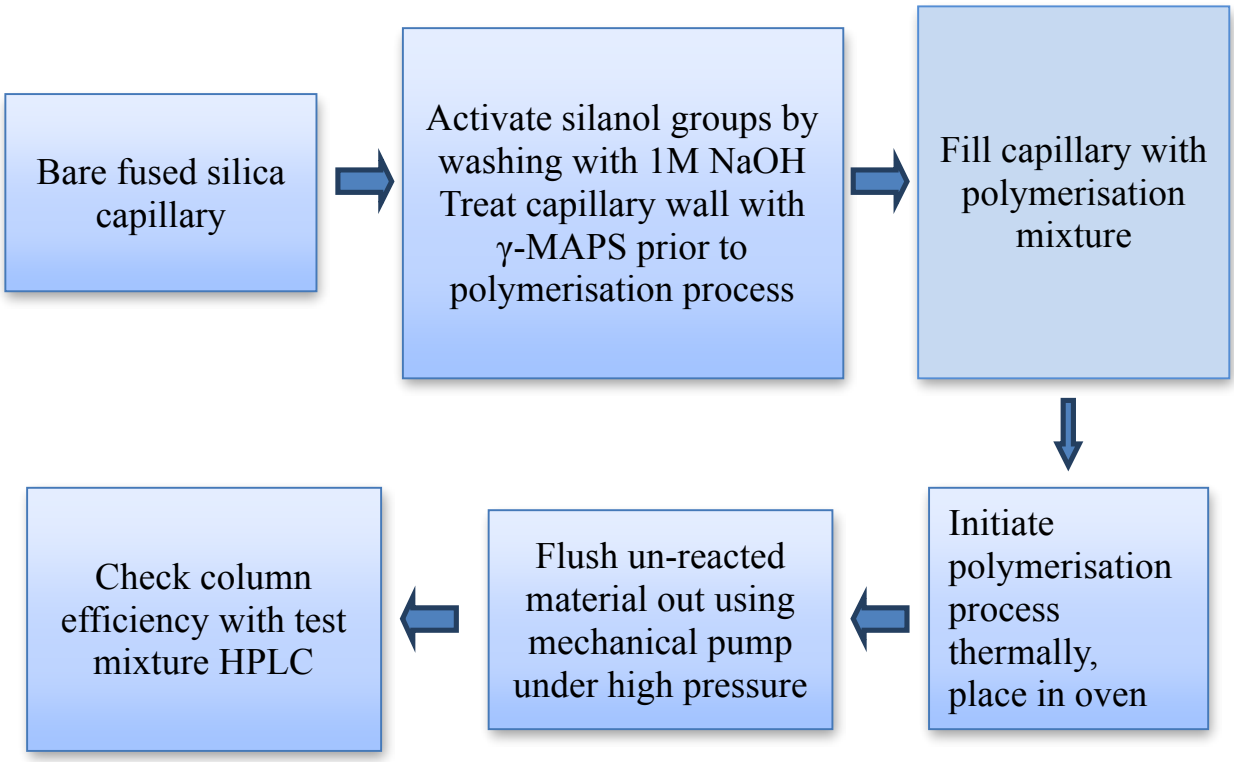

Figure 2-3: Summary of monolithic fabrication.

2.1.1. **Experimental conditions for monolith fabrication**

The following section describes the experimental conditions used for the fabrication of monolithic columns in subsequent Chapters.

Step 1: Treatment of the fused-silica capillary with alkaline media to activate the surface via conversion of Si-O-Si (silica) to Si-OH (silanol)

- The fused silica capillary was flushed with 1 M NaOH for 10 mins in order to activate the silanol groups under low pressure, using the setup illustrated in Figure 2.4.

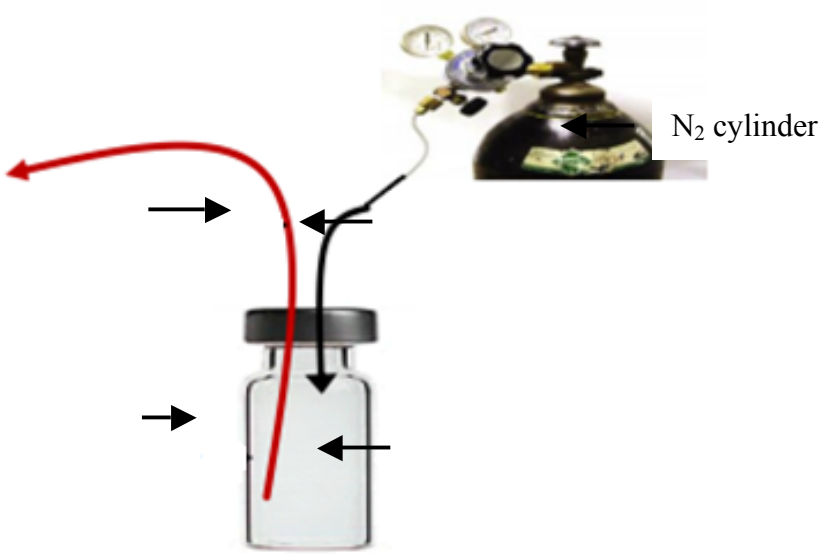

Figure 2-4: Set up used to introduce 1M NaOH, γ-MAPS solution and polymerisation mixture into the fused silica capillary under N_2 gas.

- Next, the capillary was sealed with GC septum and placed in an oven at 100 ^{0}C for approximately 12 hrs, as shown in Fig 2.5.

Figure 2-5: Capillary placed in an oven for activation.

- The capillary was purged with de-ionised water until the pH of the effluent water reached 7; pH indicator paper was used to confirm the pH value, with a yellow moderate color being an indication that the pH was close to 7.
- The capillary was subsequently flushed with MeOH for about 30 mins, then dried with N_2 under low pressure (20-60 psi) for 30 mins using the set up shown previously in Fig.2.4.

Step 2: Derivatisation of the silanol groups on the inner surface of the fused-silica capillary with 3-(trimethoxysilyl) propyl methacrylate (γ-MAPS)

- At this point, the capillary was ready for the introduction of γ-MAPS in MeOH (as a 1:1 solution). The γ-MAPS was introduced in order to add vinyl groups to the silanol groups present on the walls of the capillary, as explained previously (section 2.1). These vinyl groups would be subsequently available for the reaction with the polymerisation mixture when introduced at a later stage, as explained above.
- After addition of the γ-MAPS solution, the capillary was placed into the oven for 24 hrs at 60 °C.
- The capillary was flushed with MeOH and purged with N_2 gas under low pressure (20-60 psi) for an hour using the set up shown previously in Fig.2.4.

Step 3: In-situ thermal polymerisation of a monomer with a cross-linker in the presence of a porogen system and an initiator

- 100 ul of the polymerisation mixture was introduced into the capillary under low pressure (20-60 psi) using the set up shown previously in Fig.2.4.
- The capillary was then placed in the oven at 60 °C for 12 hrs (or otherwise specified the amount of time, depending on the experimental design).

Step 4: Thorough washing of the fabricated monolith with an organic solvent in order to wash out un-reacted materials and porogens

- The capillary was washed with MeOH using the high-pressure pump (1000-6000 psi) shown in Figure 2.6. Often a low-pressure pump is not capable of removing un-reacted materials as well as the porogenic solvents due to the porosity of the monolith.

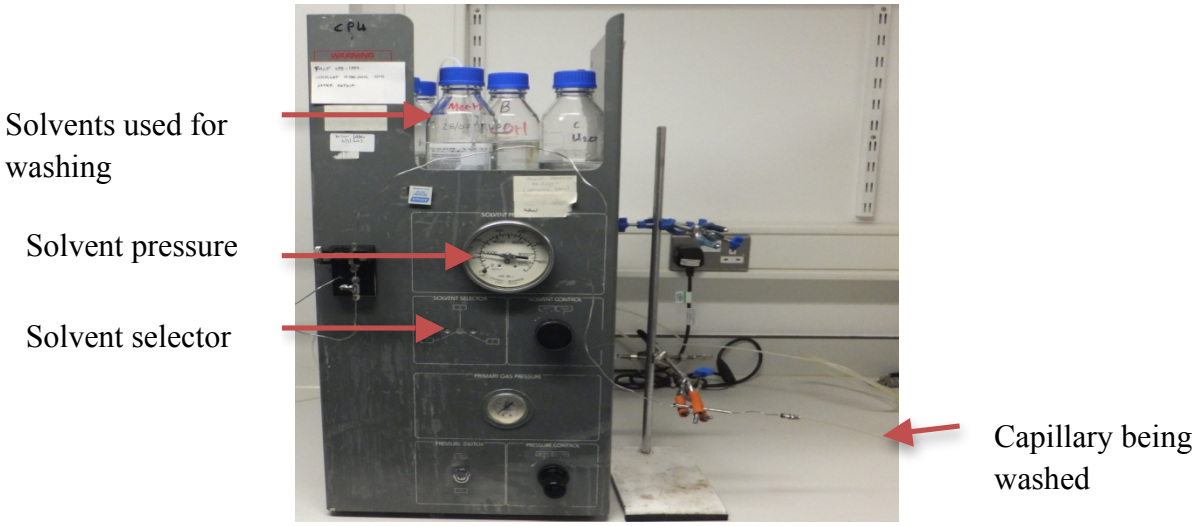

Figure 2-6: High pressure pump used for column washing.

- Both ends of the capillary were cut with a diamond capillary column cutter in order to obtain even ends.
- A thermal wire-stripper device, as shown in Fig.2.7, was used to create a 2 to 3 mm long detection window at a distance of 5 cm from one end of the capillary. At this stage, the monolithic material became pyrolysed.

Figure 2-7: Thermal wire stripper.

- The capillary was flushed once more with MeOH for 30 min under high pressure, in order to wash out any pyrolysed material produced during the creation of the detection window.
- Finally, the capillary was cut to the desired length and was connected to a nano-HPLC system for further evaluation and characterization.
-

2.1.2. **Guidelines and considerations when fabricating monoliths**

There are some practical tips that need to be taken into consideration when synthesising a monolithic column so that an efficient column could be synthesised.

- When purging with 1 M NaOH, make sure there are no bubbles present inside the fused silica capillary. Any bubbles might lead to a non-homogenous activated surface which will ultimately lead to weaken the bonds between the inner surface and γ-MAPS resulting in an unstable monolith. If bubbles are present, these can be removed by additional flushing of the capillary. Similarly, no bubbles should be present when filling the capillary with γ-MAPS, as the presence of bubbles will lead to an uneven coating of the fused silica capillary. This will result in a loss of interaction between the polymerisation mixture and γ-MAPS which ultimately lead to an unstable monolith or void being formed, as shown in Fig.2.8, resulting in poor column efficiency.

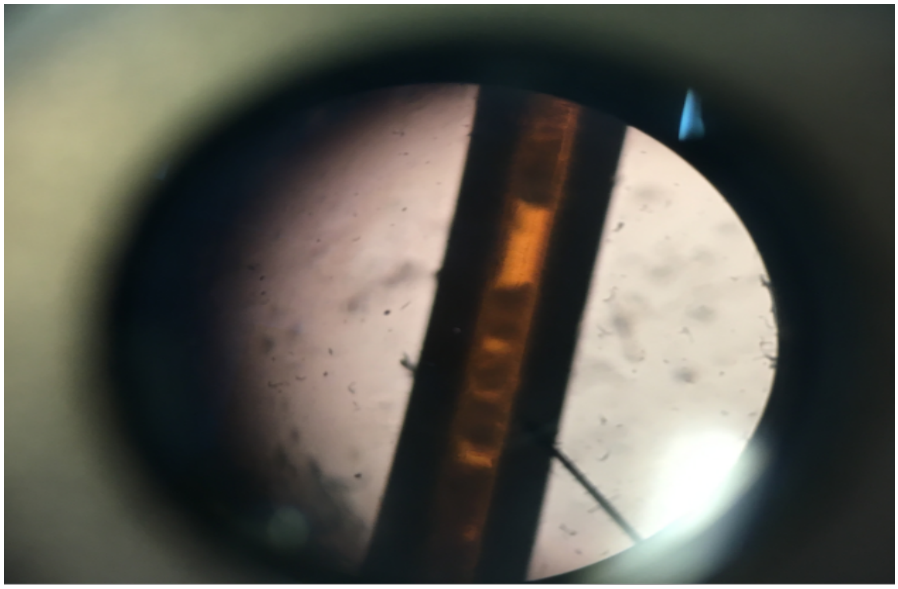

Figure 2-8: Example of the presence of voids.

- When filling the capillary with the γ-MAPS/polymerisation mixture, both ends should be sealed as soon as some liquid is observed eluting from the capillary. This ensures that the solution stays within the capillary, and minimizes the formation of bubbles. Failure to do this practice would lead to a failure of the fabrication process.
- It is important to note that before introducing the polymerisation mixture into the capillary, it has to be purged with nitrogen gas for 5 min in order to remove any dissolved gases. The presence of these gases could disturb the polymerisation process and subsequent formation of the monolith inside the capillary.
- A washing step is strongly recommended as soon as the polymerisation process comes to an end. Delaying this step could lead to the unreacted materials and porogens drying out inside the capillary. This results in difficulty in washing them out. Consequently, the capillary would become non- porous and ultimately a high back pressure would be experienced.

- When cutting both ends of the capillary, the use of a ceramic or diamond cutter is highly recommended in order to obtain even ends. This is because failure to do so would lead to bad chromatograms to be obtained due to the undesired interactions of the injected sample with the layers of the capillary, as shown in Fig.2.9. Another issue with uneven ends is that a high back pressure would be observed when washing or connecting to a HPLC system for chracterisation.

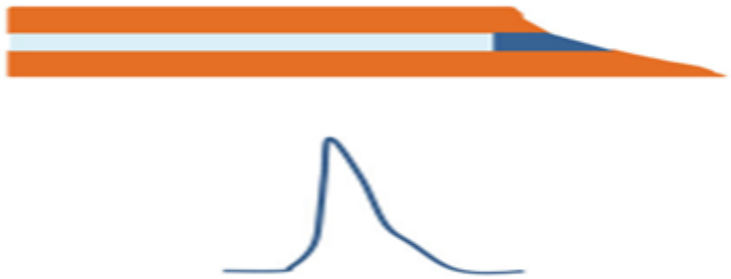

Figure 2-9: Effect of poor cutting [78].

- When introducing NaOH, the γ-MAPS solution or the polymerisation mixture during the monolith fabrication, it is important to ensure that the ends of the capillary are neither blocked nor badly cut. This is because either of these situations will prevent elution of the solution from the capillary or a high back pressure would be generated, as shown in Fig. 2.10.

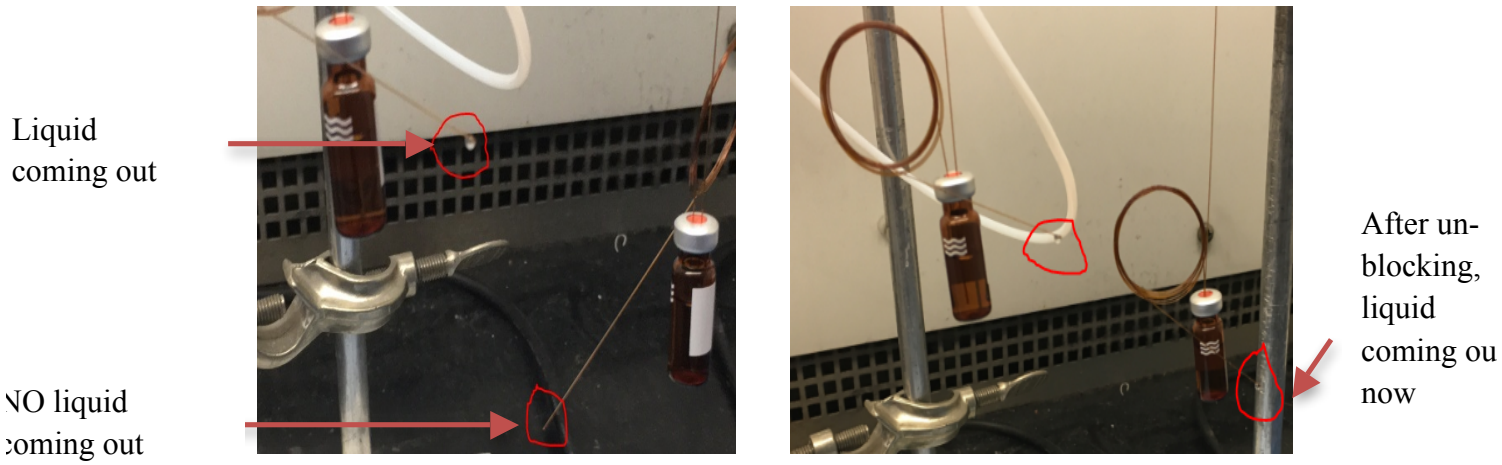

Figure 2-10: Examples of blocking when introduced solution.

- When connecting the monolithic capillary to a Valco injection valve, it is important to observe some liquid eluting from the end of the capillary before connecting to the UV detector, otherwise blocking could have occurred, as shown in Fig.2.11.

Figure 2-11: Blocking check.

- It is also important when installing the monolithic capillary into the injection valve to make sure that the monolithic capillary is secured into the injector properly. This is achieved using a sleeve with PEEK tubing and securing in place with a male nut and Valco ferrule. This is because failure to do so could result in very broad peaks as the injected sample would not be fully introduced into the monolithic capillary as shown in Fig.2.12. Fig.2.13 illustrates the same monolithic capillary poly (HMA-co-1,6-HEDA) after installing it properly into the Valco valve.

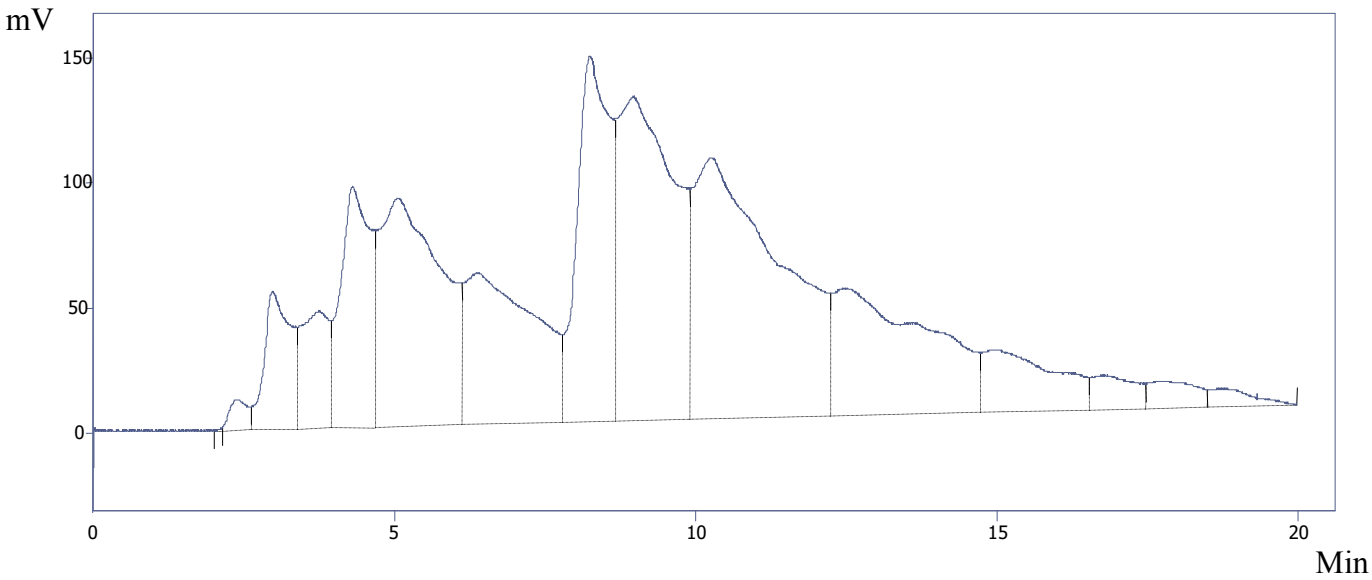

Figure 2-12: Bad installing of the column into the injector.

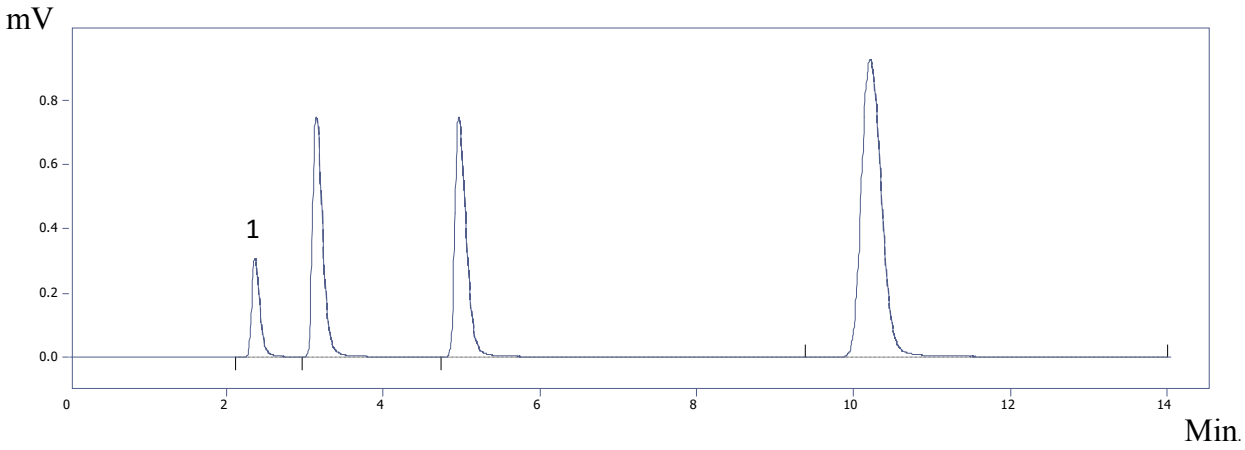

Figure 2-13: Proper installation of monolithic into injection valve. Experimental conditions: column dimension 100 um i.d. x 375 um o.d., mobile phase 40:60 (V/V) (H2O: ACN), detection wavelength 210 nm, flow rate 1000 nL/min, injection volume 100 nl, samples: 1) thiourea, 2) dimethyl phthalate, 3) anisole, 4) naphthalene.

- In addition, the fabricated detection window should be positioned in the middle of the UV cell. The cell used with our detector is shown in Fig. 2.14. If incorrectly placed, it would not be possible to zero the detector, and as a result, no signal would be obtained.

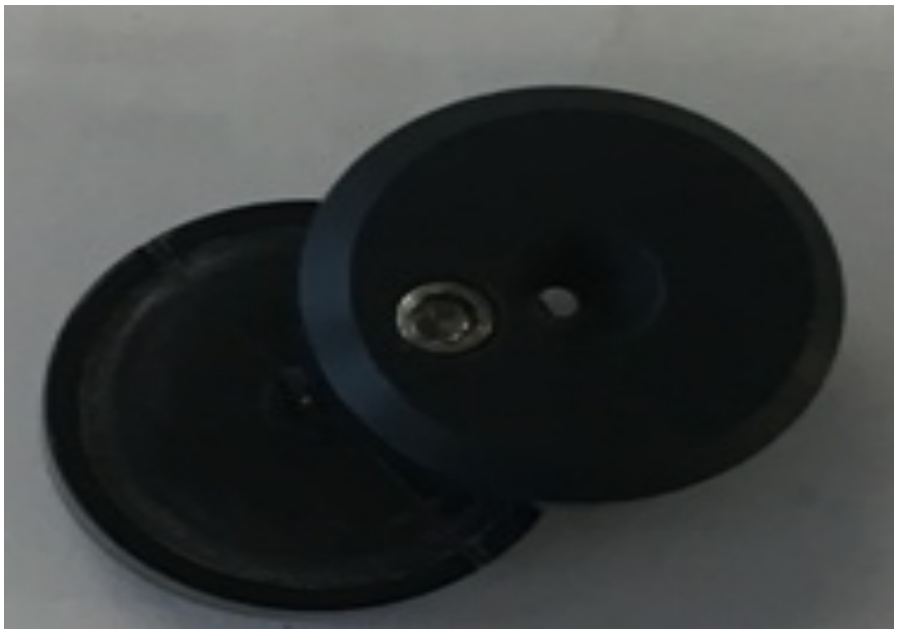

Figure 2-14: UV cell used for detection.

- It is also significant to have a clean UV cell, free from any buffer that might deposit on it. A dirty cell will lead to poor detector response as shown in Fig. 2.15.

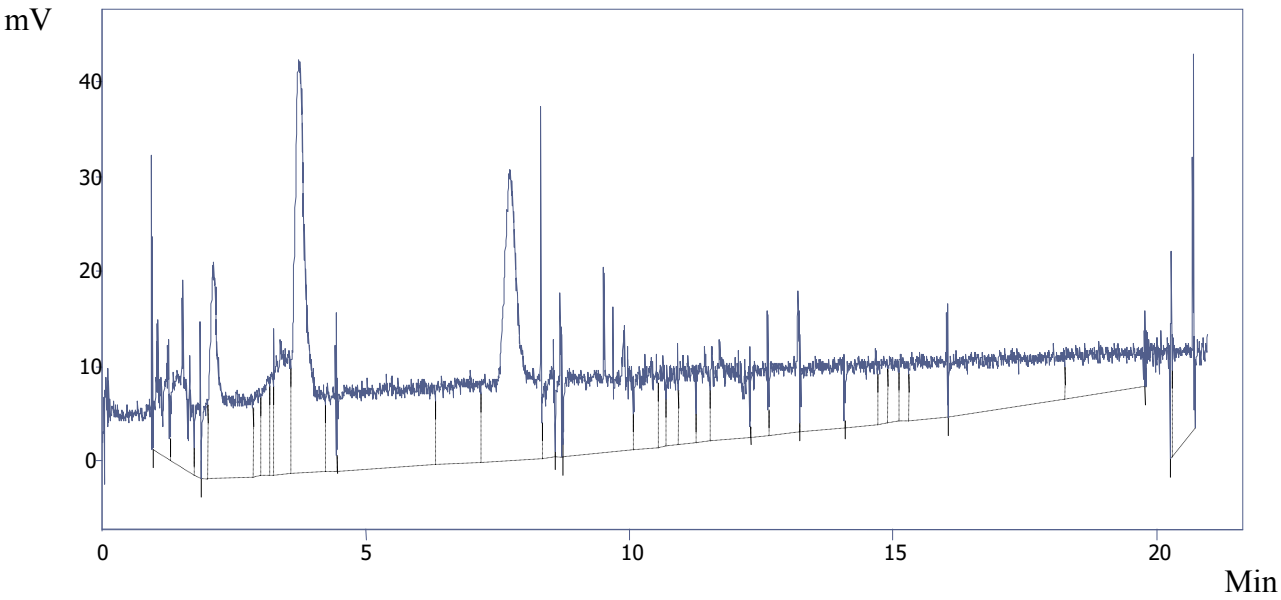

Figure 2-15: Example of dirty UV cell window.

- When making the detection window using the thermal wire stripper, previously shown in Fig.2.7, it is important not to over-heat the monolithic capillary as doing so will hinder the detection. Fig. 2.16 is an illustration of both scenarios, for well-heated and over-heated detection windows.

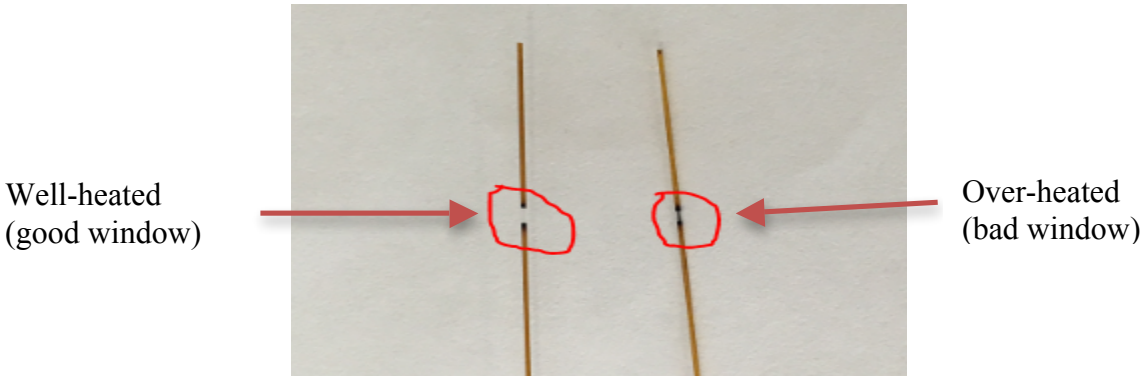

Figure 2-16: illustration of both scenarios, for well-heated and over- heated detection windows.

- Sealing the vials used to introduce either γ-MAPS or the polymerisation mixture into the capillary is highly recommended. Failure to do so will create a low pressure inside the vials. Consequently, the introduction of the solutions into the capillary resulting will be prevented leading to incomplete filling.
- When dealing with fused silica capillaries possessing I.d.s ≥ 200 μm, the cleaving process of capillaries needs to be conducted with extra care to avoid the phenomenon of brittleback as shown in Fig.2.17. Brittleback is the process whereby glass particulates fall into the internal dimension of the capillary from the cleaved end face. Additionally, when placing these fused silica capillaries in the oven in order to initiate the polymerisation process, it is important to avoid contact with any metal shelves as this can lead to damage to the capillary, as will be shown in Chapter **5**.

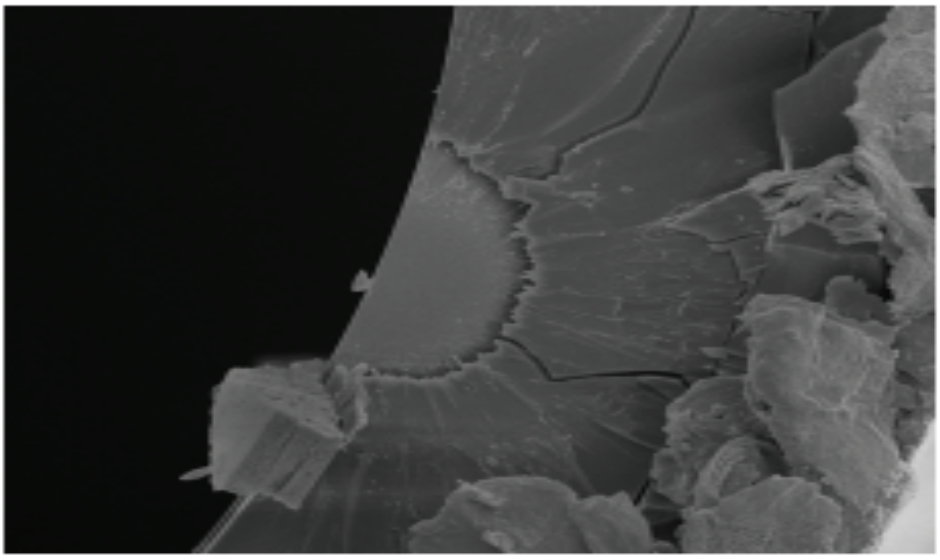

Figure 2-17: Brittleback phenomenon- internal damage of the fused silica capillary due to bad handling.

- When the monolithic capillary is not in use, it is recommended to keep it“wet”, as shown in Fig.2.18, in order to prevent it from drying out. If a monolithic column goes dry, this tends to create crevices and cracks inside the monolithic bed. These crevices and cracks, therefore, have a very negative impact on the performance of the monolithic column.

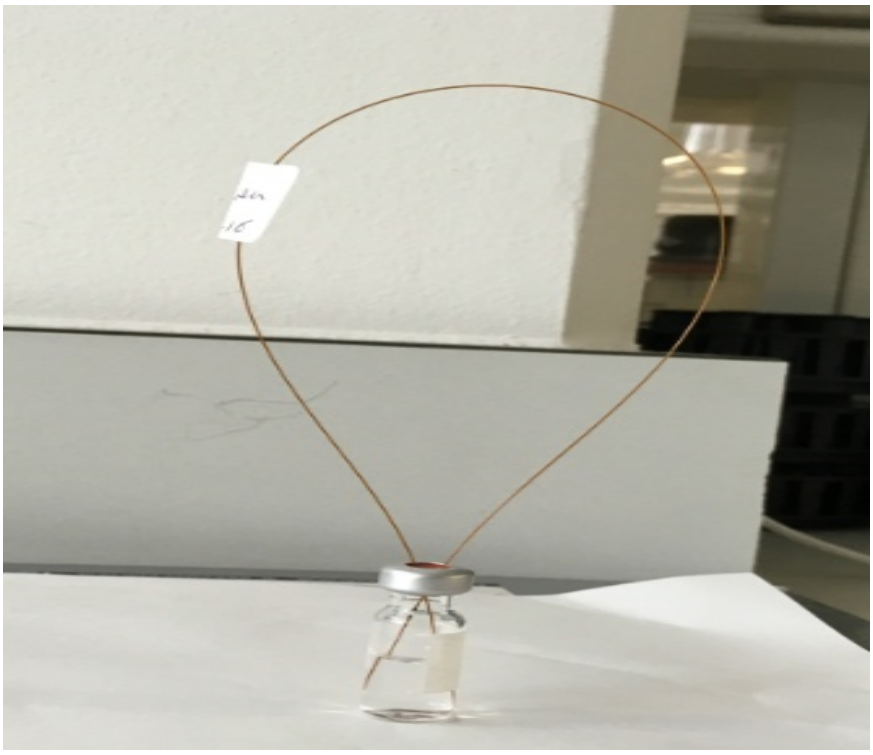

Figure 2-18: keeping the monolithic capillary in solution.

2.2. Instrumentation employed throughout the project.

A number of different instruments/techniques were used in this work, namely Nano-HPLC, MS, SEM, microscope, centrifuge, and Fourier Transform Infrared Spectroscopy (FTIR).

2.2.1. **Nano-HPLC with Dina pump**

As mentioned in the previous Chapter (section 1.2), a splitless pump was used to generate nano-flow. The Nano-HPLC system employed in this research is re-shown in Fig.2.19 and consisted of a Dina gradient pump supplied by KYA Technologies, Tokyo, Japan. The maximum pressure limit for the system is 20 MPa (200 bar, 2900 psi). The pumping system is controlled using Dina software. Injection is made via a four port Valco injection valve (model Inj-P4-100) with a fixed 100 nl internal loop (Texas, USA), and detection is accomplished using an Applied Biosystems 783A programmable absorbance detector (CA, USA) fitted with the capillary cell shown previously in Fig 2.14. All micro-HPLC data was processed using Clarity chromatography software from Data Apex version 6.

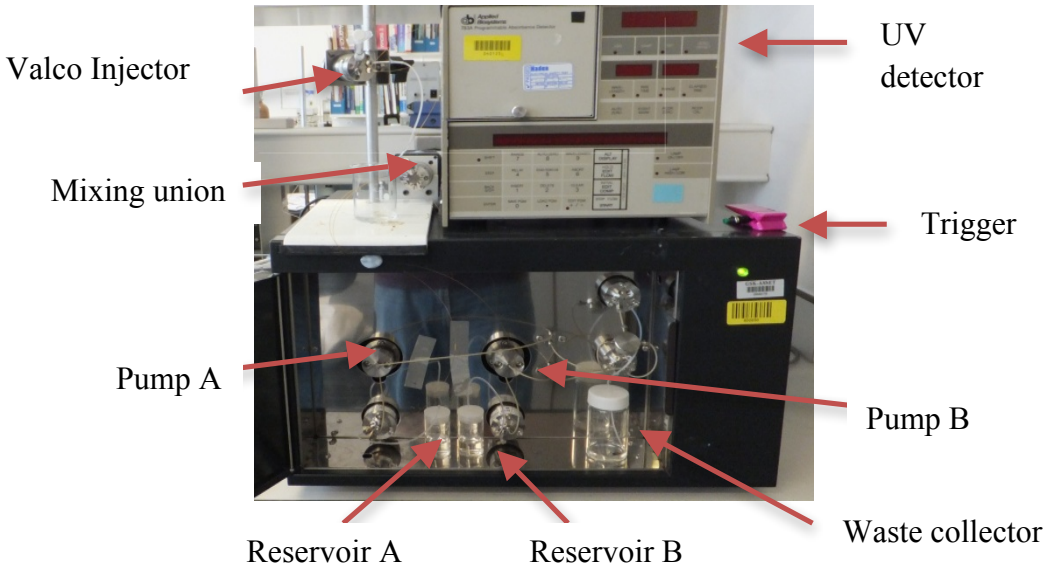

Figure 2-19: Nano-HPLC system used in this project work.

As mentioned previously (section 2.1.1), the detection window is made by removing the polyamide coating of the fused silica capillary. The detection window permits on-line UV detection and overcomes the phenomenon of band broadening (section 1.6.2) caused by extra-column volume in the UV cell, thus leading to better chromatographic performance. However, this online detection setup has a short path length, corresponding to the i.d. of the monolithic capillary, which results in lower sensitivity as per Beer's law [79]. To resolve this issue, multiple methods have been suggested to increase the path length, one of which is to bend the capillary to create a 'U' shape and orienting the UV cell so that the light passes parallel to the axis of the capillary (Figure 2.20).

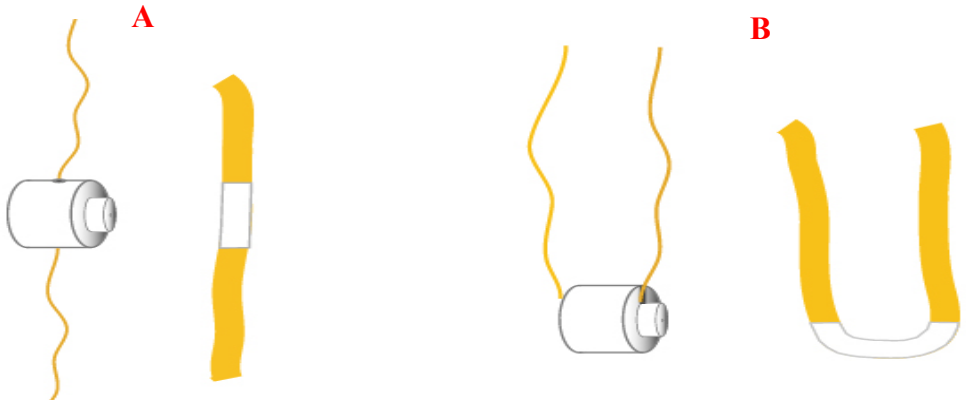

Figure 2-20: A) On-line detection, B) U shape detection, adopted from [79].

Although this approach does increase the short path by 5-8 mm resulting in an increase in sensitivity, the U-shape possesses poor optical characteristics owing to the light scattering as it passes through the cell [79], as shown in Fig.2.21.

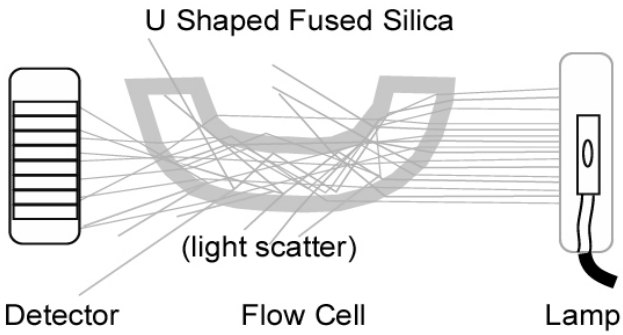

Figure 2-21: illustration of light lost via U shape bent, adopted from [79].

2.2.2. **Mass spectrometry (MS)**

The MS used in this research, as shown in Fig.22, was supplied by Thermo Scientific, (Finnigan model LCQ Deca), Waltham, USA. It consists of an ionisation source (ESI), a mass analyser (ion trap) and a detector.. The data was processed using Finnigan LCQ version 2, Xcalibur software.

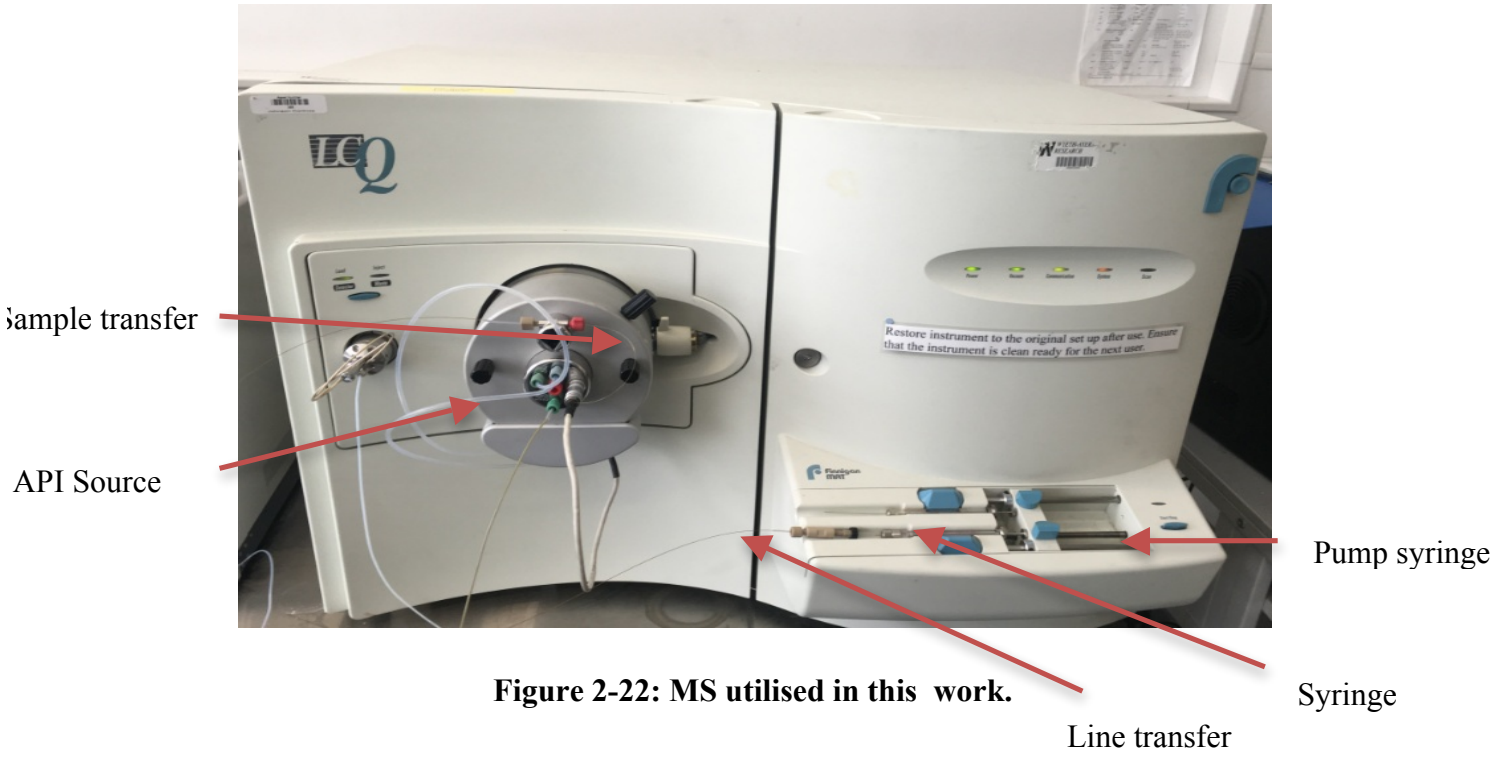

Figure 2-22: MS utilised in this work.

2.2.3. **Centrifuge**

The centrifuge used (Power 310W, Voltage 230 VAC) was supplied by Thermo Electron LED GmbH (Germany) and was used to sediment suspended solids.

2.2.4. **Scanning electron microscopy (SEM)**

A Hitachi S-4000 SEM was supplied by Hitachi High-Tech (Tokyo, Japan), and was used to investigate the morphology of the monolith, poly (HMA-co-1,6-HEDA). Relevant data will be shown in Chapter **4**. The data was processed using INCA elemental analysis software.

.

2.2.5. **Fourier transform infrared spectroscopy (FTIR)**

FTIR was performed using a Perkin Elmer Frontier instrument. This was used to identify and verify the chemical modification of poly (GMA-co-EDMA) when reacted with Congo red (CR); relevant data will be shown in Chapter **6**. The data was processed using Spectrum software, version 10.4.00. .

2.2.6. **Microscope**

A Jencons Plus microscope (model No. 00035160) was used to investigate the presence of air bubbles inside the capillary column and confirm the introduction of the polymerisation mixture within the capillary.

Chapter 3

Fabrication of stearyl methacrylate monolithic column for the quantification of caffeine in Arabic coffee using capillary chromatography

3. Introduction

Capillary-high performance liquid chromatography (Cap-HPLC) has become one of the most significant developments in the domain of separation technology in the past two decades. This is due to the low sample and solvent consumption, high sensitivity (less dispersion) and ease of hyphenating with either MS or NMR. Conventionally, Cap-HPLC employs fused silica capillaries packed with various stationary phases used to separate a wide diversity of analytes including bases, acids, neutral compounds, peptides and proteins [74]. However, the packing of capillary columns is not a straightforward process due to the challenges stated previously in Chapter **1**, section 1.7.

The ease of chromatographic column fabrication combined with maintaining their separation efficiency has become one of the most important targets in the field of separation techniques. Monolithic columns could be,as a result, considered a great candidate for this purpose due to their unique characteristics mentioned previously (section 1.7) [80].

Methacrylate-based polymers are considered to be one of the most widely investigated monoliths and were first assessed as polymeric chromatographic packing materials in 1978 by Svec and co-workers [81]. Methacrylates are one of the most common polymer chemistries employed as separation media due to several advantages. [82] These include high stability at high pH, ease of preparation, a wide variety of monomer available with a broad range of polarities helping to enhance selectivity. Moreover, methacrylate functionalisation is easy when using monomers such as glycidyl methacrylate (GMA) containing a very reactive epoxy group. Nevertheless, owing to solubility issues associated

with long alkyl chain hydrophobic methacrylate monomers, the majority of the methacrylate type monoliths were based on short alkyl chain monomers ranging from butyl to lauryl methacrylate [83-85].

In order to overcome the issue of solubility, there have been various solutions proposed by different research groups including Li et al. [86] who synthesised an octadecyl alkylated poly-methacrylate monolith via co-polymerisation of GMA with EDMA in the presence of two porogens (dodecanol and toluene) followed by the derivatisation with stearoyl chloride. Moreover, another study conducted by Ericson et al. [87] who published a three-step process to fabricate an octadecyl monolithic capillary using a BF_3-cataysed reaction between epoxy and hydroxy groups in a pre-prepared monolith and the epoxide group in 1,2 epoxyoctadecane. However, this three-step approach makes the fabrication of the monoliths less attractive and complicated and increases the risk of irreproducibility.

Jiang et al. [74] synthesised in situ stearyl methacrylate monoliths in 100 µm i.d. fused silica capillaries for the use in capillary liquid chromatography and the results obtained were promising, as shown previously in the Chapter (section 1.7.10). In their work, a binary porogen system consisting of iso-amyl alcohol and 1,4-butanediol was used. In our study, one of the porogens, namely iso-amyl alcohol, was replaced with 1-propanol in order to investigate its effect on porosity and efficiency.

Caffeine beverages such as coffee, cocoa and tea are considered to be one of the most consumed in the world. Additionally, caffeine may also be considered to be one of the most drugs utilised worldwide. It is a stimulant for muscles, heart, central nervous system, and circular systems of the body. Moreover, caffeine encourages the relaxation of the bronchial muscle, behaving as a diuretic and therefore intensifying brain activity [88]. Furthermore, the concentration of caffeine in vivo is thought to be a marker for several disorders such as kidney malfunction, asthma, and heart disease [89]. Having high doses of caffeine could

cause several unwanted symptoms and in some cases cause severe health effects in particular for children and infants, for instance, gastrointestinal problems, irritability, and loss of appetite. A lethal dosage of caffeine is thought to be more than 170 mg/kg body weight [90, 91].

Several analytical approaches have been employed for the determination of caffeine in different matrices (food, plants, environmental). These include UV–Vis [89], thin- layer chromatography coupled with HPLC (TLC) [92], FT- Raman [93], HPLC with different columns and detectors [94-96], Gas chromatography (GC) [97], FT-IR spectroscopy [98], NMR spectroscopy [99], and capillary electrophoresis (CE) [100].

In the light of these adverse effects of caffeine mentioned above, it is vital to observe caffeine in drinks and food via the use of a precise, simple, fast and cheap analytical method.

In this study, the effect of choosing a different porogen, namely 1-propanol instead of iso-amyl alcohol was investigated in terms of efficiency and porosity. Characterisation of the fabricated monolith was conducted including porosity, permeability, reproducibility, and mode of separation. Furthermore, the monolithic capillary was applied to a real life sample, namely caffeine in Arabic coffee.

3.1. Experimental section

3.1.1. **Reagents and Materials**

Stearyl methacrylate (SMA), ethylene dimethacrylate (EDMA), 3-methyl-1-butanol (iso-amyl alcohol), 3-(trimethoxysilyl) propyl methacrylate (γ-MAPS), 1,4-butanediol, 1-propanol, azobisisobutyronitrile (AIBN), sodium hydroxide, thiourea, dimethyl phthalate, anisole, and naphthalene were all obtained from Aldrich Chemicals (Steinheim, Germany). HPLC-grade methanol and acetonitrile were supplied by Fisher Scientific (Leicestershire, UK). The water used throughout all experiments was purified using a Millipore System model no. SYNSV0000. A pH indicator paper was purchased from Camlab House (Cambridge, UK). The fused silica capillaries were supplied by CM scientific (Silsden, United Kingdom, Part no. TSP100375). Caffeine and theophylline were purchased from Lancaster *(*Eastgate, White Lund Industrial Estate, UK), and Arabic coffee was purchased from a local shop (Jeddah, Saudi Arabia). A 25 mm syringe filter w/0.45 μm PTFE membrane, sodium dihydrogen phosphate and disodium hydrogen phosphate anhydrous were all purchased from VWR International Ltd (Ballycoolin, Dublin, Ireland).

3.1.2. **Instrumentations**

An oven was employed for the thermal polymerisation. A microscope was used for investigating the presence of air bubbles inside the capillary column and the confirmation of the introduction of the polymerisation mixture within the capillary. Nano-HPLC experiments were carried out using a Dina system. More details about these instruments, i.e. model/make, manufacturer's details have already been stated in Chapter **2** (section 2.2).

3.1.3. Preparations solutions

3.1.3.1. Preparation of the test mixture used for monolith characterisation

The test mixture consisted of 10 mg thiourea, 60 µl dimethyl phthalate, 57 µl anisole, and 16 mg naphthalene dissolved in 10 ml of 50% ACN (HPLC-grade) and 50% water (HPLC-grade) (V/V). The mixture was then diluted 50 times in order to avoid column overloading and to obtain a reasonable UV response.

3.1.3.2. Preparation of solutions for caffeine analysis

A standard 0.5 mM stock solution of caffeine was prepared in HPLC-grade water. The working standard solutions ranging from 0.025 mM to 0.2 mM were prepared by appropriate dilutions of the stock solution using HPLC-grade water. HPLC-grade water was employed as a blank and injected. In order to check the selectivity of the method, a 0.4 mM stock solution of theophylline was prepared and diluted when required. A buffer solution consisting of sodium dihydrogen phosphate and disodium hydrogen phosphate was prepared to the required concentrations and then adjusted to the required pH using either HCl or NaOH.

3.1.3.3. Sample preparation and extraction process

50 mg of ground Arabic coffee was accurately weighed and then dispersed in 25 ml of HPLC- grade water and then sonicated for 60 min until completely dissolved. Then, a 20 ml aliquot of the resulting solution was filtered through a 0.45 µm membrane filter and injected (100 nl) into the HPLC system for quantification [101].

3.1.3.4. **Preparation of poly (SMA-co-EDMA) monolithic column**

The general protocol followed in synthesising this monolithic column has already been mentioned in the previous Chapter, specifically section 2.1.1. The co-polymerisation scheme of the selected monomers and porogens is illustrated in Fig 3.1. Table 3.1 shows the composition of the polymerisation mixture.

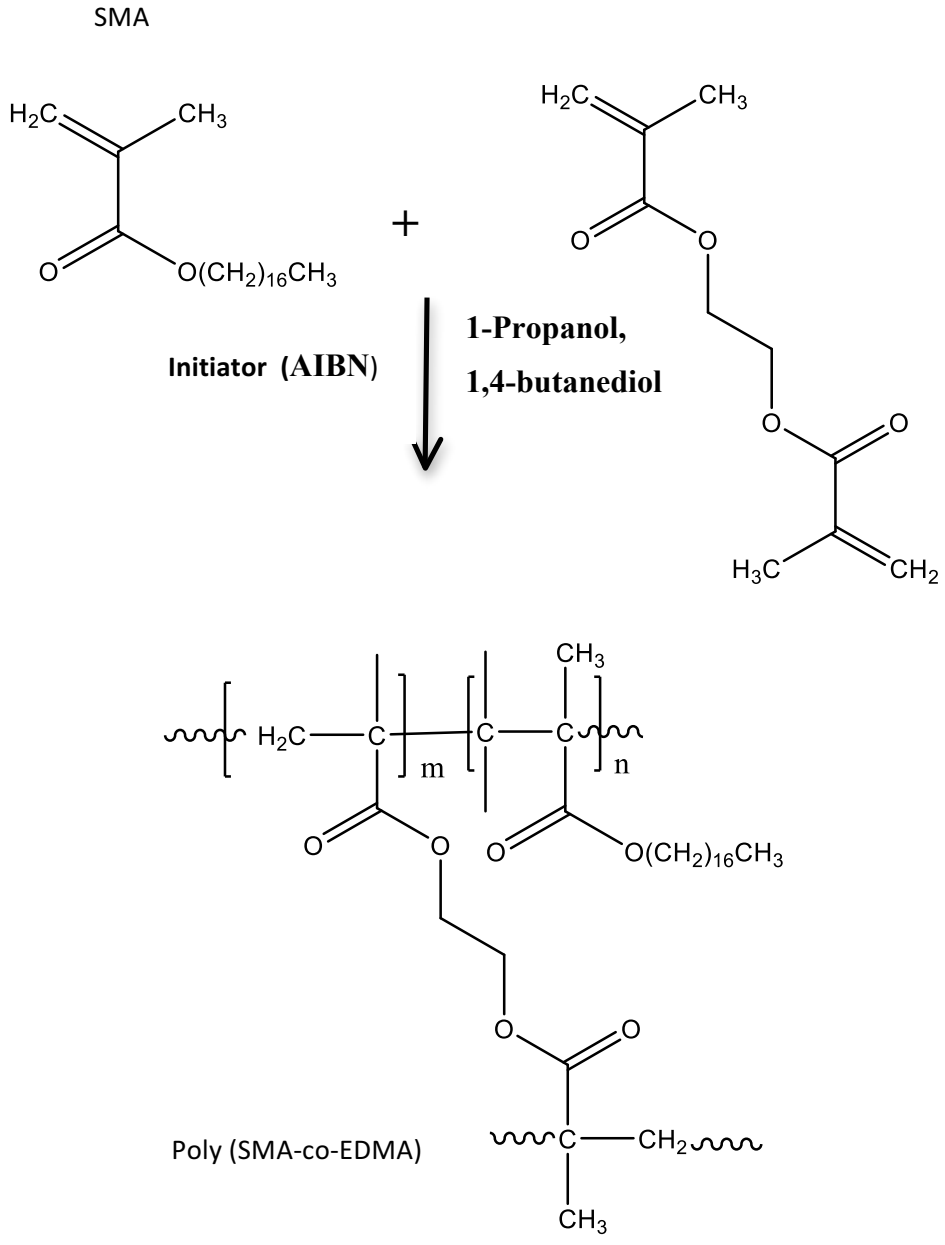

Figure 3-1: Structure of poly stearyl methacrylate monolithic capillary (poly (SMA-co-EDMA).

Table 3-1: Illustration of the composition of the polymerisation mixture.

	Monomer mixture		Porogen system		Initiator
Name of the monolith	Monomer (%, w/w)	Crosslinker (%, w/w)	1, 4-butanediol (%, w/w)	1-propanol (%, w/w)	AIBN*
SMA-co-EDMA	27%	8%	54%	11%	1%

* 1% with respect to the Monomer mixture.

3.1.4. **Chromatographic conditions**

For the analysis of the test mixture consisting of thiourea, dimethyl phthalate, anisole, and naphthalene and caffeine, the mobile phase used was H_2O/ACN in a ratio of 50:50 (V/V). When measuring the performance of all monolithic columns, a UV detector at 210 nm was employed, for the analysis of the test mixture, 210, 220, and 274 nm for the analysis of caffeine.

3.2. Results and discussions

3.2.1. Investigation into the prepared monolithic column Poly (SMA-co-EDMA)

The investigation into the prepared monolithic column was conducted using a test mixture of thiourea, dimethyl phthalate, anisole, and naphthalene. The chemical structures of these compounds with their associated logP were previously illustrated in Fig. 1.23. It could be observed from the logP that, used to indicate the polarity of a compound, this mixture contained two similar hydrophobic compounds, dimethyl phthalate and anisole as well as the highly hydrophobic naphthalene in the presence of thiourea as a dead volume marker [102].

3.2.2. Separation of test mixture

In order to resolve the test mixture, changes were made to the percentage of ACN in the mobile phase and the concentration of analytes in the mixture. The best resolution between the analytes under investigation was achieved in the presence of 50% ACN and 50% water (V/V) as shown in Fig. 3.2.

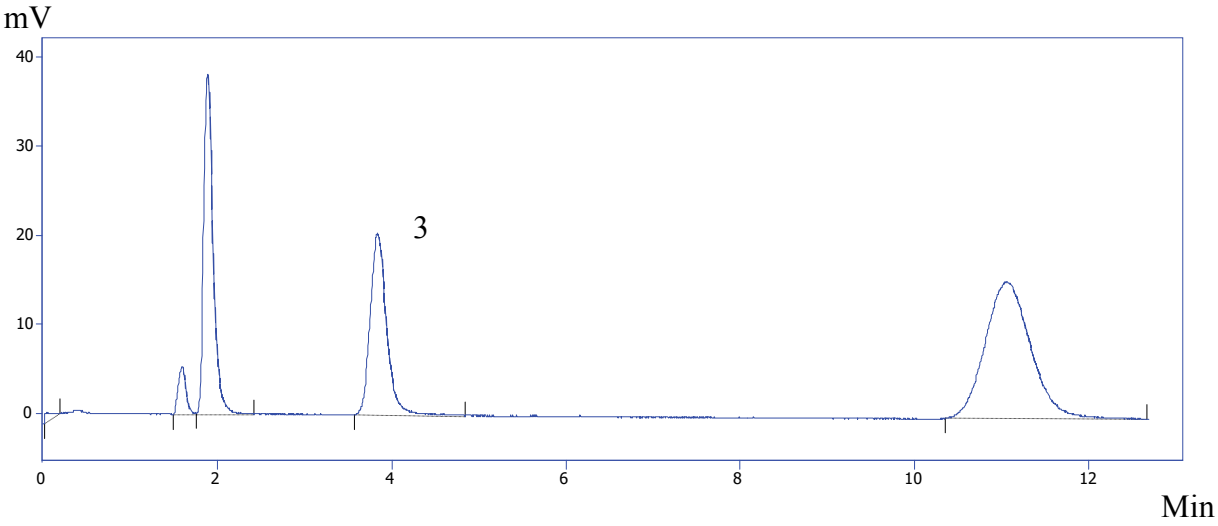

Figure 3-2: Chromatogram of test mixture with experimental conditions: column dimension 100 µm x 375 µm i.d., mobile phase 50% ACN 50% water (V/V), detection wavelength 210 nm, flow rate 1000 nl/min, injection volume 100 nl, samples: 1) thiourea, 2) dimethyl phthalate, 3) anisole, 4) naphthalene.

The next steps after resolving the mixture were the investigation of the separation mechanism of the prepared monolith, the column reproducibility, the column efficiency, column permeability, column porosity, and the application to the real sample.

As stated previously (section 1.7.8), the separation mechanism of a monolith is ascertained via the calculation of the retention factors (K) of the test mixture components in relation to the concentration of ACN in the mobile phase. If log K decreases linearly with the increase of the concentration of ACN, the mode of separation is RP-HPLC. If the opposite behavior is observed, the mode of separation is HILIC. The results obtained from this work confirmed that log k decreased linearly with an increase in the content of ACN illustrating the fact that the prepared monolith was governed by a reversed-phase mechanism. These results were in line with a previous study reported for the same monolith, using the same approach to determine the separation mode [74].

As mentioned in section 1.8.7, the reproducibility of a monolith is evaluated via the preparation of three monolithic columns from three different batches of monomers then calculating the RSD of the retention time of the test mixture. The obtained RSDs for thiourea, dimethyl phthalate, anisole and naphthalene were 1.09%, 0.92%, 0.45% and 0.45% respectively. Therefore, the prepared monolith exhibited good reproducibility.

3.2.3. **Column efficiency**

This was calculated via the equation presented in section 1.4.7. The number of theoretical plates per meter was around 7000 which was under the acceptable range. This low efficiency was attributed to the low amount of mesopores responsible for the separation, present in the prepared monolith [102]. However, the resolution of the separation looked promising, as shown previously in Fig. 3.2.

The efficiency of small molecules with organic monoliths is not as high as with silica monoliths. This is because the number of mesopores present in the former (organic monolith) is lower than those observed in the silica monolith. However, there are several approaches that can be used to make organic monoliths more suitable for small molecule analysis including optimising the polymerisation mixture including the concentration of monomers, concentration and types of porogenic solvent, and concentration of initiator. Additionally, there are less common approaches that have been adopted in the literature recently. , These include the use of a single crosslinker, a hyper-cross linker [103], a more polar cross linker, changing the polymerisation time, or using longer crosslinkers [104-106]. The following Chapter will investigate the effect of longer crosslinkers on the efficiency of the organic monoliths.

3.2.4. **Porosity Analysis**

For our research, a micro-HPLC system was employed to calculate the porosity using equation 1.18, presented in section 1.8.4.26. The porosity was calculated from the retention volume of the un-retained molecule thiourea. The porosity of the prepared monolith was calculated to be 0.69. This value was to some extent in line with a similar monolithic column manufactured previously following the same protocol, 0.72 [74].

This difference is due to the fact that the porogen system (1-propanol and 1,4-butanediol) used in this work was different to the ones used (1-propanol and iso-amyl alcohol) with same monomer mixture (SMA and EDMA). This, in turn, resulted in a decrease in porosity since the ratio and the type of porogenic solvents dramatically changed the porosity of the monolith, as stated in section 1.8 [74]. In order to improve the porosity of a monolith, the choice of porogenic solvents and controlling the amount of crosslinker have to be considered.

The choice of porogenic solvents affects the porosity directly as the porosity is dependent on the solubility of the polymer in the porogens. If the solubility is high, the separation phase taking place during the polymerisation process will be long leading to the formation of small pores, and ultimately the prepared monolith becomes non-porous. If the reverse occurs, large pores will be formed resulting in an increase in the void volume which ultimately affects the efficiency of the prepared column, as previously described in section 1.7.3.

3.2.5. **Permeability Analysis**

This was undertaken by pumping different mobile phases through the monolith including acetonitrile and water at flow rates ranging from 500 nl/min -2000 nl/min. The permeability of the prepared monolith was found to be 1.8.4.1, $12.04*10^{-14}$ and $11.86*10^{-14}$ for water and ACN respectively, calculated using the Darcy equation presented previously in Chapter 1. Figs 3.3 and 3.4 demonstrate the relationship between the flow rate and back pressure for permeability analysis when 100% ACN and 100% water were used as eluents respectively.

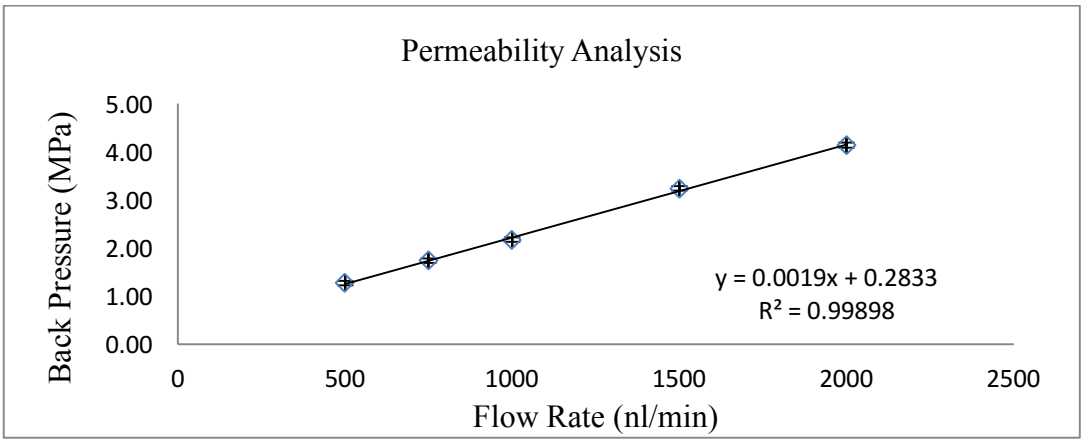

Figure 3-3: Demonstration of the relation between flow rate and back pressure for permeability analysis when 100% ACN was used as an eluent.

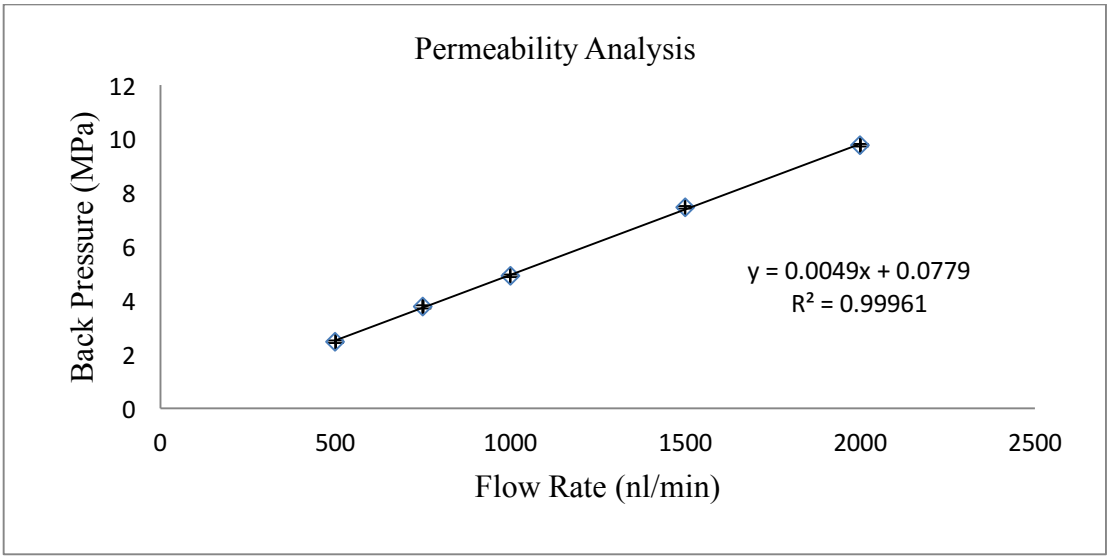

Figure 3-4: Demonstration of the relation between flow rate and back pressure for permeability analysis when 100% water was used as an eluent.

It is also evident from Figs. 3.3 and 3.4 that the relationship between the back pressure at different flow rates using water and ACN as eluents was linear with an excellent correlation coefficient (R^2) and as a result, the prepared monolith was deemed to be mechanically stable [74].

This linearity between the back pressures at different flow rates was also in agreement with both the Hagen–Poiseuille and Darcy's Laws. This law states that the pressure across a column is proportional to the viscosity of an eluent. Additionally, it was observed that the backpressure exhibited by ACN was lower than that exhibited by water under the investigated flow rates. This observation, therefore, indicated that the prepared monolithic columns showed no sign of swelling in the organic solvent. The swelling/shrinking of organic monoliths in organic solvents is considered to be one of their main disadvantages [20].

3.2.6. **Application of poly (SMA-co-EDMA)**

The analysis of caffeine in Arabic coffee was used to investigate the applicability of the prepared column for a real sample. Furthermore, since the prepared monolith is neutral, it was thought that the basic molecules studied in this work would not suffer from peak tailing observed customarily with RP-HPLC phases when basic molecules are analysed. The tailing is due to the secondary interaction between basic molecules and the ionised silanol groups which have a pKa of around 4.5. It is also postulated that the relatively polar site present in the prepared monolith, seen in Fig 3.1, would interact with the polar site of caffeine [72].

3.2.6.1. **Method development**

Firstly, a standard solution of caffeine was prepared and injected under the same conditions published previously [56, 101], particularly at 90% water and 10% ACN as seen in Fig. 3.5. However, due to a moderately high back pressure of around 10 MPa (100 bar, 1450 psi), near the upper limit of 15 MPa set by the pump manufacturer, a lower concentration of water was used in the mobile phase (50%) for subsequent analyses.

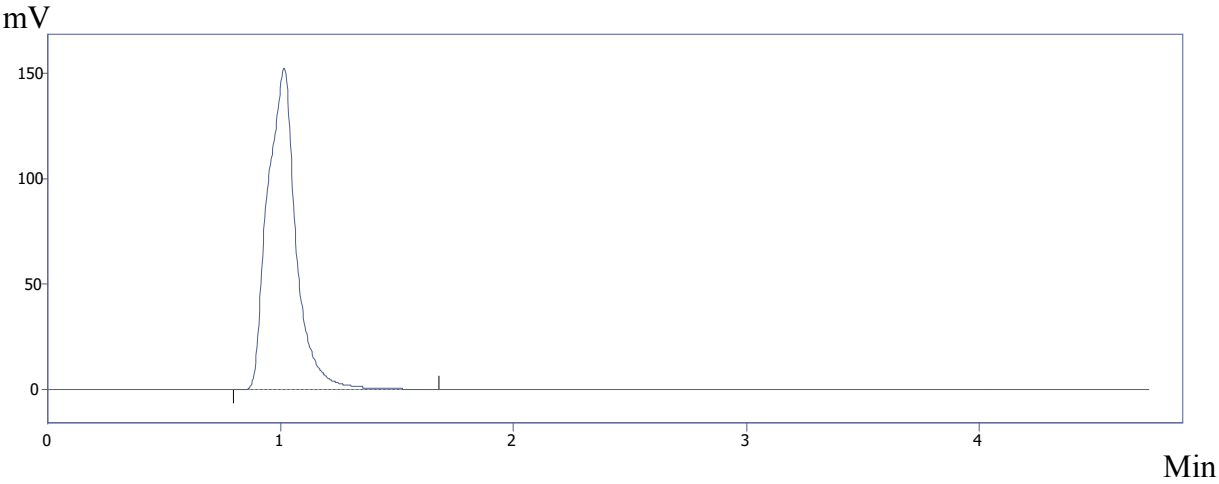

Figure 3-5: Caffeine chromatogram. Conditions: column dimension 100 um x 375 µm i.d., mobile phase 10% ACN 90% water (V/V), detection wavelength 274 nm, flow rate 1000 nl/min, injection volume 100 nl.

Secondly, based on the preliminary results, it was noticed that a wavelength of 210 nm was the best choice in terms of detector response (sensitivity) at the same concentration among all the investigated wavelengths i.e. 274, 220 and 210 nm, as seen in Fig 3.6. The choice of the investigated wavelengths was based on what has been published in the literature [56, 101].

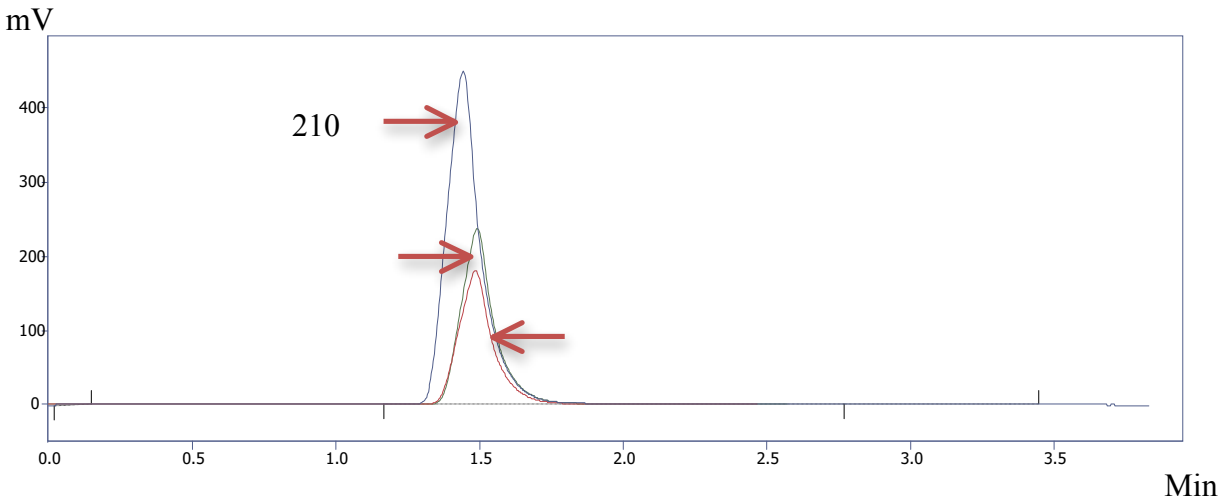

Figure 3-6: Chromatograms of caffeine mobile phase 50% ACN 50% water (V/V), detection wavelength (274, 220 and 210 nm). Other conditions are as stated in Fig.3.5.

3.2.6.2. **Method validation**

The developed method was validated based on the International Conference on Harmonisation (ICH) guidelines to check the reliability of the method [107]. The developed HPLC assay was validated in terms of linearity, precision, accuracy, L.O. D and L.O.Q, and selectivity.

3.2.6.2.1. Linearity

A series of working solutions were prepared ranging from 0.025 to 1.75 mM to construct a linear calibration curve in order to check the linearity of the developed method, as shown in Fig. 3.7.

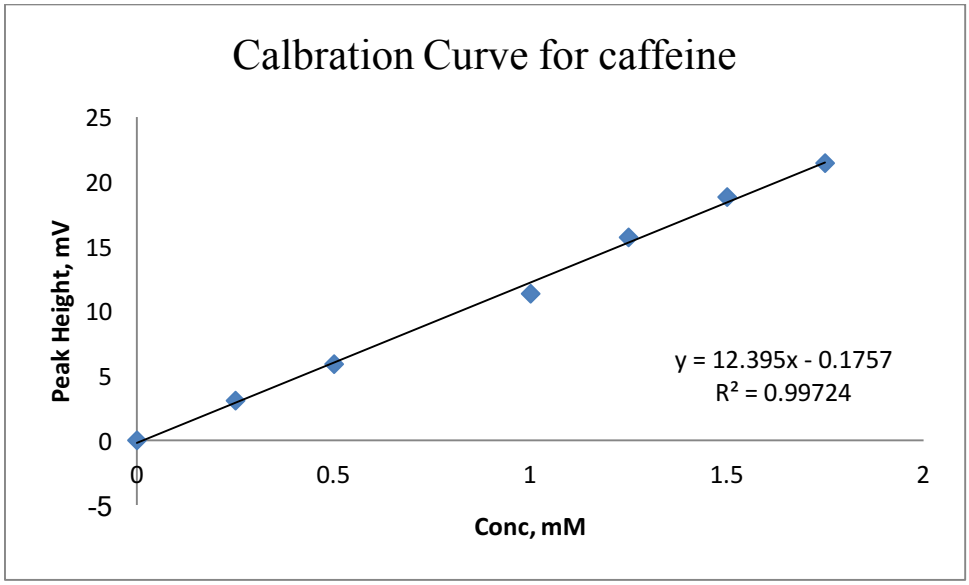

Figure 3-7: The calibration curve built for the developed method.

As can be observed from Fig.3.7, the correlation coefficient was higher than 0.995 indicating that the developed method was fit for the linearity within the investigated concentration range, 0.025 to 1.75 mM.

3.2.6.2.2. Precision

The repeatability of the retention time of caffeine was tested, n=3, and it was observed that the standard deviation was +/- 0.005 indicating that the method was precise, as illustrated in Table 3.2.

Table 3-2: The calibration curve built for the developed method.

Name of analyte	Run 1 (min)	Run 2 (min)	Run 3 (min)	Mean	SD
Caffeine	1.45	1.44	1.45	1.44	+/- 0.005

3.2.6.2.3. Accuracy

This was calculated by injecting a known concentration, 0.075 mM, of a reference standard caffeine solution and comparing the obtained result with the linearity equation, shown in Fig. 3.7. From the comparison, the method was found to be accurate as the recovery was in the acceptable range, (80%-120%) [107].

3.2.6.2.4. Limit of detection and limit of quantification (L.O.D, L.O.Q)

There are several ways to calculate L.O.D and L.O.Q, one of which is through the constructed calibration curve above using the equations mentioned below.

$$\mathbf{L.O.D} = \frac{\mathbf{3.3\,\sigma}}{\mathbf{S}} \qquad 3.1$$

$$\mathbf{L.O.Q} = \frac{\mathbf{10\sigma}}{\mathbf{S}} \qquad 3.2$$

Where S is the slope of the calibration curve and σ is standard deviation, both calculated via Excel software, Microsoft office 2010.

Based on the equation obtained from the calibration curve, observed in Fig 3.7, and the equations mentioned above (3.1, 3.2), the L.O.D and L.O.Q were 0.0023 mg/ml and 0.0071 mg/ml respectively. Therefore, the developed method showed higher sensitivity for the determination of caffeine in comparison to the previous work. This was attributed to the difference of the chromatographic method in this work to what was found previously in the literature [56, 101].

3.2.6.2.5. Selectivity

The selectivity of the developed method was examined via probing the efficiency of separation of the chromatographic system under the developed conditions against a compound structurally similar to caffeine which was in our case was theophylline, as seen in Fig 3.8.

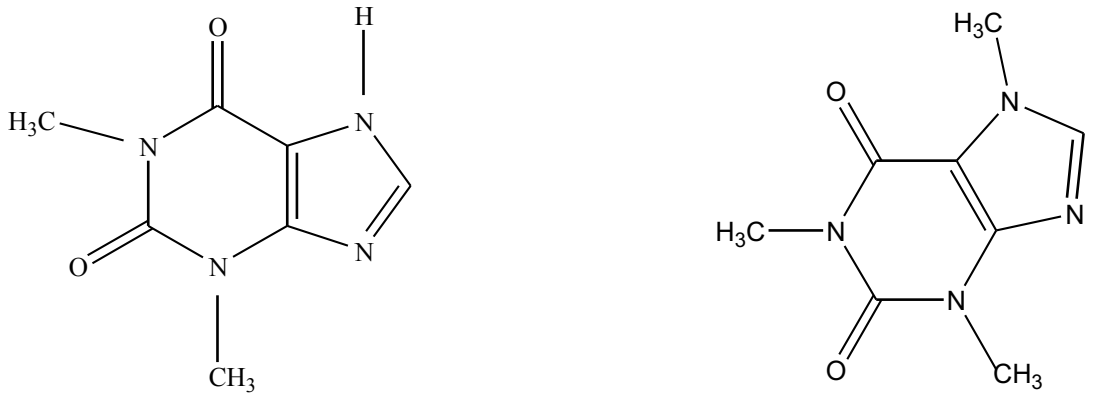

Theophylline **Caffeine**

Figure 3-8: Structures of molecules used for the selectivity test.

Several attempts have been made to separate these two molecules including investigation of the effect of organic solvent ACN (50%/40%/20%/10%), V/V, and investigation of the effect of pH including (12/9/7/3/2).

All the attempts employed to resolve these test probes failed, despite the use of a neutral monolith and the presence of relatively polar ester groups in the monolith structure (Fig 3.1). The ester group was expected to play a major role in separating the two polar basic polar molecules in this work since this poly (SMA-co-EDMA) monolith was previously used by Chaisuwan et al. to separate two polar molecules, β- and ɤ-tocopherol.

The relatively polar ester groups of the monolith interacted with the hydroxyl group on the structure of the tocopherols, so providing better selectivity than the previously used C_{18} and C_8 columns, the most used RP-HPLC phases [72]. However, the test analytes used here (caffeine and theophylline) can alternatively be separated on a silica monolith using 90% water and 10 % ACN as the mobile phase [101] or using HILIC mode [108].

3.2.7. **Analysis of a real sample**

3.2.7.1. **The efficiency of the extraction method used to analyse caffeine in Arabic coffee.**

It is vital to validate an extraction method so that the obtained results are reliable and precise; otherwise, the obtained results would be misleading and inaccurate [109]. The extraction procedure followed in this work for the determination of caffeine in coffee samples has already been validated and published in previous work, giving accurate and precise results [56].

3.2.7.2. **Determination of caffeine in coffee sample**

This was undertaken via the determination of caffeine in an Arabic coffee as an application for the prepared monolithic column.

The concentration of caffeine in the Arabic coffee was found to be 0.03 mg/ml, calculated using the calibration equation shown previously in Fig 3.7. This concentration is also in line with that found previously indicating that the adopted extraction method was carried out precisely [56, 110]. It could, therefore, be suggested that the method adopted in this work is transferable and reproducible, as it has led to the same result as previously published.

The extraction method adopted in this work is considered to be more environmentally friendly [111] than the previous method of extracting caffeine from coffee (i.e. with chloroform), as only water was used for the extraction.

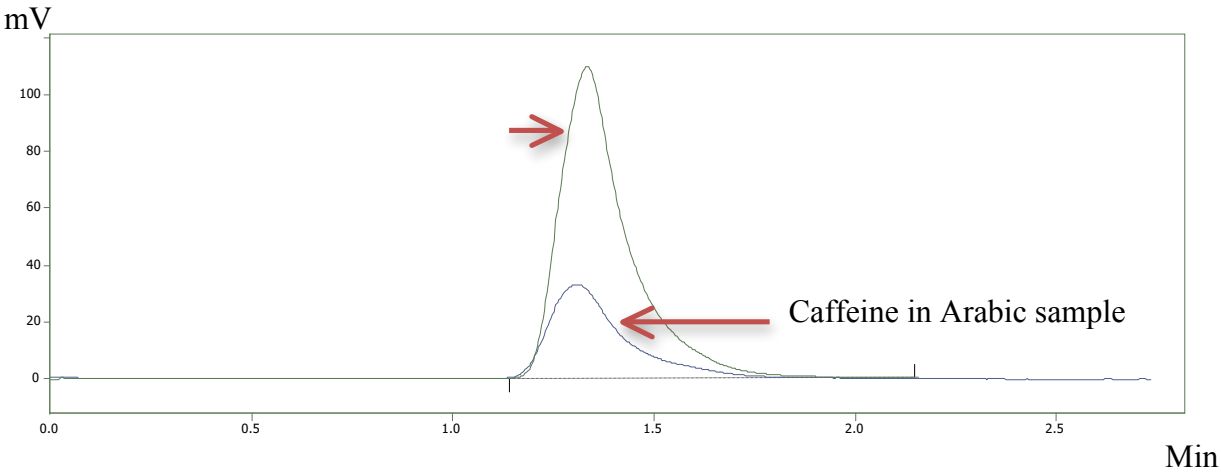

Figure 3-9: Chromatograms represent the caffeine with coffee sample for comparison. Other conditions are as stated in Figure 3.7.

It is clear from Fig 3.9 that the retention time of the peak attributed to caffeine from the Arabic coffee was identical to that obtained with the caffeine standard under the same chromatographic conditions, thus confirming the presence of caffeine.

There are various approaches which could be used to ascertain whether or not co-elution takes place, including the comparison of mass spectra [112], or scanning UV-VIS spectra [89], with those of standards. Since these techniques could not be incorporated into the micro-HPLC instrumental set-up when this piece of work was conducted, components which co-elute with caffeine in the coffee extract could not be entirely ruled out.

3.3. Conclusion

The poly (SMA-co-EDMA) monolithic column in a 100 μm i.d. fused silica capillary was fabricated and used as a stationary phase in capillary liquid chromatography. The fabricated column was assessed in terms of mechanism of separation, reproducibility of the monolith, porosity, and permeability. Furthermore, the fabricated monolith lacked any shrinking or swelling issues which could be considered as an advantage because of the known issues of shrinking/ swelling with organic monoliths when using organic solvents as stated previously (section 1.7.9). Moreover, modifying the monomer mixture from what was published previously by changing the porogen from iso-amyl alcohol to 1-propanol did not improve the porosity suggesting that the polymerisation mixture needs to be carefully modified in order to obtain the desired porosity and efficiency. Additionally, the reproducibility of fabrication in terms of the retention times of the analytes investigated was found to be high. The efficiency of this monolith was however not high due to the low amounts of mesopores (low surface area).

Furthermore, the monolith prepared was applied for the determination of the concentration of caffeine in Arabic coffee. It was also noted that when the criterion of selectivity was investigated, the probes used (caffeine and theophylline) were not resolved indicating that either silica or HILIC monoliths could be better candidates for resolving such polar analytes. It was also observed that caffeine was poorly retained on the monolith since its retention time was similar to un-retained thiourea. However, a linear relationship between the peak height and the concentration of caffeine was successfully obtained as observed in Fig. 3.7.

Since this project is focused on the fabrication of efficient monoliths, the following Chapter will therefore concentrate on the improvement of the efficiency of organic monoliths via the use of longer crosslinkers.

Chapter 4

Efficiency improvement of organic monoliths using longer cross-linker

4. Introduction

Over the past decade, great interest has been directed towards micro-HPLC and its rapid development for various applications, including those in the life sciences, the pharmaceutical industry, and environmental analyses. However, the inherent limitations of conventional packed columns, such as slow mass transfer, large void times and the difficultly of designing well-packed columns, have simultaneously driven the growth of alternative separation materials such as monoliths [49].

Polymer-based monoliths are commonly prepared by in situ polymerisation, employing either thermal initiation [113, 114] or photo-chemical initiation [115], via free-radical cross-linking polymerisation. The alternative ring-opening metathesis polymerisation (ROMP) can also be used as a common approach to synthesise polymer- based monoliths [116-118]. ROMP employs a transition metal as a catalyst for the polymerisation of the monolith [118].

Organic based monoliths are often characterised by a monomodel macropores pore size distribution and are, therefore, used for the separation of large molecules such as proteins and peptides. This limitation for organic monoliths is due to the low number of mesopores [115, 119]. Previously, several approaches have been employed to allow the separation of small molecules on organic based monoliths including optimisation of polymerisation conditions by increasing or decreasing the temperature for initiation of the polymerisation process [120, 121], changing monomers [103], and changing porogens and changing the time for polymerisation [122]. However, these approaches did not improve the applicability of the organic monoliths to the desired degree and also involve tedious optimisation work [123,

124]. More recently, several alternative approaches have been reported in the literature to enhance the applicability of organic monoliths for the separation of small molecules. These include an early termination of the polymerisation process [125], using single crosslinkers [126, 127], application of hyper-crosslinking [103], utilisation of carbon nanostructure [128], using longer crosslinkers for reversed-phase chromatography (RP-HPLC) [106], or using more polar crosslinkers when applying hydrophilic liquid chromatography (HILIC) [129].

In the study described here, the effects of crosslinker length on the separation efficiencies of small molecules have been investigated by utilising two crosslinkers (their chemical structures are shown below in Fig.4.1). The crosslinkers used in this investigation were ethylene dimethacrylate (EDMA) and 1,6-hexanediol ethoxylate diacrylate (1,6-HEDA). The efficiency of the 1,6-HEDA based monolith was found to be superior to the EDMA based column; accordingly, the porosity, permeability, and reproducibility of the 1,6-HEDA based monolith poly HMA-co-1,6-HEDA were solely further characterised. Furthermore, the effect of ACN content in the mobile phase on the retention factor and plate height for the retained molecules (anisole, naphthalene) was investigated for 1, 6-HEDA based monolith. The van Deemter plot for the most retained molecule (naphthalene) was also examined. In addition, the poly (HMA-co-1,6-HEDA) monolith was used for the separation of neutral non-polar molecules, weak acid molecules, and basic molecules to demonstrate the monolith's various applications. Furthermore, the poly (HMA-co-1,6-HEDA) was utilised to quantify amitriptyline in commercial pharmaceutical tablets.

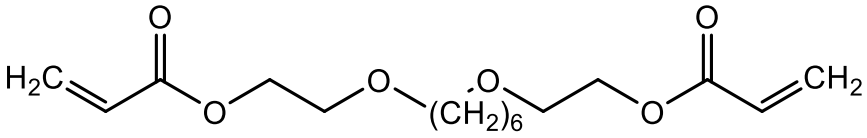

1,6 HEDA (Cross-linker)

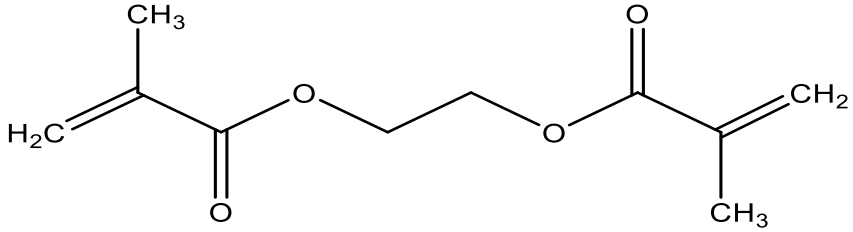

EDMA (Cross-linker)

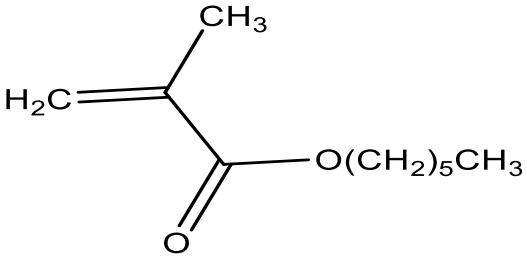

HMA (Monomer)

Figure 4-1: Monomer and crosslinkers used in the study.

4.1. Experimental

4.1.1. Reagents and materials

Hexyl methacrylate (HMA) was purchased from Lancaster, United Kingdom. 1,6-hexanediol ethoxylate diacrylate (1,6-HEDA) was purchased from Santa Cruz Biotechnology, Germany. Ethylene dimethacrylate (EDMA), 3-(trimethoxysilyl) propyl methacrylate (γ-MAPS), 1, 4-butanediol, 1-propanol, azobisisobutyronitrile (AIBN), sodium hydroxide, thiourea, dimethyl phthalate, anisole, naphthalene, phenol, and nortriptyline were all obtained from Aldrich Chemicals (Steinheim, Germany). Ammonium bicarbonate was purchased from Fluka (Steinheim, Germany). HPLC-grade methanol and acetonitrile (ACN) were bought from Fisher Scientific (Leicestershire, UK). Disodium hydrogen phosphate anhydrous was purchased from Fisons Scientific Equipment (Loughborough, UK). Ammonium formate, acetophenone, butyrophenone, valerophenone, hexanophenone, 4-methoxy-phenol, p-chlorophenol, p-bromophenol, quinine, and amitriptyline were all obtained from Aldrich (Poole, UK). Pharmaceutical tablets were kindly provided by King's College Pharmacy Department. Water used throughout all experiments was purified using a Millipore System model no. SYNSV0000. pH indicator paper was purchased from Camlab House (Cambridge, UK). The fused silica capillaries were supplied from CM Scientific (Silsden, United Kingdom, Part no. TSP100375).

4.1.2. **Instrumentations**

An oven was employed for the thermal polymerisation. A microscope was used for investigating the presence of air bubbles inside the capillary column and the confirmation of the introduction of the polymerisation mixture within the capillary. Nano-HPLC experiments were carried out using Dina system. A centrifuge was used to sediment suspended solids. A SEM was used to investigate the morphology of the monolith, more details about these instruments, i.e. model/make, manufacturer's details have already been stated in Chapter **2** (section 2.2).

4.1.3. **Monolithic preparations**

The general protocol followed in synthesising the monolithic columns in this Chapter has been already mentioned in Chapter **2**, specifically, section 2.1.1. The co-polymerisation scheme of the selected monomers and porogens is demonstrated in Fig 4.2. Table 4.1 illustrates the composition of the polymerisation mixture.

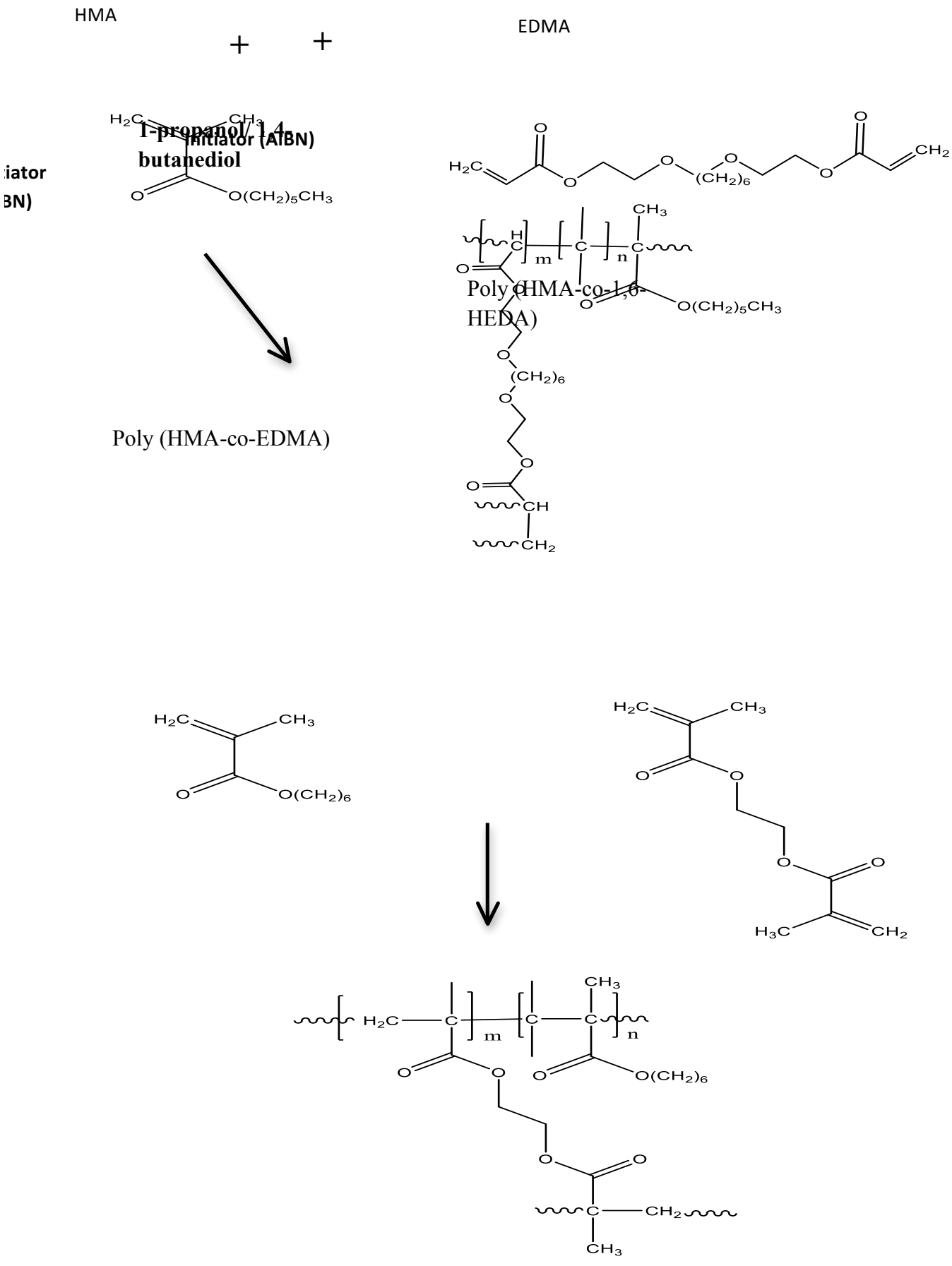

Figure 4-2: The co-polymerisation scheme of the selected monomers and porogens: A, poly (HMA-co-1,6-HEDA), B, poly (HMA-co-EDMA).

Table 4-1: Compositions of the mixtures used for preparation of monolithic columns (g/wt. %)*

	Monomer mixture		Porogen system		initiator
Name of the monolith	Monomer (%, w/w)	Crosslinker (%, w/w)	1, 4-butanediol (%, w/w)	1-propanol (%, w/w)	AIBN*
HMA-co-EDMA	12%	18%	35%	35%	1%
HMA-co-1,6 HEDA	12%	18%	35%	35%	1%

* 1% with respect to the Monomer mixture.

[130, 131].

4.1.4. **Preparation of stock solutions**

The appropriate amount of ammonium formate was dissolved in HPLC-grade water to obtain the required concentration. Additionally, the appropriate amount of di-sodium hydrogen phosphate was dissolved in HPLC-grade water and then adjusted with sodium hydroxide to the desired pH. Furthermore, the proper amount of ammonium bicarbonate was dissolved in HPLC-grade water followed by adjusting with sodium hydroxide to obtain the required pH. All mobile phases were filtered through a 0.22 µm membrane filter prior to use. All analyte mixtures were prepared in the relevant mobile phase in order to obtain good shape peaks and avoid peak distortion.

4.1.5. **Preparation of stock solutions for amitriptyline analysis**

A standard 1 mg/ml stock solution of amitriptyline was prepared by dissolving it in the mobile phase used (34% 5 mM ammonium bicarbonate (pH 12)/ 66% ACN), V/V, in order to obtain good shape peaks.

The working standard solutions ranging from 200 -6.4 µg/ml were prepared by appropriate dilutions of the stock solution using the mobile phase as diluent. 5 mM ammonium bicarbonate solution was made and adjusted to the required pH 12 using ammonium hydroxide.

4.1.6. **Extraction process of the amitriptyline tablet**

10 tablets were weighed in order to exactly identify the average weight of each tablet, 140 mg. Then, the tablets were ground using a mortar and pestle to obtain a fine powder. Subsequently, 140 mg was dissolved in 15ml of the corresponding mobile phase used for analysis. This solution was then sonicated for 20 mins followed by centrifuging for 20 mins at 2500 RPM.

4.1.7. **Chromatographic conditions**

For the analysis of the test mixture consisting of thiourea, dimethyl phthalate, anisole, and naphthalene, the mobile phase used was H_2O /ACN in a 40:60 ratio,(V/V). For the separation of neutral non-polar compounds including acetophenone, butyrophenone, valerophenone, and hexanophenone, the mobile phase was 5 mM ammonium formate (pH 6.4)/ACN in a 50:50 ratio (V/V). As to the analysis of weakly acidic compounds consisting of 4-methoxy-phenol, phenol, p-chlorophenol, p-bromophenol, the mobile phase was 5 mM sodium phosphate (pH8)/ACN in a 50:50 ratio, (V/V). 5 mM ammonium bicarbonate (pH 12) combined with ACN in a 34:66 ratio (V/V) was employed as the mobile phase for the separation of basic compounds including Quinine, amitriptyline and amitriptyline. A UV detector was employed using a wavelength of 210 nm for the analysis of the test mixture measuring the performance of all monolithic columns, and 214 nm for the analysis of neutral non-polar compounds, weak acids, and basic compounds and the quantification of amitriptyline in the marketed pharmaceutical tablets.

4.2. Results and discussions

4.2.1. Separation efficiency for 1,6-HEDA and EDMA monoliths using a test mixture

Often separation efficiencies using organic monoliths for small molecules are not high compared with silica monoliths. This is because the numbers of mesopores in organic monoliths (less than 50 nm) are not as high as present in silica monoliths. However, several approaches reported in the literature that enable organic monoliths to be employed for the analysis of small molecules. These include optimising the concentration of monomers, concentration and types of porogen solvent, and concentration of initiator [115, 119]. Recently, some more successful approaches have been adopted which includes the use of single crosslinkers, hyper-crosslinkers, using shorter polymerisation times, and using longer crosslinkers [105, 106].

In this study, the monomer HMA was employed with two different crosslinkers including EDMA and 1,6-HEDA in order to investigate the effect of cross-linker length on efficiencies for small molecules. To that end, a test mixture consisting of thiourea, dimethyl phthalate, anisole, and naphthalene was used. In order to obtain a reliable comparison, the same chromatographic conditions including mobile phase concentrations, flow rate, and wavelength were employed for both 1,6-HEDA-based and EDMA-based columns. As shown in Fig 4.3a, baseline separation was achieved for the 1,6-HEDA monolith, while in Fig 4.3b it can be seen that thiourea co-eluted with dimethyl phthalate on the EDMA monolith. Also, it was observed that the 1,6-HEDA-based monolith gave an efficiency of 32000 p/m for the retained molecule naphthalene, while the efficiency for the same compound on the EDMA monolith based was 3548 p/m.

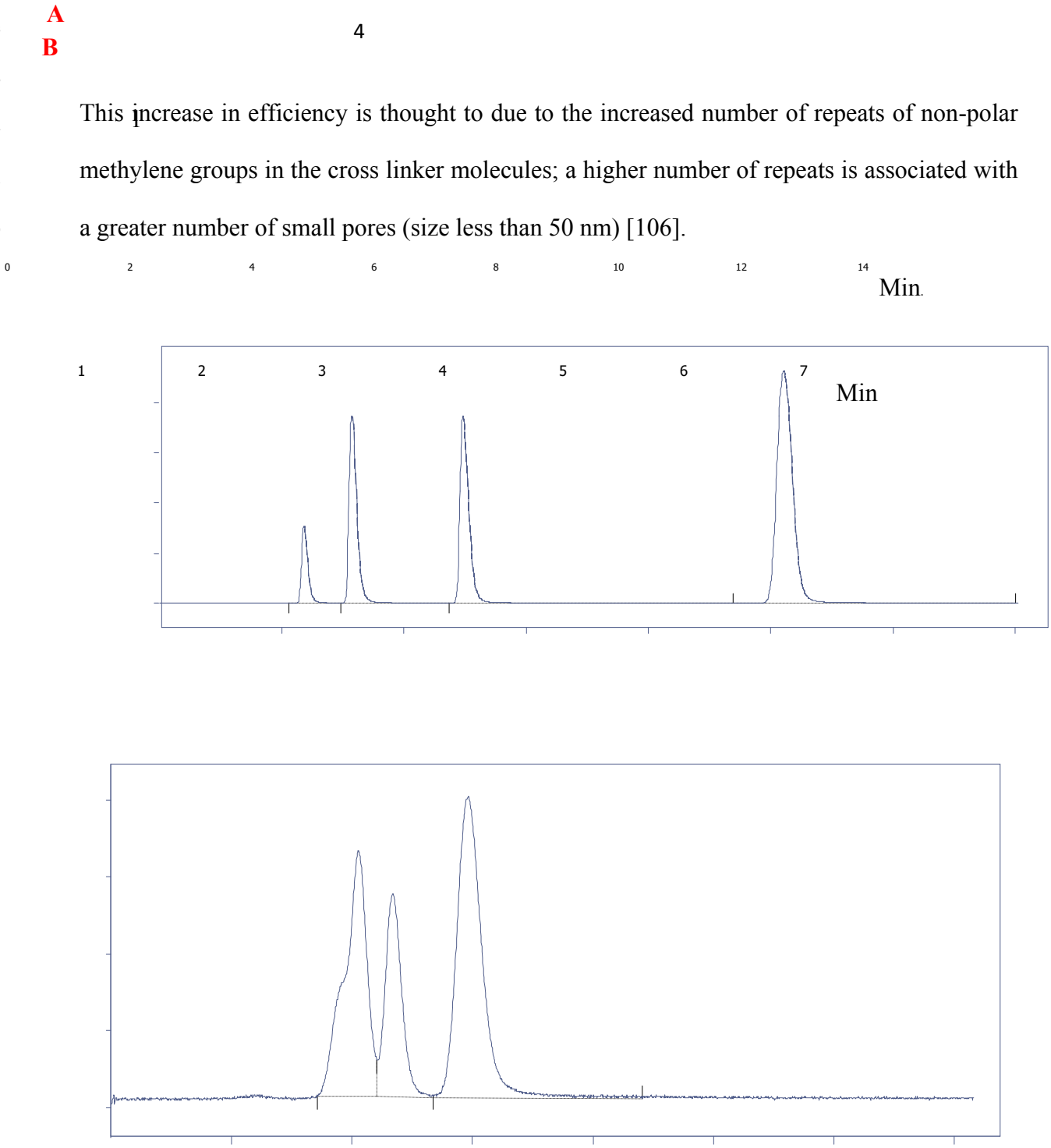

This increase in efficiency is thought to due to the increased number of repeats of non-polar methylene groups in the cross linker molecules; a higher number of repeats is associated with a greater number of small pores (size less than 50 nm) [106].

Figure 4-3: Efficiency test, (A) Illustration of the chromatogram of test mixture using the 1,6-HEDA based monolith (B) Illustration of the chromatogram of test mixture using the EDMA based monolith. Experimental conditions: column dimension 100 µm i.d. x 375 um o.d., mobile phase 40:60 (V/V) (H2O: ACN), detection wavelength 210 nm, flow rate 1000 nL/min, injection volume 100 nl, samples: 1) thiourea, 2) dimethyl phthalate, 3) anisole, 4) naphthalene.

The results obtained in this Chapter are in agreement with the previous findings; Pavel et al. [106, 129] have conducted two extensive studies on the effect of crosslinkers on the efficiency for small molecule separation on capillary monolithic columns using RP-HPLC and HILIC. In the study of RP-HPLC, three different crosslinkers namely EDMA, BUDMA, and HEDMA co-polymerised with the functional monomer LMA were compared. it was found that the efficiency increased with an increase in the number of repeats of non-polar methylene groups from two to six in the cross linker molecules attributed to higher amounts of small pores with size less than 50 nm (more surface area) [106]. This result was also in line with another study conducted by Wang et al. [132] in which several alkyl dimethacrylate crosslinkers differing in the methylene groups from two to nine were compared; it was found that the efficiency increased as the chain length of the crosslinker increased. In a recent study, Fuh et al. [104] prepared three monoliths with three different crosslinkers and found that as the polarity of the cross-linker increased, the resolution, efficiency and separation for polar small molecules increased. In another study carried out by Li et al. on poly (SMA-co-PEGMEMA-co-EDMA), it was also found that the hydrophilic PEG functionality assisted in increasing the efficiency and retention for small molecules [133].

The efficiency of 1,6-HEDA-based monoliths in this Chapter showed a higher efficiency (32000 p/m) when compared with a study reported by Lin et al. In the Lin's study, the crosslinker 1,6-HEDA when co-polymerised with other functional monomers (namely BMA, LMA, and SMA) gave efficiencies for the most retained molecule 2,3,5- trichlorophenol (2,3,5 TCP) of 15600, 25100, 27300 p/m respectively [104]. Chromatographic characteristics on poly (HMA-co-1,6-HEDA) monolith including separation efficiency, plate heights, retention factor and resolution for the retained molecules are summarised in Table 4.2.

Table 4-2: Chromatographic characteristics on poly (HMA-co-1,6 HEDA) monolith[a].

Analyte	Separation efficiency (P/M)	Plate height (um)	Retention factor (k) [b]
Anisole	24635	13.40	1.15
Naphthalene	32000	10.32	3.38

Chromatographic conditions as shown in Fig 4.2a. [b] k= (t_0-tm/t_0) equation, t_0 is the elution time of the thiourea and tm is the time of the retained molecule.

In the light of the studies mentioned above [104, 129, 132] and results presented in Fig.4.3, the 1,6-HEDA-based monoliths performed markedly better than the EDMA-based column in terms of separation efficiency. Hence, the 1,6-HEDA-based monolith was only considered for further characterisations.

4.3. Characterisation of 1,6-HEDA- monolith based.

4.3.1. **Porosity (Ɛ)**

It is well established that the porosity of a methacrylate ester based monolith column can be changed with slight alterations to the total polymerisation mixture. Mercury intrusion porosimetry is commonly employed to investigate the mean pore size of monoliths [74]; unfortunately, such an instrument was not available during this research program [134]. In order to evaluate the porosity of the synthesised monolith, SEM and micro-HPLC were employed. The total porosity of the monolith was 84% based on micro-HPLC, as shown in Table 4.3, and was calculated from the elution time/volume of an un-retained molecule (thiourea) and the geometrical volume of the column, calculated using equation 1.18 (Chapter **1**)

This result indicated the presence of large-pores which explained the observed low back pressure [104].

4.3.2. **Permeability (K)**

As defined previously, permeability describes the degree of resistance of the prepared monolith to the flow of mobile phase. The goal of conducting permeability analysis was to determine whether the prepared monolith suffers from the phenomenon of shrinking or swelling [74]. The permeability was found to be 7.2×10^{-14} and 1.4×10^{-13} for ACN and water respectively, using the equation 1.17, stated in Chapter **1**.

It was also observed that the relationship between the back pressure at different flow rates with the eluents used, water and ACN, was linear giving a high correlation coefficient (R^2) 0.995, shown in Fig. 4.4. As a result, the prepared monolith was deemed to be mechanically stable [135]. The viscosity of water and ACN at room temperature are 0.890×10^{-3}, and 0.369×10^{-3} Pa.s, respectively [136]).

Figure 4-4: Permeability analysis.

As stated previously, this linearity between back pressure *vs.* flow rates was also in agreement with Hagen–Poiseuille and Darcy's Law [74]. It was also observed that the back pressure exhibited in ACN was lower than that seen in water at the investigated flow rates. This observation demonstrated the stability of the prepared monolithic columns and lack of any swelling/shrinking in the presence of organic solvents [68].

Table 4-3: Chracterisation of a poly (HMA-co-1, 6 HEDA) monolith.

Monolith	Porosity [a] (%)	Permeability [b] (K)	Efficiency [c](p/m)
HMA-co-1,6-HEDA	84	$7.2*10^{-14}$	31989

a) The total porosity was calculated based on equation 1.18 .
b) The permeability was calculated based on equation 1.17, using ACN.
c) Column efficiency was measured for the most retained molecule, naphthalene.

4.3.3. **Evaluation of 1,6-HEDA based monolith for reversed-phase capillary chromatography**

In order to further investigate the performance of the prepared monolith, the retained molecules including anisole and naphthalene were used to assess the effect of % ACN in the mobile phase on the retention factor shown in Fig 4.5. It can be seen from Fig. 4.5 that the retention factors for the retained molecules decreased as the % ACN in the mobile phase increased, demonstrating a typical RP-HPLC behavior [134, 135, 137]. This typical non-linear behavior was also seen in the study carried out by Lin et al. on the poly (LMA-co-1,6-HEDA) monolith. In the study, four small aromatic molecules (benzyl alcohol, phenol, benzene, and toluene) were used to examine the influence of ACN concentration in the mobile phase on the retention factor. This behavior is thought to be due to the variation of partition and adsorption phenomenon of the retained molecules with the mobile phase composition [138].

Figure 4-5: Effect of ACN on retained molecules.

Fig.4.6 shows the effect of % ACN in the mobile phase on plate height. At 50% ACN the plate heights for anisole and naphthalene were 13.29 μm and 10.20 μm. Then, the associated plate heights decreased linearly as the concentration of ACN increased, reaching 9.68 μm and 8.22 μm at 65%ACN, followed by a noticeable rise at 70% reaching 15.34 μm and 12.44 μm respectively. This apparent rise was also observed in a study conducted by Causon et al. [137]. In the study, the plate heights of some small molecules including benzene, toluene, ethylbenzene, phenol, and benzene alcohol soared as the concentration of ACN increased, reaching a plate height maximum at 90%, in particular for the most retained molecules.

Figure 4-6: Effect of % ACN in the mobile phase on plate height.

Fig.4.7 depicts the plate height curve for the most retained molecule (naphthalene) at 60% ACN at room temperature within the range of 0.82 mm/s to 2.01 mm/s. The plate heights for naphthalene were < 10 μm and the optimum linear velocity at 1.01 mm/s gave the lowest plate height specifically 8 μm. These figures were calculated using equation 1.9 (Chapter **1**, section 1.6) . The small plate heights were also found on the poly (LMA-co-1,6- HEDA) monolith synthesised by Lin et al. [104]. Therefore, the small plate heights at high linear velocity could indicate the possible rapid separation for small molecules on the synthesised monolith (HMA-co-1,6-HEDA).

Fig.4.7 also shows that the plot was not noticeably affected by higher linear velocities demonstrating that the wide range of usable linear velocities with less peak dispersion (no sacrifice in efficiency). This wide range of linear velocities is considered to be a great advantage [73].

Figure 4-7: Illustration of the plate height curve for the most retained molecule (naphthalene) at 60%.

4.3.4. **Reproducibility**

The reproducibility of the monolith was evaluated by fabricating three monolithic columns from the same polymerisation mixture, using the same test mixture mentioned in Fig.4.3, then calculating the RSDs of their retention times [139]. The RSDs obtained for thiourea, dimethyl phthalate, anisole and naphthalene were 1.12%, 0.66%, 1.5%, and 2.39% respectively indicating that the prepared monolith exhibited good reproducibility.

4.4. Applications on a poly (HMA-co-1, 6-HEDA) monolith

4.4.1. **Separation of neutral non-polar compounds**

Since this monolith displayed a reversed-phase separation mechanism, a set of alkylphenones including acetophenone, butyrophenone, valerophenone, and hexanophenone was used to analyse its separation capabilities. As illustrated in Fig 4.8, baseline separation was achieved using isocratic elution in 50:50 (V/V) 5 mM ammonium formate (pH 6.4)/ACN. As anticipated, the elution order achieved was in agreement with a reversed-phase mechanism; as recently verified with a reversed-phase monolith consisting of poly (AOD-co-EDMA), hydrophobic interactions are responsible for the retention of the analysed compounds [140].

1

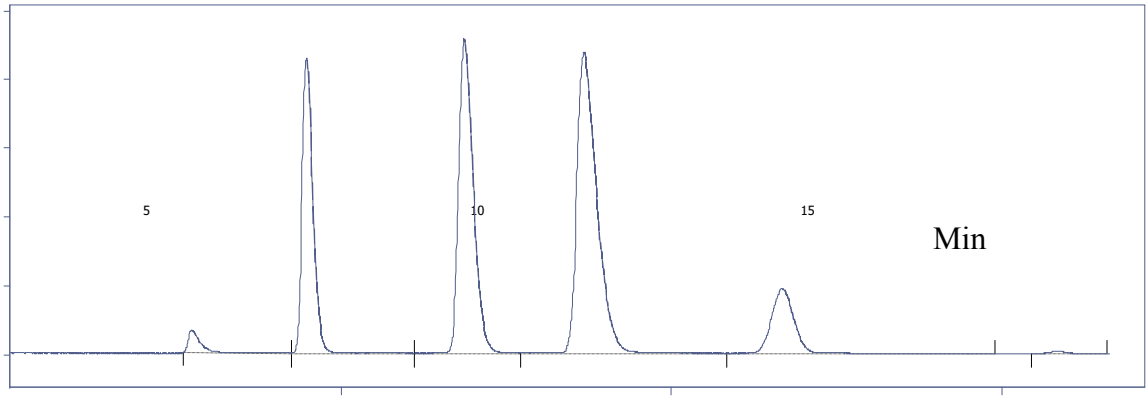

Figure 4-8: Separation of neutral compounds, a poly (HMA-co-1,6-HEDA) monolith with experimental conditions: 50:50 (V/V) (5mM ammonium formate pH 6.4: ACN), detection wavelength 214 nm, samples: 1) acetophenone, 2) butyrophenone, 3) valerophenone, 4) hexanophenone. Other conditions are as stated in Fig.4.3.

4.4.2. **Separation of weak acids**

Phenols represent a large class of environmental pollutants; therefore, the separation of four phenols was investigated on the poly (HMA-co-1,6-HEDA) monolith using an isocratic method with 50:50 (V/V) 5 mM phosphate (pH 8)/ACN as the mobile phase. A typical resultant chromatogram is shown in Fig.4.9, and it can be observed that baseline separation for all four compounds was obtained in under 8 mins. The elution order of the compounds investigated was in agreement with a reversed-phase monolith consisting of poly (PEDAS-co-SEMA-co-EDMA), confirming that hydrophobic interaction was responsible for retention of the analysed compounds [139].

1

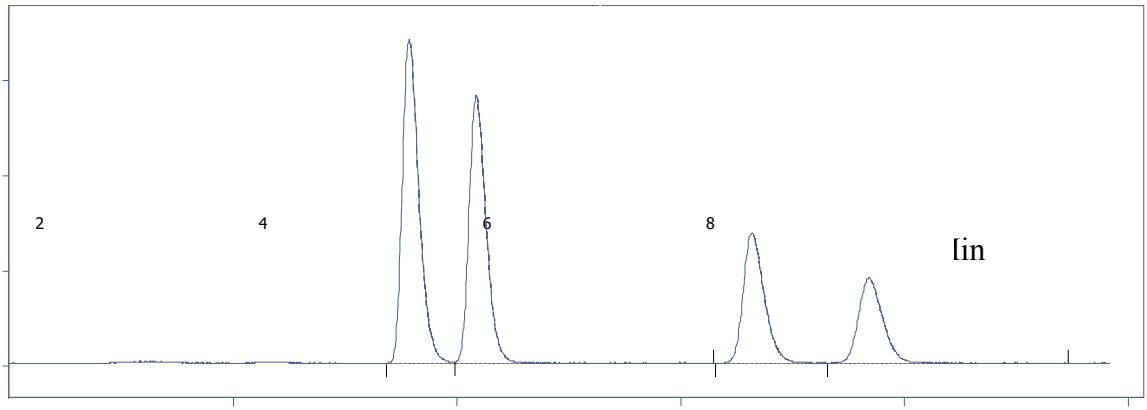

Figure 4-9: Separation of weak acids on a poly (HMA-co-1,6-HEDA) monolith with experimental conditions: mobile phase: 50:50 (V/V) (5 mM phosphate pH 8: ACN), detection wavelength 214 nm, samples: 1) 4-methoxy-phenol, 2) phenol, 3) 4-Cl phenol (3), 4) 4-Br phenol. Other conditions are as stated in Fig.4.3.

4.4.3. **Separation of basic compounds**

The analyses of basic compounds using silica-based phases in RP-HPLC represents a challenge, due to the secondary interactions between basic compounds and the stationary phase [74]. Since the surface of the (HMA-co-1,6-HEDA) monolith prepared is neutral, such interaction should be eliminated. As illustrated in Fig 4.10 baseline separation of basic molecules including quinine, nortriptyline, and amitriptyline (with pKa values of 8.6, 9.7, and 9.4 respectively) was achieved using 5 mM ammonium bicarbonate (pH 12)/ACN at a ratio of 34:66 (V/V). The isocratic mobile phase did not require any competing amines, such as triethylamine (TEA), in the mobile phase to enhance peak shapes, as is standard practice when analysing basic molecules [141].

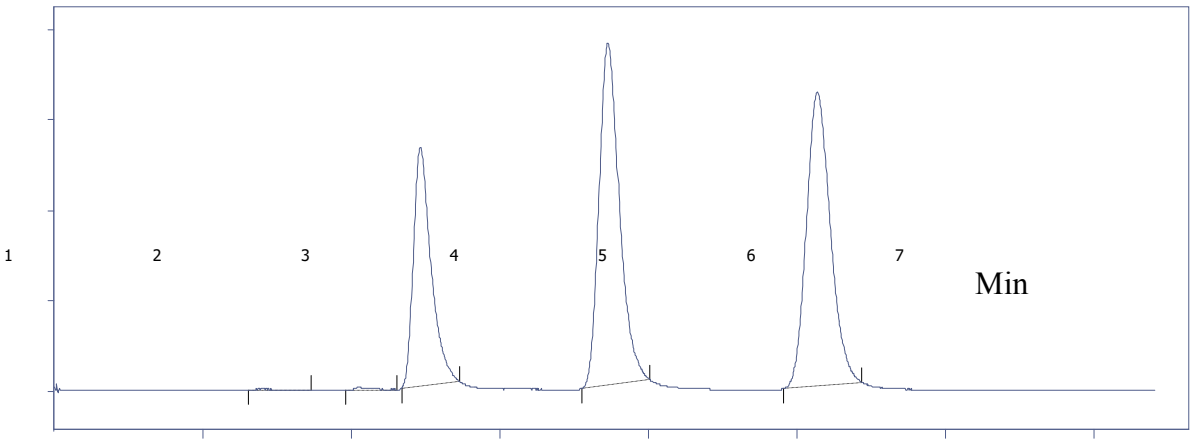

Figure 4-10: Separation of basic molecules on a poly (HMA-co-1,6-HEDA) monolith with experimental conditions: mobile phase 34:66 (V/V) (5 mM ammonium bicarbonate pH 12:ACN), detection wavelength 214 nm, samples: 1) quinine, 2) nortriptyline, 3) amitriptyline (3). Other conditions are as stated in Fig.4.3.

A high pH mobile phase was used to neutralise the compounds investigated, as is customary when analysing basic compounds in order to gain good peak shapes and better selectivity [139]. Quinine and amitriptyline, along with other basic molecules, were separated using a Phenomenex Luna C18 bonded silica column [139]. However, when these compounds were analysed, 0.1% TEA was employed as an additive in the mobile phase in order to enhance the peaks shape, but no chromatographic data was provided in their paper [139]. The asymmetry factors for nortriptyline and amitriptyline when analysed by the prepared monolith were 1.5 and 1.3 respectively, calculated by the Clarity chromatography software using the asymmetry factor (A_s) equation, mentioned previously in Chapter **1**.

4.4.3.1. Quantification of amitriptyline in marketed pharmaceutical tablets

The amount of amitriptyline in each tablet is reported to be 10 mg, as shown in Fig.4.11. Therefore, an appropriate amount of the amitriptyline ground powder was dissolved in the mobile phase in order to obtain the concentration of 50 µg /ml. Subsequently, this concentration was injected, and then the recovery was calculated with a known concentration of 50 µg /ml. The recovery obtained was around 99%, which is within the acceptable limit according to the ICH guidelines [107]. This approach of quantification is called 'single point quantification'.

Figure 4-11: Amitriptyline 10mg package.

As can be seen in Fig.4-12, the peak height of the amitriptyline in the tablet is to a high degree equal to the standard amitriptyline with a slight shift in the retention time. This shift in the retention time could have been due to the unknown interaction between the table's excipient and the stationary phase.

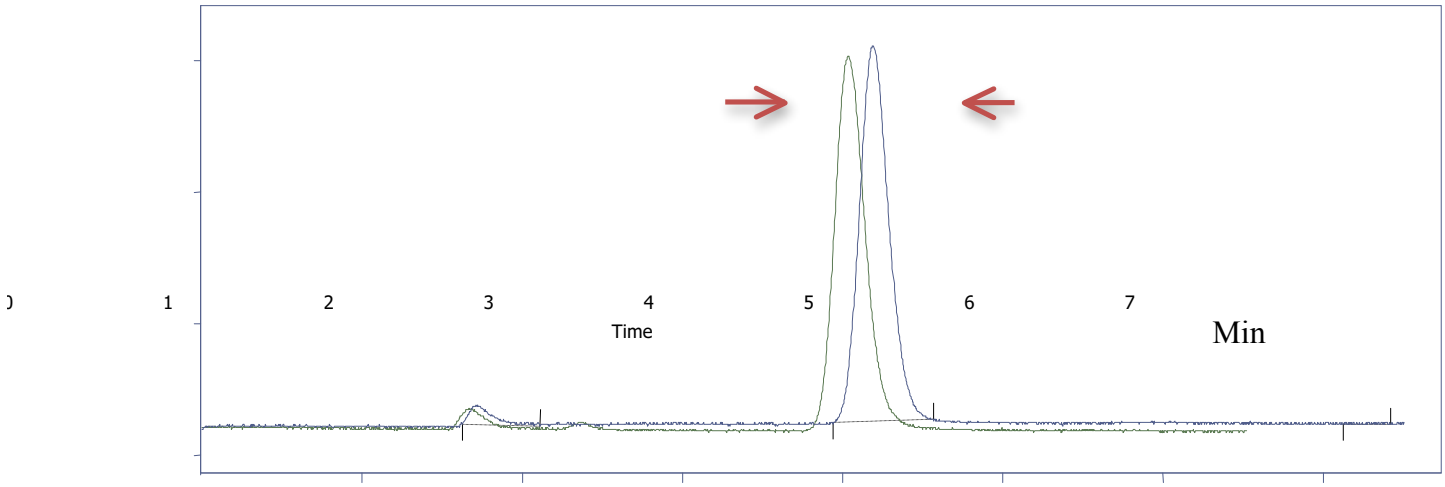

Figure 4-12: Comparison of the concentration of amitriptyline in the tablet (blue) and standard solution (green). Other conditions are as stated in Fig.4.11.

The result shown in Fig. 4-12 demonstrates the successful quantification of amitriptyline in the marketed pharmaceutical tablets using the synthesised monolith, poly (HMA-co-1,6-HEDA), indicating its utility for quantification of these types of drugs in commercial tablets.

4.5. Conclusion

A porous poly (HMA-co-1,6-HEDA) monolithic column, synthesised thermally, was successfully employed as a stationary phase in micro-HPLC. As illustrated in this study, organic monoliths can be employed for the separation of small molecules using longer crosslinkers, providing more mesopores (more surface area). The 1,6-HEDA based monoliths based showed high porosity, high reproducibility, and high stability with no indication of swelling or shrinking during the use of organic solvents. Furthermore, the monolithic column fabricated demonstrated high selectivity for neutral non-polar molecules, weak acid molecules, and basic molecules.

Additionally, the 1,6-HEDA based monolith was used employed to quantify amitriptyline in pharmaceutical tablets. The result obtained was in agreement with what reported by the manufacture indicating that the extraction approach was accurately conductedand the fabricated monolith could be utilised for the quantification of this drug in the marketed tablets.

Since the results obtained from the fabricated monolith are promising, the following Chapter will, therefore, be centred on the investigation of hyphenation of the monolithic capillary to mass spectrometry.

Chapter 5

Investigation into the connection of a small fused silica monolithic capillary to Mass Spectrometry

5. Introduction

High liquid chromatography coupled with mass spectrometry (HPLC-MS) is considered to be a revolutionary instrument in both chemical and life sciences. HPLC-MS is gathering impetus chemical research by providing robust separations and identification tool for chemists and biologists in various domains [142]. The combination of HPLC and MS affords to the chemical analysts the potential to analyse nearly any molecular species. In addition, HPLC-MS is capable of providing valuable information with regards to a given sample, for instance, structure, molecular weights, empirical formula, and quantitative information.

Regardless the efficiency of Gas chromatography-Mass Spectrometry (GC-MS) technique, many compounds cannot be analysed with this method. This is because of the lack of suitable volatility of the analyte molecules. HPLC-MS technique, on the other hand, aids the analysis of samples that conventionally have been difficult to analyse with the former technique (GC-MS). Furthermore, the range of samples analysed by HPLC-MS includes small pharmaceutical compounds to large proteins [26]. Additionally, HPLC-MS is suitable for the analysis of large, ionic, polar, involatile, and thermally unstable compounds. Having mentioned this, some of these compounds can also be analysed by GC-MS, however they need to be derivatised (chemical modification), via an extra step which is considered to be a disadvantage (time-consuming). However, HPLC-MS eliminates the requirement for time-

consuming chemical modifications permitting MS analysis of charged molecules, non-volatile, or thermally labile.

Fig. 5.1 illustrates the type of an ion source and the technique used for various types of compounds. This classification is based on the polarity of a given sample and molecular weight [26].

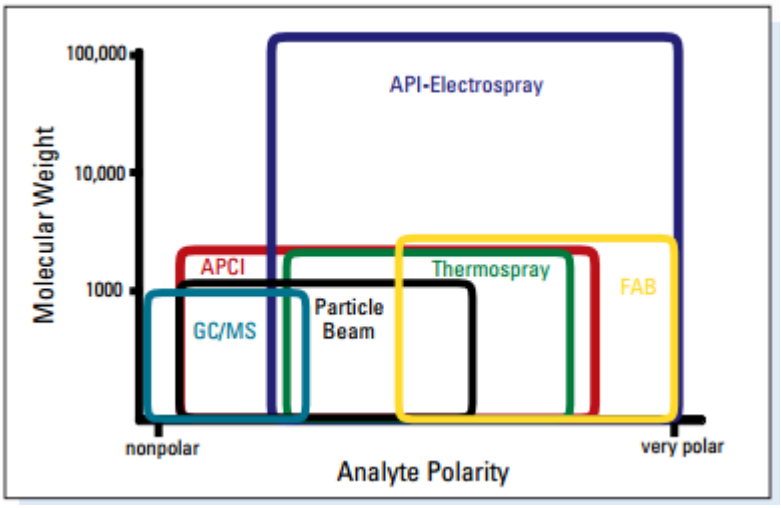

Figure 5-1: Illustrates the type of an ion source and the technique used for various types of compounds, adopted from [26].

5.1.1. **Why mass Spectrometry?**

HPLC resolves components of a sample but affords little information as to what these components are. Furthermore, it is difficult with HPLC to be confident that a particular peak is pure and represents only a single compound. Coupling MS to HPLC provides significant additional information about the sample, notably the masses of all components present, even for co-eluting species. Its use, therefore, facilitates compound identification and allows assessment of peak purity [142].

5.1.2. **Why chromatography?**

It could be thought that since the MS can distinguish various analytes all mixed together based on their *m/z* ratio, it is attractive not to employ HPLC to resolve the analyte first with chromatography. Yet, there are a few reasons why HPLC separation is highly recommended prior to MS analysis [142]: firstly, isomers (having the same mass) cannot be resolved on the basis of *m/z* differences. Resolving such isomers can be really vital when one of the enantiomers is toxic. Secondly, when a mixture is introduced directly into the MS source, its components could interact with each other in a manner that negatively affects their ionisation; this phenomenon is called ion suppression and can lead to poor sensitivity. The ion suppression can be problematic when required to detect a minor component (low concentration) or poorly ionised components (lack of ionisable functional groups) in the presence of a large amount of something else, for instance, buffer from the sample [142].

5.1.3. **Hyphenating monolithic capillary with MS**

As mentioned previously in Chapter **1** (section 1.2), there are two approaches utilized to produce a nano flow, including the use of an incorporated flow splitter with a conventional HPLC pump leading to diversion of excessive flow from a HPLC system. The second choice is via the use of nano flow technology in which a HPLC pump is capable of delivering precisely a flow in a nano range.

Since the type of ion source (ESI) for MS employed in this project is classical (not the nano ion source), the minimum flow rate set by the manufacture in order to obtain a stable MS signal and ultimately quantify a given sample, is 4 μl/min. Therefore, utilisation of the same monolithic capillary's i.d. (100 μm) used in the previous Chapter is not feasible.

This is because using a high flow rate (4 μl/min) with a 100 μm capillary could lead to damage the capillary due to the generation of a high back pressure. Hence, it was necessary to fabricate a monolithic capillary in an i.d. $\geq$ 200 μm so that a high flow rate could be utilised in order to meet the conventional ESI's requirement.

As will be illustrated in the section 5.3.2, when connecting the monolithic capillary to the MS's ion source, it is highly recommended to use the corresponding fittings (micro union, male nuts and female nuts, union Tee and etc.). This is because failure to do so would either lead to lose of the sample injected or system dispersion which ultimately has a negative impact on efficiency and sensitivity. Fig. 5.2 shows the final set up employed for the Nano-HPLC-MS work.

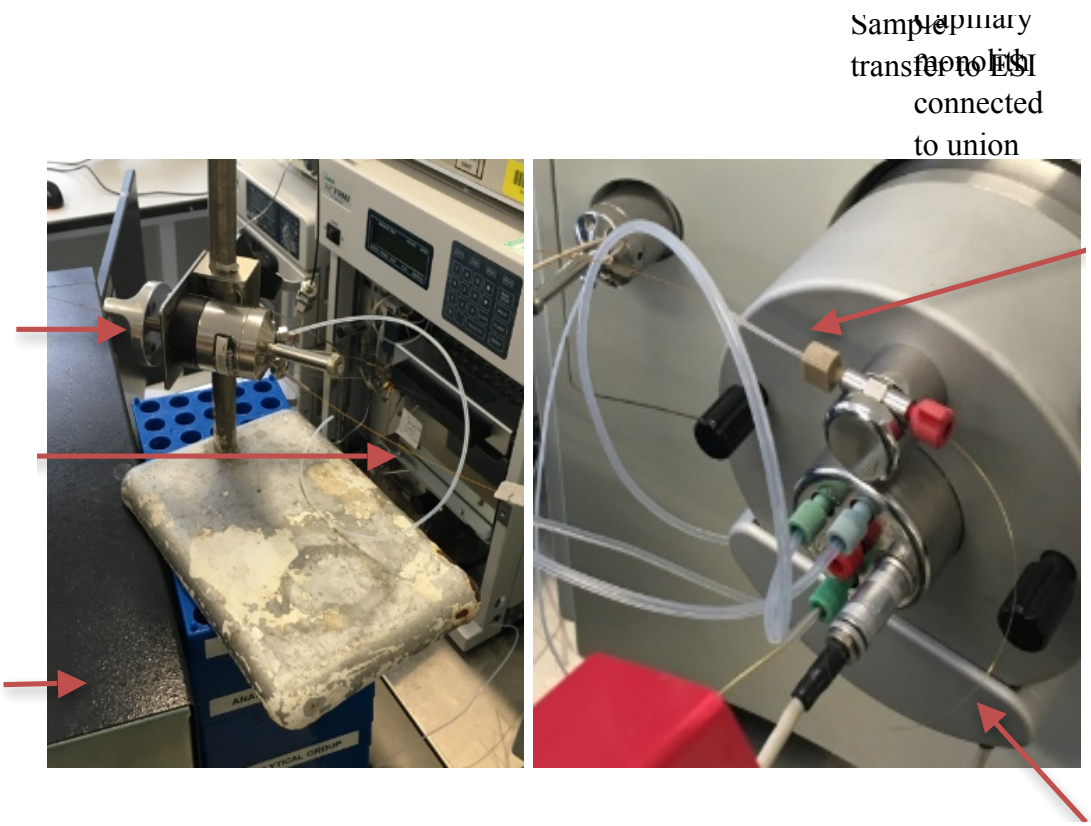

Figure 5-2: Nano-HPLC-MS set up.

5.2. Experimental section

5.2.1. Reagent and materials

Hexyl methacrylate (HMA) was purchased from Lancaster, United Kingdom, 1,6-hexanediol ethoxylate diacrylate (1,6-HEDA) was purchased from Santa Cruz Biotechnology, Germany. 3-(trimethoxysilyl) propyl methacrylate (γ-MAPS), azobisisobutyronitrile (AIBN), sodium hydroxide, thiourea, dimethyl phthalate, anisole, naphthalene, nortriptyline, 1,4-butanediol dimethacrylate (1,4-BDDMA), and 1,10-decamethylene dimethacrylate (1,10-DMDMA) were all obtained from Aldrich Chemicals (Steinheim, Germany). Ammonium bicarbonate was purchased from Fluka (Steinheim, Germany). HPLC-grade methanol and acetonitrile (ACN) were bought from Fisher Scientific (Leicestershire, UK). Disodium hydrogen phosphate anhydrous was purchased from Fisons Scientific Equipment (Loughborough, UK). Amitriptyline was purchased from Aldrich (Poole, UK). Water used throughout all experiments was purified using a Millipore System model no. SYNSV0000. pH indicator paper was purchased from Camlab House (Cambridge, UK). The fused silica capillaries were supplied from CM Scientific (Silsden, United Kingdom, Part no. TSP100375). 1/16" PEEKsil, 25 cm x 530 um i.d. (Part no. 0624370) were provided by SGE (Milton Keynes, United Kingdom).

5.2.2. **Instrumentations**

An oven employed for thermal polymerisation. A microscope used for investigating the presence of air bubbles inside the capillary column and the confirmation of the introduction of the polymerisation mixture within the capillary. Nano-HPLC-MS experiments were carried out on the Dina system coupled with MS ion trap; more details about these instruments, i.e. model/make, manufacturer's details have already been stated in Chapter **2** (section 2.2).

5.2.3. **Monolithic preparation**

The general protocol followed in synthesising the monolithic column has been already mentioned in Chapter **2**, specifically section 2.1.1. The co-polymerisation schemes of the selected monomers and porogens are demonstrated in Fig 5.3. Table 5.1 illustrates the composition of the polymerisation mixture.

Table 5-1: Composition of the polymerisation mixture.

	Monomer mixture		Porogen system		initiator
Name of the monolith	Monomer (%, w/w)	Crosslinker (%, w/w)	1, 4-butanediol (%, w/w)	1-propanol (%, w/w)	AIBN*
HMA-co- 1,6-HEDA	12%	18%	35%	35%	1%
HMA-co- 1,4-BDDMA	12%	18%	35%	35%	1%
HMA-co- 1,10-DMDMA	12%	18%	35%	35%	1%

* 1% with respect to the Monomer mixture.

HMA

B

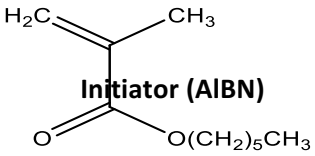

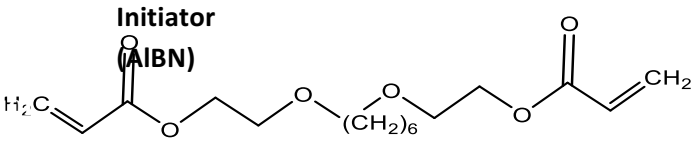

Poly (HMA-co 1,6-HEDA)

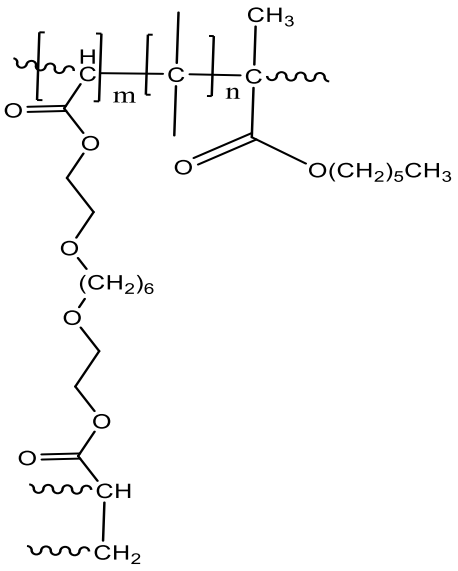

Poly (HMA-co- 1,10-DMD

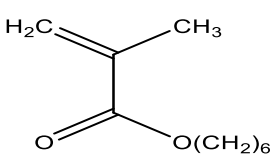

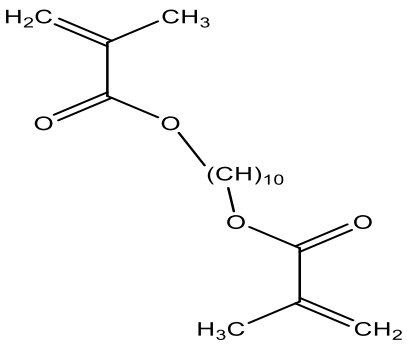

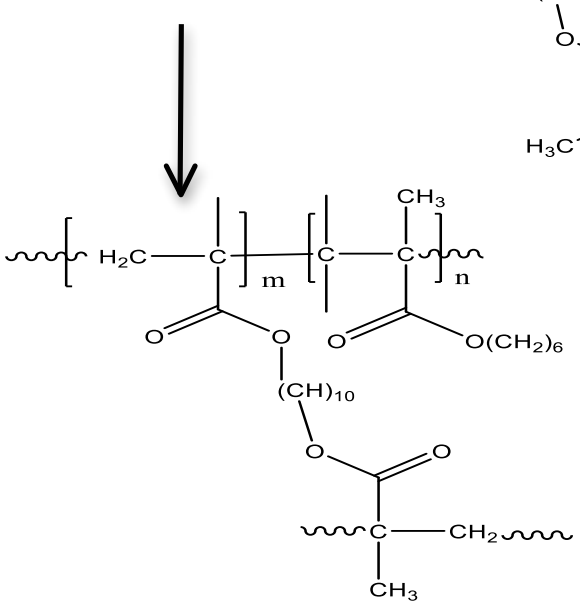

C

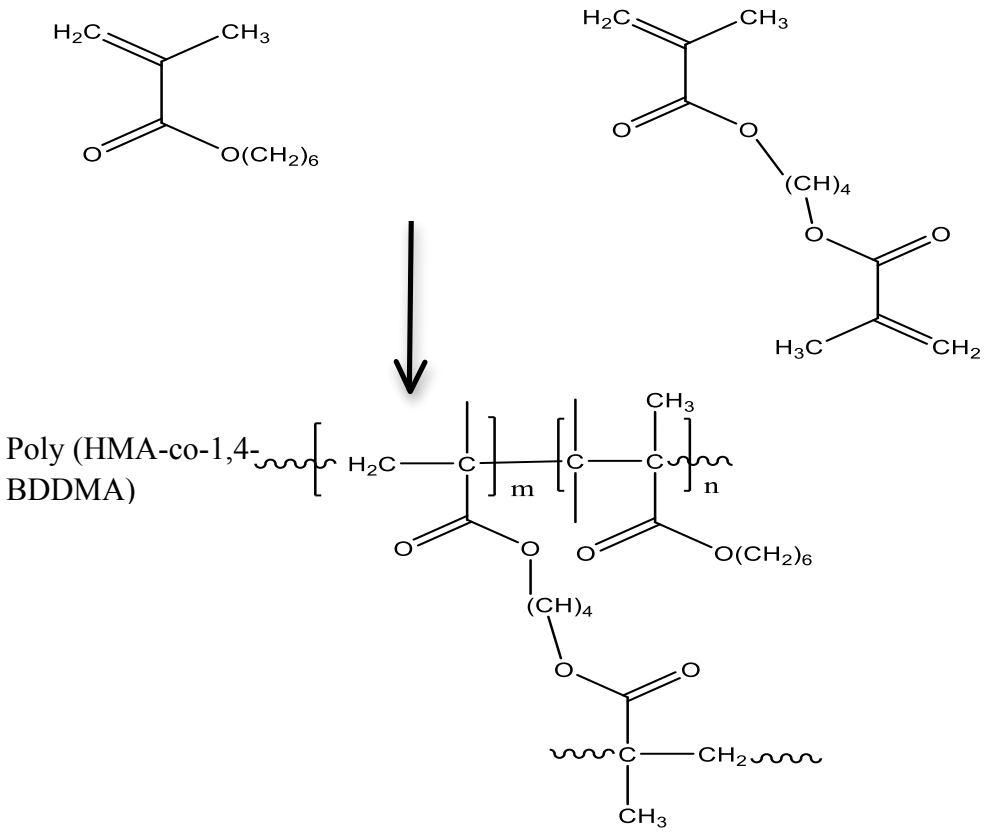

Figure 5-3: The co-polymerisation scheme of the selected monomers and porogens for A) poly (HMA-co 1,6-HEDA), B) poly (HMA-co- 1,10-DMDMA), C) poly (HMA-co- 1,4-BDDMA).

5.2.4. **Preparation of solutions**

The test mixture consisted of 10 mg thiourea, 60 µl dimethyl phthalate, 57 µl anisole, and 16 mg naphthalene dissolved in 10 ml of 50% ACN (HPLC-grade) and 50% water (HPLC-grade) (V/V). The mixture was then diluted 50 times in order to avoid column overloading and to obtain a reasonable UV response. Amitriptyline and nortriptyline were dissolved in the mobile phase used (5 mM ammonium bicarbonate (pH 12) combined with ACN in a 34:66) (V/V) in order to avoid any peak distortion.

5.2.5. **Chromatographic conditions**

For the analysis of the test mixture consisting of thiourea, dimethyl phthalate, anisole, and naphthalene, the mobile phase used was H_2O/ACN in a ratio of 40:60 (V/V). When measuring the performance of all monolithic columns in fused silica capillary (i.d. 100 µm, 200 µm), and PEEKsil (i.d. 530 µm), a UV detector at 210 nm was employed for the analysis of the test mixture. 5 mM ammonium bicarbonate (pH 12) combined with ACN in a 34:66 (V/V) ratio was employed as the mobile phase for the separation of basic compounds including amitriptyline and amitriptyline. A UV detector was employed at a wavelength of 214 nm for their analysis.

5.2.6. **Mass spectrometry conditions**

For ɤ-MAPS analysis, the MS was operated in the positive mode, the source voltage was set at 4.00 kV, the sheath and auxilliary gases were set at 19. Additionally, the capillary temperature was 60 ^{0}C. The capillary voltage was set at 23 V. As for amitriptyline and nortriptyline analysis, the MS was operated in a positive mode, the source voltage was set at 4.00 kV, the sheath and auxilliary gases were set at 60 and 0.0 units respectively. Additionally, the capillary temperature was 175 ^{0}C. The capillary voltage was set at 15 V.

5.3. Results and discussion

5.3.1. Hyphenating monolithic capillary to MS

Since the i.d. of the monolithic capillary used in the previous Chapter is small (100 µm) and was initially intended to be coupled with UPLC-MS (the pump range 100 µl/min-10 ml/min), a flow splitter was,therefore, required in order to avoid the generation of a high back pressure that could damage the monolithic capillary. Table 5.2 below shows the initial trials conducted to couple the monolithic capillary to the MS.

Table 5-2: Trial conditions for coupling of the monolithic capillary to MS.

Type and ID size	Result	Explanation	Next step
Fused silica capillary (100 µm and 200 µm i.d. [a])	Capillaries damaged	Fused silica capillary unable to withstand high back pressures	Use a bigger i.d. (530 µm)
Fused silica capillary (530 µm i.d.)	Repeated breakage observed before use	Larger ID fused silica capillary very fragile	Use PEEKsil i.e. polymer-sheathed fused silica tubing (1/16 inch i.d. 530 µm)
PEEKsil (1/16 inch or 530 µm i.d.)	Good separation with Nano-HPLC and high efficiency, shown in Fig.5.4		Couple the PEEKsil to HPLC pump (for 10 µl-10 ml flow-rates) without a splitter.
PEEKsil (1/16 inch i.d. 530 µm)	Monolith extruded from the PEEKsil, shown in Fig.5.5	High back pressure generated	Decrease the length of the tubing used for the connection between the pump and the detector.
PEEKsil (1/16 inch i.d. 530 µm)	Monolith shrank	High back pressure generated	Connect the monolith column straight to the pump's valve
PEEKsil (1/16 inch i.d. 530 µm) connected directly to the pump's valve	Monolith shrank but lower back pressure was obsvered	High back pressure generated	Investigate the synthesis process

a) Notes in fabricating in 200 µm i.d. will be stated in section 5.3.2.1.

Fig.5.4 illustrates the successful synthesis of the poly (HMA-co-1,6-HEDA) monolith in PEEKsil format and can show that a baseline separation was achieved within 13 mins. This result also indicates that monoliths could be synthesised in PEEKsil, this type of tubing to the best of knowledge has not been investigated for such use. Fig.5.5 is a demonstration of monolith extrusion when high back pressure is applied.

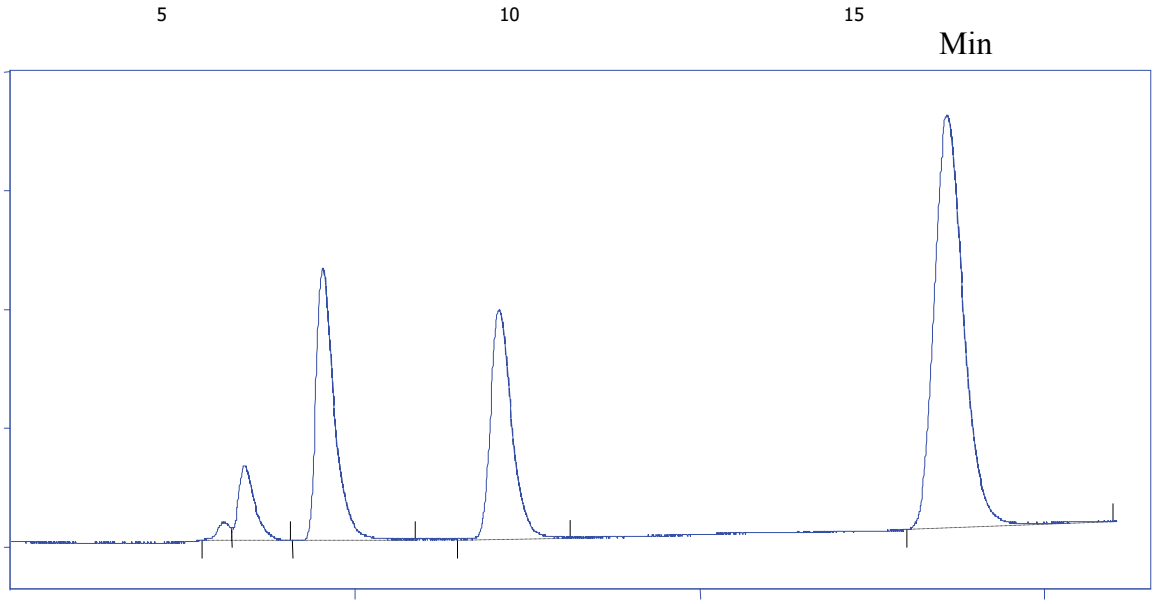

Figure 5-4: Efficiency test, Illustration of the chromatogram of test mixture using the HEDA based monolith. Experimental conditions: PEEKsil dimension 530 µm i.d., length 20 cm, flow rate 5000 nl/min, samples: 1) thiourea, 2) dimethyl phthalate, 3) anisole, 4) naphthalene. Other conditions are as stated in Fig. 4.3.

Figure 5-5: The monolith extruded from the PEEKsil capillary.

Clearly, it can be deduced from Table 5.2 above that the monolithic capillary was not able to handle a high back pressure. The initial thoughts on this problem (handling high back pressure) could have been either through the presence of air bubbles in one of the main steps involved in monolithic fabrication or because the ɤ-MAPS solution was not introduced in the fused silica capillary properly, which in both cases leads to unstable monoliths as stated previously in Chapter **2** (section 2.1.2). Therefore, a careful investigation into these two possibilities was carried out, as illustrated in Table 5.3 below.

Table 5-3: Investigation into the expected causes for high back pressure instability.

Attempt	Result	Cause	Decision made
Repeating the synthesis with paying the attention that no bubbles present.	Monolith got shrunk and some voids were present	Unknown at this stage	Repeating the synthesis with paying the attention to the ɤ-MAPS process
Repeating the synthesis with paying the attention the ɤ-MAPS application.	Some voids were present	Unknown at this stage	Decided to investigate the main steps involved in the synthesis of monoliths so that the cause of these voids could be allocated

As stated in Table 5.3 that even when great care was taken when fabricating the monolithic capillary, it could still not handle the high back pressure. Consequently, as mentioned in the table above, a systematic investigation into the main steps involved in the monolithic fabrication combined with an investigation into the polymer mixture components was conducted. Table 5.4 illustrates the role of the main steps employed in the synthesis of a monolithic capillary. In addition, Table 5.5 shows the attempts conducted to ascertain the cause of monolithic instability under high back pressure.

Table 5-4: The main steps involved in the synthesis of monoliths.

No	Step	Role
1	Introduction of NaOH	Converting the Si-O-Si to Si-OH
2	Introduction of ɤ-MAPS	Keeping the monoliths within the capillary
3	Introduction of polymer mixture	Formation of monolith

Table 5-5: Systematic investigation into the main steps involved in monolithic fabrication.

Step	Why this step	Result	Decision made
Preparation of fresh NaOH	Thought caustic might have gone off	Some voids were present	Investigating the ɤ-Maps solution's stability
Using a new bottle of ɤ- MAPS	Suggested by the suppler (Sigma) ɤ-MAPS's solution stability needs to be checked annually to make sure it functions properly, MS results shown in Fig 5.6	Some voids were present	Only Changing the cross-linker (1,6 - HEDA) to another cross liner (keeping other polymer mixture the same, i.e., monomer and porogens)
Introducing a new crosslinker 1,4 - BDDMA	Checking if the cause of these voids due to the crosslinker (1,6-HEDA) used	NO voids were present, and four peaks were observed, shown in Fig. 5.7	Repeating the synthesis using another crosslinker
Introducing a new crosslinker 1,10 - DMDMA	To double check the cause of these voids is the crosslinker (1,6-HEDA)	NO voids were present, and four peaks were observed, shown in Fig. 5.8	**Elimination of 1,6 HEDA with classical pump, **adjusting the monomer mixture or ** application of low flow rate (2 µl/ml) with 100 µm i.d.

As shown in Fig. 5.6, the two MS spectra indicate that there were not any noticeable differences between the old and the new ɤ-MAPSproving that its stability was not an issue and ultimately was not the cause of the monolith's instability under the high back pressure, as proved in Table 5.5 above.

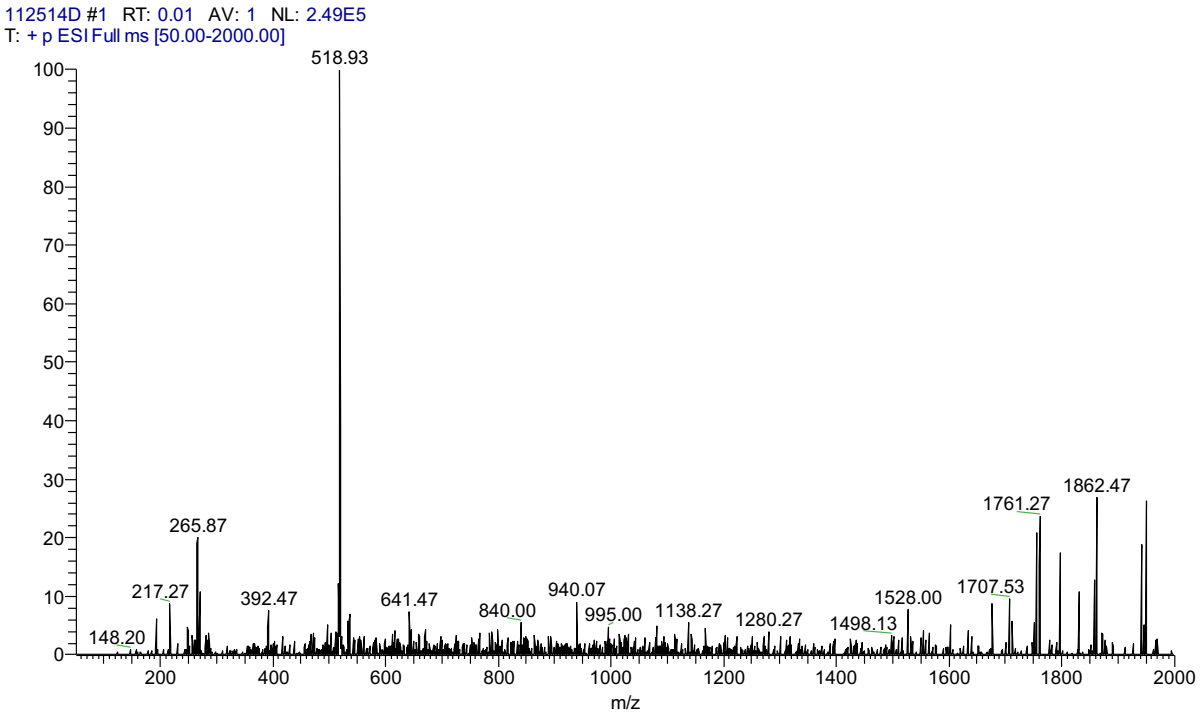

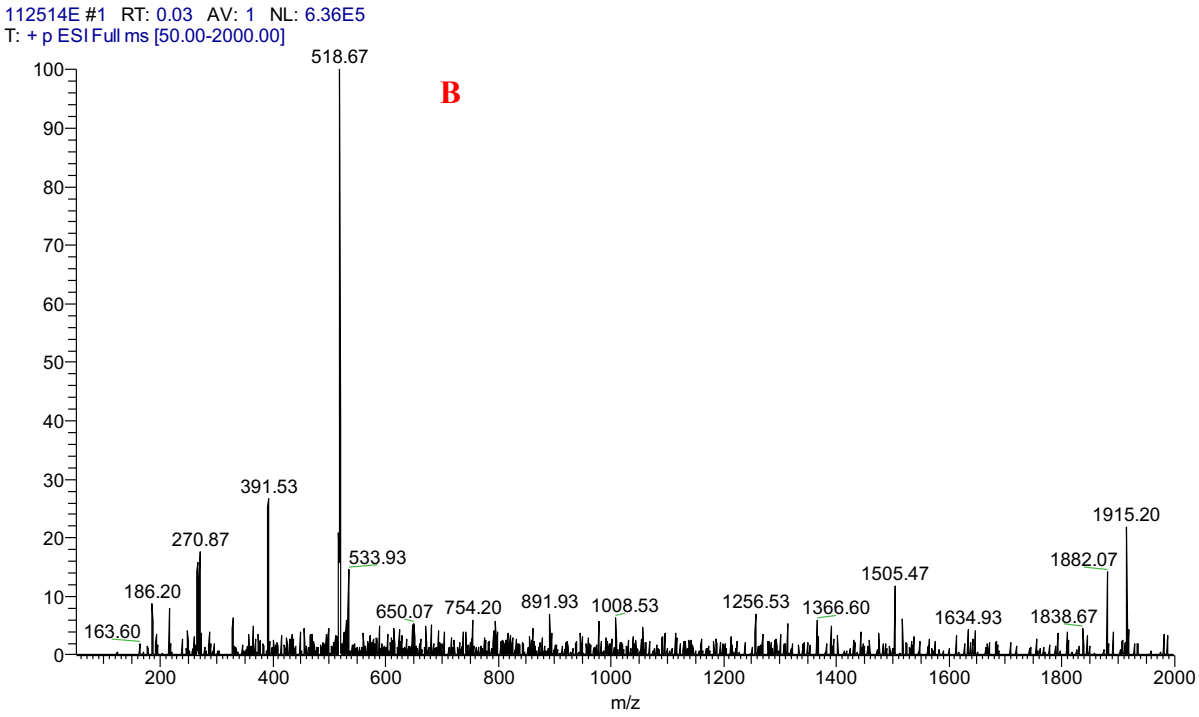

Figure 5-6: Checking ɤ-MAPS stability: A) is the old ɤ- MAPS, B) is the new one bottle of ɤ- MAPS.

From Table 5.5, Fig. 5.7 and Fig. 5.8, it is evident that the monolith instability under the high back pressure was caused by either the low concentration of the crosslinker, 1,6-HEDA in the polymerisation mixture or the unsuitable ratio of monomer to porogen.

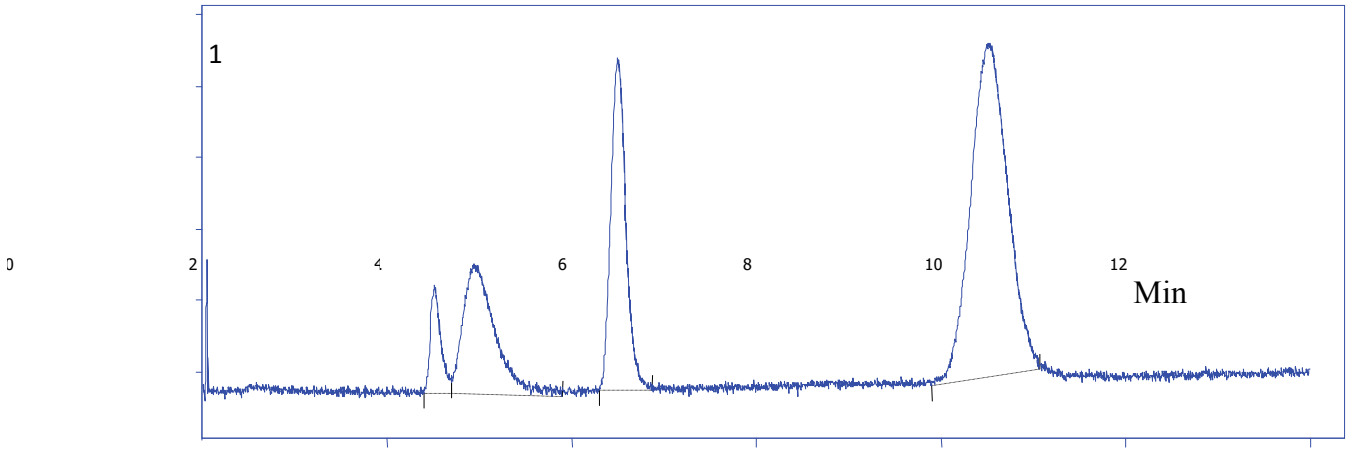

Figure 5-7: Illustration of the chromatogram of test mixture using the 1,4-BDDMA based monolith. Experimental conditions: column dimension 100 µm i.d. x 375 o.d. column length 30 cm, flow rate 1000 nl/m, samples: 1) thiourea, 2) dimethyl phthalate, 3) anisole, 4) naphthalene. Other conditions are as stated in Fig. 5.4.

Furthermore, since the purpose of employing these new crosslinkers was merely ascertaining the cause for monolith instability, no additional efforts were made to enhance the separation in Fig.58.

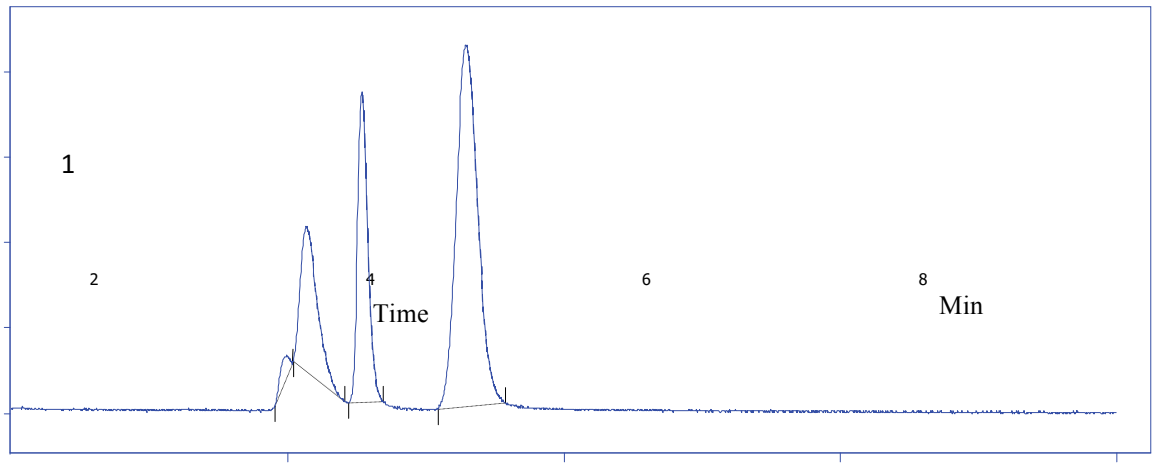

Figure 5-8: Illustration of the chromatogram of test mixture using 1,10-DMDMA based monolith. Experimental conditions: capillary dimension 100 µm i.d. Other conditions are as stated in Fig. 5.7.

After the comprehensive investigation into monolith instability described in the tables and the figures above, it could be concluded that either the concentration of the crosslinker 1,6-HEDA in the monomer mixture or the ratio of monomers to porogen was the cause of monolith instability under the high back pressure. Therefore, the composition of the polymer mixture needs to be modified so that the monolith composition can handle high back pressures.

The same finding was observed in a study by Yuan et al. [73] when they synthesised a poly (SPDA-co-MBA) monolith. They found that when the concentration of the crosslinker (MBA) in polymer mixture was 10%, the monolith could not handle the back pressure at/above 200 bar (20 MPa, 2900 psi) and consequently the monolith got extruded. Subsequently, they increased the concentration of MBA from 10% to **15%;** and the monolith was, therefore, able to resist the high back pressure. By the same token, when they adjusted the ratio of monomers to porogens from 30:70 to 25:75 for the same concentration of MBA **(15%)** in order to obtain a better efficiency, the monolith could not handle the back pressure

< 200 bar and, as a result, was extruded. Likewise, another study carried out by X. Bai et al. [143]. In the study, they fabricated a poly (trimethylolpropane triacrylate -co-EDMA) monolith, they found that when the concentration of crosslinker (EDMA) in monomer mixture was 8%, the monolith could not handle a high back pressure. Hence, they modified the percentage of EDMA from 8% to 10%; whereby the monolith was able to handle the high back pressure.

In the light of the above studies , the cause for monolith instability under the high back pressure is considered to be either due to the formation of very large pores formed together making the skeleton structure of monoliths loose. This loose structure is due to the low concentration of crosslinker in the polymerisation mixture. Alternatively, the ratio of monomers to porogens is not the suitable to be used with such back pressure.

In our case, the concentration of the crosslinker (1,6-HEDA) was to some extent high (18%), yet the monolith was not capable of withstanding the high back pressure. This could point out that the ratio of monomers to porogens should be adjusted carefully so that the stability of the monolith under a high back pressure could be improved. Therefore, a thorough investigation needs to be carried out to prove this hypothesis and, therefore, ascertain the right ratio that withstands a high back pressure if a conventional pump was in use.

5.4. Hyphenating Nano-HPLC to MS

Since the monolithic materials developed in the previous sections were shown to be incompatible with the conventional HPLC, the Dina Nano-HPLC was coupled to the MS instead of the HPLC. The same polymerisation poly (HMA-1,6-HEDA) monolith used in the previous Chapter (Table 4.1) was employed for the hyphenation.

As mentioned previously, the MS used in the project requires at least 4 µl/min so as to obtain a stable signal. Additionally, 2 µl/min is the maximum flow rate that can be used with the Dina pump. It was, thus decided to utilise a 4 µl/min flow rate, where 2 µl/min comes from the Dina pump and 2 µl/min comes from the built-in syringe pump on the MS. The flow from both sources was combined using a union tee device so that the minimum flow rate required for stable signal is satisfied.

This type of union tee has several applications in chromatography including splitting the HPLC eluent flow before the MS inlet. Another application is to supply the so-called 'make-up' solvent, in which another apparatus (syringe pump in our case) is used to supply a secondary solvent before the MS inlet.

When using a 100 µm ID monolithic capillary with two types of union tees it was found that even though a high concentration of sample (1 mg/ml) was injected, no mass was observed suggesting that these types of tees were not compatible with this i.d.

Therefore, in order to overcome such a challenge, two approaches could be used including the utilisation of the correct fittings (unions and tees) between the monolithic capillary and MS inlet so that no dead volume occurs. The second option is to fabricate the monolith in a bigger i.d., for example, ≥ 200 µm. Since the latter option would lead to the elimination of any extra column band broadening issue, it was decided to fabricate the monolith poly

(HMA-co-1,6- HEDA) in a bigger 200 µm i.d. capillary so that a direct connection from the monolith capillary to the MS inlet without the need for a tee would be implemented.

5.4.1. **Utilisation of 200 µm i.d. fused silica capillary for hyphenation with MS**

As stated in Chapter **2** (section 2.1.2), when required to introduce any solution/liquid into a fused silica capillary, the flow rate of any liquid needs to be controlled to avoid the formation of air bubbles creating voids in the monolithic capillary, as shown previously in Fig. 2.8. This is because such presence leads to poor monoliths or generation of a high back pressure. Consequently, a syringe pump was used to introduce the liquid into the fused silica capillary due to the difficulty in controlling the flow with the same set up used for 100 µm i.d. capillaries, shown previously (Fig.2.4). Fig.5.9. illustrates the set up used for introduction of liquid into 200 µm i.d. fused silica capillary.

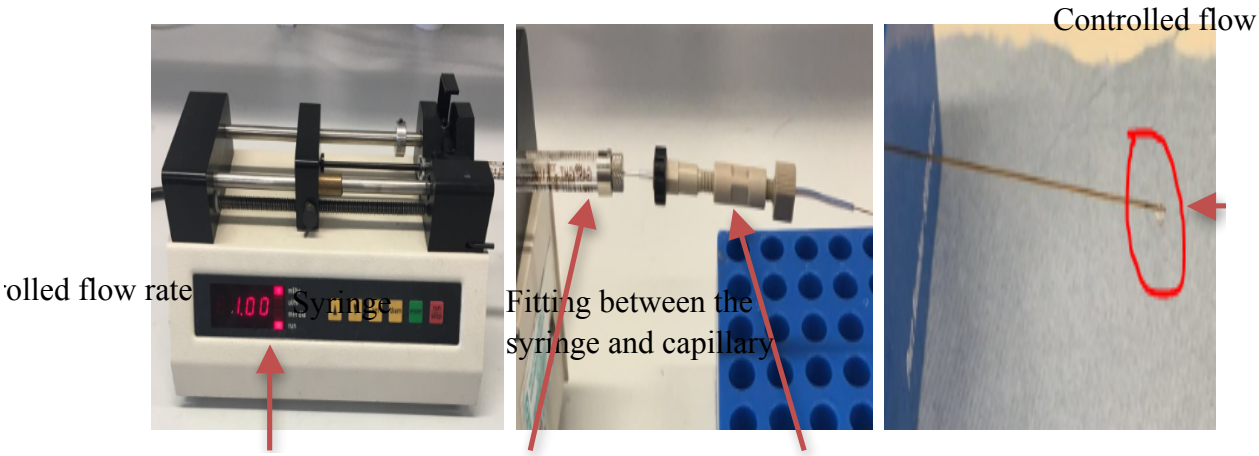

Figure 5-9: Set up used for introduction of liquid into the capillary.

When started fabricating the monolith into the 200 µm fused silica capillary, it was noticed that once the capillary was placed into in the oven at 100 ^{0}C for the derivatisation, the capillary got damaged, as shown in Fig.5.10.

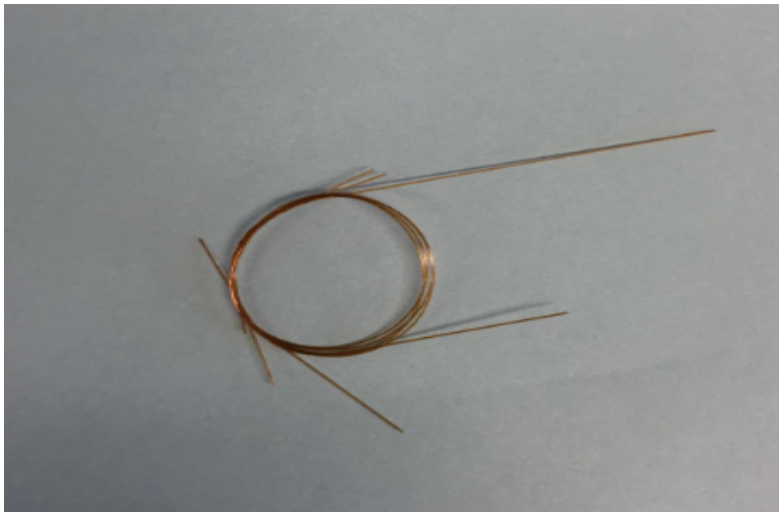

Figure 5-10: Damage caused by the direct contact of capillary with the metal of the oven.

This damage is not observed with 100 µm i.d. x 375 µm o.d. capillary and could be due to the direct contact between the fused silica capillary and the metal of the oven as the thickness of the 200 µm i.d. x 350 µm o.d.is not as thick as it is with 100 µm i.d. x 375 µm o.d. Therefore, in order to tackle this problem, it was thought that the fused silica capillary should have no contact with the metal so that such damage is prevented. One of the ways to prevent happening is to place the capillary onto a watch glass then place the glass inside the oven as shown in Fig.5.11.

Figure 5-11: Set up used to avoid damage of capillary.

This practice has, as a result, proven to be effective and prevented the capillary from the damage, reflected in obtaining a good separation shown in Fig 5.12.

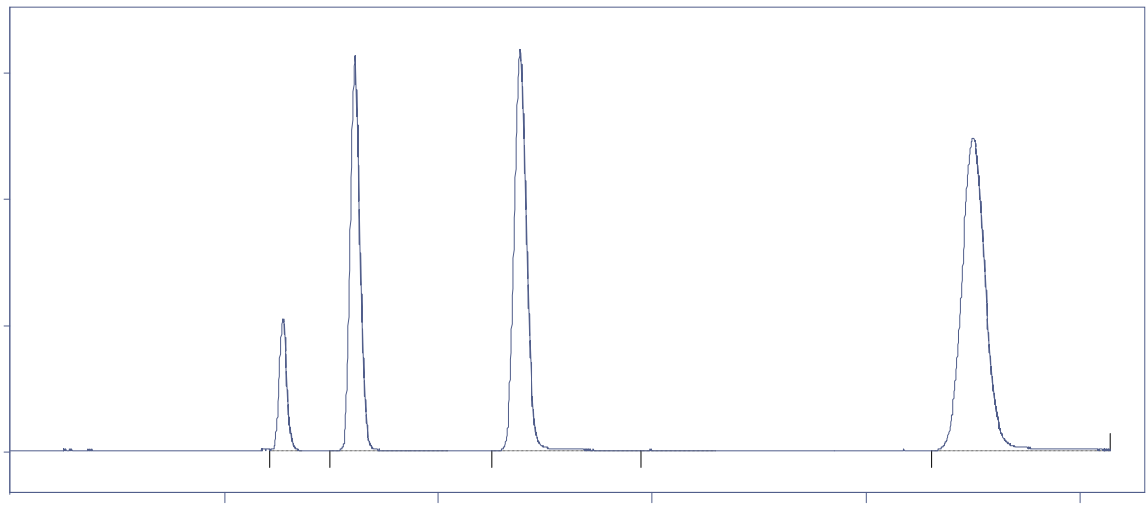

Figure 5-12: Illustration of successful fabrication in 200 µm fused silica capillary, experimental conditions: flow rate 4000 µl/min, samples: 1) thiourea, 2) dimethyl phthalate, 3) anisole, 4) naphthalene. Other conditions are as stated in Fig. 5-4.

5.4.2. **Evaluation of the hyphenation of Nano-HPLC-MS**

In order to investigate the final set-up employed for the hyphenation, a mixture of amitriptyline and nortriptyline was prepared and injected. Fig.5.13 illustrates the obtained result from the hyphenation indicating that the set up used was successful.

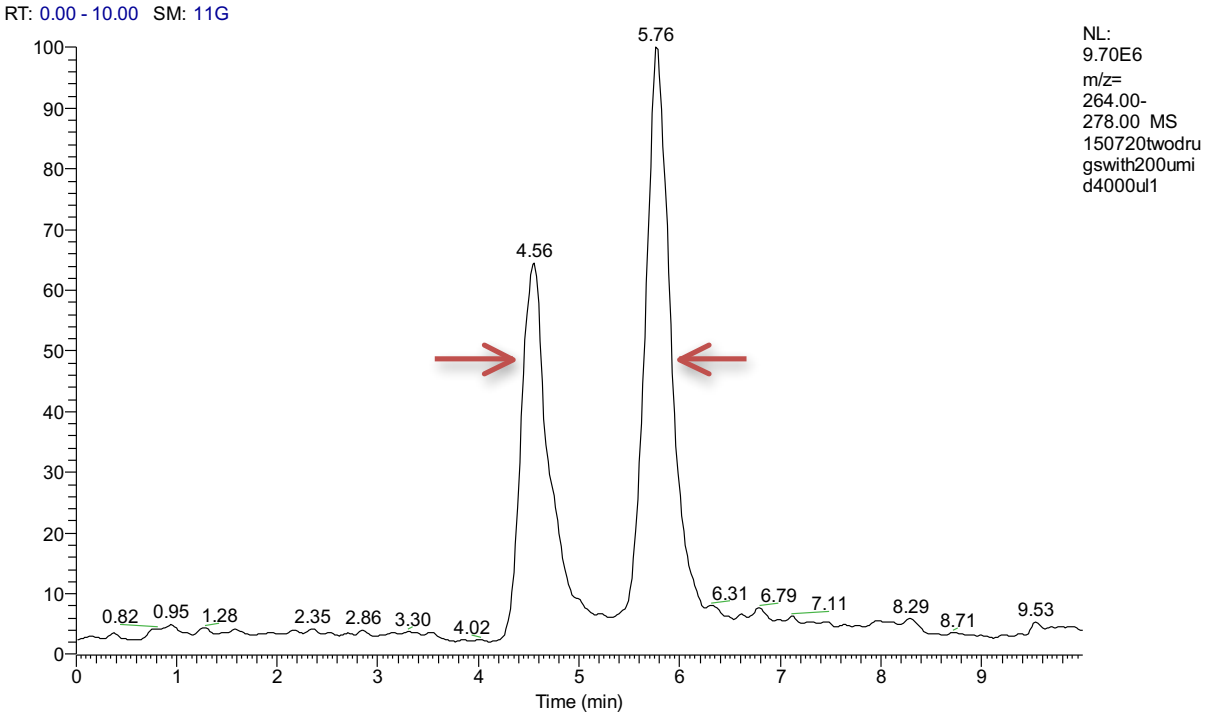

Figure 5-13: Separation of nortriptyline and amitriptyline using 200 µm monolithic capillary using Nano-HPLC-MS. Experimental conditions: flow rate 3 µl/min. Other conditions are as stated in Fig. 4.12.

Fig. 5.14 is the illustration of mass spectra for both analytes (amitriptyline and nortriptyline). The results in Figs. 5.13 and 5.14 demonstrates that the set-up is effective and can be applicable for the direct hyphenation of small i.d. fused silica capillary with conventional ion source MS without loss of efficiency.

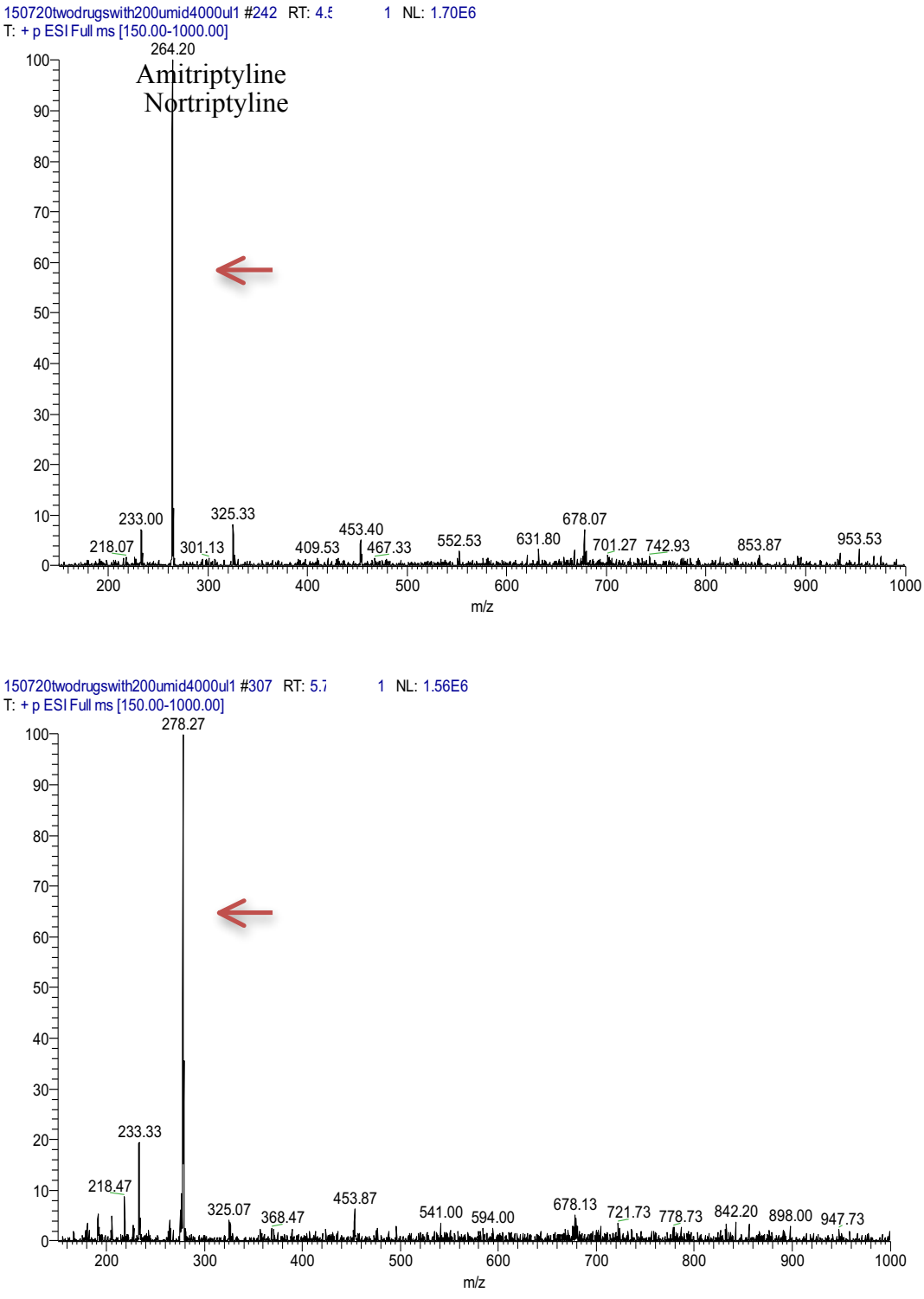

Figure 5-14: Illustration of mass spectra for amitriptyline and nortriptyline.

5.5.Conclusion

HPLC-MS technique is considered to be an innovative instrument in both chemical and life sciences. The technique accelerates the chemical research through affording robust separations and identification tool for chemists and biologists in various domains. Furthermore, HPLC-MS is suitable for the analysis of large, ionic, polar, involatile, and thermally unstable compounds. Some of these compounds can be analysed by GC-MS, but it requires an additional step (derivatisation),,thus, HPLC-MS is better and fast from this prospective.

As discussed, coupling HPLC to MS has been gone through various developments until getting to the current stage. This is due to the requirement of reducing of liquid entering the MS, as it cannot handle a high volume of liquid. In addition, it is considered that the API interfaces are the reason behind the increased interest in the MS applications owing to their sensitivity and ruggedness.

As illustrated in this Chapter, it seems that there are several reasons for monolith instability under high back pressure including the presence of air bubbles when introducing liquids into the fused silica capillary. This, as a result, causes non-homogenous surface leading ultimately to the weaker bonds between the inner surface and γ-MAPS resulting in an unstable monolith. A second reason includes the concentration of crosslinker in the polymerisation mixture, which if not high enough leads to unstable monolith under high back pressure. A third reason is the ratio between the monomers to the porogens, if not chosen properly high back pressure cannot be handled. Therefore, when synthesising a monolith, a systematic investigation needs to be carried out to establish the correct ratio so that a monolith would withstand a high back pressure if a conventional pump was in use.

When fabricating a monolith in fused silica possessing i.d. ≥ 200 μm, extra care needs to be taken especially when the capillary's ID is above 100 um and an oven is used as the device for the thermal initiation.

The final set-up established has illustrated the successful coupling between the small i.d. fused silica capillaries with the conventional MS without any additional fittings and can be used, therefore, for HPLC-MS analysis.

In order to widen the application of Reversed-phase monoliths, the following Chapter will be focused on the fabrication of a newly monolithic material namely poly (GMA-co-EDMA) followed by the incorporation of Congo Red, which contains several functional groups including SO_3H. This will then be evaluated by separating some reversed-phase and HILIC mixtures. This monolith would behave in a mixed mode chromatography manner.

Chapter 6

Derivatisation of Glycol methacrylate with Congo red for capillary liquid chromatography

6. Introduction

Due to the development of modern analytical techniques and the increasing significance of chromatographic analysis, single mode chromatography, such as conventional RP-HPLC does not meet the demands of many current separations applications. This is because RP-HPLC is limited in its ability to separate semi-polar and non-polar analytes, while normal-phase HPLC is limited to resolving moderately polar analytes. Consequently, mixed-mode stationary phases open the door for wider applications in comparison with RP-HPLC, normal HPLC or ion-exchange. There are several advantages of utilising mixed-mode stationary phases including the use of the same column either in a single mode (RP-HPLC mode or ion-exchange mode) or in a combination modes (RP-HPLC mode with ion-exchange mode) while changing only the mobile phase compositions or by using additives. Another advantage of the mixed mode is cost-effectiveness since only one column need to be purchased [144]. Due to these advantages, several mixed-mode stationary phases have recently been introduced. Emily Hilder et al. [145] synthesised a mixed mode monolith by polycondensation polymerisation of an epoxy monomer glycidyl ether with ethylenediamine in the presence of two porogens, polyethylene glycol (M=1000) and 1-decanol at 80 °C for 22 hrs. Then, the monolith was modified by a simple acid hydrolysis of the residual epoxides. The acid hydrolysis was conducted via pumping a solution consisting of 1 M 2- aminoethyl hydrogen sulphate dissolved in 1 M carbonate buffer adjusted to 10.5 with 5 M sodium hydroxide solution, for 24 hrs at 75 °C. This mixed-mode monolith showed HILIC and ion exchange

(IEX) interactions when applied to the separation of a range of benzoic acid derivatives utilising variations in the eluent pH, ionic strength, and organic solvent concentrations. Likewise, Jiang et al. [146] synthesised two phospholipids functionalized monolithic columns. These monoliths were thermally fabricated via the co-polymerisation of 12-Methacryloyl dodecylphosphocholine (MDPC) with EDMA in the presence of two porogens (iso-propanol and 1,4-butanediol) and AlBN as an initiator, to produce poly (MDPC-co-EDMA). The second monolith was produced by co-polymerisation of two monomers including MDPC, 12-methacryloyl dodecylphosphoserine (MDPS) using the same crosslinker, the porogens and the initiator, to produce poly (MDPC-co- MDPS-co-EDMA). When these monoliths were applied to the separation of eight neutral alkylphenones differing in their alkyl chain, it was found that their Rt on both monoliths followed a typical RP-HPLC mechanism, where the Rt of alkylphenones increased as the length of chain increased, indicating that an hydrophobic interaction was responsible for the separation. It is also noted that the Rt for the analytes investigated was very similar on both monoliths. In addition, as characterised by ζ potential analysis, the surface of poly (MDPC-co-EDMA) is negatively charged indicating the possibility of electrostatic interaction with charged analytes. Since the surface of MDPS is also negatively charged, its inclusion in the second monolith, poly (MDPC-co- MDPS-co-EDMA), would, therefore, be expected to enhance the electrostatic interaction. In order to examine this hypothesis (the possible behavior of electrostatic interaction), a set of six analytes including two neutral (phenacetin and nitrendipine), two acidic (diclofenac and indomethacin) and two basics (trimipramine and chlorphentermine) were investigated. The Rt of neutral analytes on both monoliths remained virtually constant, while the Rt of the charged analytes changed. For the acidic analytes (negatively charged), less electrostatic interaction was observed on the second monolith compared with the first monolith, while, for the basic analytes (positively charged), more electrostatic interaction was

noticed on the second monolith compared with the first monolith. These results indicated that both hydrophobic and electrostatic interactions were responsible for the changes in the retention times of the investigated analytes and proved of the successful fabrication of the mixed-mode monoliths.

Sulfonic- azobenzene is a type of mixed-mode stationary phase in chromatography. With this sort of mixed-mode phases, there are various possible mechanism interactions between the analytes and the phases. This is due to the rigidly functionalised azobenzene and the ionised sulfonic acid. These possible interactions include hydrophobic interactions, ion exchange interaction, and the intermolecular π–π interactions affording a wider range of applications. Azobenzene dye, methyl orange (MO), provides a stationary phase with good chromatographic performance [147]. The synthesis of this phase employs bonded silica or chemical modification of counter-ion in the ionic liquid polymer phase [148]. The MO stationary phase was used for the separation of poly-aromatic hydrocarbons (PAHs) and steroids and illustrated excellent separation characteristics [147]. Another example of sulfonic-azobenzene dye is Congo red (CR), which is regularly used as an acid–base indicator [149]. With CR, when the pH is within 3.0–5.2, the two azo groups are protonated giving rise to a colour change of the dye from blue to red [149]. CR has for the first time been synthesised and then used as a mixed-mode chromatographic stationary phase for chromatographic separation [144]. CR derivatised silica (Sil-CR) was synthesised via the bonding of CR to glycidoxypropyl-modified silica. The resulting Sil-CR was subsequently packed into a capillary for Nano-HPLC evaluation. This stationary phase illustrated different chromatographic modes including RP-HPLC, aqueous liquid chromatography (PALC), and HILIC when various types of analytes were investigated including parabens, nucleosides and some bases.

Additionally, the chromatographic material was also successfully used in a mixed-mode (RP-HPLC and ion-exchange) for the separation of benzoic acid derivatives and sulphonamides [144].

In this Chapter, instead of using the glycidoxypropyl modified silica as conducted in the study above, a newly monolith was thermally synthesised via the co-polymerisation of (GMA-co-EDMA) in the presence of two porogens (1-propanol and 1,4-butanediol) and AlBN as an initiator. Here, CR was reacted using with the very reactive epoxy group embedded in the GMA. The monolith demonstrated different chromatographic modes including RP-HPLC and HILIC, illustrated by the separation of different compounds.

6.1. Experimental section

6.1.1. **Materials and reagents**

Glycol methacrylate (GMA), ethylene dimethacrylate (EDMA), 3-(trimethoxysilyl) propyl methacrylate (γ-MAPS), 1, 4-butanediol, 1-propanol, azobisisobutyronitrile (AIBN), sodium hydroxide, thiourea, dimethyl phthalate, anisole, naphthalene, acrylamide, toluene, and Congo Red, were all obtained from Aldrich Chemicals (Steinheim, Germany). HPLC-grade methanol (MeOH), ethanol (EtOH), acetonitrile (ACN), N,N-dimethylformamide (DMF), and dimethyl sulfoxide (DMSO), triethylamine (TEA) were all purchased from Fisher Scientific (Leicestershire, UK). Water used throughout all experiments was purified using a Millipore System model no. SYNSV0000. pH indicator paper was purchased from Camlab House (Cambridge, UK). The fused silica capillaries were supplied from CM Scientific (Silsden, United Kingdom, Part no. TSP200350).

6.1.2. **Instrumentation**

An oven employed for the thermal polymerisation. A microscope used for investigating the presence of air bubbles inside the capillary column and the confirmation of the introduction of the polymerisation mixture within the capillary. IR was used to study the chemical modification of GMA with CR; more details about these instruments, i.e. model/make, manufacturer's details have already been stated in Chapter **2** (section 2.2).

6.1.3. **Solution preparation**

The test mixture consisted of 10 mg thiourea, 60 µl dimethyl phthalate, 57 µl anisole, and 16 mg naphthalene dissolved in 10 ml of 50% ACN (HPLC-grade) and 50% water (HPLC-grade) (V/V). The mixture was then diluted 50 times in order to avoid column overloading and to obtain a reasonable UV response. 400 mg Congo red was dissolved in 4 ml dry DMF and 150 ul TEA. The point of the addition the base (TEA) was to increase reactivity, as will be discussed later (section 6.2.2).

6.1.4. **Derivatisation of GMA-co-EDMA with CR**

Firstly, poly (GMA-co-EDMA) monolith was synthesised following the general protocol mentioned previously in Chapter **2** (specifically section 2.1.1). Secondly, the epoxy groups embedded in the monolith was reacted with CR to functionalise the monolith via the ring-opening reaction of the epoxy group. The CR solution was injected onto the monolith at a flow rate of 5 ul/min using a **3 ml** sample loop and using DMF, as eluent, while the monolith was placed in a water bath at 70 °C. This was continued till the red dye was observed eluting the column exit. Subsequently, the flow was stopped, and both ends of the capillary were sealed with GC septa. After that, the monolith was left in the water bath overnight. Next, the derivatised GMA-CR monolithic column was first extensively washed with DMF to wash out any un-reacted materials, followed by flushing with ACN. Fig.6.1 is a schematic of the reaction of GMA with CR with selected monomers and porogens.

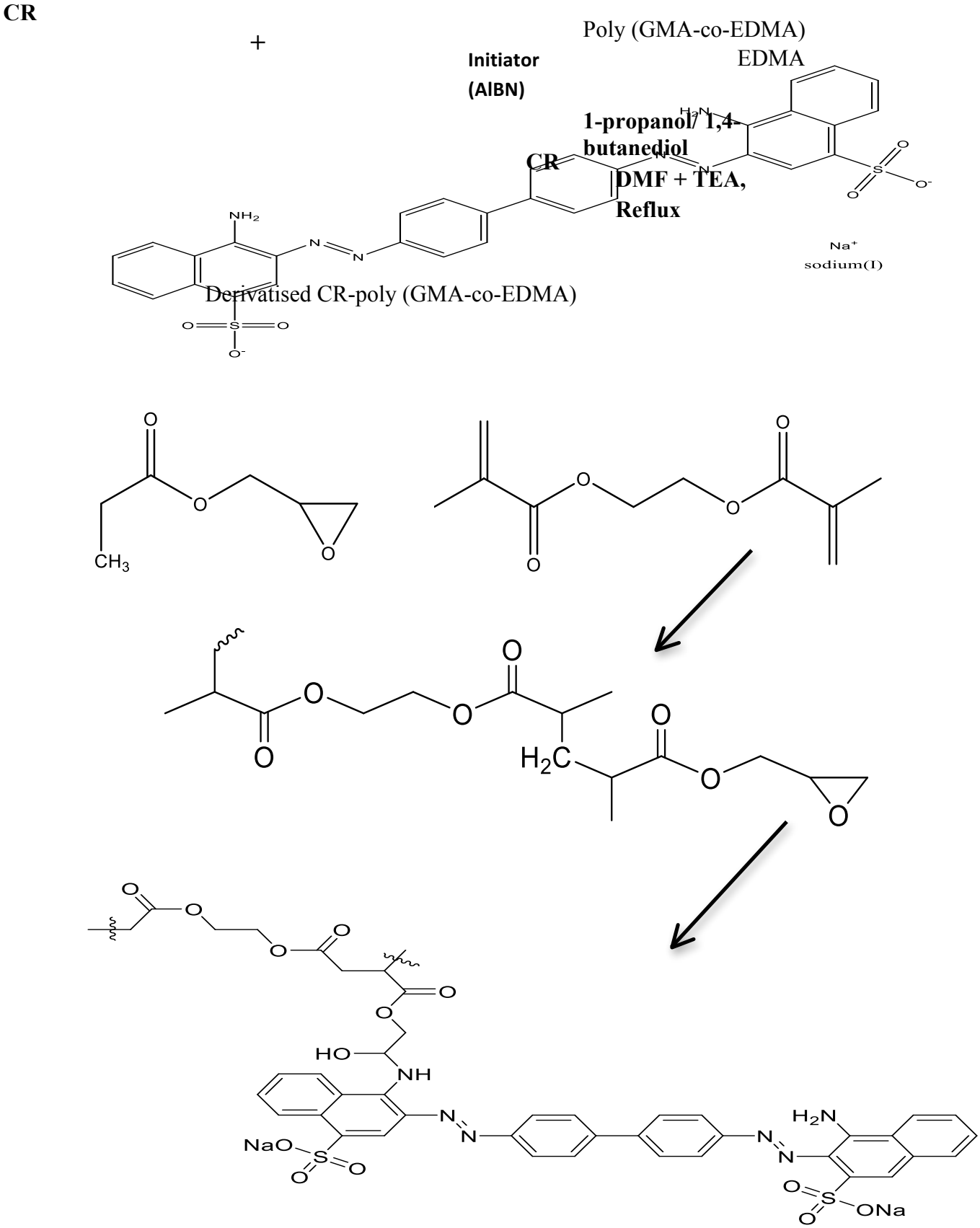

Figure 6-1: The co-polymerisation scheme of the selected monomers and porogens for GMA-co-EDMA derivatised with CR.

CR after eluting from the capillary 7125 injection valve

Fig.6.2 is illustrates the set up used to introduce CR into the (GMA-co-EDMA) monolith.

Table 6.1 shows the composition of the polymerisation mixture.

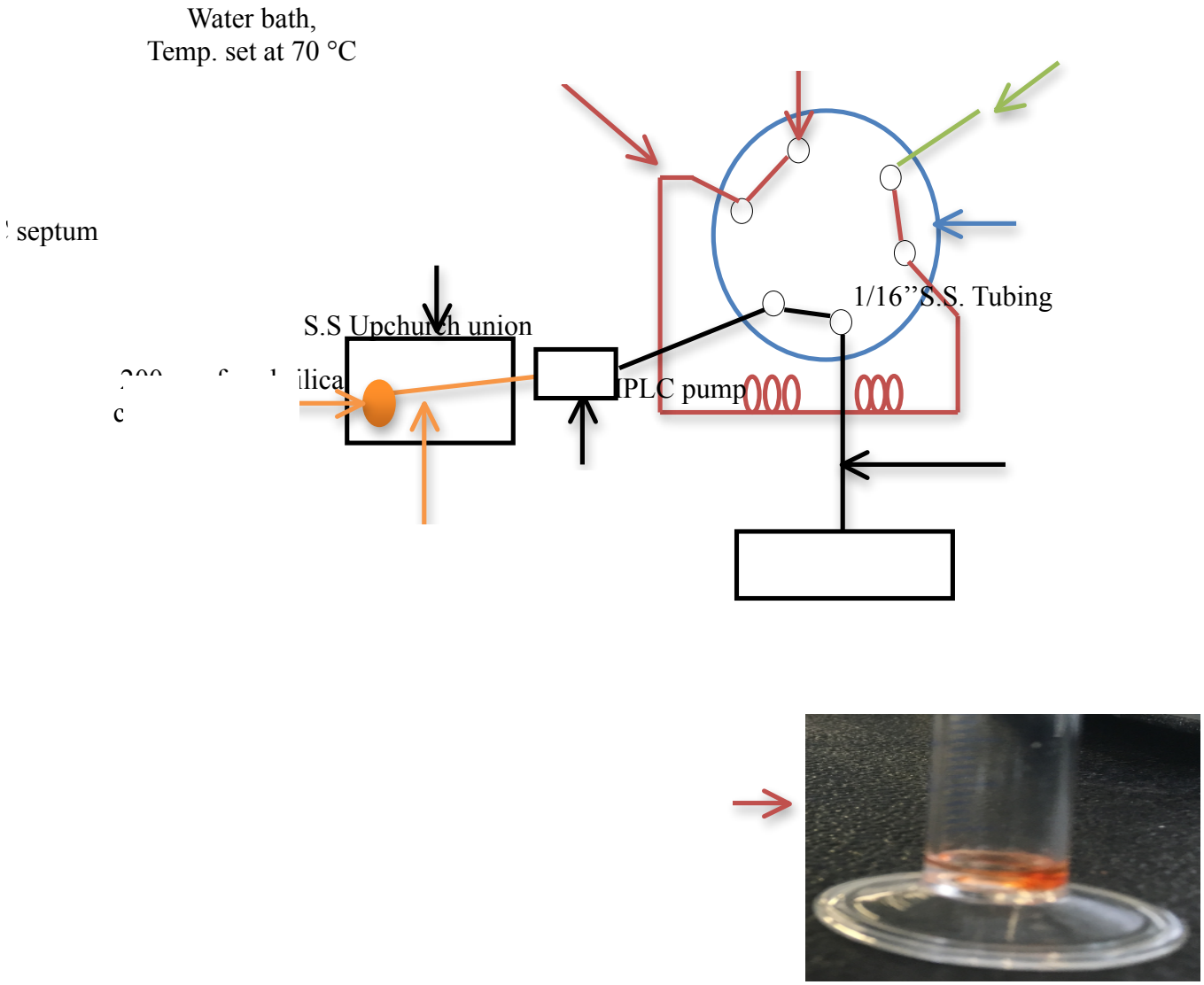

Figure 6-2: Set-up employed for the introduction of CR into the poly (GMA-co-EDMA).

Table 6-1: Composition of the polymerisation mixture.

	Monomer mixture		Porogen system		initiator
Name of the monolith	Monomer (%, w/w)	Crosslinker (%, w/w)	1, 4-butanediol (%, w/w)	1-propanol (%, w/w)	AIBN*
GMA-co- EDMA	20%	20%	30%	30%	1%

* 1% with respect to the Monomer mixture.

6.1.5. **Characterisation of derivatised CR-GMA using IR**

In order to examine the chemical modification of GMA with CR, IR was utilised. For the poly (GMA-co-EDMA) monolith, a bulk polymerization of the mixture was prepared in a 2-ml glass vial in parallel to the polymerization within the capillaries. Subsequently, the resulting bulk polymer (monolith), shown in Fig. 6.3, was removed from the glass vial and ground with a mortar and pestle carefully to avoid any formation of clusters that might cause blockage or low porosity. Afterwards, the bulk polymer was washed extensively with acetone and methanol.

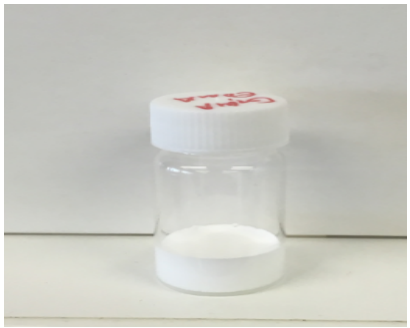

Figure 6-3: Bulk polymerisation mixture.

Then, the bulk polymer was left overnight to dry using a vacuum desiccator. As for the derivatised CR-GMA, 112 mg of dried bulk polymer (GMA-EDMA) was placed in a 25 ml round bottom flask. Next, 400 mg of CR was dissolved in a 4 ml dry DMF and 150 µl TEA and then was shaken for 30 s before being transferred to the round bottom flask containing the dried bulk polymer. Subsequently, the solution was refluxed at 70 °C overnight. After that, the reaction was terminated, and the product was left to cool down at room temperature for about 30 mins. Afterwards, the product was ground using a mortar and pestle to obtain a fine powder and avoid any formation of clusters, followed by an extensive wash with DMF and acetone. Then, the product was left to dry overnight using a vacuum desiccator.

B

After that, both the dried bulk polymers (GMA-co-EDMA) and (CR-GMA), shown in Fig. 6.4, were used for the IR analysis.

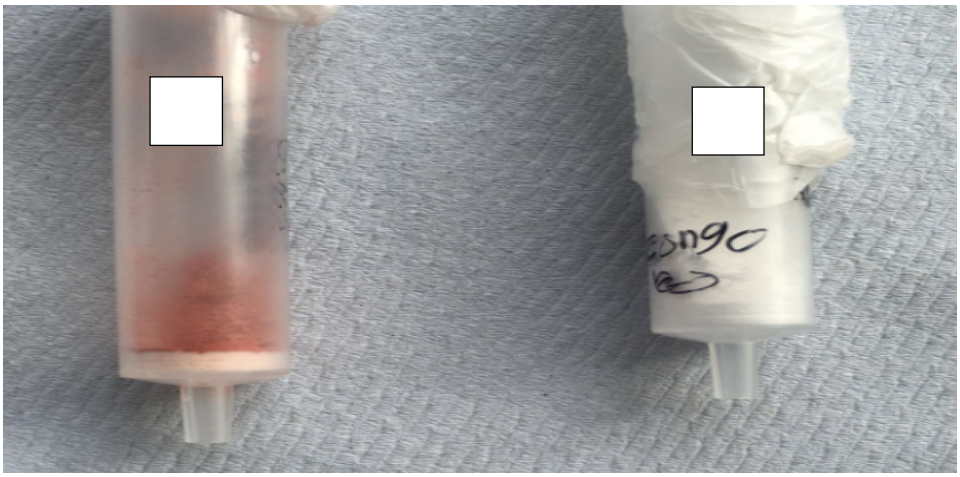

Figure 6-4: Dried bulk polymerisation mixture, A: poly (GMA-co-EDMA), B: derivatised poly (GMA-co-EDMA-CR).

A

6.2. Results and discussions

6.2.1. Characterisation of poly (GMA-co-EDMA) and poly (GMA-co-EDMA-CR) using IR

IR spectroscopy is considered to be a very useful approach for the precisely identifying molecular structures and verifying any chemical modifications [144]. As shown in Fig.6.5, there are some clear differences, highlighted in red, between poly (GMA-co-EDMA) and the derivatised poly (GMA-co-EDMA-CR) monoliths. The differences showed in the derivatised spectrum (B) illustrated the characteristic IR singles around 1650 cm^{-1} and 1100 cm^{-1}. These IR bands and in particular at 1650 cm^{-1} were considered to be attributed to the stretching vibrations of phenyl bond of sulfonic acid azobenzene confirming the successful reaction of CR with the reactive epoxy group [144].

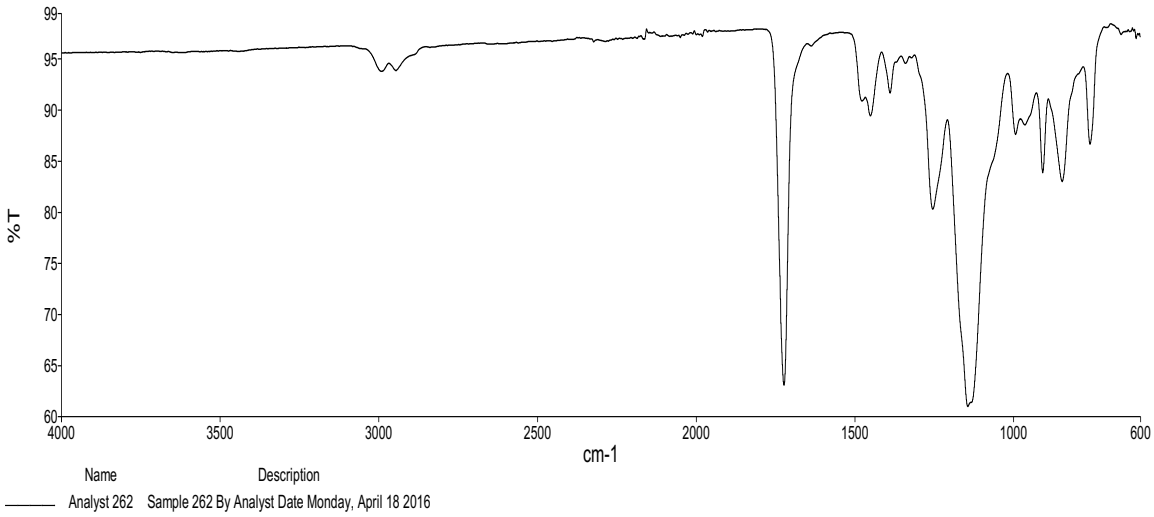

B

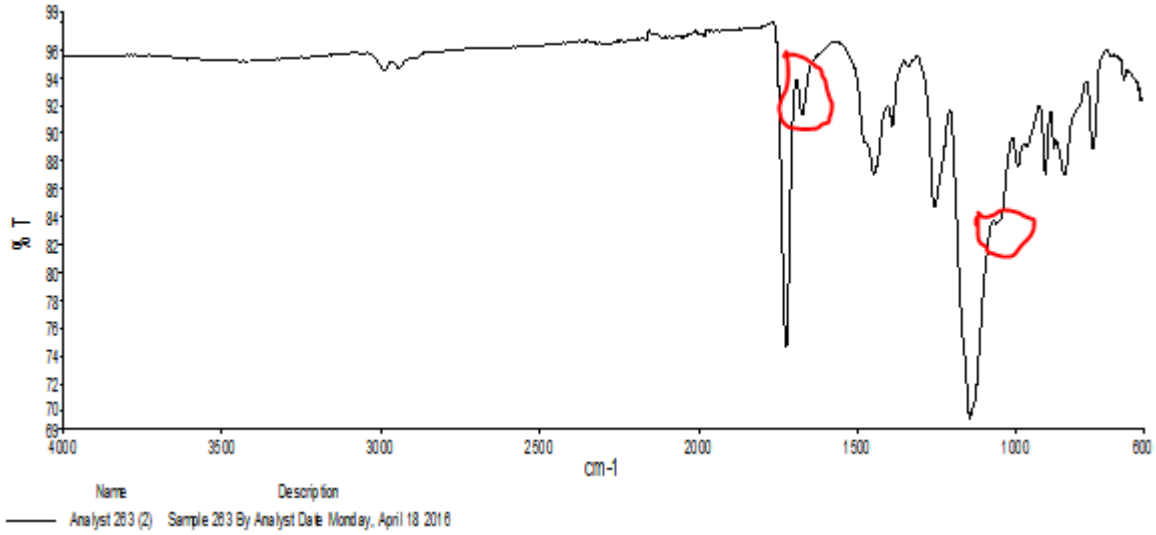

Figure 6-5: illustration of IR spectra for both monoliths, A: poly (GMA-co-EDMA), B: poly (GMA-co-EDMA-CR).

6.2.2. Investigation into the synthesised monolithic column Poly (GMA-co-EDMA)

Investigation into the poly (GMA-co-EDMA) monolith using two porogens (toluene and 1-decanol) in the presence of AlBN as initiator was conducted using a test mixture consisting of thiourea, dimethyl phthalate, anisole, and naphthalene, chemical structures of these compounds with their associated logP were previously illustrated, Chapter **1** Fig. 1.33. As expected [150], their retention behavior followed a typical RP-HPLC mechanism which is in line with their associated logP values. Fig.6.6 shows the analysis of the test mixture using a mobile phase consisting of 70% ACN and 30% H_2O (V/V). It can be observed that a good baseline separation was achieved within 23 mins. In addition, it was noticed that with only a **700 nl/min** flow rate, a very high back pressure was observed 12 MPa (120 bar, 1740 psi) which is very close to the upper limit pressure of the Dina pump 15 MPa (150 bar, 2175 psi).

In order to overcome this challenge, it was decided to synthesise the monolith in a bigger i.d. (200 µm) capillary so that a lower back pressure would be obtained, when CR was introduced for derivatisation.

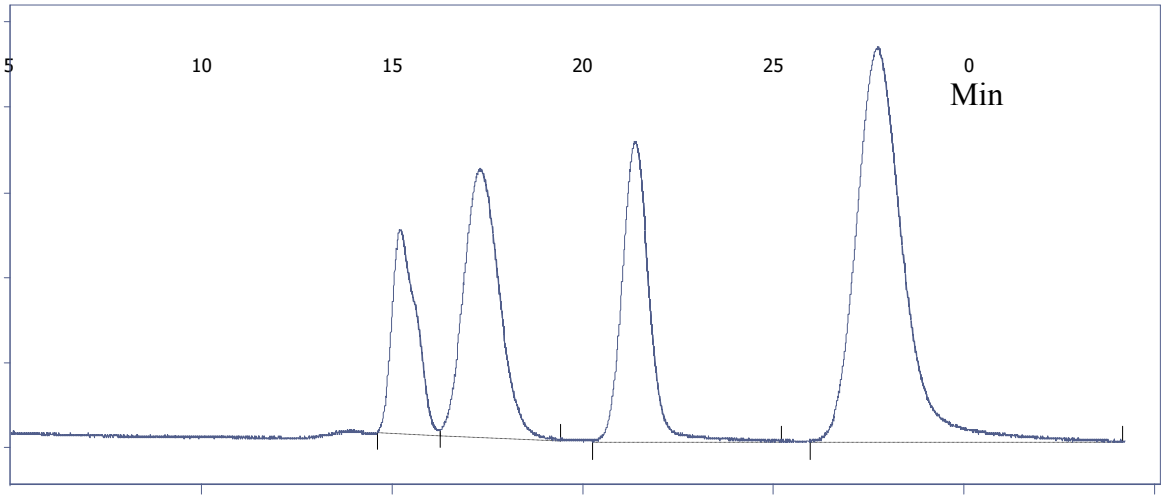

Figure 6-6: Illustration of test mixture separation on poly (GMA-co-EDMA). Experimental conditions: mobile phase 70:30 (V/V) (ACN: H_2O), flow rate 700 nl/min, column 100 µm i.d. x 375 µm o.d. Injection volume: 100 nl, wavelength 210 nm, samples: 1) thiourea, 2) dimethyl phthalate, 3) anisole, 4) naphthalene.

6.2.3. **Derivatisation of GMA with CR**

Thiourea (most polar) and naphthalene (most non-polar) in the test mixture used in Fig.6.6, were used as probes in order to investigate the synthesis of poly (GMA-co-EDMA) and its derivatisation with CR.

After the successful preparation of a poly (GMA-co-EDMA) monolithic column using the set-up shown in Fig.6.2, a CR solution (**35%** purity) dissolved in EtOH, suggested by Qingjiang Wang et al. [144], was passed through the monolithic column,using EtOH as an eluent. This process aimed to derivatise the GMA via the reactive epoxy group inside the 200 μm i.d. capillary. Then, several issues were observed after the termination of the reaction, via quenching of the heat source.. These observations concluded that the **35%** CR was barely soluble in EtOH (shown later in Fig.6.9) and the **35%** CR was not bonded to the surface of the monolith reflected in a typical RP-HPLC mechanism being observed under HILIC conditions, as shown in Fig.6.7. Additionally, even though a bigger i.d. capillary was used (200 μm), a very similar back pressure was observed when a flow rate of **1000 nl/min** was employed. This high back pressure indicated that the use of a bigger i.d. capillary did not reduce the back pressure to the desired level of 7 MPa (70 bar, 1015 psi). The latter back pressure is virtually half of the maximum pressure which the Dina pump can handle, 15 MPa (150 bar, 2175 psi). Obtaining the desired back pressure of around 7 MPa would afford the opportunity to increase flow rate, use of high concentration of H_2O (higher viscosity compared with ACN), or use of high viscous solvents with a moderate flow rate.

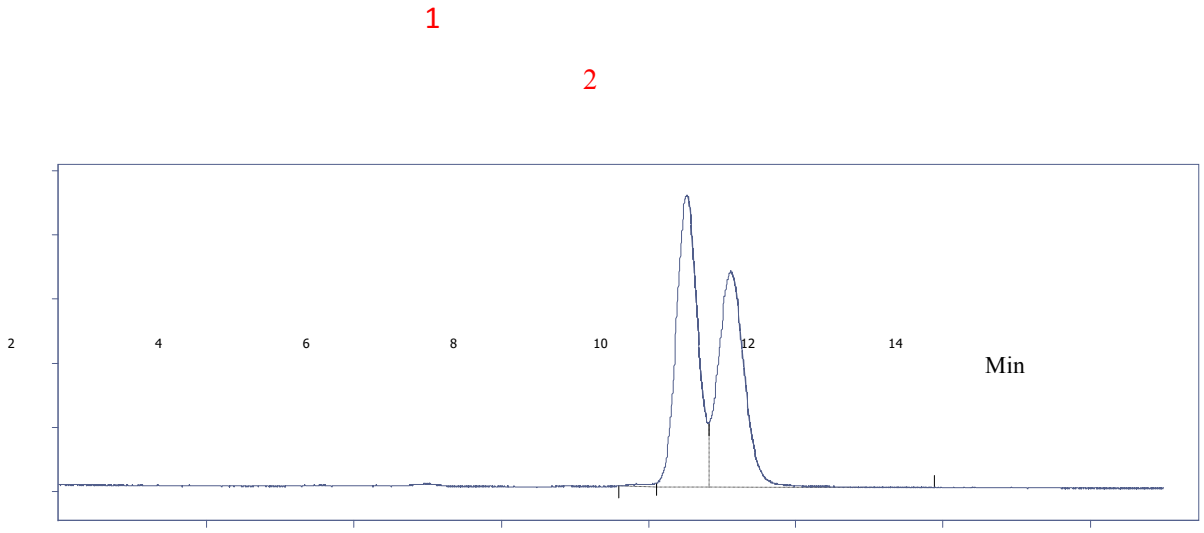

Figure 6-7: Illustration of test mixture on derivatised GMA with low purity '35%' CR. Experimental conditions: column dimension (200 µm i.d. x 350 µm o.d), flow rate 1000 nl/min, mobile phase 5:95 (H2O: ACN) (V/V), samples: 1) thiourea, 2) naphthalene. Other conditions are as stated in Fig.6.6.

In the light of the above, in order to tackle these three issues (low solubility of CR in EtOH, lacking of bonding of **35%** CR with the reactive epoxy group, and the observation of high back pressure). It was decided first to tackle the issue of the high back pressure so that a high back pressure would not be observed when introducing the CR. This was performed through an extensive investigation upon the polymerisation mixture ratio, as illustrated in Table 6.2. As mentioned in Chapter **1** (section 1.8.3.1), porogen selection is one of the main critical parameters in monolith formation. This is because choosing the correct porogens leads to the production of an efficient and porous monolith, whereas incorrect porogen selection adversely affects monolith performance [115].

Table 6-2: Illustration of an extensive study for ratio modifications.

No of trials	GMA (w/v%)	EDMA (w/v %)	Toluene (w/v%)	1-Decanol (w/v%)	AIBN (mg)	Ratio of monomer to porogen (w/ v%)	Observation
1	24%	6%	25%	25%	1%	30:70	Not formed
2	32%	8%	25%	25%	1%	40:60	Not formed
3	20%	20%	20%	40%	1%	40:60	Formed monolith
4	20%	20%	40%	20%	1%	40:60	Formed monolith
5	20%	20%	45%	15%	1%	40:60	Formed monolith
6	25%	15%	20%	40%	1%	40:60	Formed monolith
7	15%	25%	20%	40%	1%	40:60	Formed monolith
New Porogens	GMA (w/ v%)	EDMA (w/ v%)	1-Propanol (w/ v %)	1,4 Butanediol (w/ v%)	AIBN (mg)	Ratio of monomer to porogen	Observation
8	20%	20%	30%	30%	1%	40:60	Formed monolith

As observed in Table 6.2, when the first and second ratios were selected, no monolith was formed indicating that these ratios were not suitable for the monolith synthesis. The reason for choosing these ratios was that it is thought that the ratio between monomer to crosslinker within the polymerisation mixture is commonly to be either 90%-10% or 80%-20% [73, 139, 150, 151]. However, this commonly used ratio did not seem to be applicable with this monolith. Hence, it was decided to go back to the adopted ratio [152], ratio **3**. This ratio consisted of 20% GMA, 20% EDMA, 20% toluene and 40% 1-decanol and this led to the formation of a monolith which produced the baseline separation shown previously in Fig.6.7. Although a baseline separation was obtained, the back pressure was high at 12 MPa (120 bar, 1740 psi) under low flow rate, **1000 nl/min**. This high back pressure indicated that the synthesised monolith lacked large through-pores and consequently had low porosity.

Therefore, it was decided to modify this polymerisation ratio in order to synthesise a monolith with low back pressure (large-through pores). This alteration was performed by keeping the ratio of monomer to porogen (40:60) and the ratio within the monomers (20:20) constant but modifying the ratio within the porogens (toluene and 1-decanol). Since 1-decanol was expected to act as 'good solvent' (more soluble in the monomers) leading to the formation of small pores ultimately generating a high back pressure [119]. It was, thus, decided to decrease the concentration of 1-decanol from 40% to 20% (ratio **4**) expecting that a lower back pressure would be observed. Although, a monolith was formed, a high back pressure was generated, observed when washing the synthesised monolith. Therefore, a further reduction in the concentration of 1-decanol from 20% to 15% (ratio **5**) was conducted, however, the same phenomenon (high back pressure) was also noticed. Subsequently, it was decided to keep the ratio of monomer to porogen (40:60) and the ratio within porogens (20%:40%) constant and altering the ratio within the monomers (GMA and EDMA). As stated beforehand in Chapter **1** (section 1.8.3.2), an increase in the concentration of a crosslinker would result in the formation of small pores which eventually forms a dense bed. This, as a result, leads to the generation of high back pressure [74, 139]. Therefore, it was decided to decrease the concentration of the crosslinker (EDMA) from 20% to 15% (ratio **6**), a monolith was formed but the back pressure was unexpectedly still high, observed when washing the monolith. This observation of high back pressure with a decrease in the concentration of EDMA in the polymerisation mixture has been recently observed in a study conducted by Zhenghua Liu et al.[153]. They fabricated a poly (N, N-dimethyl-N-(3-methacryl-amidopropyl)-N-(3-(sulfopropyl) ammonium betaine (SPP)-co-EDMA) and observed that a decrease in EDMA concentration led to an increase in the back pressure surprisingly, but no explanation was provided.

Then, it was decided to increase the crosslinker form 20% to 25% (ratio **7**), but the back pressure was still high.

In the light of the attempts conducted above, it was decided to replace the porogen system (toluene and 1-decanol) with a new porogen system for the reason that the choice of 'correct porogens system' has a profound effect on monolith's pores formation and efficiency [115, 154].

One of the common porogen systems employed for monoliths fabrication is the combination of 1-propanol and 1,4-butanediol [69, 155-158]. Therefore, it was decided to replace the original porogen system (toluene and 1-decanol) with this commonly used combination (1-propanol and 1,4-butanediol), as shown in the ratio **8**. The monomers were readily soluble in the new porogen system (1-propanol and 1,4-butanediol), and a monolith was also formed with large through-pores. These large through-pores afforded a very low back pressure around 10 MPa (100 bar, 1450 psi) under a high flow rate, **3000 nl/min,** three folds higher than what was used with the original porogens (toluene and 1-decanol). Additionally, a good baseline separation was obtained, as shown in Fig.6.8. As expected [150], a typical RP-HPLC mechanism was observed when the concentration of ACN decreased from 99% to 65%, reflected in longer Rt for naphthalene.

A B

2 1

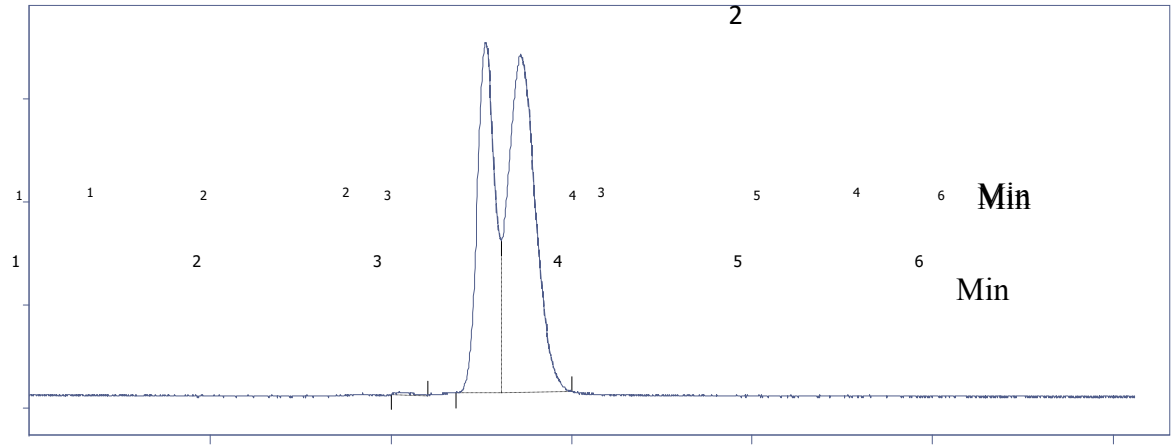

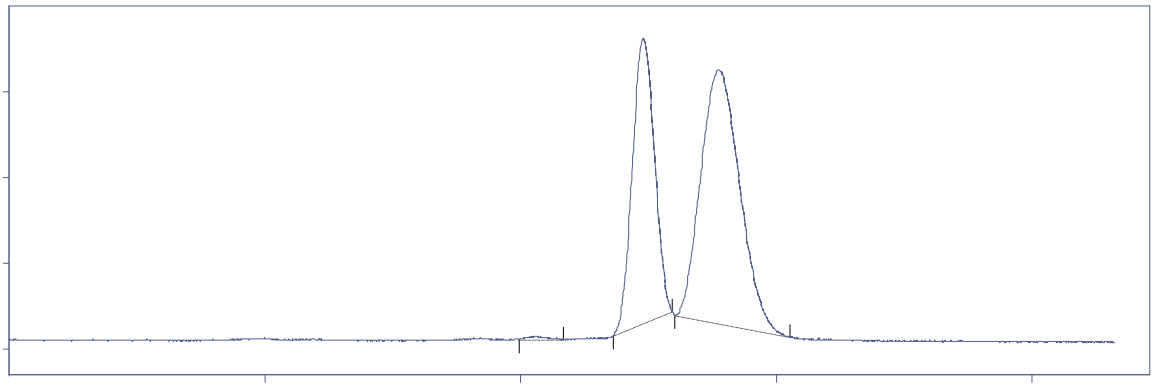

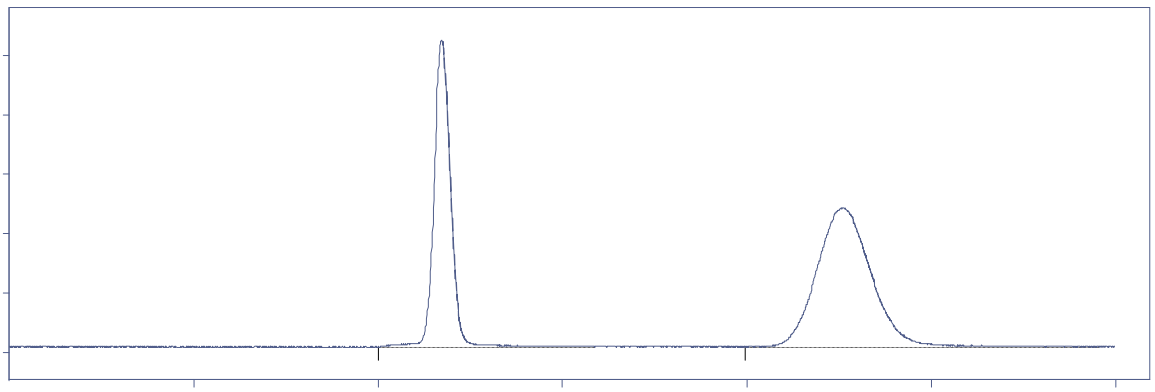

D

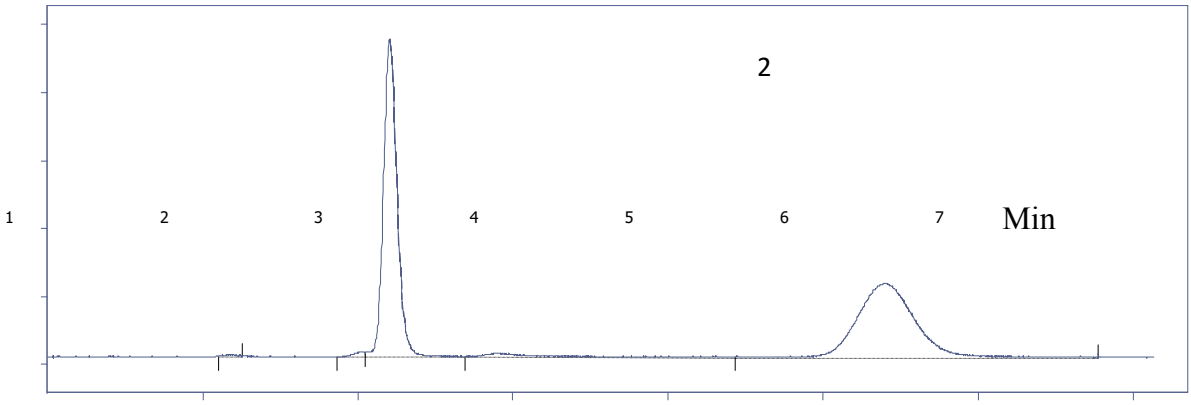

Figure 6-8: illustration of ratio 8 for the separation of test mixture, Experimental conditions: mobile phase mobile phase (A) 1:99 (H2O: ACN), (B) 5:95 (H2O: ACN), (C) 30:70 (H2O: ACN), (D) 35:65 (H2O: ACN) (V/V), samples: 1) thiourea, 2) naphthalene. Other conditions are as stated in Fig.6.7.

After tackling the issue of high back pressure, it was next decided to investigate the second problem, which was the low solubility of CR in EtOH. This was simply performed via running a solubility test using four different solvents differing in their polarity including H_2O, EtOH, DMSO, and DMF. As can be observed from Fig.6.9, CR was not readily soluble in EtOH and was soluble in H_2O and quickly soluble in DMF and DMSO. Since H_2O water could compete in the nucleophilic attack to GMA causing unwanted ring-opening with consequent loss of CR derivatisation, it was, therefore, disqualified from the choice. For a matter of choice, DMF was selected over DMSO.

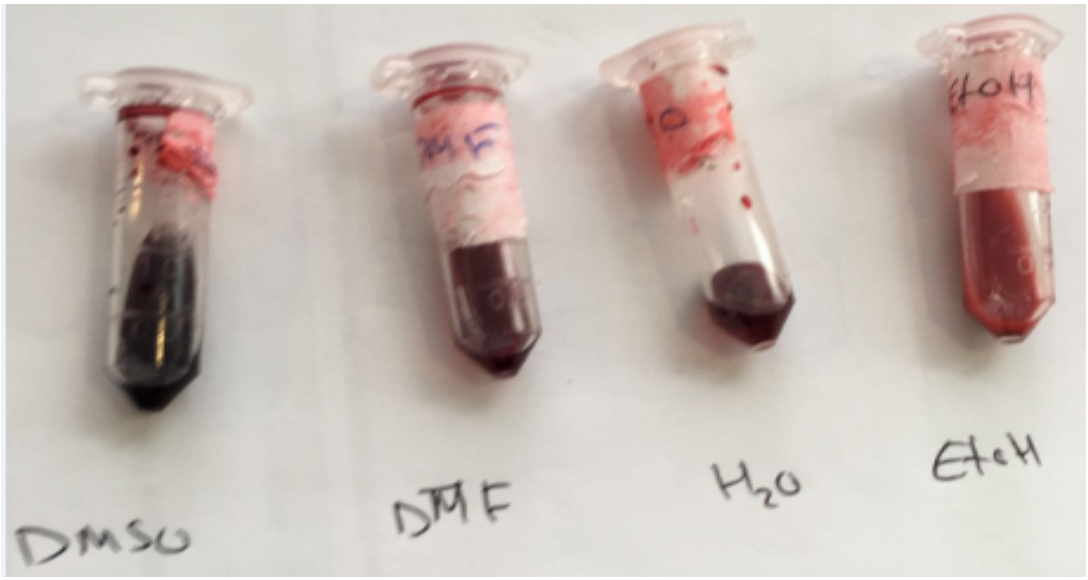

Figure 6-9: Solubility test using four solvents.

After tackling the issue of solubility, it was then decided to investigate the third issue, which was the enhancement of the reactivity of CR. This would ultimately lead to the improvement in the bonding of CR to the reactive epoxy group embedded in the GMA monolith. This improvement was accomplished via utilising two steps, including purer CR and the addition of a base (TEA). The purity of CR utilised in the first attempt was only **35%** indicating a very low concentration of CR present, and therefore, there was not much of CR that would react with the reactive epoxy group. Therefore, purer CR was utilised, specifically **85%**.

The second step was the addition of a tertiary base (TEA). This is because the derivatisation of CR to GMA is not a straightforward reaction due to the aromatic amine of CR, given the resonance effect of the lone pair of electrons on the nitrogen atom making it difficult to react with the epoxide of GMA. Hence, it was decided to add the tertiary base (in the reaction mixture in order to enhance the reactivity of the aromatic CR amine. This addition of the base combined with the high purity CR (85 **%**) has led to the formation of a deep-red polymer, suggesting a higher CR incorporation than the previously reported polymer-CR conjugates [144].

A
A1

1

This was further confirmed by the IR analysis, shown previously Fig.6.5, whereby a new strong peak at 1650 cm^{-1} appeared when compared with the control poly (GMA-co-EDMA).

This band was attributed to the phenyl stretch of sulfonic acid azobenzene, confirming CR presence in the polymer [159]. This approach (purer CR and the addition of TEA) has proven to be effective resulting in bonding of CR to the reactive epoxy group reflected in the observation of the HILIC mode, as shown in the Fig.6.10.

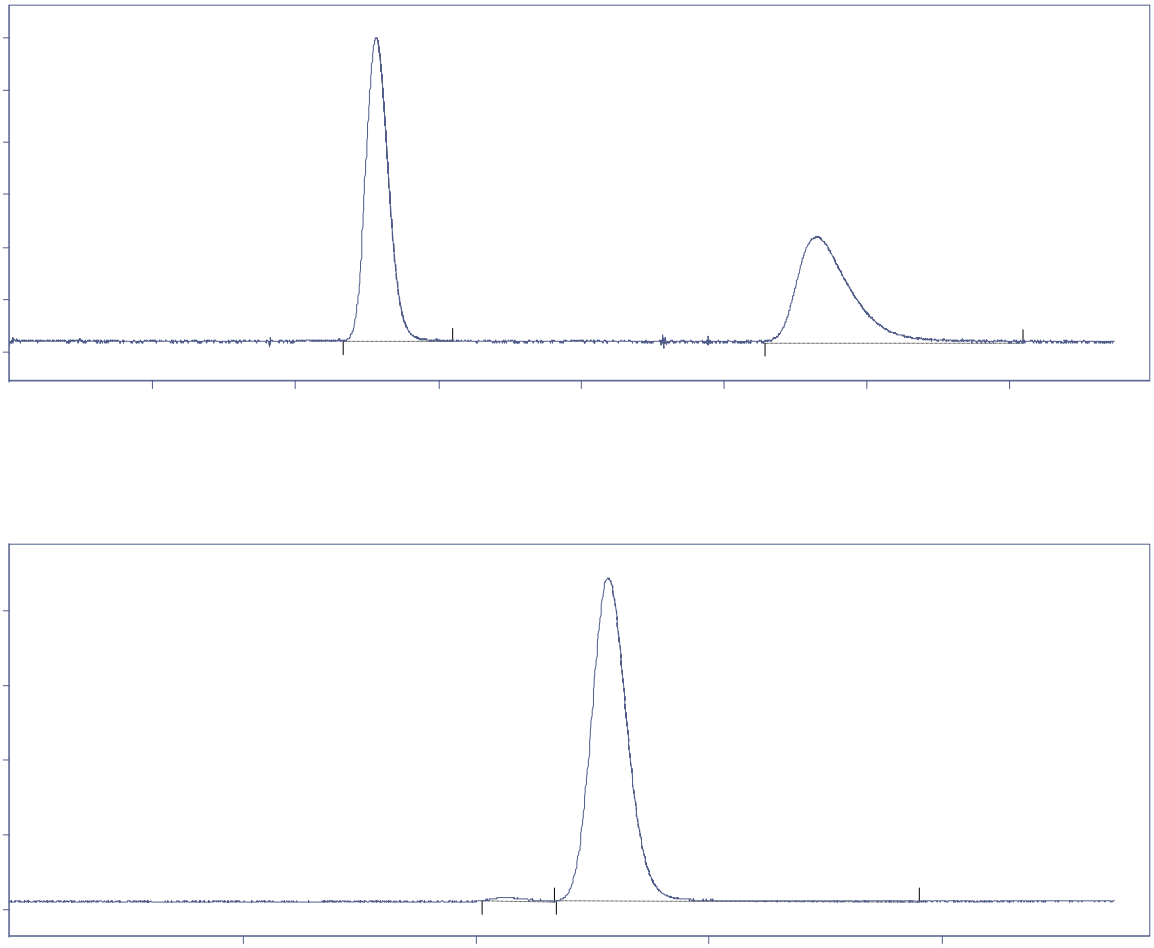

100
80
60
40
20
0
0

1

A2C
B

1

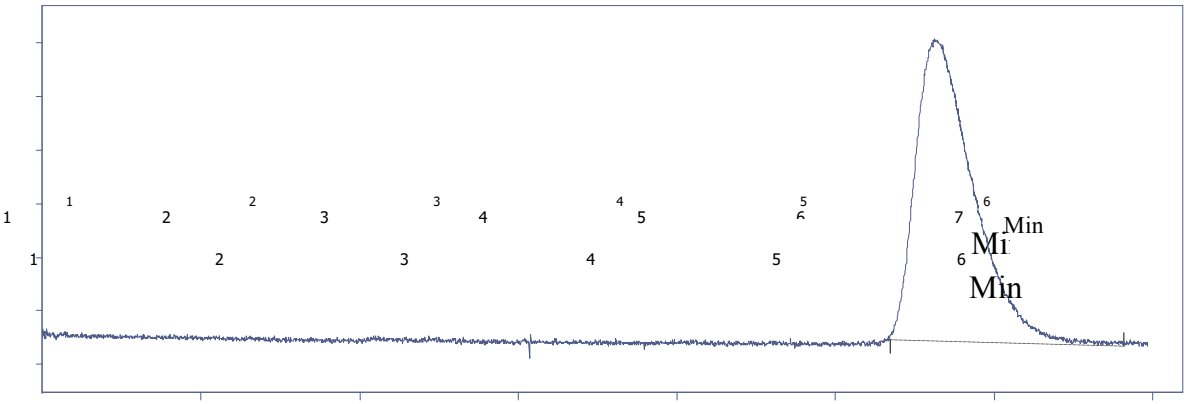

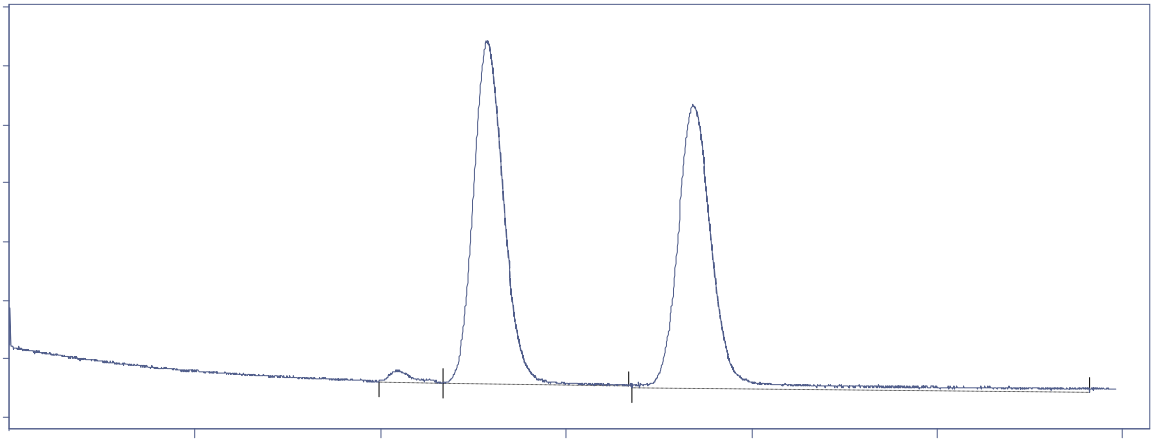

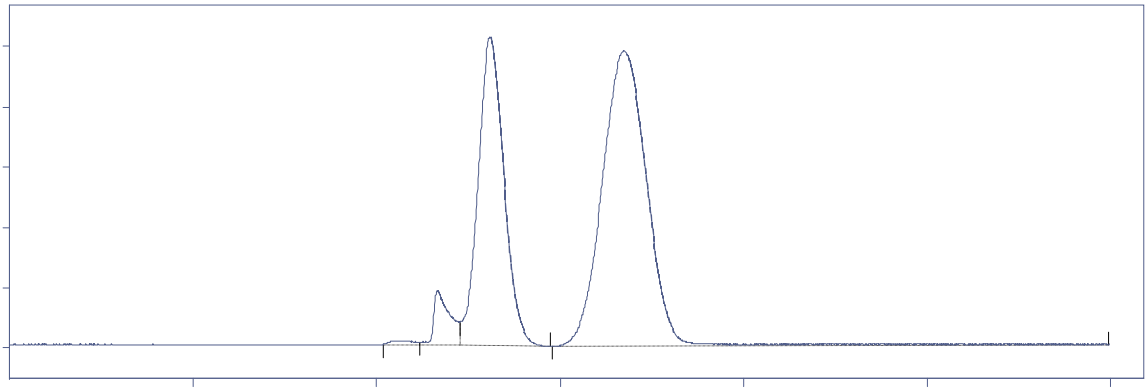

D1

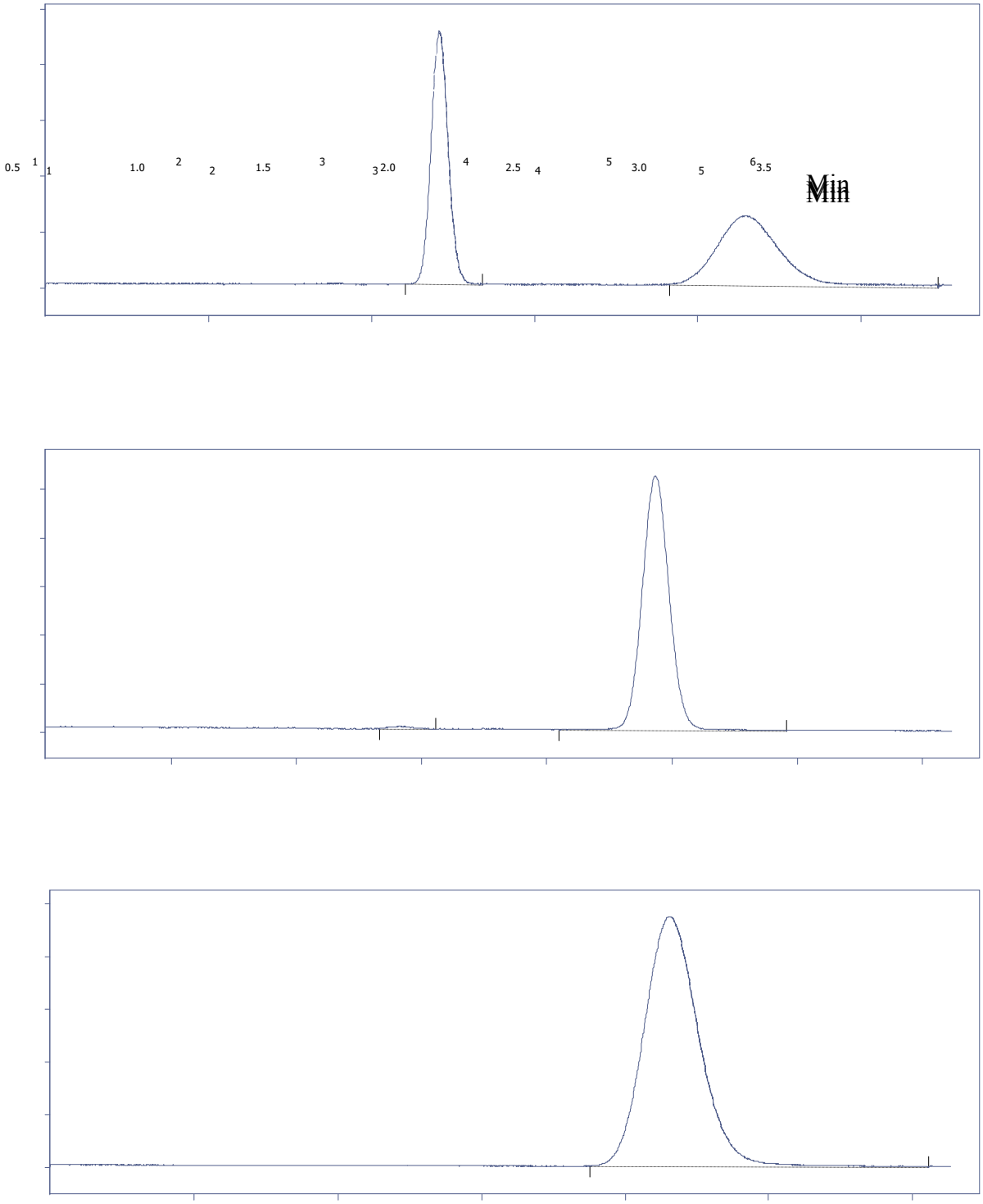

Figure 6-10: Illustration of HILIC and RP-HPLC separation. Experimental conditions: mobile phase mobile phase (A) 1:99 (V/V) (H2O: ACN), (B) 5:95 (V/V) (H2O: ACN), (C) 30:70 (V/V) (H2O: ACN), (D) 35:65 (V/V) (H2O: ACN), flow rate 3000 nl/ml, samples: 1) naphthalene, 2) thiourea. Other conditions are as stated in Fig.6.7.

Furthermore, a typical phenomenon in HILIC columns was observed, shown in Fig.6.10, as previously stated in Chapter **1** (section 1.8.6). This observation is called 'critical transition' by which at a certain concentration of organic eluent (ACN in most cases), the mechanism of RP-HPLC is observed when HILIC columns are in use. The 'critical transition' is dependent on the polarity of the HILIC column, the lower the critical transition is, the more polar the stationary phase will be. In our case, this phenomenon was observed at 65% ACN, which is similar to the HILIC monolith poly (SPE-co-EDMA) synthesised by Smith et al. [20], when they found that at 65 % ACN, a RP-HPLC mechanism was observed.

6.2.4. **Application**

In order to further investigate the derivatised monolith (GMA-co-EDMA-CR), a commonly used mixture consisting of toluene (logP 2.49), acrylamide (logP -0.27) and thiourea (logP -0.46) [160] was employed.. Fig.6.11 shows an excellent baseline separation for the analytes investigated. Additionally, when the concentration of ACN in the mobile phase increased from 95% to 98%, a better baseline separation was observed. Furthermore, a typical HILIC behavior was observed, in which the Rt of thiourea increased as the ACN concentration increased. [161].

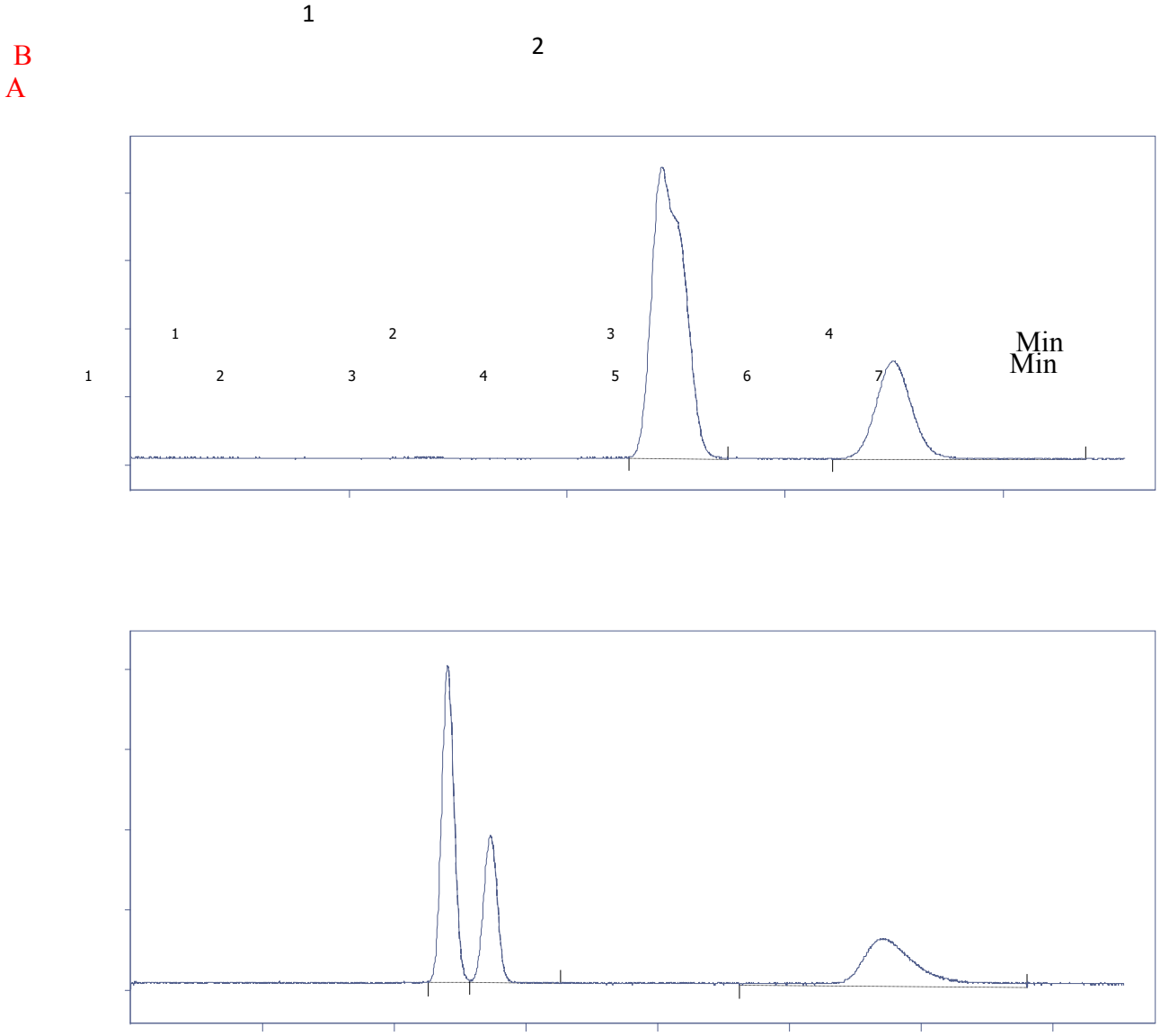

Figure 6-11: Illustration of HILIC separation. Experimental conditions: mobile phase (A) 5:95 (V/V) (H2O: ACN), (B) 1:99 (V/V) (H2O: ACN), samples: 1) toluene, 2) acrylamide, 3) thiourea. Other conditions are as stated in Fig.6.10.

To further investigate the derivatised monolith (GMA-co-EDMA-CR), another more polar mixture consisting of thymine (logP -0.46), cytosine (logP -1.24), and cytidine (logP -2.8) [160] was injected, however, no baseline separation was attained (co-elution), as illustrated in Fig.6.12.

1,2,3

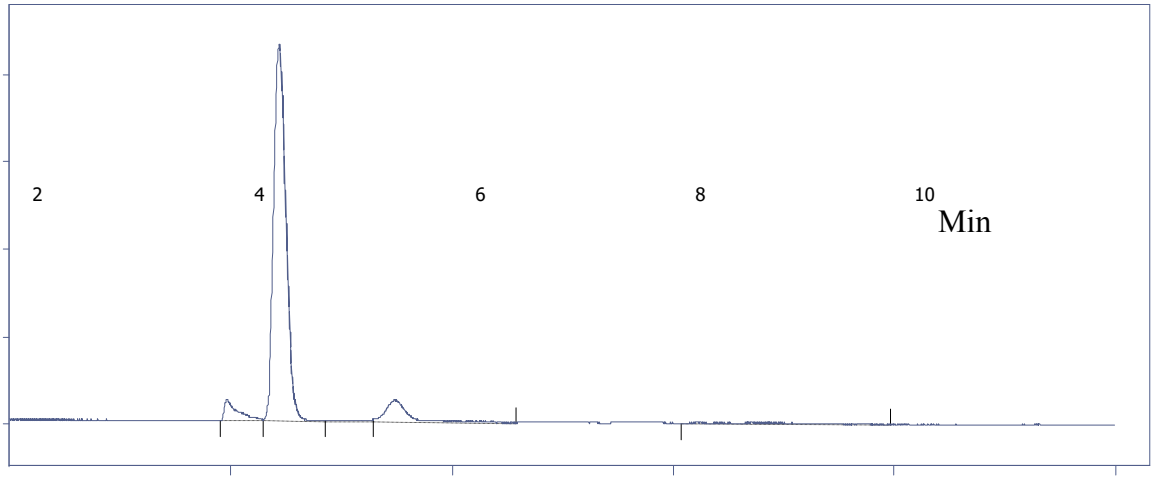

Figure 6-12: illustration of separation of polar analytes (thymine, cytosine, and cytodine). Experimental conditions: mobile phase 5:95 (V/V) (H_2O: ACN), samples: 1) thymine, 2) cytosine, 3) cytodine. Other conditions are as stated in Fig.6.10.

The suggested explanation and hypothesis for such phenomenon could be that possessing very low back pressure, as stated earlier (section 6.2.2), was the result of the presence of very large through- pores. This has led, as a result, to the application of high flow rate and ultimately fast analysis. Yet, these large through-pores could have been at the expense of the monolith's surface area. In other words, a very low surface area was available for the analytes investigated to interact with. Therefore, in order to overcome this challenge and increase the monolith's surface area, there are a number of ways that could be investigated. These include increasing the ratio of GMA to EDMA in the polymerisation mixture, for instance, from the used ratio in this Chapter (1:1) to 5:1 expecting that more of the reactive epoxy group will be present for the reaction with CR followed by the utilisation of the particle-packed bed technique. This approach could lead to an increase in the surface area of the monolith and make the monolith behave more in a HILIC mode.

The reason for utilising the particle-packed bed technique is because this technique is understood to afford a much higher surface area than that within a monolithic bed due to its nature [162]. Another approach for increasing the surface area could be via the synthesis of organic polymer beads containing the reactive epoxide group. These would be expected to have a higher concentration of these groups, potentially leading to a higher HILIC property after derivatising with the CR reagent. These both approaches are an area of study that will be further explored as part of future research projects.

6.3. Conclusion

Mixed-mode stationary phases have proven to be an alternative approach to enhance chromatographic selectivity due to the advantages mentioned beforehand in the introduction section.

The poly (GMA-co-EDMA) monolith was thermally performed using two porogen systems including toluene and 1-decaonol and 1-propanol and 1,4- butanediol. The latter porogen system was observed to be a better in terms of porosity, higher porosity (lower back pressure). DMF and DMSO afforded better solubility for CR. In addition, the utilisation of purer CR and the addition of TEA provided a better enhancement for the reactivity of the aromatic amino group illustrated in increasing its binding with the reactive epoxy group. The derivatised poly (GMA-co-EDMA-CR) monolith showed a mixed-mode separation including RP-HPLC and HILIC and the critical transition was observed at 65%.

The monolith poly (GMA-co-EDMA-CR) was also applied to separate a mixture of small molecules (toluene, acrylamide, and thiourea) and gave a good baseline separation. When more polar analytes (thymine, cytosine, and cytidine) were investigated, no baseline separation was attained and this phenomenon area will be under investigation, as shown in the next Chapter (section 7.1).

Chapter 7

Conclusion and Future work

7. Conclusion

Monolithic columns are continuous interconnected networks with large through-pores channels. This structure results in a decrease in the diffusion path and therefore affords high permeability, which results in obtaining good separation efficiency. The preferred structure of monoliths is bi-model consisting of mesopores and macropores responsible for retention and flow of mobile phase respectively. The structure also enhances the mechanical strength, and the large through-pores channels provide very low flow resistance leading to fast analysis and separation. This combination (mechanical stability and high through-pores), consequently, allows the use of smaller diameter monolithic columns employed under high flow-rates, increasing both sensitivity and throughput simultaneously. Additionally, the unique structure of monolith improves permeability and mass transfer leading to a decrease in the phenomenon of band broadening.

Furthermore, organic monolithic materials have several advantages over the silica based material. These include the resistance to high pH qualifying basic analytes to be analysed without the use of additives, such as TEA or suffer from peak tailing, as explained previously. Another advantage is the vast bank of chemistry choices enabling synthesis of organic monoliths fitting the desired applications or modes of chromatography (RPHPLC, HILIC, etc.).

Regardless of the advantages mentioned previously, there are still some shortcomings associated with organic monoliths. These include some monoliths materials are prone to swelling/shrinking under high organic solvent compositions. This negative impact leads to low stability and low efficiency. In addition, tuning the monolith morphology, including

porosity, pore-size distribution, internal pores and external pores in order to yield efficient monoliths is often associated with 'trial and error strategy' and therefore is time-consuming.

When synthesising monolith columns, there are some hints suggested to be considered so that efficient columns could be produced. Some of these considerations include avoiding the presence of air bubbles throughout the monolith's synthesis. This is because failure to do so could lead the air bubbles to be present during the introduction of NaOH, which could result in a non-homogenous activated surface. This, in turn, would weaken the bonds between the inner surface and γ-MAPS, resulting in an unstable monolith. Another negative impact associated with the presence of the air bubbles is an uneven coating of the fused silica capillary if the air bubbles are present during the introduction of γ-MAPS. In such cases, this will lead to a loss of interaction between the polymerisation mixture and γ-MAPS resulting in an unstable monolith or void being formed leading to poor column efficiency. Furthermore, it is highly recommended to purge the polymerisation mixture with N_2 gas for around 5 min in order to eliminate the presence of dissolved gases. The presence of such gases might lead to disturb the polymerisation process and eventually the formation of the monolith inside the capillary. In addition, when required to make a detection window, it is vital not to over-heat the monolithic capillary as doing so will hinder the detection, as illustrated in Fig. 2.16.

Additionally, installation of a monolithic capillary into the injector valve, when required for monolith's characterizations/analysis, is an essential step as improper installation will lead to poor chromatograms, as shown in Fig. 2.12.

The first stage of this project was focused on the synthesis of a poly (SMA-co-EDMA) monolithic column in a 100 μm i.d. fused silica capillary to be used as a stationary phase in capillary liquid chromatography, Chapter **3**. After the successful synthesis, the monolith was then characterised in terms of mechanism of separation, reproducibility of the monolith,

porosity, and permeability. Furthermore, the fabricated monolith showed no sign of shrinking or swelling issues under the use of organic solvents, considered as an advantage since many organic monoliths are prone to such phenomena. Moreover, modifying the polymerisation mixture from what was published previously via by changing the porogen from iso-amyl alcohol to 1-propanol did not improve the porosity. This suggested that the polymerisation mixture needs to be carefully modified to obtain the desired porosity and efficiency. Also, the monolith showed high reproducibility reflected in low %RSD for the analytes investigated (dimethyl phthalate, naphthalene). The monolith synthesised, however, showed low efficiency as many organic monoliths display with small molecules. This is due to the low amount of mesopores, i.e. low surface area. In order to illustrate the applicability of this monolith into 'real-life samples', a method was developed and validated based on the ICH guidelines for the quantification of caffeine in Arabic coffee.

Due to the low efficiency of the poly (SM-co-EDMA) monolith, a newly novel monolithic column was synthesised, namely poly (HMA-co-1,6-HEDA) using a longer crosslinker as a stationary phase for micro-HPLC. As the results in Chapter **4** illustrated, organic monoliths can therefore be utilised for the separation of small molecules using this approach (longer crosslinker). This is because; it affords more mesopores, responsible for the retention (more surface area). The novel monolith demonstrated a high porosity, a high reproducibility, and high stability with no sign of swelling or shrinking during the use of organic solvents. In addition, when synthesising a new monolithic material, it is recommended to show its applicability. Therefore, the novel monolith was employed to separate three sets of samples including neutral non-polar molecules, weak acid molecules, and basic molecules. The monolith demonstrated high selectivity towards these sets. Moreover, so as to show further application for the new monolith (HMA-co-1,6-HEDA), the monolith was employed to quantify amitriptyline in the pharmaceutical tablets. The result obtained was in agreement

with that reported by the manufacture indicating that the fabricated monolith could be utilised for the quantification of this drug in the marketed tablets.

After the synthesis of the new monolith (poly (HMA-co-1,6-HEDA)) for capillary chromatography, a move towards investigating the coupling of monolithic capillary column with MS was taken. As shown in Chapter **5**, it appears that there are a couple of reasons for monolith instability under high back pressure. These include the presence of air bubbles when introducing liquids into the fused silica capillary causing a non-homogenous surface leading to weaker bonds between the inner surface and the γ-MAPS resulting in an unstable monolith. A second reason includes the concentration of crosslinker in the polymerisation mixture, which if not high enough could lead a monolith to become un-stable under high back pressure. A third reason includes the ratio between the monomers to porogens, if not chosen properly could result in unstable monoliths under high back pressure. Therefore, when synthesising a monolith, a systematic investigation needs to be carried out to establish the correct ratio so that the fabricated monolith could withstand a high back pressure if a conventional pump was in use. Moreover, when fabricating a monolith in fused silica capillaries possessing i.d. ≥ 200 μm, extra care needs to be taken especially when an oven is used as the device for the thermal initiation. Furthermore, a successful coupling between small i.d. fused silica capillaries with conventional MS without additional fittings has been established and can be used, therefore, for HPLC-MS analysis. In order to widen the application and selectivity of RPHPLC stationary phases, the final Chapter in this project was focused on the mixed-mode stationary phases.

As shown in Chapter **6**, the synthesis of the poly (GMA-co-EDMA) monolith was successfully thermally fabricated. Additionally, 1-propanol and 1,4-butanediol was observed to be a better porogen system over toluene and 1-decaonol reflected in providing a higher porosity, lower back pressure. Furthermore, the utilisation of purer CR and the addition of

TEA provided a better enhancement for the reactivity of the aromatic amino group, illustrated in increasing its binding with the reactive epoxy group. The newly derivatised poly (GMA-co-EDMA-CR) monolith showed a mixed-mode separation including RP-HPLC and HILIC and 'the critical transition' was observed at 65% of ACN. The monolith poly (GMA-co-EDMA-CR) was also applied to the separation of a mixture of small molecules (toluene, acrylamide, and thiourea) and gave a good baseline separation. Additionally, when more polar analytes (thymine, cytosine, and cytidine) were investigated, all these analytes co-eluted with the solvent front, i.e. they were not retained. This odd phenomenon could be due to the fact that although the monolith's morphology showed very large through-pores reflected in the ability of the application of high flow rate (3000 ul/min), this could have had a negative impact on the surface area, i.e. low surface area was available for the interaction.

7.1. Future work

As mentioned in Chapter **3**, caffeine co-eluted with the un-retained molecule (thiourea) which could ring the bell that its quantification in the Arabic coffee could be questioned. This is because interference with the solvent front (thiourea) could have affected the quantification (imprecise results). Therefore, a HILIC column could be synthesised and used to verify the quantification of caffeine. The reason for not performing this suggestion in this project was that the Arabic coffee used in this analysis ran out. This was brought from author's own country and could not be replaced. In addition, since the porogen system used (1-propanol and 1,4-butanediol) did not provide high porosity in comparison with similar monolith with different porogen system (iso-amyl alcohol and 1,4-butanediol). Thus, an investigation into a different ratio of the porogen system used or use of different porogen systems could be another piece of work to be conducted.

Since the poly (HMA-co-1,6-HEDA) showed promising results in small i.d. fused silica capillary, Chapter **4**, it could be interesting to investigate how well the monolith would behave in a bigger i.d. (1 or 2.1 mm) using either stainless steel or glass lined tubing. This is because a different kind of column housing leads to a different character of resulting monolith [69, 163]. Hence, it could also be expected that column diameter provides a noticeable effect on the physical properties of the synthesised monolith including homogeneity and permeability. Moreover, another piece of work with this monolith is the analysis and quantification of more complex samples, such as soil or protein and comparing the results obtained with commercial monoliths. The point of this work is to assess the performance and efficiency with such matrices. Furthermore, another piece of work that could be performed with this monolith is that systemic investigation into the polymerisation mixture so that the resulting monolith could handle a high back pressure and be used ultimately with a classical pump. In addition, to the best of our knowledge, the stability of monolithic columns over a long term period (one year for example) has not been investigated. Hence, such an investigation would be highly recommended in order to assess whether or not monolithic materials possess high stability.This is because such characterisation (stability) is vital in the domain of analytical chemistry. Moreover, monolithic materials could be utilised as sorbents for extraction, for instance, SPE sorbents [164]. Therefore, the poly (HMA-co-1,6-HEDA) monolith could be utilised for such applications. Recently, Fuh MR et al. [165] prepared a monolith sorbent for the determination of phenylurea herbicides in water samples and the results obtained were promising. Another piece of work with poly (HMA-co-1,6-HEDA) is that since the set up between the fused silica capillary and the MS has been successfully established, Chapter **5**, it would be useful to evaluate its performance with some bio-fluid samples (urine, blood) and utilise the powerful technique (HPLC-MS).

Since the newly synthesised monolith poly (GMA-co-EDMA-CR) illustrated sort of 'mixed-mode chromatography' due to the chemical structure of the dye (Congo red), it would be interesting to explore more dyes, such as methyl orange (MO), possessing a sulfonic-azobenzene similar to CR. Another material that could be investigated in place of CR is 3-aminopropane-1-sulfonic acid, shown in Fig. 7.1; the reason for this suggestion is that this chemical has similar functional groups as CR (amino and sulfonic acid groups), but the amino group embedded in its chemical structure is aliphatic and is expected to be more reactive, as mentioned in section 6.2.

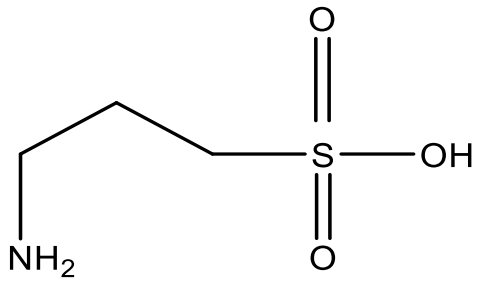

Figure 7-1: Chemical structure of 3-aminopropane-1-sulfonic acid.

To the best of our knowledge, this compound (Fig. 7.1) has not been utilised in monolith synthesis. Another piece of work which could be conducted with this material (GMA-co-EDMA-CR) to enhance the surface area is the synthesis of organic polymer beads containing the reactive epoxide group. These would be anticipated to have a higher concentration of these groups, possibly leading to a higher HILIC property after derivatising with the CR compound.

Nowadays, there has been a wide interest in the application of statistical and machine learning programs for the use with the design of experiments in the field of analytical chemistry. This is because these programs facilitate optimising the choice of factors and variables that have a great effect on a given experiment. Additionally, these programs aid to minimise the waste of time and reagents [166]. Therefore, use of such programs could be a good candidate for the use with the polymerisation mixture ratios used for monolith fabrication. This is because,as illustrated in this thesis, the choice of the best ratio for monoliths fabrication in terms of porosity, permeability, stability under high back pressure and high efficiency involves tedious work, waste of large amount of chemicals and reagents and is time-consuming. To the best of our knowledge, only a few studies have investigated the potential of these programs with monolith fabrication, one of which is a study by Milton Lee et al. [167]. In their study, they developed a statistical model employed for optimising the reagents used for monolithic fabrication. They claim that the statistical model developed could be applied to help simplifying the synthesis of organic monoliths.

Another area of investigation could be the use of monolithic columns with supercritical fluid chromatography (SFC). SFC is a form of chromatography which utilises CO_2 as a mobile phase, typically in combination with more polar co-solvents such as methanol, ethanol, and isopropyl alcohol (many other solvents can also be used e.g. acetonitrile, chloroform, ethyl acetate., [168]). Such CO_2-rich mobile phases have low viscosities and high diffusivities and are ,therefore, considered to be well suited for use as eluents in chromatography [169]. Consequently, combining SFC with monolithic materials (known for high porosity and permeability) could be an interesting future research direction. One of the main application areas in SFC is chiral separation [170]. Therefore, fabrication of chiral monoliths could be of great interest to SFC users.

Bibliography

- Derivatisation of Glycol methacrylate with Congo red for capillary liquid chromatography. Wael Alshitari, C. Legido-Quigley, N.W. Smith. **In preparation.**
- Fabrication and evaluation of an organic monolithic column based upon the polymerisation of hexyl methacrylate with 1,6-hexanediol ethoxylate diacrylate for the separation of small molecules by capillary liquid chromatography. Wael Alshitari, C. Legido-Quigley, N.W. Smith. **Talanta** 141 (2015) 103–110.

Presentation

- Effect of longer crosslinkers on the efficiency of organic monoliths for the separation of small molecules by capillary liquid chromatography, **postgraduate symposium 2015**, King's College London.

References (created using endnotes software version X6):

1. Horváth, C. and W.R. Melander, *Chapter 3 Theory of chromatography*, in *Journal of Chromatography Library*, E. Heftmann, Editor. 1983, Elsevier. p. A27-A135.
2. Wellings, D.D.A., *3 - Modes of chromatographic separation*, in *A Practical Handbook of Preparative HPLC*. 2005, Elsevier Science: Oxford. p. 29-56.
3. *High performance liquid chromatography,isocratic and gradient elution*. High perfromance liquid chromatography 2016 [cited 2016 29-02-16]; Available from: https://en.wikipedia.org/wiki/High-performance_liquid_chromatography#Isocratic_and_gradient_elution.
4. *Wikipedia.org/wiki/Elution* 2015 [cited 2016 29-02-16]; Available from: https://en.wikipedia.org/wiki/Elution#Eluotropic_series
5. L.R.Snyder, *High- performance Liquid Chromatography*. Vol. 3. 1983, USA: New York: Academic press.
6. Whungsinsujarit, S., *The development of polymer related chiral stationary phases for use with micro-separation techniques*, in *Analytical and environmental sciences* 2011, King's College London p. 247.
7. Gama, M.R., C.H. Collins, and C.B. Bottoli, *Nano-liquid chromatography in pharmaceutical and biomedical research.* J Chromatogr Sci, 2013. **51**(7): p. 694-703.
8. Chervet, J.P., M. Ursem, and J.P. Salzmann, *Instrumental requirements for nanoscale liquid chromatography.* Anal Chem, 1996. **68**(9): p. 1507-12.
9. *Column selectivity- A powerful tool when developing reversed-phase separations*. 2000 [cited 2016 03-10-2016]; Available from: http://www.agilent.com/cs/library/support/documents/f3912602612.pdf.
10. Aldrich, S. *Alternate Selectivity in HPLC 4: Embedded Polar Group (EPG) Phases*. 2015 [cited 2016 10-03-]; Available from: http://www.sigmaaldrich.com/video/analytical/hplc-alternate-selectivity-epg-phases.html.
11. J.Dolan *Ion Pairing — Blessing or Curse?* 2008. **21**, 258-263.
12. Dolan, J. *HPLC Solutions #6: What is Phase Dewetting?* 2017 [cited 2017 20-05-17]; Available from: https://www.sepscience.com/Techniques/LC/Articles/696-/HPLC-Solutions-6-What-is-Phase-Dewetting.
13. Levin, D.S. *Ion Exchange Chromatography* 2017 [cited 2017 20-05-17]; Available from: http://docplayer.net/14280096-1-dr-shulamit-levin-analytical-consulting-medtechnica.html.
14. Kahsay, G., et al., *Hydrophilic interaction chromatography (HILIC) in the analysis of antibiotics.* J Pharm Biomed Anal, 2014. **87**: p. 142-54.
15. Hemstrom, P. and K. Irgum, *Hydrophilic interaction chromatography.* J Sep Sci, 2006. **29**(12): p. 1784-821.
16. FUNA, A.M.E., *INVESTIGATIONS ON POLYMERIC CAPILLARY MONOLITHS FOR THE SEPARATION OF SMALL POLAR MOLECULES*, in *Analytical and environmental sciences* 2014, King's College London London. p. 300.
17. Rappold, B.A. and R.P. Grant, *HILIC-MS/MS method development for targeted quantitation of metabolites: practical considerations from a clinical diagnostic perspective.* J Sep Sci, 2011. **34**(24): p. 3527-37.
18. Buszewski, B. and S. Noga, *Hydrophilic interaction liquid chromatography (HILIC)—a powerful separation technique.* Analytical and Bioanalytical Chemistry, 2012. **402**(1): p. 231-247.
19. Tolstikov, V.V. and O. Fiehn, *Analysis of highly polar compounds of plant origin: combination of hydrophilic interaction chromatography and electrospray ion trap mass spectrometry.* Anal Biochem, 2002. **301**(2): p. 298-307.
20. Jiang, Z.J., et al., *Hydrophilic interaction chromatography using methacrylate-based monolithic capillary column for the separation of polar analytes.* Analytical Chemistry, 2007. **79**(3): p. 1243-1250.

21. Simon Cubbon, C.A., Julie Wilson, and Jane Thomas-Oates, *Metabolomic applications of HILIC–LC–MS.* Mass Spectrometry Reviews, 2010. **29**(5): p. 671-684.
22. Miller, J.M., *Chromatography concepts and contrasts*, 2005, WILEY: New Jersey.
23. Dolan, J. *High Performance Liquid Chromatography Solution, Back to basic, Retention Factor*. 2016 [cited 2016 05-03-2016]; Available from: https://www.sepscience.com/214-/John-Dolan.
24. Gray, N., *Studies of UHPLC-MS performance and applications to rapid, sensitive, and robust drug analysis*, in *Analytical and Environmental Sciences*2013, Kings College London: Kings College London
25. Ho, C.S., et al., *Electrospray Ionisation Mass Spectrometry: Principles and Clinical Applications.* The Clinical Biochemist Reviews, 2003. **24**(1): p. 3-12.
26. corportion, A. *Basics of LC/MS*. 1998 [cited 2016 03-10-16]; Available from: http://www.agilent.com/cs/library/Support/Documents/a05296.pdf.
27. Lemière, F., *Guide to LCMS*, in *Guide to LCMS*2016, University of Antwerp, Belgium: Dept of Chemistry p. 7.
28. Bruins, A.P., *Atmospheric-pressure-ionization mass spectrometry: I. Instrumentation and ionization techniques* TrAC Trends in Analytical Chemistry, 1994. **13**(1): p. 37-43.
29. Banerjee, S. and S. Mazumdar, *Electrospray ionization mass spectrometry: a technique to access the information beyond the molecular weight of the analyte.* Int J Anal Chem, 2012. **2012**: p. 282574.
30. Fenn, J.B., et al., *Electrospray ionization for mass spectrometry of large biomolecules.* Science, 1989. **246**(4926): p. 64-71.
31. Knappy, C., *utilisation of Mass Spectrometry for the analysis of some elemntal analysis* in *Chemistry* 2010, University of York York, UK. p. 300
32. Chromacademy. *Mass SpectrometryFundamental LC-MS Electrospray Ionisation – Theory*. 2017 [cited 2017 20-05-17]; Available from: http://www.chromacademy.com/lms/sco31/Fundamental_LC-MS_Electrospray_Ionisation_Theory.pdf.
33. Nguyen, S. and J.B. Fenn, *Gas-phase ions of solute species from charged droplets of solutions.* Proc Natl Acad Sci U S A, 2007. **104**(4): p. 1111-7.
34. Iribarne, J.V. and B.A. Thomson, *On the evaporation of small ions from charged droplets.* The Journal of Chemical Physics, 1976. **64**(6): p. 2287-2294.
35. Dole, M., et al., *Molecular beams of macroions.* The Journal of Chemical Physics, 1968. **49**(5): p. 2240-2249.
36. Schmelzeisen-Redeker, G., L. Bütfering, and F.W. Röllgen, *Desolvation of ions and molecules in thermospray mass spectrometry.* International Journal of Mass Spectrometry and Ion Processes, 1989. **90**(2): p. 139-150.
37. Thomson, B.A. and J.V. Iribarne, *Field induced ion evaporation from liquid surfaces at atmospheric pressure.* The Journal of Chemical Physics, 1979. **71**(11): p. 4451-4463.
38. Mazzeo, J.R., et al., *A new separation technique takes advantage of sub-2-mu m porous particles.* Analytical Chemistry, 2005. **77**(23): p. 460a-467a.
39. Scientific, C. *High performance Liquid Chromatography Column dimensions*. Chromatography 2016 [cited 2016 20-04-16]; Available from: http://www.chromacademy.com/chromatography-HPLC-Column-Dimensions.html.
40. Wicke, E., *J. C. Giddings: Dynamics of Chromatography. Part. I: Principles and Theory. Marcel Dekker, New York, 1965. XII und 323 Seiten. 39 Abb. Preis:$ 11.50.* Berichte der Bunsengesellschaft für physikalische Chemie, 1967. **71**(2): p. 236-236.
41. Heaton, J.C., *An Evaluation Of UHPLC-MS Technology Encompassing Elevated Temperatures, Low Viscosity Operation and Recently Developed Stationary Phase Materials*, in *Analytical and environmnetal sciences*2012, King's College London: King's Research Portal. p. 234.

42. Bristow, P.A. and J.H. Knox, *Standardization of test conditions for high performance liquid chromatography columns.* Chromatographia, 1977. **10**(6): p. 279-289.
43. Kaiser, T.J., et al., *Capillary-Based Instrument for the Simultaneous Measurement of Solution Viscosity and Solute Diffusion Coefficient at Pressures up to 2000 bar and Implications for Ultrahigh Pressure Liquid Chromatography.* Analytical Chemistry, 2009. **81**(8): p. 2860-2868.
44. David Fairhurst, B.W. *A Guide to Determination of Particle Size – Making an Effective and Reliable Measurement*. 2017 [cited 2017 22-05-17]; Available from: http://bic.com/pdf/theory/Determination%20of%20Particle%20Size.pdf.
45. Giddings, J.C., *Comparison of Theoretical Limit of Separating Speed in Gas and Liquid Chromatography.* Analytical Chemistry, 1965. **37**(1): p. 60-63.
46. Neue, U.D. *Kinetic Plots Made Easy*. 2009 [cited 2017 23-05-17]; Available from: http://www.chromatographyonline.com/kinetic-plots-made-easy-1?id=&sk=&date=&pageID=2.
47. Poppe, H., *Some reflections on speed and efficiency of modern chromatographic methods.* Journal of Chromatography A, 1997. **778**(1): p. 3-21.
48. Desmet, G., D. Clicq, and P. Gzil, *Geometry-independent plate height representation methods for the direct comparison of the kinetic performance of LC supports with a different size or morphology.* Anal Chem, 2005. **77**(13): p. 4058-70.
49. Svec, F. and J.M.J. Frechet, *Molded rigid monolithic porous polymers: An inexpensive, efficient, and versatile alternative to beads for the design of materials for numerous applications.* Industrial & Engineering Chemistry Research, 1999. **38**(1): p. 34-48.
50. Bakry, R., C.W. Huck, and G.K. Bonn, *Recent Applications of Organic Monoliths in Capillary Liquid Chromatographic Separation of Biomolecules.* Journal of Chromatographic Science, 2009. **47**(6): p. 418-431.
51. R. Asiaie, X.H., D. Farnan, and C. Horváth, *Sintered octadecylsilica as monolithic column packing in capillary electrochromatography and micro*

high-performance liquid chromatography. J. Chromatogr. A, 1998. **806**(2): p. 251–263.
52. Dulay, M.T., R.P. Kulkarni, and R.N. Zare, *Preparation and characterization of monolithic porous capillary columns loaded with chromatographic particles.* Anal Chem, 1998. **70**(23): p. 5103-7.
53. Smith, N.W. and Z. Jiang, *Developments in the use and fabrication of organic monolithic phases for use with high-performance liquid chromatography and capillary electrochromatography.* Journal of Chromatography A, 2008. **1184**(1-2): p. 416-440.
54. Gritti, F. and G. Guiochon, *Heterogeneity of the surface energy on unused C18-chromolith adsorbents in reversed-phase liquid chromatography.* J Chromatogr A, 2004. **1028**(1): p. 105-19.
55. Minakuchi, H., et al., *Effect of skeleton size on the performance of octadecylsilylated continuous porous silica columns in reversed-phase liquid chromatography.* J Chromatogr A, 1997. **762**(1-2): p. 135-46.
56. Al-Othman, Z.A., et al., *Fast chromatographic determination of caffeine in food using a capillary hexyl methacrylate monolithic column.* Food Chemistry, 2012. **132**(4): p. 2217-2223.
57. Kubin, M., P. Spacek, and Chromece.R, *Gel Permeation Chromatography on Porous Poly(Ethylene Glycol Methacrylate).* Collection of Czechoslovak Chemical Communications, 1967. **32**(11): p. 3881-&.
58. Ross, W.D. and Jefferso.Rt, *In-Situ-Formed Open-Pore Polyurethane as Chromatography Supports.* Journal of Chromatographic Science, 1970. **8**(7): p. 386-&.
59. Yang, Y.Q., et al., *Protein Chromatography Using a Continuous Stationary Phase.* Journal of Chromatography, 1992. **598**(2): p. 169-180.
60. Roper, D.K. and E.N. Lightfoot, *Separation of Biomolecules Using Adsorptive Membranes.* Journal of Chromatography A, 1995. **702**(1-2): p. 3-26.

61. Kennedy, J.F. and M. Paterson, *Application of Cellulosic Fast-Flow Column Filters to Protein Immobilization and Recovery.* Polymer International, 1993. **32**(1): p. 71-81.
62. Tennikova, T.B., B.G. Belenkii, and F. Svec, *High-Performance Membrane Chromatography - a Novel Method of Protein Separation.* Journal of Liquid Chromatography, 1990. **13**(1): p. 63-70.
63. Hjerten, S., J.L. Liao, and R. Zhang, *High-Performance Liquid-Chromatography on Continuous Polymer Beds.* Journal of Chromatography, 1989. **473**(1): p. 273-275.
64. Svec, F. and J.M.J. Frechet, *Continuous Rods of Macroporous Polymer as High-Performance Liquid-Chromatography Separation Media.* Analytical Chemistry, 1992. **64**(7): p. 820-822.
65. Minakuchi, H., et al., *Octadecylsilylated porous silica rods as separation media for reversed-phase liquid chromatography.* Analytical Chemistry, 1996. **68**(19): p. 3498-3501.
66. Ashraf Ghanem, T.I., *Recent advances in silica-based monoliths: Preparations, characterizations and applications.* Separation science 2011. **34**(16-17): p. 1945-1957.
67. Gunasena, D.N. and Z.E. Rassi, *Organic monoliths for hydrophilic interaction electrochromatography/chromatography and immunoaffinity chromatography.* Electrophoresis, 2012. **33**(1): p. 251-61.
68. Zou, H.F., et al., *Monolithic stationary phases for liquid chromatography and capillary electrochromatography.* Journal of Chromatography A, 2002. **954**(1-2): p. 5-32.
69. Tasfiyati, A.N., et al., *Evaluation of glycidyl methacrylate-based monolith functionalized with weak anion exchange moiety inside 0.5 mm i.d. column for liquid chromatographic separation of DNA.* Analytical Chemistry Research, 2016. **7**: p. 9-16.
70. Gusev, I., X. Huang, and C. Horvath, *Capillary columns with in situ formed porous monolithic packing for micro high-performance liquid chromatography and capillary electrochromatography.* Journal of Chromatography A, 1999. **855**(1): p. 273-290.
71. Svec, F., *Porous polymer monoliths: Amazingly wide variety of techniques enabling their preparation.* Journal of Chromatography A, 2010. **1217**(6): p. 902-924.
72. Kositarat, S., et al., *Repeatability in column preparation of a reversed-phase C18 monolith and its application to separation of tocopherol homologues.* Talanta, 2011. **84**(5): p. 1374-1378.
73. Yuan, G., et al., *A facile and efficient strategy to enhance hydrophilicity of zwitterionic sulfoalkylbetaine type monoliths.* Journal of Chromatography A, 2013. **1301**: p. 88-97.
74. Jiang, Z.J., et al., *Preparation and characterization of long alkyl chain methacrylate-based monolithic column for capillary chromatography.* Journal of Biochemical and Biophysical Methods, 2007. **70**(1): p. 39-45.
75. Medicine, U.N.L.O. *Open Chemistry Data Base*. 2016 [cited 2016 10-11-16

]; Available from: https://pubchem.ncbi.nlm.nih.gov/search/.
76. Pesek, J.J., M.T. Matyska, and S. Larrabee, *HPLC retention behavior on hydride-based stationary phases.* Journal of Separation Science, 2007. **30**(5): p. 637-647.
77. Courtois, J., et al., *A study of surface modification and anchoring techniques used in the preparation of monolithic microcolumns in fused silica capillaries.* J Sep Sci, 2006. **29**(1): p. 14-24.
78. Sänger, C. *CE capillary* CE solutions 2016 [cited 2016 19-05-2016

]; Available from: https://www.sepscience.com/Techniques/CE/643-/CE-Solutions-3-The-CE-Capillary.
79. source, I. *Capillary HPLC UV Detection*. 2005 [cited 2016 19-05-16]; Available from: http://www.ionsource.com/tutorial/capillary/uv.htm.
80. Grafnetter, J., et al., *Optimization of binary porogen solvent composition for preparation of butyl methacrylate monoliths in capillary liquid chromatography.* Journal of Chromatography A, 2004. **1049**(1–2): p. 43-49.

81. Lukas J, S.F., Kalal J. , *Reactive polymer: XV. polar polymeric sorbents based on glydicyl methoacrylate copolymers.* J chromatogr., 1978. **153**: p. 15-22.
82. Coufal, P., *methacrylate monolithic column for capillary liquid chromatography using ammonium peroxydisulfate as initiator.* separation science 2003. **26**(8).
83. Hoegger, D. and R. Freitag, *Acrylamide-based monoliths as robust stationary phases for capillary electrochromatography.* Journal of Chromatography A, 2001. **914**(1–2): p. 211-222.
84. Anna Maria Enlund, C.E., Stellan Hjertén, Douglas Westerlund, *Capillary electrochromatography of hydrophobic amines on continuous beds.* Electrophoresis, 2001 **22**: p. 511-517.
85. Novotny, A.P.a.M.V., *Macroporous Polyacrylamide/Poly(ethylene glycol) Matrixes as Stationary Phases in Capillary Electrochromatography.* Anal. Chem. 1997, 69, 4499-4507, 1997 **69**: p. 4499-4507.
86. Li, Y., et al., *Preparation and characterization of alkylated polymethacrylate monolithic columns for micro-HPLC of proteins.* J Sep Sci, 2004. **27**(17-18): p. 1467-74.
87. Ericson, C., et al., *Preparation of continuous beds for electrochromatography and reversed-phase liquid chromatography of low-molecular-mass compounds.* Journal of Chromatography A, 1997. **767**(1-2): p. 33-41.
88. Haenel, H., *J. E. James: Caffeine and Health. 432 Seiten. Academic Press, London, San Diego, New York* Food / Nahrung, 1992. **36**(4): p. 431-431.
89. Belay, A., et al., *Measurement of caffeine in coffee beans with UV/vis spectrometer.* Food Chemistry, 2008. **108**(1): p. 310-315.
90. Reissig, C.J., E.C. Strain, and R.R. Griffiths, *Caffeinated energy drinks—A growing problem.* Drug and Alcohol Dependence, 2009. **99**(1–3): p. 1-10.
91. Sutherland, A.H.V.J.P., *Beverages : technology, chemistry and microbiology*. Food products series, v. 2. 1994, London London : Chapman & Hall, 1994.
92. Fenske, M., *Caffeine Determination in Human Saliva and Urine by TLC and Ultraviolet Absorption Densitometry.* Chromatographia, 2007 **65**(3): p. 8.
93. Armenta, S., S. Garrigues, and M. de la Guardia, *Solid-phase FT-Raman determination of caffeine in energy drinks.* Analytica Chimica Acta, 2005. **547**(2): p. 197-203.
94. Brunetto, M.a.d.R., et al., *Determination of theobromine, theophylline and caffeine in cocoa samples by a high-performance liquid chromatographic method with on-line sample cleanup in a switching-column system.* Food Chemistry, 2007. **100**(2): p. 459-467.
95. Li, H., et al., *Simultaneous quantitation of paracetamol, caffeine, pseudoephedrine, chlorpheniramine and cloperastine in human plasma by liquid chromatography–tandem mass spectrometry.* Journal of Pharmaceutical and Biomedical Analysis, 2010. **51**(3): p. 716-722.
96. Sun, H.-w., F.-x. Qiao, and G.-y. Liu, *Characteristic of theophylline imprinted monolithic column and its application for determination of xanthine derivatives caffeine and theophylline in green tea.* Journal of Chromatography A, 2006. **1134**(1–2): p. 194-200.
97. Shrivas, K. and H.-F. Wu, *Rapid determination of caffeine in one drop of beverages and foods using drop-to-drop solvent microextraction with gas chromatography/mass spectrometry.* Journal of Chromatography A, 2007. **1170**(1–2): p. 9-14.
98. Mashkouri Najafi, N., A.S. Hamid, and R.K. Afshin, *Determination of caffeine in black tea leaves by Fourier transform infrared spectrometry using multiple linear regression.* Microchemical Journal, 2003. **75**(3): p. 151-158.
99. Talebpour, Z., Maesum, S., Jalali-Heravi, M., & Shamsipur, M, *Simultaneous determination of theophylline and caffeine by proton magnetic resonance spectroscopy using partial least squares regression techniques.* Analytical Sciences, 2003. **19**: p. 4.
100. Meinhart, A.D., et al., *Optimisation of a CE method for caffeine analysis in decaffeinated coffee.* Food Chemistry, 2010. **120**(4): p. 1155-1161.

101. Tzanavaras, P.D. and D.G. Themelis, *Development and validation of a high-throughput high-performance liquid chromatographic assay for the determination of caffeine in food samples using a monolithic column.* Analytica Chimica Acta, 2007. **581**(1): p. 89-94.
102. Urban, J., et al., *Preparation and characterization of polymethacrylate monolithic capillary columns with dual hydrophilic interaction reversed-phase retention mechanism for polar compounds.* Journal of Separation Science, 2009. **32**(15-16): p. 2530-2543.
103. Urban, J., F. Svec, and J.M.J. Frechet, *Hypercrosslinking: New approach to porous polymer monolithic capillary columns with large surface area for the highly efficient separation of small molecules.* Journal of Chromatography A, 2010. **1217**(52): p. 8212-8221.
104. Lin, S.L., et al., *Preparation and evaluation of 1,6-hexanediol ethoxylate diacrylate-based alkyl methacrylate monolithic capillary column for separating small molecules.* Journal of Chromatography A, 2013. **1298**: p. 35-43.
105. Svec, F., *Quest for organic polymer-based monolithic columns affording enhanced efficiency in high performance liquid chromatography separations of small molecules in isocratic mode.* Journal of Chromatography A, 2012. **1228**: p. 250-262.
106. Jandera, P., et al., *Cross-linker effects on the separation efficiency on (poly)methacrylate capillary monolithic columns. Part I. Reversed-phase liquid chromatography.* Journal of Chromatography A, 2013. **1274**: p. 97-106.
107. Taverniers, I., M. De Loose, and E. Van Bockstaele, *Trends in quality in the analytical laboratory. II. Analytical method validation and quality assurance.* TrAC Trends in Analytical Chemistry, 2004. **23**(8): p. 535-552.
108. Wang, X.C., et al., *Electrochromatographic characterization of methacrylate-based monolith with mixed mode of hydrophilic and weak electrostatic interactions by pressurized capillary electrochromatography.* Journal of Chromatography A, 2008. **1190**(1-2): p. 365-371.
109. Dean, J.R., *Extraction Techniques in Analytical Sciences* 2009, United Kingdom Wiley. 308.
110. Shrivas, K. and H.F. Wu, *Rapid determination of caffeine in one drop of beverages and foods using drop-to-drop solvent microextraction with gas chromatography/mass spectrometry.* Journal of Chromatography A, 2007. **1170**(1-2): p. 9-14.
111. Gałuszka, A., Z. Migaszewski, and J. Namieśnik, *The 12 principles of green analytical chemistry and the SIGNIFICANCE mnemonic of green analytical practices.* TrAC Trends in Analytical Chemistry, 2013. **50**(0): p. 78-84.
112. Niessen, W.M.A. and A.P. Tinke, *Liquid chromatography-mass spectrometry General principles and instrumentation.* Journal of Chromatography A, 1995. **703**(1–2): p. 37-57.
113. Chen, M.L., et al., *Preparation and characterization of rnethacrylate-based monolith for capillary hydrophilic interaction chromatography.* Journal of Chromatography A, 2012. **1230**: p. 54-60.
114. Lubbad, S.H. and M.R. Buchmeiser, *Fast separation of low molecular weight analytes on structurally optimized polymeric capillary monoliths.* Journal of Chromatography A, 2010. **1217**(19): p. 3223-3230.
115. Liu, K., H.D. Tolley, and M.L. Lee, *Highly crosslinked polymeric monoliths for reversed-phase capillary liquid chromatography of small molecules.* Journal of Chromatography A, 2012. **1227**: p. 96-104.
116. Lubbad, S.H., R. Bandari, and M.R. Buchmeiser, *Ring-opening metathesis polymerization-derived monolithic strong anion exchangers for the separation of 5 '-phosphorylated oligodeoxythymidylic acids fragments.* Journal of Chromatography A, 2011. **1218**(49): p. 8897-8902.
117. Gatschelhofer, C., et al., *Ring-opening metathesis polymerization for the preparation of norbornene-based weak cation-exchange monolithic capillary columns.* Journal of Chromatography A, 2009. **1216**(13): p. 2651-2657.

118. Bandari, R. and M.R. Buchmeiser, *Functional Monolithic Materials for Boronate-Affinity Chromatography via Schrock Catalyst-Triggered Ring-Opening Metathesis Polymerization.* Macromolecular Rapid Communications, 2012. **33**(16): p. 1399-1403.
119. Li, Y.Y., H.D. Tolley, and M.L. Lee, *Monoliths from poly(ethylene glycol) diacrylate and dimethacrylate for capillary hydrophobic interaction chromatography of proteins.* Journal of Chromatography A, 2010. **1217**(30): p. 4934-4945.
120. Peters, E.C., et al., *Control of porous properties and surface chemistry in "molded" porous polymer monoliths prepared by polymerization in the presence of TEMPO.* Macromolecules, 1999. **32**(19): p. 6377-6379.
121. Viklund, C., et al., *Preparation of porous poly(styrene-co-divinylbenzene) monoliths with controlled pore size distributions initiated by stable free radicals and their pore surface functionalization by grafting.* Macromolecules, 2001. **34**(13): p. 4361-4369.
122. Svobodova, A., et al., *Monolithic columns based on a poly(styrene-divinylbenzene-methacrylic acid) copolymer for capillary liquid chromatography of small organic molecules.* Journal of Chromatography A, 2011. **1218**(11): p. 1544-1547.
123. Moravcova, D., et al., *Characterization of polymer monolithic stationary phases for capillary HPLC.* Journal of Separation Science, 2003. **26**(11): p. 1005-1016.
124. Moravcova, D., et al., *Comparison of monolithic silica and polymethacrylate capillary columns for LC.* Journal of Separation Science, 2004. **27**(10-11): p. 789-800.
125. Svec, F. and J.M.J. Frechet, *Kinetic Control of Pore Formation in Macroporous Polymers - Formation of Molded Porous Materials with High-Flow Characteristics for Separations or Catalysis.* Chemistry of Materials, 1995. **7**(4): p. 707-715.
126. Kanamori, K., K. Nakanishi, and T. Hanada, *Rigid macroporous poly(divinylbenzene) monoliths with a well-defined bicontinuous morphology prepared by living radical polymerization.* Advanced Materials, 2006. **18**(18): p. 2407-+.
127. Li, Y., et al., *Preparation and evaluation of hydrophilic C18 monolithic sorbents for enhanced polar compound retention in liquid chromatography and solid phase extraction.* Journal of Chromatography A, 2011. **1218**(48): p. 8608-8616.
128. Small, H., T.S. Stevens, and W.C. Bauman, *Novel Ion-Exchange Chromatographic Method Using Conductimetric Detection.* Analytical Chemistry, 1975. **47**(11): p. 1801-1809.
129. Stankova, M., et al., *Cross-linker effects on the separation efficiency on (poly)methacrylate capillary monolithic columns. Part II. Aqueous normal-phase liquid chromatography.* Journal of Chromatography A, 2013. **1289**: p. 47-57.
130. Aggarwal, P., *High- Peformance Molymer Monoliths for Capillary Liquid Chromatography* in *Chemistry and Biochemistry* 2014, Brigham Young USA p. 200.
131. Khattab, A.K., *Fabrication, functionalization and characterization of silica monolith for forensic chemistry applications*, in *Chemistry* 2013, Hull: UK p. 230.
132. Xu, Z., L. Yang, and Q. Wang, *Different alkyl dimethacrylate mediated stearyl methacrylate monoliths for improving separation efficiency of typical alkylbenzenes and proteins.* Journal of Chromatography A, 2009. **1216**(15): p. 3098-3106.
133. Li, Y., et al., *Preparation and evaluation of hydrophilic C18 monolithic sorbents for enhanced polar compound retention in liquid chromatography and solid phase extraction.* J Chromatogr A, 2011. **1218**(48): p. 8608-16.
134. Bai, X., et al., *Preparation of a novel porous poly (trimethylol propane triacrylate-co-ethylene dimethacrylate) monolithic column for highly efficient HPLC separations of small molecules.* Talanta, 2014. **119**: p. 479-84.
135. Liu, H.Y., et al., *High-performance liquid chromatography separation of small molecules on a porous poly (trimethylol propane triacrylate-co-N-isopropylacrylamide-co-ethylene dimethacrylate) monolithic column.* Journal of Chromatography A, 2014. **1324**: p. 128-134.
136. (ED), D.R.L., *CRC Handbook of chemistry and physics* 80 ed. 1999, Boca Raton, Florida: CRC Press

137. Causon, T.J., E.F. Hilder, and I. Nischang, *Impact of mobile phase composition on the performance of porous polymeric monoliths in the elution of small molecules.* Journal of Chromatography A, 2012. **1263**: p. 108-112.
138. Nischang, I., *On the chromatographic efficiency of analytical scale column format porous polymer monoliths: Interplay of morphology and nanoscale gel porosity.* Journal of Chromatography A, 2012. **1236**: p. 152-163.
139. Jiang, Z., et al., *Mixed-mode reversed-phase and ion-exchange monolithic columns for micro-HPLC.* J Sep Sci, 2008. **31**(15): p. 2774-83.
140. Duan, Q., et al., *Preparation and evaluation of a novel monolithic column containing double octadecyl chains for reverse-phase micro high performance liquid chromatography.* J Chromatogr A, 2014. **1345**: p. 174-81.
141. Legido-Quigley, C. and N.W. Smith, *Study of short polystyrene monolith-fritted micro-liquid chromatography columns for analysis of neutral and basic compounds.* Journal of Chromatography A, 2004. **1042**(1-2): p. 61-68.
142. JIC, M.S.a. *LC-MS: Why use it, and what is it?* How LC-MS works 2013 [cited 2016; Available from: https://www.jic.ac.uk/services/metabolomics/topics/lcms/why.htm.
143. Bai, X., et al., *Preparation of a novel porous poly (trimethylol propane triacrylate-co-ethylene dimethacrylate) monolithic column for highly efficient HPLC separations of small molecules.* Talanta, 2014. **119**: p. 479-484.
144. Zhang, Y., et al., *Synthesis and characterization of a multimode stationary phase: Congo red derivatized silica in nano-flow HPLC.* Analyst, 2016. **141**(3): p. 1083-90.
145. Talebi, M., et al., *Epoxy-based monoliths for capillary liquid chromatography of small and large molecules.* Anal Bioanal Chem, 2013. **405**(7): p. 2233-44.
146. Zhao, X., et al., *A novel mixed phospholipid functionalized monolithic column for early screening of drug induced phospholipidosis risk.* J Chromatogr A, 2014. **1367**: p. 99-108.
147. Qiu, H., et al., *A sulfonic-azobenzene-grafted silica amphiphilic material: a versatile stationary phase for mixed-mode chromatography.* Chemistry, 2013. **19**(52): p. 18004-10.
148. Qiu, H., et al., *New strategy for drastic enhancement of selectivity via chemical modification of counter anions in ionic liquid polymer phase.* Chem Commun (Camb), 2010. **46**(46): p. 8740-2.
149. Sayed, R.H., et al., *Misdiagnosing renal amyloidosis as minimal change disease.* Nephrol Dial Transplant, 2014. **29**(11): p. 2120-6.
150. Jiao, X., S. Shen, and T. Shi, *One-pot preparation of a novel monolith for high performance liquid chromatography applications.* Journal of Chromatography B, 2015. **1007**: p. 100-109.
151. Liu, C., et al., *Influence of the crosslinker type on the chromatographic properties of hydrophilic sulfoalkylbetaine-type monolithic columns.* Journal of Chromatography A, 2014. **1373**: p. 73-80.
152. Norman Smith, J., Z. *Investigation of monolithic stationary phases for micro-high performance liquid chromatography*. [PostDoc position] 2009 2009; 27].
153. Liu, Z., et al., *Preparation and application of novel zwitterionic monolithic column for hydrophilic interaction chromatography.* Journal of Separation Science, 2013. **36**(2): p. 262-269.
154. Liu, K., et al., *Highly crosslinked polymeric monoliths with various C6 functional groups for reversed-phase capillary liquid chromatography of small molecules.* Journal of Chromatography A, 2013. **1321**: p. 80-87.
155. Lin, S.-L., Y.-R. Wu, and M.-R. Fuh, *Polymer monolith microextraction using poly(butyl methacrylate-co-1,6-hexanediol ethoxylate diacrylate) monolithic sorbent for determination of phenylurea herbicides in water samples.* Talanta, 2016. **147**: p. 199-206.
156. Lin, S.-L., et al., *Preparation and evaluation of 1,6-hexanediol ethoxylate diacrylate-based alkyl methacrylate monolithic capillary column for separating small molecules.* Journal of Chromatography A, 2013. **1298**: p. 35-43.

157. Alshitari, W., C.L. Quigley, and N. Smith, *Fabrication and evaluation of an organic monolithic column based upon the polymerisation of hexyl methacrylate with 1,6-hexanediol ethoxylate diacrylate for the separation of small molecules by capillary liquid chromatography.* Talanta, 2015. **141**: p. 103-110.
158. Lin, S.-L., et al., *Preparation and evaluation of poly(alkyl methacrylate-co-methacrylic acid-co-ethylene dimethacrylate) monolithic columns for separating polar small molecules by capillary liquid chromatography.* Analytica Chimica Acta, 2015. **871**: p. 57-65.
159. Wamser, D.C.C. *Chapter 15 - Carbonyl Compounds*. Organic Chemistry II 2000 [cited 2016 10-11-16]; Available from: http://web.pdx.edu/~wamserc/C335W99/15notes.htm.
160. *Structures predications and identification of chemical structures*. 2016 [cited 2016 15-11-16]; Available from: http://cds.rsc.org/.
161. Shao, W., et al., *Hydrogen-bond interaction assisted branched copolymer HILIC material for separation and N-glycopeptides enrichment.* Talanta, 2016. **158**: p. 361-367.
162. Unger, K.K., R. Skudas, and M.M. Schulte, *Particle packed columns and monolithic columns in high-performance liquid chromatography-comparison and critical appraisal.* Journal of Chromatography A, 2008. **1184**(1–2): p. 393-415.
163. Shu, S., et al., *Preparation and characterization of lauryl methacrylate-based monolithic microbore column for reversed-phase liquid chromatography.* Journal of Chromatography A, 2011. **1218**(31): p. 5228-5234.
164. Liu, Y., et al., *Biodegradable polylactic acid porous monoliths as effective oil sorbents.* Composites Science and Technology, 2015. **118**: p. 9-15.
165. Lin, S.L., Y.R. Wu, and M.R. Fuh, *Polymer monolith microextraction using poly(butyl methacrylate-co-1,6-hexanediol ethoxylate diacrylate) monolithic sorbent for determination of phenylurea herbicides in water samples.* Talanta, 2016. **147**: p. 199-206.
166. James N Miller, J.C.M., *Statistics and Chemometrics for Analytical Chemistry*. 6 ed. 2010, England Pearson Education Limited. 297.
167. Aggarwal, P., et al., *High efficiency polyethylene glycol diacrylate monoliths for reversed-phase capillary liquid chromatography of small molecules.* J Chromatogr A, 2014. **1364**: p. 96-106.
168. Yang, W., et al., *Supercritical fluid chromatography for separation and preparation of tautomeric 7-epimeric spiro oxindole alkaloids from Uncaria macrophylla.* Journal of Pharmaceutical and Biomedical Analysis.
169. Bamba, T. and E. Fukusaki, *Separation of hydrophobic metabolites using monolithic silica column in high-performance liquid chromatography and supercritical fluid chromatography.* J Sep Sci, 2009. **32**(15-16): p. 2699-706.
170. Berger, T.A. and B.K. Berger, *Minimizing UV noise in supercritical fluid chromatography. I. Improving back pressure regulator pressure noise.* J Chromatogr A, 2011. **1218**(16): p. 2320-6.